DISSERTATION

CHARACTERIZING THE GENETIC EVOLUTION OF ENDEMIC BLUETONGUE VIRUS STRAINS

Submitted by

Jennifer H. Kopanke

Department of Microbiology, Immunology, and Pathology

In partial fulfillment of the requirements

For the Degree of Doctor of Philosophy

Colorado State University

Fort Collins, Colorado

Summer 2019

Doctoral Committee:

Advisor: Christie Mayo

Rob Callan
Greg Ebel
Sue VandeWoude

ABSTRACT

CHARACTERIZING THE GENETIC EVOLUTION OF ENDEMIC BLUETONGUE VIRUS STRAINS

Bluetongue virus is an arthropod-borne virus that can cause severe disease in susceptible animals. Transmitted by biting midges in the genus *Culicoides*, the bluetongue virus particle (genus *Orbivirus*, family *Reoviridae*) is composed of ten segments of double-stranded RNA enclosed by a bi-layered, icosahedral capsid. While both wild and domestic ruminants are capable of becoming infected with bluetongue virus, sheep are most likely to develop severe disease characterized by systemic vasculitis, edema, and coagulopathy.

Due to its relatively unusual genome structure, bluetongue virus (BTV) is able to evolve via several key mechanisms, including via the accumulation of mutations over time, or more rapidly via reassortment of genome segments. Adding to this genetic complexity, bluetongue virus must maintain fitness in two very disparate hosts: the insect vector and the ruminant. While host-switching is widely accepted as an important aspect of bluetongue virus evolution, the specific features of viral adaptation in each host are poorly characterized. Limited field studies and experimental work from other labs have alluded to the presence of these phenomena at work in the evolutionary trajectory of bluetongue virus, but our overall understanding of the factors that drive or constrain this virus's genetic diversification remains incomplete.

In recent years, bluetongue virus has caused significant disease outbreaks among ruminants in enzootic regions, such as the U.S., as well as in areas where bluetongue virus was previously considered exotic, such as northern Europe. Various dynamics including vector range

expansion, movement of animals, virus evolution through reassortment and mutation, and environmental factors all may have an integral role in the occurrence of these outbreaks. Not only do bluetongue epizootics carry sometimes profound animal health consequences, but they are also associated with significant economic impacts due to production declines, costly efforts to contain disease spread, and trade restrictions. Collectively, our currently limited understanding of bluetongue virus ecology and evolution dramatically hinders our ability to predict and prevent the occurrence of epizootics associated with orbiviruses.

As whole genome sequencing approaches have become increasingly available and affordable, these tools provide a uniquely valuable platform for interrogating underlying viral genetic factors associated with bluetongue disease incursions and outbreaks. Coupling applied fieldwork, in vitro, and in vivo studies with sequencing tools and bioinformatics, the work described in this dissertation seeks to address specific knowledge gaps surrounding bluetongue evolution in North America.

In particular, we first queried how an alternating-host transmission cycle affects bluetongue's genetic diversity using an in vitro system, where we leveraged whole genome sequencing and measures of population genetics to understand the role of viral mutation during BTV evolution. We found low rates of overall mutation, leading us to consider whether reassortment is a relatively greater contributor to bluetongue's genetic diversity. Once again using an in vitro platform, we investigated reassortment frequency and segment-specific trends between two enzootic bluetongue virus strains. Our work demonstrated that global shifts in segment frequencies emerged across serial passages, possibly representing preferred reassortant segment combinations. However, most viral segments persisted – even if at very low levels – within the overall population from passage to passage. To better characterize these trends, and to

understand whether environmental factors such as temperature might affect their occurrence, we introduced these same viruses into *Culicoides sonorensis* midges – the predominant North American vector of bluetongue virus – and tracked virogenesis and reassortment across time at three different temperatures. Correlating with other studies, we found that higher temperatures were associated with more rapid virogenesis. However, we were surprised to find that one of the two virus strains replicated poorly in midges orally infected with biologically relevant titers, highlighting potential vector-based barriers to reassortment. Finally, we used whole genome sequencing to characterize circulating strains of bluetongue virus present in Colorado ruminants in 2015 and 2018. We found that numerous strains of bluetongue virus were present among sentinel animals, and that many isolates contained signatures of reassortment.

Collectively, our findings demonstrate that reassortment among virus strains is a prominent feature of bluetongue viral evolution. Importantly, there appear to be preferred segment combinations that arise following coinfection, but vector-virus interactions seem to play a central role in modulating the ultimate emergence of reassortant viruses. These studies and others promise to improve our understanding of bluetongue's evolution and ecology, ultimately contributing to the development of better predictive models and management strategies to reduce future impacts of bluetongue epizootics.

ACKNOWLEDGMENTS

This work would not have been possible without the unwavering support of an entire community of individuals who have encouraged me, challenged my thinking, supported my science, and kept me laughing. Many thanks to all of those currently in the Mayo Lab (Molly Carpenter, Justin Lee, Kirsten Reed, and Christie Mayo herself) and those who have graduated from the lab during the time I have been at CSU, including the residents and summer scholars who have joined us for a season (Anna Fagre, Teresa Garcia, Elle Holbrook, and others). Each of these prior lab mates has contributed to this body of research and added to the character of the Mayo Lab in a unique way. Special thanks to Teresa for performing much of the lab work that laid the foundation of Chapter 4 and for decorating the lab space.

I could not have completed any part of this dissertation without the help of Justin, who patiently taught me everything I know about sequencing and spent many hours brainstorming and troubleshooting with me, particularly as we tackled *Culicoides* husbandry (which turned out to be one of the most difficult tasks of my PhD). Thank you, as well, to Molly for her assistance with various project in the lab this spring, and for her boundless positive attitude and creativity. Finally, I am deeply grateful to Christie for her constant support, excellent mentorship and guidance, shared excitement at my eureka moments over the years, and willingness to take me on as her first PhD student.

I am also very appreciative of the mentorship provided by my graduate committee: Drs. Sue VandeWoude, Greg Ebel, and Rob Callan. They have brought expertise and insight to each step of this process, and we greatly value their contributions to the quality of this body of work and overall support of my graduate program.

There have been many collaborators involved in various aspects of the research presented here, but special thanks to local veterinarians and producers for their willingness to contribute to the field portions of our work. Thank you as well to Mark Stenglein, who has repeatedly assisted with project conceptualization and analysis, and all of the incredibly helpful team members at the NGS Core. We also appreciate the expertise provided by those at the USDA-ARS in Manhattan, Kansas, and are thankful for the resources they shared with us – particularly the CuVaW3 cells and *Culicoides sonorensis* midges used in our experiments.

I am also very grateful to all of those who contribute to the combined Comparative Medicine residency-degree program here at CSU, which opened the door for me to pursue a PhD following my residency. Many thanks to my mentors at Lab Animal Resources, my residency mates, and the many excellent individuals I had the opportunity to work with during my residency.

Lastly, I would not be in this position without the lifelong support of absolutely amazing family and friends. Thank you to my parents for their constant encouragement, wisdom, and humor, and for letting me grow up on a farm and follow my little girl's dream of becoming a veterinarian. I also am deeply thankful for my sister, who has always been my role model and also my friend. Finally, thank you to Jason for being by my side absolutely every step along the way since vet school. I am so grateful for the love, laughter, and adventure you bring to my life.

TABLE OF CONTENTS

LIST OF TABLES

LIST OF FIGURES

CHAPTER 1 – INTRODUCTION

History of Bluetongue Virus

First described in South Africa at the turn of the 20th century, bluetongue virus remains an economically important, re-emerging disease with substantial animal health impacts. Its significance stems from its role as the etiologic agent behind recent devastating disease outbreaks among ruminants, coupled with its ongoing expansion into new regions. Bluetongue virus, or BTV, belongs to genus *Orbivirus*, family *Reoviridae*, and is composed of ten segments of double-stranded RNA (dsRNA) surrounded by a bi-layered viral capsid. Transmitted by hematophagous midges in the *Culicoides* genus (Diptera: Ceratopogonidae), BTV is the causative agent of bluetongue disease, which is characterized by vasculitis and associated sequelae in susceptible animals. Despite more than a century of research, significant knowledge gaps regarding BTV's ecology and evolution persist, particularly in light of today's accelerating climate crisis. The transformational advancement and widespread availability of whole genome sequencing and other novel sequencing technologies offers an essential tool to explore and better understand the evolutionary dynamics of this segmented dsRNA arbovirus.

BTV is believed to have circulated subclinically among ruminants in sub-Saharan Africa long before bluetongue disease was first noted in imported Merino sheep in South Africa in the late 1800s.[1,2] Characterized by lameness and mouth lesions in the imported animals, the disease was initially simply termed "fever" or "epizootic cattarh," but later was given the name "bluetongue" for its association with cyanosis of the tongue and mucous membranes.[3–5] Theiler subsequently determined that this disease was caused by a virus or a "filterable agent" in 1906.[6] While it was circumstantially suspected early on that bluetongue virus was an insect-transmitted

disease, du Toit definitively demonstrated this was the case in 1944 when wild-caught *Culicoides imicola* – now known to be the key BTV vector in Africa and Asia – were macerated, filtered, and inoculated into sheep that subsequently developed bluetongue disease.[7] Du Toit also was able to demonstrate that *C. imicola* was a biological vector for the virus by carrying out transmission experiments from midges to sheep.[7]

Early attempts to control BTV via vaccination with an attenuated virus (generated through repeated passages in sheep) led to the discovery that multiple virus strains, or serotypes, existed.[8,9] While animals exhibited lifelong protection against the specific strain used in vaccine preparations, it was soon discovered that these vaccines did not protect against all field isolates of BTV. Defined by the vertebrate host's immune response to the BTV VP2 outer capsid protein, viral serotype is still used today to classify strains of bluetongue virus. At least 29 serotypes of BTV have been described to date, with various serotypes circulating regionally. Importantly, as early findings demonstrated, antibodies that develop in response to infection with one serotype of BTV are generally not cross-protective against other serotypes.[10,11] Hence, the introduction of novel BTV serotypes even to enzootic areas poses a concern in terms of animal health risk.

Bluetongue virus was largely believed to be confined to Africa until mid-century, when several reports of bluetongue-like disease emerged in other regions including Cyprus, the United States, and the Iberian Peninsula.[12–15] These disease outbreaks often had profound consequences and high mortality rates; nearly 180,000 sheep died in Spain and Portugal during the Iberian Peninsula epizootic.[15]

BTV was first detected in the U.S. in clinically affected sheep in Texas and California in 1952, where it was coined "soremuzzle," prior to its positive identification as bluetongue virus.[13,14] The detection of BTV outside of Africa in combination with the significant animal

health consequences associated with these outbreaks led the World Organisation for Animal Health (Office International des Epizooties, OIE) to make bluetongue infection a listed disease in the 1960s.

Bluetongue Virus Today: Expansion and Epizootics

Today, BTV has been detected on all continents except Antarctica.[16] Its range is defined by the presence of competent vector species and is classically considered to exist between 35°S to 40°N.[17] However, numerous reports in recent years indicate that this canonical distribution no longer captures the true range of BTV, likely reflecting viral evolution, vector expansion, long-distance dispersion of vectors, and animal movement, among other factors.[1,18,19]

Several high-profile, economically devastating epizootics have occurred in the last 15 years, highlighting the ability of bluetongue virus to cause explosive outbreaks of disease with little warning. Perhaps most notable among these recent events was the BTV-8 epizootic that occurred in 2006 and 2007 in Northern Europe, representing remarkable expansion of bluetongue virus to 58°N.[20] Not only was BTV infection associated with disease in sheep, but illness was also noted in other ruminant species that rarely demonstrate signs of BTV infection, such as cattle and goats.[21,22] Moreover, transplacental infection and transmission of BTV – usually an phenomenon confined to the use of live attenuated vaccine strains at certain points of gestation – was a common occurrence during this epizootic.[23,24] Collectively, animal losses, production declines, and restrictions in trade resulted in a cost of over 150 million € in the initial years of the outbreak.[25,26]

Even in enzootic regions such as the U.S., outbreaks of orbiviral disease have occurred with relative frequency in the last two decades. In 2007, 2012, and 2015, BTV and epizootic hemorrhagic disease virus (EHDV) – a closely related orbivirus – caused significant disease in

domestic and wild ruminants across the U.S.[27–30] Numerous reports worldwide indicate that non-enzootic serotypes are increasingly being identified in otherwise BTV-enzootic regions, although whether these strains become persistently established remains to be seen. At least in the United States, incursive BTV serotype 3 appears to have become widespread across the country, with recurrent detections in many states in the last decade.[31–33]

Infection and Pathology

Bluetongue disease most commonly occurs in susceptible sheep breeds – generally considered to be those of European origin, which are widely produced throughout the world. The virus preferentially replicates in endothelial cells and mononuclear phagocytes, as well as lymphocytes.[34,35] After initial replication, virus is highly associated with red blood cells and platelets, resulting in a prolonged viremia.[34,36] Affected animals develop a range of signs secondary to systemic vasculitis: coronitis and laminitis, mucosal erosions, myonecrosis, subcutaneous and fascial edema, gastrointestinal ulceration, pulmonary edema, pericardial effusion, hemorrhage, ecchymoses and petechiae, and coagulopathy, among other features.[22,34,37–39] Animals may present with lameness, swelling of the face/ears and distal limbs, ulcerations on the lips and nose, mucopurulent nasal discharge, fever, and dyspnea. Morbidity and mortality rates vary markedly depending on an infected animal's species and breed, as well as its immune status, the viral strain, and various environmental factors. Reproductive sequelae may also occur in infected or recovering animals, with abortions and fetal hydranencephaly occurring in pregnant animals, and testicular degeneration and infertility arising in males.[40–42]

Disease tends to be subclinical or less explosive in areas where BTV is enzootic. Many ruminant species have been demonstrated to become infected with BTV, although disease is not necessarily a common occurrence. Cattle and goats generally remain subclinical for infection,

and cattle are considered to be a potential reservoir host for BTV. South American camelids are susceptible to severe bluetongue disease, as well as many wildlife species, including bighorn sheep, white-tailed deer, and pronghorn in North America.[43–48] BTV infection may result in acute death in white-tailed deer and pronghorn. Worldwide, studies have indicated that most large herbivores are susceptible to infection with BTV; dromedaries, water buffalo, bison, kudu, elk, antelope, and others all have demonstrated seropositivity to BTV.[2] Dogs and wild carnivores also are occasionally infected with bluetongue virus, either through consumption of infected meat or vaccine contamination with improperly inactivated fetal bovine serum.[49–51] The role that these species play in this BTV's epidemiology remains poorly understood.

Vector Distribution and Ecology

While BTV is occasionally transmitted horizontally and vertically in vertebrate hosts, the vast majority of BTV transmission occurs via the bite of an infected female midge of the genus *Culicoides*. Of ~1,400 species of *Culicoides* distributed worldwide, only approximately 30 species have been demonstrated to be biological vectors for BTV.[52–54] *Culicoides sonorensis* is the predominant vector in North America, with *C. insignis* playing a lesser role due to its geographic constraint to the southeastern portions of the United States.[17] *C. insignis* is the key BTV vector in Central and South America and appears to have an increasing range in the U.S.[55] In Africa and western Asia, *C. imicola* has been incriminated as the major biological vector of BTV, while *C. brevitarsis* and *C. wadai* are known to transmit the virus in central and east Asia, as well as Australia.[17,56] In Europe, the *C. obsoletus* complex – composed of several closely related species of *Culicoides* – is primarily responsible for BTV transmission.[25] Importantly, numerous other species of *Culicoides* may also be competent for various strains of BTV, but robust information on the distribution and competence of many of these various species is

lacking. Moreover, as climate change advances, the range of these vectors is expected to expand, as has been seen in North America and the Mediterranean.[55,57,58]

Culicoides midges also serve as biological vectors for several other viruses with significant animal or human health impacts, including orbiviruses such as epizootic hemorrhagic disease virus (EHDV), African horse sickness virus (AHSV), and equine encephalosis virus (EEV); orthobunyaviruses such as Schmallenberg virus, Akabane virus, and Oropouche virus; and rhabdoviruses including bovine ephemeral fever virus. The interactions that occur when these viruses co-infect a single midge remain poorly characterized, although various studies have demonstrated that midges can be infected with more than one strain of bluetongue virus and may subsequently transmit more than one virus during blood-feeding on a susceptible animal.[59] These potential interactions – both between co-infecting viruses and the vector's response to each virus – have widespread implications for the epidemiology, evolution, and ecology of *Culicoides*-borne viruses.

Viral Structure, Function, and Replication

When considering the evolution of BTV, it is informative to first understand the genetic composition of this virus. Bluetongue and other viruses in the family *Reoviridae* possesses a relatively unusual genome structure, carrying from 10-12 linear segments of double-stranded RNA (dsRNA) depending on the viral species. BTV itself contains ten segments of dsRNA, which range from 822 base pairs (segment 10) in length to 3954 base pairs (segment 1). Of the viruses belonging to family *Reoviridae*, only those within the genus *Orbivirus* are vector-borne. The BTV virion is non-enveloped. Structural studies have demonstrated that BTV is composed of a bi-layered capsid that surrounds ten segments of dsRNA.[60] The dsRNA segments in the viral core are associated with three key structural proteins: the RNA-dependent RNA polymerase

(VP1, encoded by segment 1), the viral capping protein (VP4, encoded by segment 4), and the RNA helicase (VP6, encoded by segment 9).[61] Viral entry is mediated by VP2 (segment 2) and VP5 (segment 6), the two outer capsid proteins. VP2 is the receptor-binding protein and enables clathrin-mediated endocytosis, while the pH-sensitive VP5 protein is responsible for membrane fusion in the late endosome that allows ejection of the BTV inner core particle into the cytoplasm.[62,63] The inner capsid, composed of VP7 (segment 7) and VP3 (segment 3), forms an icosahedral structure that is sensitive to the presence of magnesium and NTPs, which promote a shift in arrangement that allows for the release of viral mRNAs into the cellular milieu, beginning the process of viral protein synthesis and replication.[60,64] Single-stranded positive-sense RNAs function as both the template for genome replication (i.e., the synthesis of the complementary, negative-sense RNA strand), as well as the translation of viral proteins.[65] Non-structural proteins NS1 (segment 5) and NS2 (segment 8) play an important role during viral translation and assembly; NS1 forms microtubules and specifically enhances the translation of viral proteins, and NS2 is the key component of viral inclusion bodies (VIBs) that recruit viral genomic RNAs and proteins to facilitate viral particle assembly.[66–69] NS3 (segment 10) and a truncated version of this same protein – NS3a – are associated with viral egress from the cell. NS3a is translated from a slightly downstream start site from that of the NS3 protein and is the major viral egress protein produced in *Culicoides* cells.[65,70] Viral egress is non-lytic in *Culicoides* cells and lytic in mammalian cells, but the exact mechanism by which this occurs is not fully understood. It is likely that there is some degree of non-lytic viral budding that occurs early in infection in mammalian cells.[65] Only discovered relatively recently, NS4 is an interferon antagonist (segment 9).[71]

Single-stranded viral RNAs (ssRNA) are recruited to VIBs during the assembly process. As a multi-segmented virus, BTV reportedly uses a highly ordered process to ensure all ten segments are properly incorporated into each virion.[65] Once all ten ssRNAs are integrated in nascent virions, capsid assembly and reverse transcription may occur. BTV dsRNA replication, like that of related viruses, is conservative.[61,72] Conserved untranslated regions (UTRs) at the 3' and 5' end of each segment are essential for mediating sequential recruitment of ssRNAs.[73–76] The 3' UTR of segment 10 is especially instrumental in this process and triggers the proper secondary conformational structures of subsequent segments to allow proper interactions.[73] The smallest segments (segments 7-9) are recruited first, followed by segments 4-6, and finally segments 1-3.[60] Once viral cores are equipped with a complete set of genome segments, the nascent BTV particle is released from VIBs following NS2 phosphorylation, and acquires the VP2 and VP5 outer protein layer as it exits.[60,77]

Bluetongue Virus Evolution

While the field of viral evolution is a robust and ever-growing area of research, two main considerations are essential to discuss when specifically considering bluetongue virus. First, BTV's vector-borne nature plays an important role in its overall evolutionary trajectory. Second, BTV's segmented, RNA genome is a defining characteristic for its genetic diversification. While many features of BTV are well-characterized, there are gaps in our understanding of BTV evolution that are underscored by the recent incursions of BTV into new regions, and the introduction of novel serotypes into otherwise enzootic areas. These developments require an understanding of many contributing dynamics, including environmental conditions, ruminant and vector ecology, host community structure, immunity in the vertebrate and invertebrate host, anthropogenic factors such as management and preventive strategies, and viral evolution. Here,

we focus on the knowns and unknowns of BTV evolution – with the caveat that viral evolution is inextricably linked to numerous selection pressures and exogenous factors beyond the realm of this introduction.

Evolution of RNA Viruses: Underlying Concepts

Transcribed via an RNA dependent RNA polymerase, which – in contrast to DNA polymerase – does not possess proofreading ability, many RNA viruses demonstrate an inherently high mutation rate.[78–81] The rapid generation of many progeny viruses with mutations in their genomes is believed to be an important part of the RNA virus's evolutionary repertoire.[79,82,83] Replicating at very high rates, RNA viruses such as poliovirus, vesicular stomatitis virus, foot-and-mouth disease virus, and others generate massive populations of viral progeny that possess numerous low-frequency mutations.[84–87] RNA viruses are often described as approaching the point of extinction or lethality because of their extreme mutation rate.[88–91] However, RNA viruses are believed to preserve fitness by maintaining an optimal balance between rate of mutation and population size, allowing for rapid adaptation to new fitness landscapes.[79,82,92] This concept is captured by the terms "viral quasispecies" and "mutant swarm," which are used to characterize both the genetic diversity and the vast number of virions produced during infection. Quasispecies theory posits that high mutation rates and the generation of viral swarms are evolutionarily beneficial for ultimate phenotypic flexibility. The spectrum of mutant viruses is considered in many ways to be its own evolutionary entity: selection pressures are exerted on the entire viral ensemble, with complementation, interference, and recombination amongst viruses ultimately shaping the swarm's overall fitness.[79]

Several theories have been proposed to describe underlying mechanisms that may drive this phenomenon. Mutational robustness is one explanation for the presence of viral

quasispecies; while redundancy and gene duplication serve to reduce the effect of deleterious mutations in higher-complexity organisms, a single mutation in a viral genome may be lethal.[93] Viral swarms may serve this same function, providing a rescue mechanism for high mutation rates.[94,95] Others have proposed that quasispecies allow virus populations to occupy neutral or flat fitness landscapes.[96,97] In this framework, populations with high, but narrow, fitness peaks (i.e., populations of virus that are highly fit but also highly similar) are less capable of withstanding mutation, compared to broad, low peaks (i.e., populations of viruses that may be individually less fit, but are also more diverse).[95]

In contrast, some have argued that high mutation rates in RNA viruses, such as poliovirus, are the evolutionary byproduct or fitness trade-off for rapid viral replication speeds.[98] Most mutations are deleterious, so it stands to reason that an RNA polymerase capable of higher fidelity replication would eventually evolve; however, this has not been demonstrated to occur.[91,99,100] Using a mutant poliovirus strain with an anti-mutator phenotype (apparently conferred by a single mutation in its RNA polymerase), Fitzsimmons et al. demonstrated that the reduced fitness of this virus was directly related to its slower speed of replication.[98] Fitzsimmons et al. concluded that speedy replication – with lower rates of replication fidelity – may be an acceptable trade-off for poliovirus and other RNA viruses, as it is difficult "to be both fast and accurate." [98] Other work has suggested similar paradigms with different organisms.[101,102]

Arbovirus Evolution

Compared to non-vector transmitted viruses, arboviruses demonstrate relatively stable genomes with lower mutation rates than expected, particularly for RNA viruses.[103–105] This is suspected to occur due to increased purifying selection exerted by the rigors of maintaining fitness in two highly disparate host systems – vertebrate and invertebrate. Using experimental

systems, varying results have been found using alphaviruses and flaviviruses in both in vitro and in vivo systems that recapitulate arbovirus transmission cycles.[106–111] Studies with Venezuelan equine encephalitis virus (VEEV), an alphavirus, showed increases in viremia in either the insect or vertebrate host when virus was released from replication in the opposite host, compared to when the virus was passaged alternatingly.[109] Similar findings have been described for other alphaviruses (chikungunya virus) and flaviviruses such as West Nile virus (WNV), dengue virus, and others.[103,112–114] Studies have suggested that purifying selection is especially driven by the vertebrate host, although additional work also supports the fact that both the vertebrate and invertebrate host species plays an instrumental role in the overall evolution of these arboviruses.[103,112,115,116] The multi-vector, multi-vertebrate ecology and transmission cycles of many arboviruses, including bluetongue virus, warrant further investigation to better understand host-imposed evolutionary pressures.

Repeated bottlenecks occur during viral replication in the arthropod vector, driving successive contractions and expansions in viral populations in the process of overcoming infection barriers. In mosquitoes and *Culicoides*, multiple barriers to arboviral infection and dissemination exist, including the mesenteron infection barrier, the mesenteron escape barrier, the salivary gland infection barrier, and the salivary gland escape barrier.[117–119] While salivary gland infection and escape barriers are reported to not exist in *Culicoides* midges, a "dissemination barrier" is believed to occur in these vectors.[117]

Work with Zika virus, West Nile virus, and related arboviruses using barcoded viruses or virus clones have characterized the impact of bottlenecks on viral populations in insect hosts.[115,120–122] These studies have demonstrated that repeated bottlenecks shape viral populations during infection in the insect vector. Due to the small volume of blood that vectors ingest during

blood feeding, insects are only exposed to a relatively low number of viruses when taking an infectious blood meal. *Culicoides* midges have been shown to take a blood meal volume of approximately 0.1 – 1 μL.[123] Viral titer in the blood, therefore, plays an instrumental role in the probability of infection, with higher titers associated with greater likelihood of successful infection of the vector.[122] Forrester et al. used F_{ST} to demonstrate that mosquitoes orally infected with a high titer of VEEV did not have evidence of a significant bottleneck during midgut infection.[122] However, when a more biologically relevant dose was used (4.9 $\log_{10}$ pfu/ml) for oral infection, a very strong midgut infection bottleneck occurred, with only 1.9 (±2.6) virions estimated to have initiated midgut infection. Based on simple odds, it is expected that only high frequency variants would be likely to cross the midgut infection barrier in this circumstance, unless a significant fitness advantage was conferred by an otherwise low-frequency mutant. In contrast to the multiple bottlenecks evident during vector infection, a transmission bottleneck was not detected when VEEV-infected mosquitoes were fed back on mice.[122]

Not only do infection and escape barriers and virus titer play an important role in the occurrence of population bottlenecks, but other factors such as RNA interference (RNAi) – which is known to occur in *Culicoides* midges – are also likely to contribute to viral population divergence in the invertebrate host.[121,124–127]

Bluetongue Virus: Host-Switching and Intrahost Diversity

Preliminary work with bluetongue virus has demonstrated that some of the arboviral evolutionary features described above are similarly applicable to orbivirus evolution. Early on, various groups used electropherotype to characterize the genetic heterogeneity of bluetongue virus, but unfortunately these works are difficult to relate to our understanding of BTV evolution today due to relatively poor genomic resolution provided by these early methods. With the

advent of modern sequencing techniques, additional approaches to better understand BTV genetic diversification have become readily available. However, only a few studies have investigated how BTV's alternating host transmission cycle affects its evolution.

Bonneau et al. used *Culicoides sonorensis* midges and domestic ruminants to recapitulate the natural transmission cycle of BTV.[128] A plaque-purified field isolate of BTV was used to orally infect *C. sonorensis* midges, which then fed on sheep and cattle across three transmission cycles. BTV was then plaque-isolated from ruminant blood and pools of homogenized midges between vertebrate-invertebrate transmissions. Segment 2 and segment 10 from individual viral plaques were reverse-transcribed, amplified, and cloned into plasmids, prior to sequencing. This group found infrequent synonymous and non-synonymous mutations that arose in segments 2 and 10. Ultimately, Bonneau et al. concluded that the founder effect and quasispecies generation were important features in the evolution of a single BTV strain, as evidenced by mutants that arose and then disappeared during the course of transmission, as detected by sequencing segments 2 and 10 of individual plaques from insects or ruminants. As PCR amplification itself generates errors during transcription, it is difficult to determine whether some of these putative BTV variants were artefactual.[129,130] Moreover, the true extent of viral quasispecies present in these experiments may have been masked by replication deficiencies of certain mutants, making them non-detectable by plaque assay. Today, ultra-deep sequencing approaches provide a readily available technique to query the extent of BTV quasispecies occurrence while avoiding the caveats of earlier methods.

More recent efforts to characterize aspects of intrahost viral genetic diversity have used whole genome sequencing. Caporale et al. used different cell types to isolate a strain of BTV-8 from an experimentally infected sheep.[131] Using deep sequencing, this group found that virus

sequenced from whole blood had more high-frequency (>0.4%) single-nucleotide variants (SNVs) than when the virus was isolated onto KC cells (derived from *Culicoides sonorensis*) or BHK 21 cells.[132] However, KC cells generated the highest number of SNVs, while virus propagated on BHK 21 cells demonstrated a marked reduction in variants. Two synonymous variants that were high frequency in the virus sequenced directly from whole blood went to fixation when isolated on KC cells and BHK cells (segments 1 and 4). When additional sheep were directly inoculated with either BTV-8 from whole blood or the cell-culture isolated virus, those infected directly with BTV-8 from blood developed more severe disease, despite the blood having ~100-fold lower titer of BTV than propagated virus. Caporale et al. suggested that the discrepancy in disease phenotypes manifested in infected sheep may have been due to the number of low-frequency variants and quasispecies present, although numerous other factors could have contributed to the difference in disease phenotype observed in this case.

While other studies have suggested that propagation in cell culture or eggs results in viral attenuation of BTV secondary to purifying selection and a reduction in viral quasispecies, few studies have been performed to understand whether purifying selection occurs during BTV host-switching.[133,134] Virus isolation in non-native cell types such as BHK 21 cells or embryonated chicken eggs likely enforces a dramatic bottleneck, possibly leading to a Muller's Ratchet-like phenomenon, leading to virus attenuation.[87,135,136] However, these findings are difficult to relate to the overall evolution of BTV in its native hosts.

The impact of host-switching across all ten BTV segments – and whether each segment behaves similarly – is poorly characterized. Although direct experimental approaches to this question remain few, various phylogenetic-based studies have indicated that – consistent with other arboviruses – BTV has a low overall mutation rate across its genome segments. This

implies that some of the same mechanisms that drive slower rates of mutation in ssRNA arboviruses may be at play in BTV's evolution as well. Interestingly, when Carpi et al. analyzed the sequences of four segments across 290 BTV isolates, they found that BTV demonstrated lower substitution rates than many other vector-borne viruses (mean rates of ~$0.5–7 \times 10^{-4}$ nucleotide substitutions per site, per year).[137] Others have found similar substitution rates and evidence of strong purifying selection among bluetongue virus isolates from Europe and Australia.[138,139] This is suggestive of additional stringencies that may affect BTV's genome stability, such as increased replication fidelity or stableness exerted by its double-stranded composition.

Segmented Viruses and Reassortment

Building upon early electropherotype work, whole genome sequencing efforts over the last decade have provided increasingly strong evidence that reassortment may be the primary driver of BTV genetic diversification. Reassortment can occur when a cell is co-infected by more than one virus of the same species and is a characteristic feature of many segmented viruses.[140] Viruses with segmented genomes – including those in families *Orthomyxoviridae*, *Reoviridae*, *Picobirnaviridae*, and *Birnaviridae*, as well as order *Bunyavirales* – have frequently been demonstrated to reassort, both in nature and experimentally.[141–145]

Reassortment among segmented viruses has been linked to a number of significant downstream effects, including generation of highly pathogenic hemorrhagic fevers (e.g., Ngari orthobunyavirus) and influenza pandemics.[146,147] Moreover, analysis of influenza virus indicates that reassortment increases the likelihood of viral expansion into a new host.[148] Reassortment is a prominent feature among BTV field isolates, including those that seem to cause more severe disease.[149–151]

Previous Findings: Bluetongue Virus Reassortment

While the occurrence of reassortment has long been recognized among BTV both in North America and worldwide, a suite of studies in the 1980s sought to characterize reassortment between two enzootic North American strains in a variety of systems (in vitro, insect, and mammalian).[59,152–156] Using electropherotype shifts in plaque-isolated progeny viruses following experimental coinfections as an indicator of reassortment, these studies were able to establish several important points. First, they found that BTV-10 and BTV-17 were able to reassort extensively in Vero cells, and that when viruses did not have equal multiplicities of infection (MOI), the virus with a higher MOI contributed more segments to reassortant progeny.[154] Later, *C. sonorensis* midges, cattle, and sheep were co-infected with BTV strains to determine the frequency of reassortment in vivo.[59,152,155,156] Reassortant viruses arose in all cases, although *Culicoides* seemed to support more robust levels of reassortment. Finally, El Hussein et al. found that when *Culicoides* coinfections were staggered by various lengths of time, reassortant viruses could be isolated after an appropriate incubation period from midges that had been infected with the second virus up to five days after the primary virus was introduced.[153]

More recent in vitro work by Shaw et al. using BTV-1 and BTV-8 found that reassortment between these two viruses was highly flexible.[157] When mono-reassortant viruses were generated using reverse genetics, some segment combinations demonstrated fitness disadvantages compared to others, highlighting that segment-segment interactions, segment-protein interactions, and protein-protein interactions likely affect the overall viability of reassortant BTV viruses. While certain segments were detected more frequently in reassortant viruses, Shaw et al. ultimately determined that reassortment could involve any segment between BTV-1 and BTV-8.

Although prior studies provide an important starting point for investigating BTV reassortment, these experiments have several shortcomings. First, polyacrylamide gel electrophoresis (PAGE) and related methods provide limited resolution for detecting subtle differences in the genome sequences of each segment. Thus, early studies were unable to distinguish the parental origin of several segments in reassortant progeny viruses. Moreover, variations in fitness and replication kinetics between different reassortants makes accurate detection of reassortment based solely on plaque assays potentially biased.

Shaw et al.'s approach of generating mono-reassortants via reverse genetics is a vital initial step towards fully understanding the actual viability of various segment combinations, but with 10 segments of genomic dsRNA and 1,024 possible reassortment combinations between two strains of virus, BTV poses a logistical challenge for this type of work. Compared to influenza, with just 8 segments and 256 possible segment combinations between two viruses, the number of segments present among viruses in family *Reoviridae* adds another level of difficulty to characterizing reassortment in these viruses. Therefore, novel techniques for rapid and unbiased detection of reassortment among multi-segmented viruses are needed.

Factors Restricting Reassortment

While reassortment is known to be a key feature of segmented virus evolution, our understanding of the mechanisms, restrictions, and drivers of this phenomenon remain limited. It has been suggested that reassortment is akin to "viral sex" and may serve similar purposes in terms of its contribution to accelerate adaptive fitness.[158] In the context of Muller's Ratchet, reassortment may be remarkably beneficial, particularly in small populations.[158] The evolutionary origin of segmented viral genomes is incompletely understood, but beyond the potential gains from reassortment as a mechanism to introduce genetic variability in a

population, there are fitness benefits to segmentation itself, such as improved viral stability and more rapid genome replication.[159]

For successful reassortment to transpire, several key features must be in place. First, coinfection of a single cell must occur. Second, this coinfection must occur within a time frame that permits productive coinfection. For example, reassortment between influenza viruses can occur within the first ~3 hours of a cellular infection, but thereafter cells become refractory to infection with a second virus.[160] This may be due to a number of reasons, including viral-mediated destruction of receptors on the cell surface or host cell antiviral responses.[140] Some studies indicate that viruses in the family *Reoviridae* are relatively permissible to superinfection, with a prolonged window where cells may be productively infected with more than one virus.[161] Prior work in vitro and with *Culicoides* indicates that this may be an important feature of BTV coinfection, as well.[153,154]

Physical barriers within the cell may prevent productive reassortment; if the sites of viral replication are highly isolated, only limited interactions between different viruses may occur. The mechanism by which reassortment may occur during BTV coinfection is not well understood, particularly as BTV and related viruses generate highly sequestered replication factories within the cell. Whether a trafficking mechanism exists to shuttle viral segments between bluetongue VIBs is not known. A recent study with mammalian orthoreovirus demonstrated dynamic movement of viral factories within the host cell, which was mediated in part by microtubules.[162] It is not known whether a similar mechanism might facilitate segment movement and reassortment among bluetongue viruses.

Finally, incompatibility between certain genome segments or their downstream proteins may preclude the generation of reassortant viruses. For instance, in rotaviruses, mismatches

between the viral polymerase and capsid proteins appears to limit the spectrum of reassortant viruses that are viable.[163] Packaging signals, too, play an instrumental role in the likelihood of reassortment. Marshall et al. demonstrated that reassortment between engineered, near-identical influenza A viruses (differing by rare silent mutations in each segment) was highly efficient in an in vitro system, but when heterologous packaging signals (3' and 5' UTRs) were introduced on certain segments, reassortment was dramatically limited.[164,165] Similar restrictions in reassortment mediated by incompatible packaging signals have been described for viruses in *Bunyavirales*.[166,167] While 3' and 5' UTRs are quite conserved across BTV strains, additional packaging signals contained in the coding sequences may similarly restrict inter-strain reassortment.

As with single mutations, most instances of reassortment are expected to be deleterious.[140,168] Therefore, when reassortment does occur, subsequent mutations or reassortment events are likely to follow in the course of adaptation, leading to a variety of potential downstream consequences. Moreover, the specific stringencies that BTV's alternating-host transmission cycle imposes on reassortment remain unexplored.

Summary

Clearly, many questions regarding the factors that drive or constrain BTV genetic diversification remain. Instrumental work with other vector-borne and segmented viruses provides a compelling backdrop for further investigation of BTV. The increased application of whole genome sequencing and other novel sequencing platforms promises to build upon earlier work, setting the stage for improved understanding of bluetongue and related viruses.

This dissertation seeks to address key knowledge gaps surrounding bluetongue virus evolution as identified in previous sections. By applying recent advancements in sequencing

technologies and using a variety of experimental approaches (applied fieldwork, in vitro systems, and in vivo models), we aim to characterize the relative impact of host-switching, reassortment, and environmental conditions on the overall genetic diversification of bluetongue virus. The ultimate goal of this work is to apply a refined understanding of the factors that drive or constrain BTV evolution so as to facilitate improved predictive models and preventive strategies with the intent of mitigating the risk of future bluetongue disease outbreaks.

REFERENCES

1. Maclachlan NJ. Bluetongue: History, global epidemiology, and pathogenesis. *Prev Vet Med*. 2011;102(2):107-111. doi:10.1016/j.prevetmed.2011.04.005.

2. Coetzee P, Stokstad M, Venter EH, Myrmel M, Van Vuuren M. Bluetongue: a historical and epidemiological perspective with the emphasis on South Africa. *Virol J*. 2012;9:198. doi:10.1186/1743-422X-9-198.

3. Hutcheon D. Fever of epizootic cattarrh. *Rep Coll Vet Surg*. 1881;1880:12-15.

4. Hutcheon D. Marlarial cattarrhal fever of sheep. *Vet Res*. 1902;14:629-633.

5. Spreull J. Malarial catarrhal fever (bluetongue) of sheep in South Africa. *J Comp Pathol Ther*. 1905;18:321-337. doi:10.1016/S0368-1742(05)80073-6.

6. Theiler A. Bluetongue in sheep. *Ann Rep Dir Agric Transvaal, 1906*. 1904-1905:110-121.

7. Du Toit RM. The transmission of blue-tongue and horse-sickness by *Culicoides*. *Onderstepoort J Vet Sci Anim Ind*. 1944;19(2):7-16.

8. Theiler A. The inoculation of sheep against bluetongue and the results in practice. *Vet J*. 1908;64(12):600-607. doi:10.1016/S0372-5545(17)68234-8.

9. Neitz WO. Immunological studies on bluetongue in sheep. *Onderstepoort J Vet Anim Ind*. 1948;23:93-136.

10. Maan S, Maan NS, Belaganahalli MN, et al. Full-genome sequencing as a basis for molecular epidemiology studies of bluetongue virus in India. *PLoS One*. 2015;10(6). doi:10.1371/journal.pone.0131257.

11. Wright M. Serological and genetic characterisation of putative new serotypes of bluetongue virus and epizootic haemorrhagic disease virus isolated from an alpaca. Dissertation Thesis, North-West University Potchefstroom Campus. 2013.

12. Gambles RM. Bluetongue of sheep in Cyprus. *J Comp Path Ther*. 1949;59:176-190. doi:10.1016/S0368-1742(49)80018-X.

13. McKercher DG, McGowan B, Howarth JA SJ. A preliminary report on the isolation and identification of the bluetongue virus from sheep in California. *J Am Vet Med Assoc*. 1953;122(913):300-301.

14. Hardy W, Price D. Soremuzzle of sheep. *Am J Vet Med Assoc*. 1952;120:23-25.

15. Manso-Ribeiro J, Rosa-Azevedo J, Noronha F, Braco-Forte-Junior M, Vasco-Fernandez M. Fievre catarrhale du mouton (bluetongue). *Bull Off Int Epiz*. 1957;48:350-367.

16. Maclachlan NJ. Globlal implications of the recent emergence of bluetongue virus in Europe. *Vet Clin Food Anim*. 2010;26:163-171. doi:10.1016/J.CVFA.2009.10.012.

17. Tabachnick WJ. *Culicoides* and the global epidemiology of bluetongue virus infection. *Vet Ital*. 2004;40(3):145-150.

18. Clavijo A, Munroe F, Zhou EM, Booth TF, Roblesky K. Incursion of bluetongue virus into the Okanagan Valley, British Columbia. *Can Vet J*. 2000;41:312-314.

19. Lundervold M, Milner-Gulland EJ, O'Callaghan CJ, Hamblin C. First evidence of bluetongue virus in Kazakhstan. *Vet Microbiol*. 2003;92(3):281-287. doi:10.1016/S0378-1135(02)00365-6.

20. Wilson AJ, Mellor PS. Bluetongue in Europe: past, present and future. *Philos Trans R Soc Lond B Biol Sci*. 2009;364(1530):2669-2681. doi:10.1098/rstb.2009.0091.

21. Toussaint JF, Sailleau C, Mast J, et al. Bluetongue in Belgium, 2006. *Emerg Infect Dis*. 2007;13(4):614-616. doi:10.3201/eid1304.061136.

22. Darpel K, Batten C, Veronesi E, et al. Clinical signs and pathology shown by British sheep and cattle infected with bluetongue virus serotype 8 derived from the 2006 outbreak in northern Europe. *Vet Rec*. 2007;161:253-261. doi:10.1136/vr.161.8.253.

23. Belbis G, Bréard E, Cordonnier N, et al. Evidence of transplacental transmission of bluetongue virus serotype 8 in goats. *Vet Microbiol*. 2013;166(3-4):394-404. doi:10.1016/j.vetmic.2013.06.020.

24. Desmecht D, Bergh RV, Sartelet A, et al. Evidence for transplacental transmission of the current wild-type strain of bluetongue virus serotype 8 in cattle. *Vet Rec*. 2008;163:50-52. doi:10.1136/vr.163.2.50.

25. Wilson A, Mellor P. Bluetongue in Europe: vectors, epidemiology and climate change. *Parasitol Res*. 2009;103(Suppl 1):S69-S77. doi:10.1007/s00436-008-1314-8.

26. Hoogendam K. International study on the economic consequences of outbreaks of bluetongue serotype 8 in north-western Europe Leeuwarden*: Van Hall Institute*; 2007.

27. Miller MM, Brown J, Cornish T, et al. Investigation of a bluetongue disease epizootic caused by bluetongue virus serotype 17 in sheep in Wyoming. *J Am Vet Med Assoc*. 2010;237(8):955-959. doi:10.2460/javma.237.8.955.

28. Stevens G, McCluskey B, King A, O'Hearn E, Mayr G. Review of the 2012 epizootic hemorrhagic disease outbreak in domestic ruminants in the United States. *PLoS One*. 2015;10(8). doi:10.1371/journal.pone.0133359.

29. Ruder MG, Lysyk TJ, Stallknecht DE, et al. Transmission and epidemiology of bluetongue and epizootic hemorrhagic disease in North America: current perspectives, research gaps, and future directions. *Vector-Borne Zoonot*. 2015;15(6):348-363. doi:10.1089/vbz.2014.1703.

30. Philips R. Fish and Game confirms outbreak of bluetongue disease in whitetails. Idaho Department of Fish and Game. 2015. https://idfg.idaho.gov/press/fish-and-game-confirms-outbreak-bluetongue-disease-whitetails.

31. Brenner J, Oura C, Asis I, et al. Multiple serotypes of bluetongue virus in sheep and cattle, Israel. *Emerg Infect Dis*. 2010;16(12):2003-2004. doi:10.3201/eid1612.100239.

32. White JR, Williams DT, Wang J, et al. Identification and genomic characterization of the first isolate of bluetongue virus serotype 5 detected in Australia. *Vet Med Sci*. 2019;5(2):129-145. doi:10.1002/vms3.156.

33. Schirtzinger EE, Jasperson DC, Ostlund EN, Johnson DJ, Wilson WC. Recent US bluetongue virus serotype 3 isolates found outside of Florida indicate evidence of reassortment with co-circulating endemic serotypes. *J Gen Virol*. 2018;99(2):157-168. doi:10.1099/jgv.0.000965.

34. Maclachlan NJ, Drew CP, Darpel KE, Worwa G. The pathology and pathogenesis of bluetongue. *J Comp Pathol*. 2009;141(1):1-16. doi:10.1016/j.jcpa.2009.04.003.

35. Barratt-Boyes SM, Rossitto PV, Stott JL, Maclachlan NJ. Flow cytometric analysis of in vitro bluetongue virus infection of bovine blood mononuclear cells. *J Gen Virol*. 1992;73:1953-1960.

36. Bonneau K, DeMaula C, Mullens B, MacLachlan N. Duration of viraemia infectious to *Culicoides sonorensis* in bluetongue virus-infected cattle and sheep. *Vet Microbiol*. 2002;88:115-125. doi:10.1016/S0378-1135(02)00106-2.

37. Pierce CM, Balasuriya UB, MacLachlan NJ. Phylogenetic analysis of the S10 gene of field and laboratory strains of bluetongue virus from the United States. *Virus Res*. 1998;55(1):15-27. doi:10.1016/S0168-1702(98)00024-0.

38. Maclachlan NJ, Mayo CE, Daniels PW, Savini G, Zientara S, Gibbs EPJ. Bluetongue. *Rev Sci Tech*. 2015;34(2):329-340. doi:doi.org/10.20506/rst.34.2.2360.

39. Schwartz-Cornil I, Mertens PPC, Contreras V, et al. Bluetongue virus: virology, pathogenesis and immunity. *Vet Res*. 2008;39(46). doi:10.1051/vetres:2008023.

40. Puggioni G, Pintus D, Melzi E, et al. Testicular degeneration and infertility following arbovirus infection. *J Virol*. 2018;92(19). doi:10.1128/JVI.01131-18.

41. MacLachlan N, Conley A., Kennedy P. Bluetongue and equine viral arteritis viruses as models of virus-induced fetal injury and abortion. *Anim Reprod Sci*. 2000;60-61:643-651. doi:10.1016/S0378-4320(00)00105-6.

42. Schultz G, Delay PD. Losses in newborn lambs associated with bluetongue vaccination of pregnancy ewes. *J Am Vet Med Assoc*. 1955;127(942):224-226.

43. Ortega J, Crossley B, Dechant JE, Drew CP, MacLachlan NJ. Fatal bluetongue virus infection in an alpaca (*Vicugna pacos*) in California. *J Vet Diagn Invest*. 2010;22:134-136. doi:10.1177/104063871002200129.

44. Meyer G, Lacroux C, Léger S, et al. Lethal bluetongue virus serotype 1 infection in llamas. *Emerg Infect Dis*. 2009;15(4):608-610. doi:10.3201/eid1504.081514.

45. Robinson RM, Hailey TL, Livingston CW, Thomas JW. Bluetongue in the desert bighorn sheep. *J Wildlife Manage*. 1967;31(1):165. doi:10.2307/3798372.

46. Noon TH, Wesche SL, Cagle D, et al. Hemorrhagic disease in bighorn sheep in Arizona. *J Wildlife Dis*. 2002;38(1):172-176.

47. Vosdingh RA, Trainer D, Easterday BC. Experimental bluetongue disease in white-tailed deer. *Can J Comp Med Vet Sci*. 1968;32:382-387.

48. Hoff GL, Trainer DO. Bluetongue virus in pronghorn antelope. *Am J Vet Res*. 1972;33(5):1013-1016.

49. Gaudreault NN, Jasperson DC, Dubovi EJ, Johnson DJ, Ostlund EN, Wilson WC. Whole genome sequence analysis of circulating bluetongue virus serotype 11 strains from the United States including two domestic canine isolates. *J Vet Diagn Invest*. 2015;27(4):442-448. doi:10.1177/1040638715585156.

50. Evermann JF, McKeiman AJ, Wilbur LA, et al. Canine fatalities associated with the use of a modified live vaccine administered during late stages of pregnancy. *J Vet Diagn Invest*. 1994;6(3):353-357. doi:10.1177/104063879400600312.

51. Jauniaux TP, De Clercq KE, Cassart DE, et al. Bluetongue in Eurasian lynx. *Emerg Infect Dis*. 2008;14(9):1496-1498. doi:10.3201/eid1409.080434.

52. Foxi C, Delrio G, Falchi G, Marche MG, Satta G, Ruiu L. Role of different *Culicoides* vectors (Diptera: Ceratopogonidae) in bluetongue virus transmission and overwintering in Sardinia (Italy). *Parasit Vectors*. 2016;9(1):440. doi:10.1186/s13071-016-1733-9.

53. Borkent A. World Species of Biting Midges (Diptera: Ceratopogonidae); 2016. https://www.inhs.illinois.edu/files/4514/6410/0252/CeratopogonidaeCatalog.pdf.

54. Meiswinkel R, Gomulski LM, Delécolle J-C, Goffredo M, Gasperi G. The taxonomy of *Culicoides* vector complexes-unfinished business. *Vet Ital*. 2004;40(3):151-159.

55. Vigil SL, Ruder MG, Shaw D, et al. Apparent range expansion of *Culicoides* (Hoffmania) *insignis* (Diptera: Ceratopogonidae) in the southeastern United States. *J Med Entomol*. 2018;55(4):1043-1046. doi:10.1093/jme/tjy036.

56. Venter GJ, Paweska JT, Van Dijk AA, Mellor PS, Tabachnick WJ. Vector competence of *Culicoides bolitinos* and *C. imicola* for South African bluetongue virus serotypes 1, 3, and 4. *Med Vet Entomol*. 1998;12(4):378-385. doi:10.1046/j.1365-2915.1998.00116.x.

57. Guichard S, Guis H, Tran A, Garros C, Balenghien T, Kriticos DJ. Worldwide niche and future potential distribution of *Culicoides imicola*, a major vector of bluetongue and African horse sickness viruses. *PLoS One*. 2014;9(11). doi:10.1371/journal.pone.0112491.

58. Jacquet S, Huber K, Pagès N, et al. Range expansion of the bluetongue vector, *Culicoides imicola*, in continental France likely due to rare wind-transport events. *Sci Rep*. 2016;6:27247. doi:10.1038/srep27247.

59. Samal BK, El-Hussein A, Holbrook FR, Beaty BJ, Ramig RF. Mixed infection of *Culicoides variipennis* with bluetongue virus serotypes 10 and 17: evidence for high frequency reassortment in the vector. *J Gen Virol*. 1987;68:2319-2329.

60. Roy P, Jardetsky T, Kuhn R, Lamb R. Bluetongue virus structure and assembly. *Curr Opin Virol*. 2017;24:115-123. doi:10.1016/j.coviro.2017.05.003.

61. Roy P. Bluetongue virus: dissection of the polymerase complex. *J Gen Virol*. 2008;89(8):1789-1804. doi:10.1099/vir.0.2008/002089-0.

62. Forzan M, Marsh M, Roy P. Bluetongue virus entry into cells. *J Virol*. 2007;81(9):4819-4827. doi:10.1128/JVI.02284-06.

63. Zhang X, Patel A, Celma CC, Yu X, Roy P, Zhou ZH. Atomic model of a nonenveloped virus reveals pH sensors for a coordinated process of cell entry. *Nat Struct Mol Biol*. 2016;23(1):74-80. doi:10.1038/nsmb.3134.

64. Kar AK, Iwatani N, Roy P. Assembly and intracellular localization of the bluetongue virus core protein VP3. *J Virol*. 2005;79(17):11487-11495. doi:10.1128/JVI.79.17.11487-11495.2005.

65. Patel A, Roy P. The molecular biology of bluetongue virus replication. *Virus Res*. 2014;182:5-20. doi:10.1016/j.virusres.2013.12.017.

66. Kerviel A, Ge P, Lai M, et al. Atomic structure of the translation regulatory protein NS1 of bluetongue virus. *Nat Microbiol*. 2019;4:837-845. doi:10.1038/s41564-019-0369-x.

67. Boyce M, Celma CCP, Roy P. Bluetongue virus non-structural protein 1 is a positive regulator of viral protein synthesis. *Virol J*. 2012;9(178). doi:10.1186/1743-422X-9-178.

68. Kar A, Bhattacharya B, Roy P. Bluetongue virus RNA binding protein NS2 is a modulator of viral replication and assembly. *BMC Mol Biol*. 2007;8(1):4. doi:10.1186/1471-2199-8-4.

69. Lymperopoulos K, Noad R, Tosi S, Nethisinghe S, Brierley I, Roy P. Specific binding of bluetongue virus NS2 to different viral plus-strand RNAs. *Virology*. 2006;353:17-26. doi:10.1016/j.virol.2006.04.022.

70. Han Z, Harty RN. The NS3 protein of bluetongue virus exhibits viroporin-like properties. *J Biol Chem*. 2004;279(41):43092-43097. doi:10.1074/jbc.M403663200.

71. Ratinier M, Shaw AE, Barry G, et al. Bluetongue virus NS4 protein is an interferon antagonist and a determinant of virus virulence. *J Virol*. 2016;90(11):5427-5439. doi:10.1128/JVI.00422-16.

72. Silversteint SC, Schonberg M, Levin DH, Acs G. The Reovirus replicative cycle: conservation of parental RNA and protein. *Proc Natl Acad Sci*. 1970;67(1):275-281.

73. Sung PY, Roy P. Sequential packaging of RNA genomic segments during the assembly of bluetongue virus. *Nucleic Acids Res*. 2014;42(22):13824-13838. doi:10.1093/nar/gku1171.

74. Fajardo T, Sung PY, Roy P. Disruption of specific RNA-RNA interactions in a double-stranded RNA virus inhibits genome packaging and virus infectivity. *PLoS Pathog*. 2015;11(12):e1005321. doi:10.1371/journal.ppat.1005321.

75. Boyce M, Mccrae MA, Boyce CM. Rapid mapping of functional *cis*-acting RNA elements by recovery of virus from a degenerate RNA population: application to genome segment 10 of bluetongue virus. *J Gen Virol.* 2015;96:3072-3082. doi:10.1099/jgv.0.000259.

76. Boyce M, McCrae MA, Boyce P, Kim JT. Inter-segment complementarity in orbiviruses: a driver for co-ordinated genome packaging in the *Reoviridae*? *J Gen Virol*. 2016;97:1145-1157. doi:10.1099/jgv.0.000400.

77. Mohl BP, Roy P. Cellular casein kinase 2 and protein phosphatase 2A modulate replication site assembly of bluetongue virus. *J Biol Chem*. 2016;291(28):14566-14574. doi:10.1074/jbc.M116.714766.

78. Steinhauer DA, Domingo E, Holland JJ. Lack of evidence for proofreading mechanisms associated with an RNA virus polymerase. *Gene*. 1992;122(2):281-288. doi:10.1016/0378-1119(92)90216-C.

79. Andino R, Domingo E. Viral quasispecies. *Virology*. 2015;479-480:46-51. doi:10.1016/j.virol.2015.03.022.

80. Holland J, Spindler K, Horodyski F, Grabau E, Nichol S, Vandepol S. Rapid evolution of RNA genomes. *Science*. 1982;215(4540):1577-1585.

81. Drake J, Holland J, Brault AC, Powers AM, Tripet F, Weaver SC. Mutation rates among RNA viruses. *Proc Natl Acad Sci.* 2008;96(24):13910-13913. doi:10.1073/pnas.96.24.13910.

82. Lauring AS, Andino R. Quasispecies theory and the behavior of RNA viruses. *PLoS Pathog*. 2010;6(7). doi:10.1371/journal.ppat.1001005.

83. Dow N, Chernick A, Orsel K, Van Marle G, Van Der Meer F. Genetic variability of bovine viral diarrhea virus and evidence for a possible genetic bottleneck during vertical transmission in persistently infected cattle. *PLoS ONE*. 2015;10(7). doi:10.1371/journal.pone.0131972.

84. Ward CD, Flanegan JB. Determination of the poliovirus RNA polymerase error frequency at eight sites in the viral genome. *J Virol*. 1992;66(6):3784-3793.

85. Elena SF, Moya A. Rate of deleterious mutation and the distribution of its effects on fitness in vesicular stomatitis virus. *J Evol Biol*. 1999;12(6):1078-1088. doi:10.1046/j.1420-9101.1999.00110.x.

86. Elena SF, Gonzhlez-Candelas F, Novella IS, et al. Evolution of fitness in experimental populations of vesicular stomatitis virus. *Genetics*. 1996;142:673-679.

87. Escarmís C, Dávila M, Charpentier N, Bracho A, Moya A, Domingo E. Genetic lesions associated with Muller's Ratchet in an RNA virus. *J Mol Biol*. 1996;264(2):255-267. doi:10.1006/jmbi.1996.0639.

88. Domingo E. Viruses at the edge of adaptation. *Virology*. 2000;270(2):251-253. doi:10.1006/viro.2000.0320.

89. Sanjuán R, Nebot MR, Chirico N, Mansky LM, Belshaw R. Viral mutation rates. *J Virol*. 2010;84(19):9733-9748. doi:10.1128/JVI.00694-10.

90. Peck KM, Lauring AS. Complexities of viral mutation rates. *J Virol*. 2018;92(14). doi:10.1128/JVI.

91. Gerrish PJ, Colato A, Perelson AS, Sniegowski PD. Complete genetic linkage can subvert natural selection. *Proc Natl Acad Sci*. 2007; 104(5):6266-6271. doi/10.1073/pnas.0607280104.

92. Martin V, Domingo E. Influence of the mutant spectrum in viral evolution: focused selection of antigenic variants in a reconstructed viral quasispecies. *Mol Biol Evol*. 2008;25(8):1544-1554. doi:10.1093/molbev/msn099.

93. Krakauer DC, Plotkin JB. Redundancy, antiredundancy, and the robustness of genomes. *Proc Natl Acad Sci*. 2002;99(3):1405-1409. doi10.1073pnas.032668599

94. Elena SF, Sanjuán R. Adaptive value of high mutation rates of RNA viruses: separating causes from consequences. *J Virol*. 2005;79(18):11555-11558. doi:10.1128/JVI.79.18.11555-11558.2005.

95. Lauring AS, Frydman J, Andino R. The role of mutational robustness in RNA virus evolution. *Nat Rev Microbiol*. 2013;11(5):327-336. doi:10.1038/nrmicro3003.

96. Wilke C. Adaptive evolution on neutral networks. *Bull Math Biol*. 2001;63(4):715-730. doi:10.1006/bulm.2001.0244.

97. Schuster P, Swetina J. Stationary mutant distributions and evolutionary optimization. *Bull Math Biol*. 1988;50(6):635-660. doi:10.1007/BF02460094.

98. Fitzsimmons WJ, Woods RJ, McCrone JT, et al. A speed–fidelity trade-off determines the mutation rate and virulence of an RNA virus. *PLOS Biol*. 2018;16(6). doi:10.1371/journal.pbio.2006459.

99. Acevedo A, Brodsky L, Andino R. Mutational and fitness landscapes of an RNA virus revealed through population sequencing. *Nature*. 2014;505(7485):686-690. doi:10.1038/nature12861.

100. Visher E, Whitefield SE, McCrone JT, Fitzsimmons W, Lauring AS. The mutational robustness of influenza A virus. *PLOS Pathog*. 2016;12(8). doi:10.1371/journal.ppat.1005856.

101. Dulin D, Vilfan ID, Berghuis BA, et al. Elongation-competent pauses govern the fidelity of a viral RNA-dependent RNA polymerase. *Cell Rep*. 2015;10(6):983-992. doi:10.1016/j.celrep.2015.01.031.

102. Banerjee K, Kolomeisky AB, Igoshin OA. Elucidating interplay of speed and accuracy in biological error correction. *Proc Natl Acad Sci*. 2017;114(20):5183-5188. doi:10.1073/PNAS.1614838114.

103. Jerzak G, Bernard KA, Kramer LD, Ebel GD. Genetic variation in West Nile virus from naturally infected mosquitoes and birds suggests quasispecies structure and strong purifying selection. *J Gen Virol*. 2005;86(8):2175-2183. doi:10.1099/vir.0.81015-0.

104. Jenkins GM, Rambaut A, Pybus OG, Holmes EC. Rates of molecular evolution in RNA viruses: a quantitative phylogenetic analysis. *J Mol Evol*. 2002;54:156-165. doi:10.1007/s00239-001-0064-3.

105. Holmes EC, Twiddy SS. The origin, emergence and evolutionary genetics of dengue virus. *Infect Genet Evol*. 2003;3(1):19-28. doi:10.1016/S1567-1348(03)00004-2.

106. Vasilakis N, Deardorff ER, Kenney JL, Rossi SL, Hanley KA, Weaver SC. Mosquitoes put the brake on arbovirus evolution: experimental evolution reveals slower mutation accumulation in mosquito than vertebrate cells. *PLoS Pathog*. 2009;5(6). doi:10.1371/journal.ppat.1000467.

107. Greene IP, Wang E, Deardorff ER, Milleron R, Domingo E, Weaver SC. Effect of alternating passage on adaptation of Sindbis virus to vertebrate and invertebrate cells. *J Virol*. 2005;79(22):14253-14260. doi:10.1128/JVI.79.22.14253-14260.2005.

108. Weaver SC, Brault AC, Kang W, Holland JJ. Genetic and fitness changes accompanying adaptation of an arbovirus to vertebrate and invertebrate cells. *J Virol*. 1999;73(5):4316-4326.

109. Coffey LL, Vasilakis N, Brault AC, Powers AM, Tripet F, Weaver SC. Arbovirus evolution in vivo is constrained by host alternation. *Proc Nat Acad Sci*. 2008;105(19):6970-6975. doi10.1073pnas.0712130105.

110. Chen WJ, Wu HR, Chiou SS. E/NS1 Modifications of dengue 2 virus after serial passages in mammalian and/or mosquito cells. *Intervirology*. 2003;46:289-295. doi:10.1159/000073208.

111. Ciota AT, Lovelace AO, Ngo KA, et al. Cell-specific adaptation of two flaviviruses following serial passage in mosquito cell culture. *Virology*. 2007;357(2):165-174. doi:10.1016/j.virol.2006.08.005.

112. Deardorff ER, Fitzpatrick KA, Jerzak GVS, Shi PY, Kramer LD, Ebel GD. West Nile virus experimental evolution in vivo and the trade-off hypothesis. *PLoS Pathog*. 2011;7(11):e1002335. doi:10.1371/journal.ppat.1002335.

113. Coffey LL, Vignuzzi M. Host alternation of chikungunya virus increases fitness while restricting population diversity and adaptability to novel selective pressures. *J Virol*. 2011;85(2):1025-1035. doi:10.1128/jvi.01918-10.

114. Lequime S, Fontaine A, Ar Gouilh M, Moltini-Conclois I, Lambrechts L. Genetic drift, purifying selection and vector genotype shape dengue virus intra-host genetic diversity in mosquitoes. *PLoS Genet*. 2016;12(6):e1006111. doi:10.1371/journal.pgen.1006111.

115. Grubaugh ND, Weger-Lucarelli J, Murrieta RA, et al. Genetic drift during systemic arbovirus infection of mosquito vectors leads to decreased relative fitness during host switching. *Cell Host Microbe*. 2016;19(4):481-492. doi:10.1016/j.chom.2016.03.002.

116. Grubaugh ND, Ebel GD. Dynamics of West Nile virus evolution in mosquito vectors. *Curr Opin Virol*. 2016;21:132-138. doi:10.1016/j.coviro.2016.09.007.

117. Fu H, Leake CJ, Mertens PPC, Mellor PS. The barriers to bluetongue virus infection, dissemination and transmission in the vector, *Culicoides variipennis* (Diptera: Ceratopogonidae). *Arch Virol*. 1999;144:747-761.

118. Agarwal A, Parida M, Dash PK. Impact of transmission cycles and vector competence on global expansion and emergence of arboviruses. *Rev Med Virol*. 2017;27(5):e1941. doi:10.1002/rmv.1941.

119. Jennings DM, Mellor PS. Variation in the responses of *Culicoides variipennis* (Diptera, Ceratopogonidae) to oral infection with bluetongue virus. *Arch Virol*. 1987;95(3-4):177-182.

120. Weger-Lucarelli J, Garcia SM, Rückert C, et al. Using barcoded Zika virus to assess virus population structure in vitro and in *Aedes aegypti* mosquitoes. *Virology*. 2018;521:138-148. doi:10.1016/j.virol.2018.06.004.

121. Grubaugh ND, Rückert C, Armstrong PM, et al. Transmission bottlenecks and RNAi collectively influence tick-borne flavivirus evolution. *Virus Evol*. 2016;2(2):vew033. doi:10.1093/ve/vew033.

122. Forrester NL, Guerbois M, Seymour RL, Spratt H, Weaver SC. Vector-borne transmission imposes a severe bottleneck on an RNA virus population. *PLoS Pathog*. 2012;8(9):e1002897. doi:10.1371/journal.ppat.1002897.

123. Leprince D, Higgings J, Church G, Issel C, Mcmanus J, Foil L. Body size of *Culicoides variipennis* (Diptera: Ceratopogonidae) in relation to bloodmeal size estimates and the ingestion of *Onchocerca cervicalis* (Nematoda: Filarioidea) microfiliariae. *J Am Mosq Control Assoc*. 1989;5:100-103.

124. Mills MK, Nayduch D, Michel K. Inducing RNA interference in the arbovirus vector, *Culicoides sonorensis*. *Insect Mol Biol*. 2015;24(1):105-114. doi:10.1111/imb.12139.

125. Schnettler E, Ratinier M, Watson M, et al. RNA interference targets arbovirus replication in *Culicoides* cells. *J Virol*. 2013;87(5):2441-2454. doi:10.1128/jvi.02848-12.

126. Brackney DE, Beane JE, Ebel GD. RNAi targeting of West Nile virus in mosquito midguts promotes virus diversification. *PLoS Pathog*. 2009;5(7). doi:10.1371/journal.ppat.1000502.

127. Olson KE, Blair CD. Arbovirus–mosquito interactions: RNAi pathway. *Curr Opin Virol*. 2015;15:119-126. doi:10.1016/j.coviro.2015.10.001.

128. Bonneau KR, Mullens BA, Maclachlan NJ. Occurrence of genetic drift and founder effect during quasispecies evolution of the VP2 and NS3/NS3A genes of bluetongue virus upon passage between sheep, cattle, and *Culicoides sonorensis*. *J Virol*. 2001;75(17):8298-8305. doi:10.1128/jvi.75.17.8298-8305.2001.

129. Pienaar E, Theron M, Nelson M, Viljoen HJ. A quantitative model of error accumulation during PCR amplification. *Comput Biol Chem*. 2006;30(2):102-111. doi:10.1016/j.compbiolchem.2005.11.002.

130. Orton RJ, Wright CF, Morelli MJ, et al. Distinguishing low frequency mutations from RT-PCR and sequence errors in viral deep sequencing data. *BMC Genomics*. 2015;16(1):229. doi:10.1186/s12864-015-1456-x.

131. Caporale M, Gialleonorado L Di, Janowicz A, et al. Virus and host factors affecting the clinical outcome of bluetongue virus infection. *J Virol*. 2014;88(18); 10399-10411. doi:10.1128/JVI.01641-14.

132. Nayduch D, Cohnstaedt LW, Saski C, et al. Studying *Culicoides* vectors of BTV in the post-genomic era: resources, bottlenecks to progress and future directions. *Virus Res*. 2014;182:43-49. doi:10.1016/j.virusres.2013.12.009.

133. Gould AR, Eaton BT. The amino acid sequence of the outer coat protein VP2 of neutralizing monoclonal antibody-resistant, virulent and attenuated bluetongue viruses. *Virus Res*. 1990;17:161-172.

134. Lean FZX, Neave MJ, White JR, et al. Attenuation of bluetongue virus (BTV) in an in ovo model is related to the changes of viral genetic diversity of cell-culture passaged BTV. *Viruses*. 2019;11(481). doi:10.3390/v11050481.

135. Escarmís C, Dávila M, Domingo E. Multiple molecular pathways for fitness recovery of an RNA virus debilitated by operation of Muller's ratchet. *J Mol Biol*. 1999;285(2):495-505. doi:10.1006/JMBI.1998.2366.

136. Muller HJ. The relation of recombination to mutational advance. *Mutat Res*. 1964;1:2-9. doi:10.1016/0027-5107(64)90047-8.

137. Carpi G, Holmes EC, Kitchen A. The evolutionary dynamics of bluetongue virus. *J Mol Evol*. 2010;70:583-592. doi:10.1007/s00239-010-9354-y.

138. Boyle DB, Amos-Ritchie R, Broz I, et al. Evolution of bluetongue virus serotype 1 in northern Australia over 30 years. *J Virol*. 2014;88(24):13981-13989. doi:10.1128/JVI.02055-14.

139. Nomikou K, Hughes J, Wash R, et al. Widespread reassortment shapes the evolution and epidemiology of bluetongue virus following European invasion. *PLoS Pathog*. 2015;11(8). doi:10.1371/journal.ppat.1005056.

140. Lowen AC. It's in the mix: reassortment of segmented viral genomes. *PLOS Pathog*. 2018;14(9). doi:10.1371/journal.ppat.1007200.

141. Briese T, Calisher CH, Higgs S. Viruses of the family *Bunyaviridae*: are all available isolates reassortants? *Virology*. 2013;446:207-216. doi:10.1016/j.virol.2013.07.030.

142. Conceição-Neto N, Mesquita JR, Zeller M, et al. Reassortment among picobirnaviruses found in wolves. *Arch Virol*. 2016;161(10):2859-2862. doi:10.1007/s00705-016-2987-4.

143. Steel J, Lowen AC. Influenza A virus reassortment. *Curr Top Microbiol Immunol*. 2014;385:377-401. doi:10.1007/82_2014_395.

144. Campbell E, Wells J, Gray A, Broadbent A. Characterising *Birnaviridae* replication and reassortment in vitro: virus factories derived from distinct input viruses form in the cytoplasm of co-infected cells and coalesce over time. *Access Microbiol*. 2019;1. doi:10.1099/acmi.ac2019.po0147.

145. Komoto S, Tacharoenmuang R, Guntapong R, et al. Reassortment of human and animal rotavirus gene segments in emerging DS-1-like G1P[8] rotavirus strains. *PLoS One*. 2016;11(2). doi:10.1371/journal.pone.0148416.

146. Gerrard SR, Li L, Barrett AD, Nichol ST. Ngari virus is a Bunyamwera virus reassortant that can be associated with large outbreaks of hemorrhagic fever in Africa. *J Virol*. 2004;78(16):8922-8926. doi:10.1128/JVI.78.16.8922–8926.2004.

147. Taubenberger JK, Kash JC. Influenza virus evolution, host adaptation, and pandemic formation. *Cell Host Microbe*. 2010;7(6):440-451. doi:10.1016/j.chom.2010.05.009.

148. Ma EJ, Hill NJ, Zabilansky J, Yuan K, Runstadler JA, Delong EF. Reticulate evolution is favored in influenza niche switching. *Proc Nat Acad Sci*. 2016;113(19):5335-5339. doi:10.1073/pnas.1522921113.

149. Shafiq M, Minakshi P, Bhateja A, Ranjan K, Prasad G. Evidence of genetic reassortment between Indian isolate of bluetongue virus serotype 21 (BTV-21) and bluetongue virus serotype 16 (BTV-16). *Virus Res*. 2013;173(2):336-343. doi:10.1016/j.virusres.2013.01.009.

150. Batten CA, Maan S, Shaw AE, Maan NS, Mertens PPC. A European field strain of bluetongue virus derived from two parental vaccine strains by genome segment reassortment. *Virus Res*. 2008;137(1):56-63. doi:10.1016/ j.virusres.2008.05.016.

151. Youssef L, Nomikou K, Mounir K, Mohammed B, Ouafaa F, Mehdi E. Bluetongue in Morocco 2004 to 2015: an overview. *J Infect Dis Epidemiol*. 2017;3(1). doi:10.23937/2474-3658/1510023.

152. Samal SK, Livingston CW, Mcconnell S, Ramig1 RF. Analysis of mixed infection of sheep with bluetongue virus serotypes 10 and 17: evidence for genetic reassortment in the vertebrate host. *J Virol*. 1987;61(4):1086-1091.

153. El Hussein A, Ramig RF, Holbrook FR, Beaty BJ. Asynchronous mixed infection of *Culicoides variipennis* with bluetongue virus serotypes 10 and 17. *J Gen Virol*. 1989;70:3355-3362.

154. Ramig RF, Garrison C, Chen D, Bell-Robinson D. Analysis of reassortment and superinfection during mixed infectino of Vero cells with bluetongue virus serotypes 10 and 17. *J Gen Virol*. 1989;70:2595-2603.

155. Stott JL, Oberst RD, Channell MB, Osburn BI. Genome segment reassortment between two serotypes of bluetongue virus in a natural host. *J Virol*. 1987;61(9):2670-2674.

156. Oberst RD, Stott JL, Blanchard-Channell M, Osburn BI. Genetic reassortment of bluetongue virus serotype 11 strains in the bovine. *Vet Microbiol*. 1987;15:11-18.

157. Shaw AE, Ratinier M, Nunes SF, et al. Reassortment between two serologically unrelated bluetongue virus strains is flexible and can involve any genome segment. *J Virol*. 2013;87(1):543-557. doi:10.1128/JVI.02266-12.

158. Turner PE. Searching for the advantages of viral sex. *Orig Life Evol Biosph*. 2003;33:95-108.

159. Ojosnegros S, García-Arriaza J, Escarmís C, et al. Viral genome segmentation can result from a trade-off between genetic content and particle stability. *PLoS Genet*. 2011;7(3). doi:10.1371/journal.pgen.1001344.

160. Dou D, Hernández-Neuta I, Wang H, et al. Analysis of IAV replication and co-infection dynamics by a versatile RNA viral genome labeling method. *Cell Rep*. 2017;20:251-263. doi:10.1016/j.celrep.2017.06.021.

161. Ramig RF. Superinfecting rotaviruses are not excluded from genetic interactions during asynchronous mixed infections in vitro. *Virology*. 1990;176:308-310.

162. Bussiere LD, Choudhury P, Bellaire B, Miller CL. Characterization of a replicating mammalian orthoreovirus with tetracysteine-tagged μNS for live-cell visualization of viral factories. *J Virol*. 2017;91(22). doi:10.1128/jvi.01371-17.

163. Patton JT, Jones MT, Kalbach AN, He YW, Xiaobo J. Rotavirus RNA polymerase requires the core shell protein to synthesize the double-stranded RNA genome. *J Virol*. 1997;71(12):9618-9626. doi:10.1128/jvi.00409-09.

164. Marshall N, Priyamvada L, Ende Z, Steel J, Lowen AC. Influenza virus reassortment occurs with high frequency in the absence of segment mismatch. *PLoS Pathog*. 2013;9(6). doi:10.1371/journal.ppat.1003421.

165. White MC, Steel J, Lowen AC. Heterologous packaging signals on segment 4, but not segment 6 or segment 8, limit influenza A virus reassortment. *J Virol*. 2017;91(11). doi:10.1128/JVI.00195-17.

166. Tilston-Lunel NL, Shi X, Elliott RM, Olszanski Acrani G. The potential for reassortment between Oropouche and Schmallenberg orthobunyaviruses. *Viruses*. 2017;9(220). doi:10.3390/v9080220.

167. Iroegbu CU, Pringle CR. Genetic interactions among viruses of the Bunyamwera complex. *J Virol*. 1981;37(1):383-394.

168. Villa M, Lässig M. Fitness cost of reassortment in human influenza. *PLOS Pathog*. 2017;13(11). doi:10.1371/journal.ppat.1006685.

CHAPTER 2 – CHARACTERIZING THE GENETIC DIVERSIFICATION OF A SINGLE BLUETONGUE VIRUS STRAIN USING AN IN VITRO MODEL OF HOST-SWITCHING

Introduction

Bluetongue virus (BTV; family *Reoviridae*, genus *Orbivirus*) is a globally distributed, arthropod-borne virus that can cause profound disease in both domestic and wild ruminants. BTV is the etiologic agent of bluetongue disease, which manifests as a systemic vasculitis in susceptible animals and is transmitted by biting midges in the genus *Culicoides*. Affected animals may develop thrombosis, pulmonary edema, pericardial effusion, cyanosis, mucosal erosions, and coronitis secondary to widespread vascular permeability and inflammation.[1,2] Sheep are considered to be relatively more susceptible to severe disease compared to other ruminants, although cattle and wildlife species also may succumb to infection and illness.

At least 29 serotypes of BTV have been recognized globally.[3,4] BTV is considered endemic in North America, with serotypes 2, 10, 11, 13, and 17 circulating seasonally in many parts of the United States.[5–7] Recent evidence also indicates the incursion and likely permanent establishment of previously exotic BTV-3 in North America (see Chapter 5).[8]

The global distribution of this virus is defined by the presence of its insect vector, which is – with few exceptions – necessary for natural disease transmission between ruminants.[9,10] In North America, the predominant vector species is *Culicoides sonorensis*, although additional vectors exist in certain locations such as Florida (i.e., *C. insignis*).[11–14] *Culicoides* midges that become infected with BTV through an infective blood meal do not appear to manifest adverse effects and remain persistently infected and capable of transmitting virus to ruminant hosts throughout their life.[15]

The BTV genome is composed of ten segments of double-stranded RNA (dsRNA) which encode 12 distinct proteins, as well as a novel ORF in segment 10.[16] Segments 2 and 6 encode the proteins VP2 – the serotype-defining protein – and VP5, respectively, which form the outer capsid of the virion and are involved with virus entry into host cells.[17–20] VP3 (segment 3) and VP7 (segment 7) form an inner core structure, while segment 1 encodes the RNA-dependent RNA polymerase, VP1.[21–23] In addition to VP1, VP4 (segment 4) and VP6 (segment 9) are components of the transcription machinery, with VP6 acting as the RNA helicase and VP4 enzymatically adding 5' caps to mRNAs.[24] BTV also encodes several non-structural proteins, including NS1 (segment 5), which facilitates tubule formation and enhances translation; NS2 (segment 8), which is essential for the formation of viral inclusion bodies and viral factories; NS3/3a (segment 10), which is involved in viral egress; and NS4 (segment 9), which acts an interferon antagonist.[25–28] In addition, BTV's RNA segments play an important role in virion assembly, with segment 10 untranslated regions (UTRs) initiating sequential packaging of RNA segments.[29,30] Various RNA-RNA and RNA-protein interactions occur during virion assembly, thereby ensuring successful packaging of all ten genome segments.[29,31]

BTV's segmented dsRNA composition enables the virus to evolve via several mechanisms, including through the occurrence of mutations and reassortment in a viral population. Reassortment is a key evolutionary feature of segmented viruses such as those in families *Orthomyxoviridae* and *Reoviridae*, as well as those in order *Bunyavirales* (Rift Valley fever virus, Schmallenberg virus, etc.). Reassortment permits the generation of progeny containing genome segments from more than one parent strain of virus, thereby contributing to genetic diversification and opportunities for host-switching and expansion into new niches.[32–34]

Arboviruses such as BTV face distinct evolutionary pressures. These vector-borne viruses must maintain functionality in two divergent host systems (invertebrate and vertebrate), each of which contributes additional, host-specific constraints. Arboviruses such as West Nile virus, dengue virus, and others have been found to undergo purifying selection during transmission from invertebrate to vertebrate hosts, likely due to fitness trade-offs.[35–39] While insect vectors are believed to exert less dramatic purifying selection on arboviruses, repeated bottlenecks and the founder effect are considered important modulators of genetic diversity in the vector.[40,41] While large viral population sizes, high rates of mutation, and mutant swarms (so-called quasispecies) appear to contribute to the overall ability of single-stranded RNA (ssRNA) arboviruses to maintain fitness in vertebrate and invertebrate hosts, little is known about whether similar factors come into play for BTV during its transmission cycle.[42–44] Caporale et al. found that BTV derived directly from the blood of infected animals had higher levels of low-frequency mutations than virus that had been cell culture isolated, particularly when the virus was propagated on BHK cells, indicating that naturally infected hosts may support more genetically diverse viral populations.[45] However, some studies have suggested that dsRNA virus mutation rates are less dramatic than those of ssRNA viruses, despite the lack of RNA polymerase proof-reading ability in both cases.[46,47] Additionally, given BTV's segmented genome, it is unclear whether each segment experiences similar selection pressures across transmission cycles, or whether there are differential effects across the ten genome segments.

While it is presumed that purifying selection plays an essential role in the maintenance of viral fitness in BTV transmission, only a handful of studies have experimentally investigated BTV's genetic evolution in vertebrate and invertebrate hosts.[48–51] However, these studies predominantly occurred before the advent of next-generation, whole-genome sequencing (WGS),

and as a result only were able to emphasize the genetic changes occurring within one or two segments of the BTV genome, or were based upon earlier methods to detect genetic differences, such as electropherotype.[48–51] Thus, although there is good evidence that at least two segments (2 and 10, encoding VP2 and NS3/3a, respectively) remain relatively unchanged through 2-3 alternating passages in *Culicoides sonorensis* and domestic ruminants, to date there has not been a robust investigation of the effect of BTV's alternating life cycle across all ten segments of its genome over multiple generations.[48] Here, we use an in vitro system that leverages cell lines derived from two of BTV's natural hosts (*Culicoides sonorensis* and cattle) and whole genome sequencing to answer fundamental questions regarding the population makeup and genetic diversity of this virus as it alternates between host systems.

Materials and Methods

Virus isolation

A field isolate of BTV-17 from California was isolated from BTV-positive whole blood during a naturally occurring infection in a clinically affected sheep and passaged as described by DeMaula et al.[52] Virus was expanded prior to initiation of the current experiment by a single passage in BHK 21 cells and infectious titer was determined via 50% tissue culture infectious dose (TCID50) using the Reed-Muench method.[53]

Cells

Bovine pulmonary artery endothelial cells (BPAEC) were maintained in Advanced MEM (Gibco, Dublin, Ireland) supplemented with 1% non-essential amino acids, 1% penicillin-streptomycin (10,000 U/ml), and 10% heat-inactivated fetal bovine serum (FBS). Cells were held at 37°C with 5% CO_2 supplementation and were passaged every 3-4 days when approximately 80-90% confluent.

CuVaW3 cells, derived from *Culicoides sonorensis* embryos, were maintained in a modified Schneider's Drosophila Media supplemented with 15% FBS and passaged every 3-4 days when ~90% confluent (Appendix 1).[54] CuVaW3 cells were held at 27°C without additional CO_2 supplementation.

Virus infections

BTV-17 (BTV17-INPUT) was used to infect confluent monolayers of BPAEC or CuVaW3 cells at an MOI of 1 in duplicate under three different conditions. Virus was either passaged serially in BPAEC (BTV17-BPAEC), serially in CuVaW3 cells (BTV17-CUVA), or alternatingly between bovine and insect cell lines (BTV17-ALT) for 10 consecutive passages. After initial infection at MOI 1, virus was passaged blindly every 96 hours to avoid freeze-thaw cycles.

Virus was harvested from each passage when bovine cells showed >80% cytopathic effect (CPE). Insect cells did not demonstrate CPE, but the presence of BTV was confirmed with qRT-PCR at each passage. Virus collected from each passage was used to initiate each subsequent round of infection, and remaining stocks were stored immediately at -80°C for downstream applications.

qRT-PCR

Nucleic acid from viral supernatant collected at each passage was extracted using MagMAX Pathogen RNA/DNA kit (Applied Biosystems, Foster City, CA) according to manufacturer's instructions for low cell content samples. Extracted samples were prepared for qRT-PCR using a universal one-tube fluorogenic probe-based reaction that detects BTV segment 10 as described by Ortega et al.[55] Reactions were prepared using SuperScript™ III One-step

qRT-PCR kit (Invitrogen, Carlsbad, CA) at half-reaction volumes and were thermocycled as previously described.[55]

WGS library preparation

Input virus (BTV17-INPUT) and duplicates from each condition (BTV17-CUVA, BTV17-ALT, and BTV17-BPAEC) collected after passages 1, 3, 6, 9, and 10 were prepared for whole genome sequencing (WGS). To maximize dsRNA recovery, extracted samples were treated with 4 U of DNase (TURBO DNA-*free*™ kit, Invitrogen) according to manufacturer's instructions. Extracted and DNased nucleic acids were then incubated with LiCl (final concentration 2.0 M) for 14-18 h at 4°C to selectively precipitate single stranded RNA and maximize dsRNA yield. Following incubation, samples were centrifuged at 4°C x 20 min at 18,000 x *g*. Supernatant was collected and excess salts were removed via a 1.25x MagMAX Pathogen RNA/DNA kit clean-up step.

Libraries for each sample were then prepared for whole genome metagenomic sequencing using ScriptSeq v2 RNA-Seq library preparation kit (Epicentre, Madison, WI) according to manufacturer's instructions, except RNA fragmentation time was reduced to 2 min 30 seconds at 85°C. Unique 6-mer barcodes (ScriptSeq Index PCR Primers, Epicentre) were annealed to each sample. Libraries were cleaned using a 1x Agencourt AMPure XP (Beckman Coulter, Brea, CA) magnetic bead-based clean-up, and concentration and quality of each library was measured using Agilent's High Sensitivity D1000 ScreenTape assay on the TapeStation 2200 instrument (Agilent, Santa Clara, CA). Samples were pooled to achieve roughly equal concentrations prior to size-selection. Pooled, indexed products between 300-700 base pairs (bp) in length were manually selected by fractionating the pooled library on a 1% agarose gel, followed by excising the desired region and performing gel extraction according to kit

instructions (QIAquick Gel Extraction Kit, Qiagen, Hilden, Germany). Concentration, quality, and size-distribution of pooled, size-selected libraries were then once again quantified via High Sensitivity D1000 ScreenTape. Library concentration was confirmed using KAPA Library Quantification qPCR (KAPA Biosystems, Basel, Switzerland) according to manufacturer's instructions.

Four initial samples were sequenced on the Illumina MiSeq instrument using 300 cycle (2 x 150) MiSeq v2 reagents (Illumina Inc., San Diego, CA). Subsequently, batches of 15-16 samples were sequenced on the Illumina NextSeq using 300 cycle (2 x 150) NextSeq v2 reagents (Illumina Inc.) to achieve sufficient sequencing depth across all ten segments.

Bioinformatics

Libraries were demultiplexed and reads from each sample were quality-filtered via a pre-processing bioinformatics pipeline that uses TrimAL to remove bases and sequences with low quality scores, as well as adapter sequences.[56] Trimmed reads were then processed using Cd-hit to eliminate duplicate reads (those where two or more reads had ≥ 96% pairwise identity in the first and last 30 base pairs).[57] Reads were then aligned to the consensus sequence of the parental input virus (BTV17-INPUT) in Bowtie2 using default parameters.[58] Finalized sequences were examined in Geneious v.10.2.2 to confirm alignment accuracy.

Quality-filtered reads in BAM format from BTV17-INPUT and virus replicates from passages 3, 6, and 9 were analyzed for single nucleotide variants (SNVs) and insertions-deletions (indels) using LoFreq.[59] Indel qualities were added to BAM data using `--lofreq indelqual` with `--dindel` option. Default LoFreq parameters, which include stringent thresholds based on alignment quality, base quality, and mapping quality, were used for SNV and indel detection.

Only LoFreq-detected variants in the coding sequence of each segment were included in downstream analyses.

Variants with significant strand-bias were pre-filtered based on LoFreq default parameters. Output .vcf files were imported into Geneious v.10.2.2 and visually inspected along with alignments.

Population Genetics

Viral population diversity was assessed in several ways. Genetic distance was determined for each sample by summing coding sequence SNV frequencies generated by LoFreq for each segment.[41] Richness was also measured using viral population-specific modifications: the number of SNV sites detected within the coding sequence of each of the ten genome segments was tabulated for each sample, and then normalized by the total number of BTV reads aligning per segment.[41,60]

Shannon entropy across samples and segments was calculated as a measure of population complexity to better characterize the genetic makeup of the viral milieu generated in each condition. The following equation, based on previously published papers was used:

$$S_{i,s} = -p_s(\ln p_s) + (1 - p_s) \times \ln(1 - p_s)$$

where the within-host viral population's Shannon entropy ($S_{i,s}$) is estimated as the mean S across all nucleotide positions (s) using the SNV frequency (p) at each nucleotide position.[41] Mean Shannon entropy across all sites was determined for each segment and/or sample.

Changes in the fixation index (F_{ST}) between the input virus and along the lineage of each replicate were calculated as a measure of genetic diversification across conditions and passages. F_{ST} was estimated by method-of-moments technique as described by Reynolds and refined for WGS datasets by Fumagalli et al.[61,62] As has been performed for other viral deep sequencing

datasets, *n* - or the number of individuals sampled in each population - was set to the mean BTV coverage depth for each segment's coding sequence (segment 1: 1604; segment 2: 2423; segment 3: 1375; segment 4: 1726; segment 5: 3014; segment 6: 3217; segment 7: 1866; segment 8: 5332; segment 9: 5282; segment 10: 2664).[41] The LoFreq-detected frequencies of non-reference variants (those that differed from the consensus sequence) were estimated as $p_{i,s}$, $p_{j,s}$ and $p_{s,}$ for populations *i*, *j*, and *i*+*j*, respectively, at site *s*. All other sites where non-reference variants were not detected were set to $p = 0$. Genetic variance at a single site, *s*, was then calculated based on the following equations:

$$a_s = \frac{(4n_i(p_{i,s} - p_s)^2 + 4n_j(p_{j,s} - p_s)^2 - b_s)}{2(2n_i n_j/(n_i + n_j)}$$

and

$$b_s = \frac{(n_i\alpha_{i,s} + n_j\alpha_{j,s})}{(n_i + n_j - 1)}$$

where

$$\alpha_{i,s} = 2p_{i,s}(1 - p_{i,s}), \text{ and } \alpha_{j,s} = 2p_{j,s}(1 - p_{j,s})$$

F_{ST} at a single site *s* is then estimated as $\frac{a_s}{(a_s + b_s)}$, and cumulatively across a coding sequence locus (*m* sites) as $\frac{\sum_{s=1}^{m} a}{\sum_{s=1}^{m}(a+b)}$. F_{ST} between input and passaged viruses and along lineages of each replicate was calculated for each segment. F_{ST} between two populations may range from 0 to 1, with an F_{ST} of 1 representing highly divergent populations.

To estimate degree of selection, d_N/d_S was calculated for each sample. Total nonsynonymous (N_s) and synonymous (S_s) sites for the coding region of each segment across passages 3, 6, and 9 were determined using DnaSP 6 via the Nei-Gojobori method.[63,64] Based on recommendations for viral data, nonsynonymous substitutions (N_d) and synonymous

substitutions (S_d) were calculated as the sum of LoFreq-generated nonsynonymous and synonymous substitution frequencies, respectively.[36,41] The d_N/d_S ratio was then calculated based on the Jukes-Cantor formula:[65]

$$d_S = \frac{-3 \times \ln(1 - ((4S_d/S_s)/3))}{4}$$

and

$$d_N = \frac{-3 \times \ln(1 - ((4N_d/N_s)/3))}{4}$$

A d_N/d_S ratio >1 suggests positive selection, while a d_N/d_S ratio of <1 indicates negative selection. While d_N/d_S provides an estimate of selection, it is considered a relatively insensitive measure for intra-host virus populations, and is therefore only interpreted as a guide towards general trends in this dataset.[66]

Statistics

Statistical analyses were carried out using GraphPad Prism 8.1.0. Unless otherwise noted, two-way repeated measures ANOVA with Tukey's post-hoc test was used to analyze the effect of condition (CuVaW3, BPAEC, or alternating propagation) and genome segment on measures of viral population genetics, with $p < 0.05$ considered significant.

Results

Despite passage in a relaxed in vitro system, BTV-17 remains remarkably stable regardless of cell culture condition

A field isolate of BTV-17 was passaged in duplicate serially under three different cell culture conditions (BTV17-CUVA, BTV17-ALT, and BTV17-BPAEC), and WGS was subsequently used to assess the impact of alternating host transmission on BTV's genetic diversification over time (Figure 2.1). The in vitro system used here leverages cell lines derived

from two of BTV's natural North American hosts, *Culicoides sonorensis* and cattle. By using these native cell types, we hoped to capture the scope of BTV genetic diversification that occurs in a system without adaptive immunity to allow relatively unchecked viral evolution.

In addition to the development of cytopathic effect in BPAEC cells, qRT-PCR was used as an estimate of viral replication, and Ct values remained consistently low across conditions and passages (Ct range: 13.4 - 16.0, data not shown). Whole genome sequencing was coupled with variant detection to establish single nucleotide variant (SNV) frequencies for the input (BTV17-INPUT) and passaged viruses. Depth of BTV coverage across the coding sequences of all samples and segments varied (Table 2.1), with a mean depth of 3,528. Only coding sequence SNVs above 0.2% frequency and without significant strand bias (as identified by LoFreq default parameters) were included in analyses. Mean SNV depth across all samples was 3,084 (SD: 2,541).

While the occurrence of SNVs varied across samples, the consensus sequence of BTV17-INPUT shared 100% nucleotide identity with output viruses across all conditions in segments 1, 2, 3, 4, 6, 7, 8, and 9, and >99.8% nucleotide identity in segments 5 and 10. Consensus sequences for BTV17-CUVA, BTV17-ALT, and BTV17-BPAEC were identical across all ten segments at each time point examined by WGS (passages 1, 3, 6, 9, and 10).

Single nucleotide consensus changes arose and approached fixation in segments 5 (nonsynonymous, residue 229I → R) and 10 (synonymous, nucleotide 360A → G) after a single passage in CuVaW3 cells or BPAEC cells and were conserved across remaining passages in all three cell culture conditions (segment 5 229I → R frequency: 99.35-99.96%, and segment 10 360A → G frequency: 97.39-99.89% across all samples). No further consensus changes occurred with additional passages, and resequencing of an additional aliquot of original BTV17-INPUT

confirmed that neither variant was present as the consensus nucleotide (i.e., >50% frequency) in the input virus.

Measures of genetic diversity remain relatively consistent across passages, regardless of cell culture condition

Whole genome sequencing data was analyzed for low frequency variants and insertions-deletions (indels) using LoFreq. Various measures of genetic diversity, including distance, richness, complexity, divergence, and selection were assessed across conditions and segments to better understand genetic variation in a relaxed, in vitro model of BTV transmission.

Genetic distance was approximated for the input virus and for viruses collected from passages 3, 6, and 9 as the sum of all SNV frequencies per coding sequence. BTV17-CUVA, BTV17-ALT, and BTV17-BPAEC exhibited similar genetic distances; overall distance (assessed across all segments and passages) was similar between passaged viruses and BTV17-INPUT (Figure 2.2) and did not differ between passaged viruses when analyzed by segment (Figure 2.3). Consistent with the consensus mutations that occurred in passaged viruses, BTV17-CUVA, BTV17-ALT, and BTV17-BPAEC demonstrated nearly two-fold greater genetic distance compared to BTV17-INPUT in segments 5 and 10 (Figure 2.3). When assessed for trends during the progression of passages, viruses exhibited similar genetic distances across all 10 segments regardless of cell culture condition (Figure 2.4). BTV17-ALT and BTV17-BPAEC demonstrated relatively variable genetic distances in segments 1, 2, and 3 across passages.

Richness, defined as the number of unique SNV sites present per 10,000 BTV reads, was calculated for each sample. Relatively wide variation was detected across samples and segments (Figures 2.5 and 2.6). When analyzed across all three cell culture conditions (BTV17-CUVA, -ALT, and -BPAEC), overall richness was significantly lower in segments 8 and 9 than in the

other eight segments ($p < 0.0001$). Segments 1 and 3 demonstrated the highest overall richness ($p < 0.05$). Interestingly, BTV17-INPUT richness was dramatically greater than that detected in any of the subsequent passages, regardless of cell culture condition ($p < 0.0005$) (Figure 2.5a). When assessed for trends in richness arising across passages, BTV17-CUVA, BTV17-ALT, and BTV17-BPAEC demonstrated substantial variability within each segment (Figure 2.6).

We then measured population complexity using Shannon entropy as an estimator of uncertainty within a viral population. Mean Shannon entropy was calculated for each sample and segment across passages. When data from all segments and passages was combined, BTV17-ALT was the least complex viral population, with significantly lower Shannon entropy than BTV17-INPUT, BTV17-CUVA, and BTV17-BPAEC ($p < 0.005$) (Figure 2.7). When analyzed for segment-specific trends, segment 10 had the greatest Shannon entropy across all conditions ($p < 0.05$) (Figure 2.8). However, no significant differences were detected between cell culture conditions, and no overt trends were noted along the progression of passages (Figure 2.9).

Novel SNVs and indels arose in each condition and passage, although the number of new variants varied across samples (Figure 2.10). The occurrence of novel indels - which are presumed to be universally deleterious due to shifts in reading frame – was approximately ten-fold less than the occurrence of novel SNVs. Several novel variants and indels re-occurred across samples or passages, disappearing in one passage and then reoccurring later (data not shown). This may reflect a predisposition for variants or indels to occur repeatedly in certain parts of the genome, or it may indicate subtle variations in sequencing quality that resulted in failure to detect these very low-level variants in certain samples.

BTV-17 exhibits marked genetic divergence from input virus in segments 5 and 10 early in passage series across all cell culture conditions

Genetic divergence was estimated by calculation of F_{ST}, or the fixation index. This measure is used to approximate the divergence between two populations and was applied to understand how viral populations shifted from BTV17-INPUT (passage 0) to passage 3, and then within each replicate, how populations diverged from passages 3 to 6 and 6 to 9. Marked divergence from BTV17-INPUT was detected in segments 5 and 10 across all samples (segment 5 mean F_{ST} = 0.67 (range 0.64-0.70); segment 10 mean F_{ST} = 0.73 (range 0.70-0.74)), consistent with consensus changes that arose in these segments (Figure 2.11). Less strikingly, segments 1 and 2 also demonstrated moderate divergence from BTV17-INPUT (mean F_{ST} 0.12 and 0.24, respectively) across all samples by passage 3. Remaining segments had very low F_{ST} values from BTV17-INPUT (passage 0) to passage 3 viruses, with segments 6, 8, and 9 demonstrating the lowest divergence from the input virus across all three conditions. Subsequent to initial passages, when most marked divergence was detected, F_{ST} values exhibited relatively consistent rates of divergence between passages 3 and 6, and passages 6 and 9. F_{ST} values were similar among cell culture conditions and segments, and while BTV17-ALT showed slightly higher F_{ST} values than matched BTV17-CUVA and BTV17-BPAEC samples across all segments, this trend was non-significant.

BTV-17 exhibits purifying selection regardless of cell culture condition

The proportion of nonsynonymous to synonymous changes (d_N/d_S) was calculated as an estimate of selection across segments and passages. The proportion of nonsynonymous sites across the entire BTV coding sequence (*pN*) for BTV17-INPUT was 0.77, and this measure remained relatively unchanged across segments and samples for subsequent passages (data not

shown). Propagation on BHK cells (BTV17-INPUT) appeared to result in purifying selection for most segments (mean $d_N/d_S = 0.35$) (Figure 2.12a), although segments 3 and 7 had d_N/d_S ratios closer to 1 (0.97 and 1.03, respectively), indicating more neutral selection (Figure 2.12b). In contrast, after passage in CuVaW3 and BPAEC cells, segments 4 and 5 generally exhibited positive selection (mean d_N/d_S across all conditions: 1.13, range 0.60-1.71; and 1.07, range 0.61-1.58, respectively) (Figure 2.12b). When assessed across the coding sequence of all ten segments, BTV demonstrated negative, or purifying selection, in all conditions and passages. However, purifying selection appeared to be relatively stronger in BTV17-INPUT (propagated in BHK cells) compared to BTV propagated in BPAEC and CuVaW3 cells. When individual segments were analyzed across passages, d_N/d_S was quite varied from passage to passage, and between cell culture conditions (Figure 2.12c).

Discussion

By using a relaxed system of propagation, we sought to remove the impact of varying host-derived features (i.e., adaptive immunity, overall health status, species variation) on BTV's genetic diversification, instead capturing the virus's inherent capacity to develop low-frequency mutations in vertebrate and invertebrate host systems. Insect and mammalian hosts presumably exert differing selection pressures that have the potential to be amplified when alternating transmission is eliminated (i.e., single cell type passages) versus when alternating transmission is maintained (i.e., alternating cell type passages), as transmission between vertebrate and invertebrate hosts is believed to drive purifying selection in many arboviruses, including BTV.[35,37,38,43,48,67–70] Arboviruses with RNA genomes generally evolve more slowly than other RNA viruses, reportedly due to the selective pressures exerted by their transmission cycle.[43,71]

Here, we provide evidence that BTV remains highly stable in a relaxed in vitro system emulating BTV's natural transmission cycle.

Several studies have demonstrated that arboviruses diversify to a greater extent in the insect host, possibly due to common mechanisms of immune response (RNA interference, RNAi) compared to that of the vertebrate.[43,72,73] While there is evidence for the existence of RNAi in *Culicoides* and *Culicoides*-derived cell lines, the presence of RNAi in the cell line used in our study (CuVaW3) has yet to be demonstrated.[74,75] Contrary to our expectation of increased genetic diversity in virus passaged solely in CuVaW3 cells, we found that BTV-17 viral populations remained largely constant regardless of cell culture condition. In fact, for some measures, the most dramatic changes occurred when transitioning from BHK 21 cells (BTV17-INPUT) into our in vitro system (CuVaW3 and BPAEC cell lines). Individual consensus changes in segments 5 and 10 arose after only a single passage in BPAEC or CuVaW3 cells, but consensus sequences thereafter remained the same in all cell culture conditions, and the majority of diversity measures stayed roughly equivalent across passages and conditions.

Despite passaging BTV-17 in a relaxed model with relatively few constraints on genetic diversification, we found that this virus exhibited marked genetic consistency between passages. BTV diversity found among field isolates most likely reflects numerous factors, including host immune response (both in the vertebrate and invertebrate), vaccination status, host species, infectious titer, possible co-infecting viruses, and repeated bottlenecks that occur due to small number of infectious particles that *Culicoides* expectorate or imbibe during blood meals. The underwhelming degree of genetic diversity detected in our study is corroborated by studies demonstrating that electropherotype of BTV does not change across prolonged infection in ruminant hosts and that experimental in vivo transmission between *C. sonorensis* and sheep and

cattle results in minimal changes in the overall genetics of BTV.[48,50,51] Bonneau et al. also described the occurrence of the founder effect during transmission between *C. sonorensis* and ruminant hosts.[48]

Studies of West Nile virus and Venezuelan equine encephalitis virus has demonstrated that mosquitoes expectorate unique populations of virus with each feeding.[60] While viral bottlenecks are minimal during transmission from the insect to vertebrate host, profound bottlenecks occur when the vector takes a bloodmeal.[40,41,60] It is possible that a similar phenomenon exists during transmission of bluetongue virus. As a result, the high MOI (1) used in this experiment may have prevented the development of genetic diversification secondary to bottlenecking, as a relatively constant, large-sized virus population was carried from passage to passage. This large population size and subsequent avoidance of bottlenecks due to a low number of "individuals" (i.e., genome equivalents) would inherently abolish the occurrence of founder effect.

Divergence of passaged viruses (BTV17-CUVA, -ALT, and -BPAEC) from the input strain (BTV17-INPUT) likely indicates that BHK 21 cells exert different selection pressures than BPAEC or CuVaW3 cells. The disproportionately high genetic richness (total SNV sites normalized by BTV reads) of BTV17-INPUT coupled with unremarkable genetic distance (sum of SNV frequencies) across all segments indicates that most SNVs in BTV17-INPUT are low-frequency. In addition, BTV17-INPUT demonstrated the lowest d_N/d_S ratio of our samples, indicating relatively dramatic negative selection. While these findings seem contradictory, they may in fact demonstrate that strong purifying selection in BHK cells is coupled with increased frequency of neutral – or even deleterious – alleles that are not purged from the population.[76] This phenomenon, described by Cvijovic et al. using a forward-time model, can result in

distortions of genetic measures that mimic population expansion and is particularly evident in larger populations.[77] Alternatively, interferon-deficient BHK 21 cells may promote "tolerance" of viral variants, causing a similar net outcome in our various diversity measures.[77,78]

Consistent with the work of Bonneau et al., who found that segment 10 developed nonsynonymous mutations with relatively high frequency during transmission from *Culicoides* to ruminants, we detected high complexity (Shannon entropy) and divergence (F_{ST}) for segment 10, regardless of cell culture condition. This suggests that increased population heterogeneity may be a characteristic feature of BTV segment 10. While this segment is generally considered to be one of the more conserved BTV segments, other groups have also identified relatively high substitution rates for segment 10.[70,79,80] While underlying mechanisms for this trend are unclear, segment 10 plays an essential role in recruiting RNA segments during viral replication and generation of cytopathic effect, and thus the low-level genetic heterogeneity detected here and in other studies may be explained by its functional role in virus replication. Alternatively, there may be secondary structures that affect sequencing chemistry and falsely increases the number of variants detected.

Our work also corroborates findings by Caporale et al., who described a decrease in variants isolated from whole blood, particularly when passaged in BHK 21 cells.[45] It is likely that isolating BTV on this non-native cell type causes a population bottleneck and purifying selection. We suspect that the consensus changes that arose in segments 5 and 10 when BTV-17 was transitioned from BHK 21 cells to bovine or *Culicoides* cells may reflect a reversion from BHK-specific adaptations in these segments. While segment 5 and 10 RNAs are known to interact, these interactions occur at different sites than those detected in our work.[81] However, the current understanding of RNA-RNA, RNA-protein, and protein-protein interactions in BTV

assembly and maturation are not exhaustive, so potential for additional interactions beyond those currently characterized exists.

Importantly and interestingly, variants that arose across passages in all conditions were often not present in the parent strain but then occurred at low frequency in several of the passaged viruses, possibly representing certain hotspots in the viral genome that are associated with increased diversity. Alternatively, secondary DNA structures can impact sequencing chemistry, and may result in similar findings. Certainly, a caveat to this work and all deep-sequencing projects is that variant detection is not free of bias. LoFreq default parameters include stringent quality filters that reduce the incidence of false-positives.[59] However, various bioinformatics studies have demonstrated that false positives are relatively common regardless of sequencing platform and variant detector used, and that sensitivity often varies between variant programs.[82] By performing our work in duplicate and eliminating any PCR amplification steps aside from the initial creation of libraries, we have tried to reduce as many variables as possible. However, sequencing chemistry, structural features of DNA-DNA interactions, and inherent sequencing errors may all contribute to uncertainty in our data.

In summary, few studies have utilized a comprehensive approach to evaluate contributions of viral genetic diversity and how the existence of multiple genotypes within alternate host passage may influence BTV evolution. Improved understanding of BTV genetic variability during host-switching is critical for predicting the emergence and impact of *Culicoides*-transmitted viruses in different ecosystem contexts with disease transmission models.

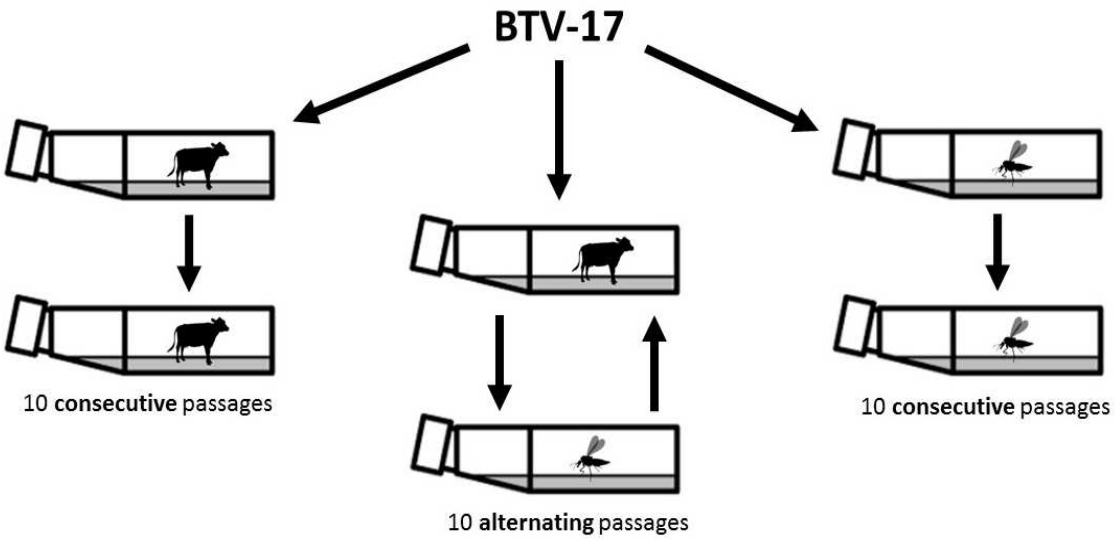

Figure 2.1 – Schematic of Experimental Set-up. A field isolate of BTV-17 (BTV17-INPUT) was passaged under three different cell culture conditions: serial passages in bovine cells (BTV17-BPAEC); serial passages in *Culicoides sonorensis* cells (BTV17-CUVA); and alternating passages in bovine and *C. sonorensis* cells (BTV17-ALT) for 10 consecutive passages.

Table 2.1 – Samples Demonstrate Similar Sequencing Coverage. Mean depth of sequencing coverage across the coding sequence of each BTV segment of BTV17-INPUT and all samples from passages 3, 6, and 9.

		Passage 3						Passage 6						Passage 9					
Segment	BTV17-INPUT	BTV17-CUVA p3a	BTV17-CUVA p3b	BTV17-ALT p3a	BTV17-ALT p3b	BTV17-BPAEC p3a	BTV17-BPAEC p3b	BTV17-CUVA p6a	BTV17-CUVA p6b	BTV17-ALT p6a	BTV17-ALT p6b	BTV17-BPAEC p6a	BTV17-BPAEC p6b	BTV17-CUVA p9a	BTV17-CUVA p9b	BTV17-ALT p9a	BTV17-ALT p9b	BTV17-BPAEC p9a	BTV17-BPAEC p9b
1	877	2282	1705	1675	1783	1783	1835	2655	2944	1041	1668	1724	1499	859	1789	1106	1191	1775	1492
2	1103	3333	2282	2317	2392	2731	2490	3590	4072	1538	2321	2319	2066	1344	2463	2428	1578	2823	2095
3	818	2072	1309	1230	1324	1641	1705	2271	2799	1042	1478	1539	1518	903	1689	848	790	1485	1169
4	1007	2616	1780	1638	1567	2219	2008	2519	3542	1436	1872	1893	1993	1168	2372	1126	1118	1823	1534
5	1207	5481	3254	3238	3259	3903	3840	5111	6518	2601	3307	3376	3171	2048	3903	2375	2212	3859	3088
6	1242	5519	3393	3358	3277	4275	4385	4554	6276	2768	3518	3589	3426	2080	3959	2308	2262	4076	3350
7	1065	3193	1816	1850	1749	2713	2263	3257	4560	1863	2258	2063	2471	1573	2477	1368	1306	2014	1778
8	1810	8831	5795	5802	5338	7711	7598	8742	11297	5039	6124	6269	6047	4226	6971	3696	3811	6664	5468
9	2831	9179	5823	5792	5494	8085	9362	7743	11195	5230	5930	5419	5885	4417	7104	3211	3992	7033	5669
10	1412	6204	3676	3411	3592	3859	3648	4785	6370	2479	3180	3374	3228	2008	4008	2914	2469	3901	3211

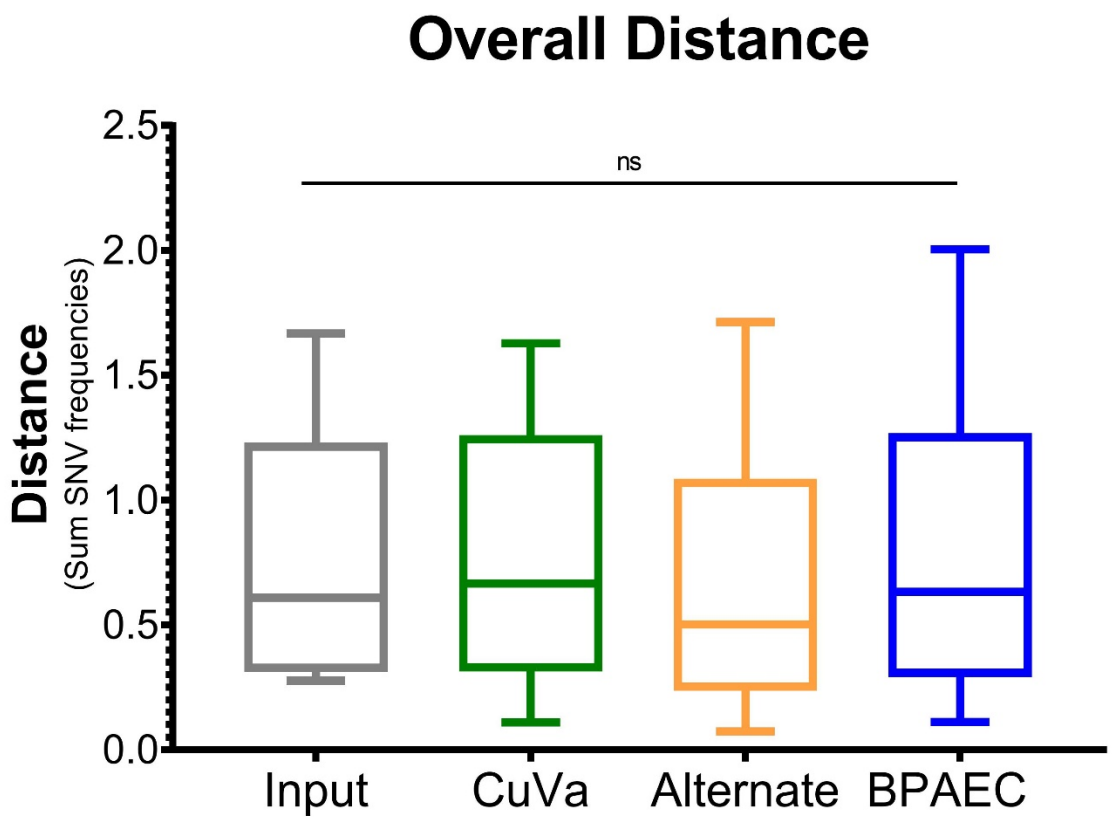

Figure 2.2 – Overall Genetic Distances do not Differ by Cell Culture Condition. Genetic distances (i.e., the sum of SNV frequencies) across the coding sequences of BTV17-INPUT, BTV17-CUVA, BTV17-ALT, and BTV17-BPAEC do not differ regardless of cell culture condition. Distance was calculated for each segment, and cumulative data from all segments is shown by box-and-whisker plots (median, interquartile range, and min/max are depicted). Box-and-whisker plots for BTV17-CUVA, -ALT, and -BPAEC were constructed using the genetic distances of all segments across passages 3, 6, and 9.

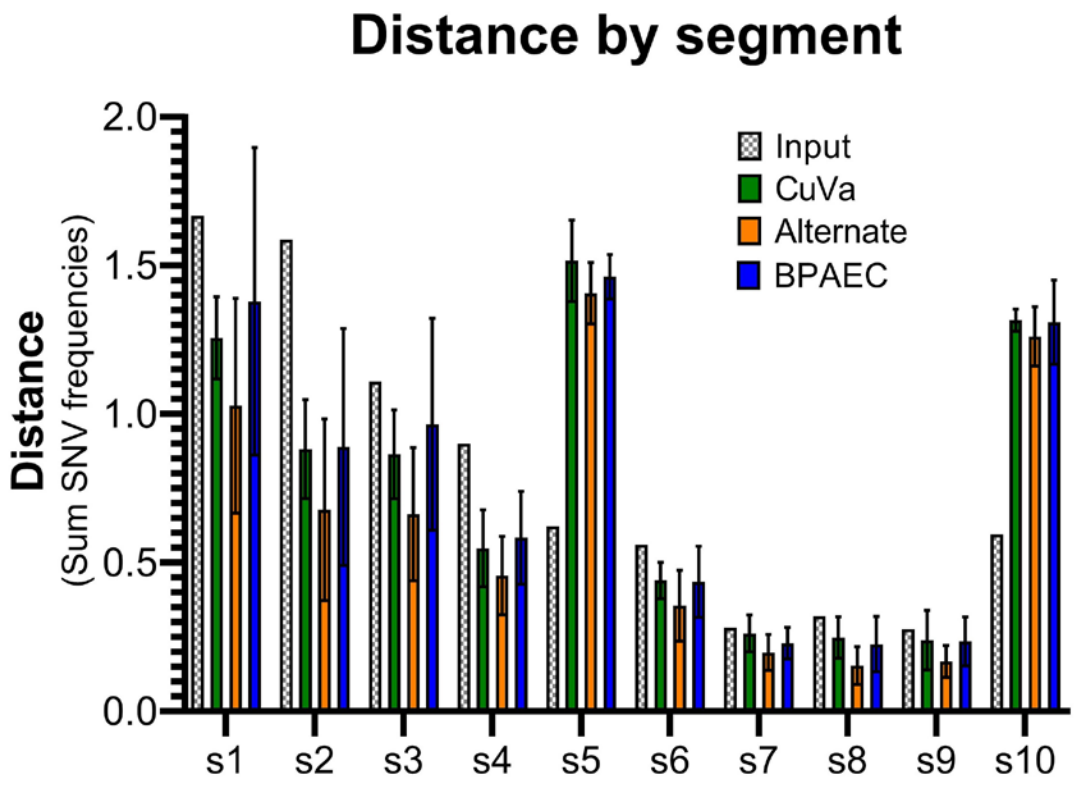

Figure 2.3 – Segments 5 and 10 from Passaged Viruses Demonstrate Increased Genetic Distances. BTV17-CUVA, -ALT, and -BPAEC demonstrate increased genetic distance compared to input virus (BTV17-INPUT) in segments 5 and 10, consistent with consensus variants that arose in across all three cell culture conditions. For BTV17-CUVA, -ALT, and -BPAEC, mean distance (and standard deviation) for each segment across passages 3, 6, and 9 is shown.

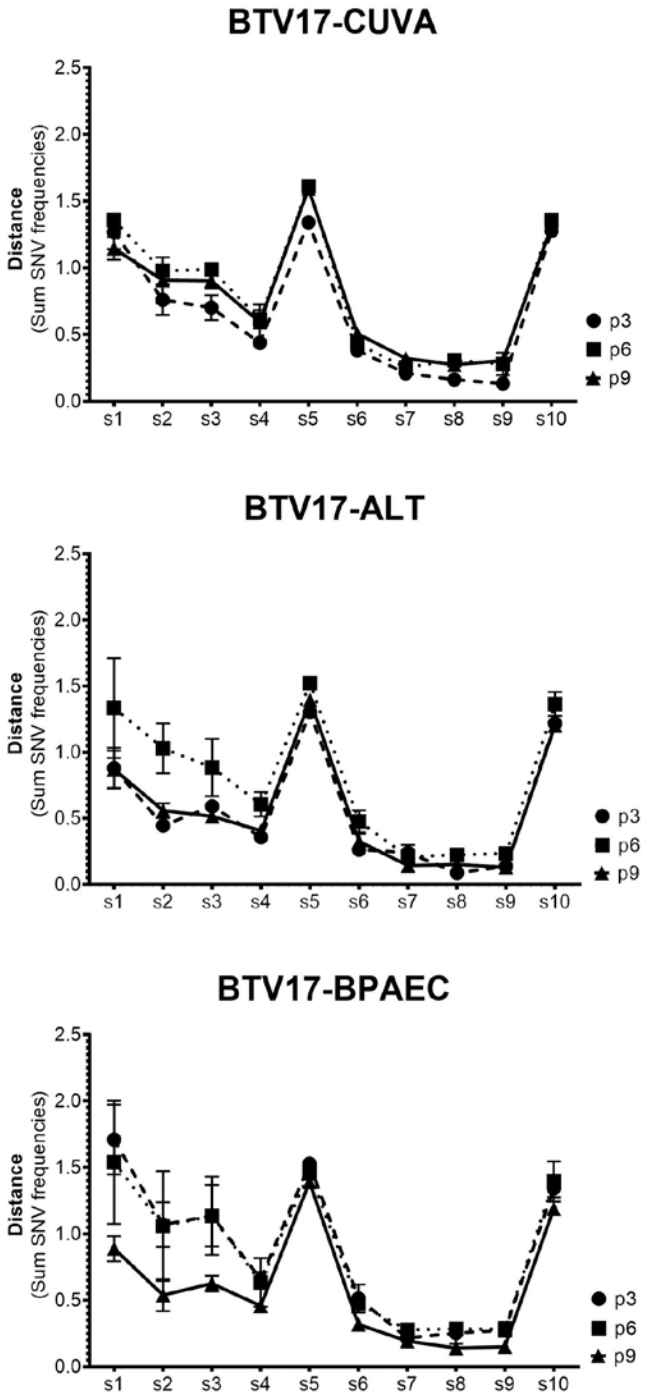

Figure 2.4 – Genetic Distances across Passages are Similar between Cell Culture Conditions. BTV17-CUVA, -ALT, and -BPAEC demonstrate similar genetic distances within each segment across passages 3, 6, and 9. Mean distance (and range) for each segment and passage is shown. Virus harvested from passage 3 is connected by dashed line; virus from passage 6 is connected by dotted line; virus from passage 9 is connected by solid line.

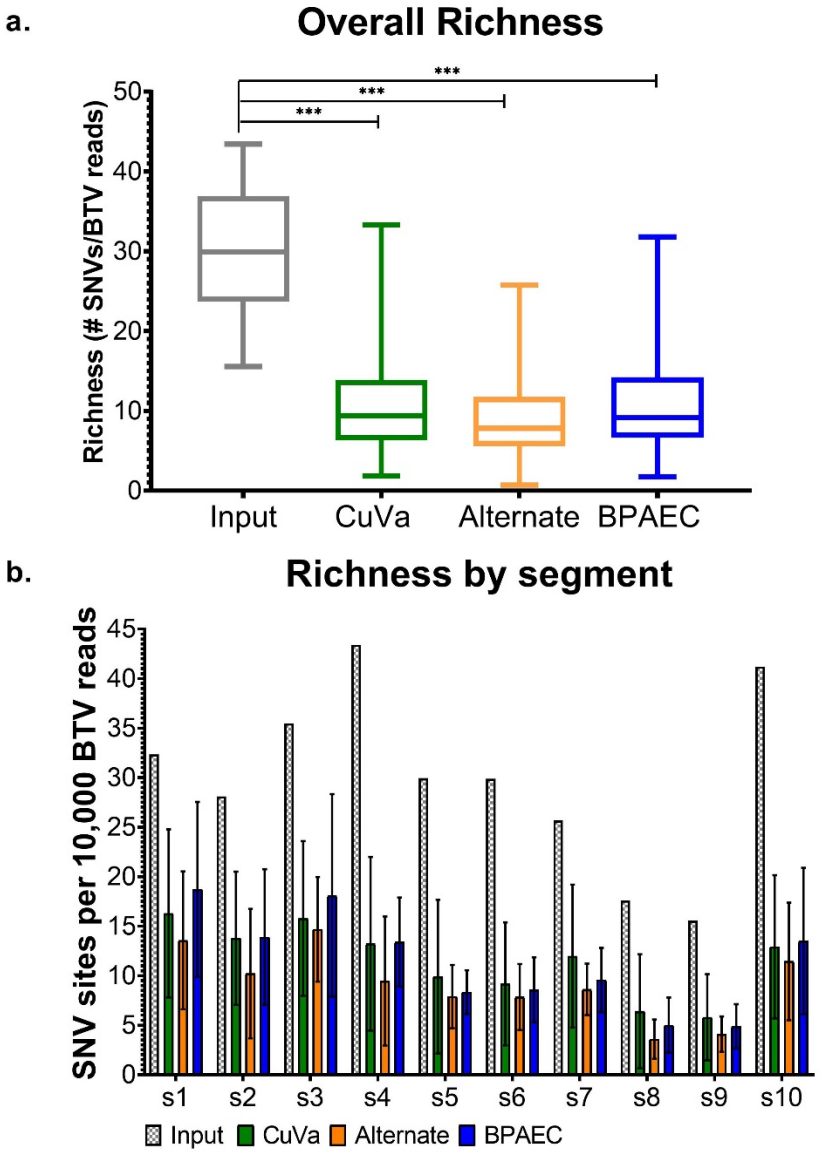

Figure 2.5 – Input Virus Demonstrates Significantly Greater Genetic Richness. BTV17-CUVA, -ALT, and -BPAEC demonstrate decreased richness compared to BTV17-INPUT. **a)** Richness across the entire coding sequence of BTV17-INPUT is significantly higher ($p < 0.0005$) than that detected across the coding sequences of BTV17-CUVA, BTV17-ALT, and BTV17-BPAEC. Richness of each segment was calculated as the sum of SNV sites normalized by the number of BTV reads (i.e., variant sites per 10,000 BTV reads), and collective data across all segments is shown by box-and-whisker plots (median, interquartile range, and min/max are depicted). Box-and-whisker plots for BTV17-CUVA, -ALT, and -BPAEC were constructed using the richness of all segments across passages 3, 6, and 9. **b)** Mean richness and standard deviation for each segment is shown. Bars depicting BTV17-CUVA, -ALT, and -BPAEC represent collective data from passages 3, 6, and 9.

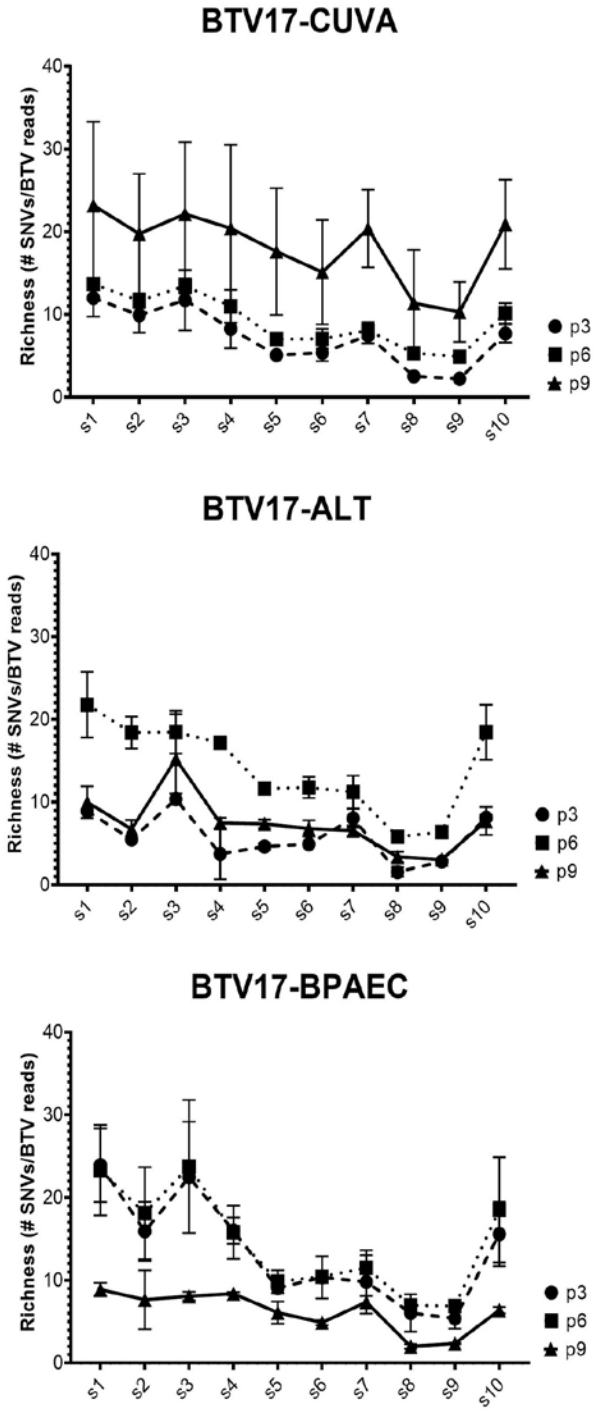

Figure 2.6 – Genetic Richness is Variable across Passages and Segments. BTV17-CUVA, -ALT, and -BPAEC demonstrate variable richness within each segment across passages 3, 6, and 9. Mean richness (and range) for each segment and passage is shown. Virus harvested from passage 3 is connected by dashed line; virus from passage 6 is connected by dotted line; virus from passage 9 is connected by solid line.

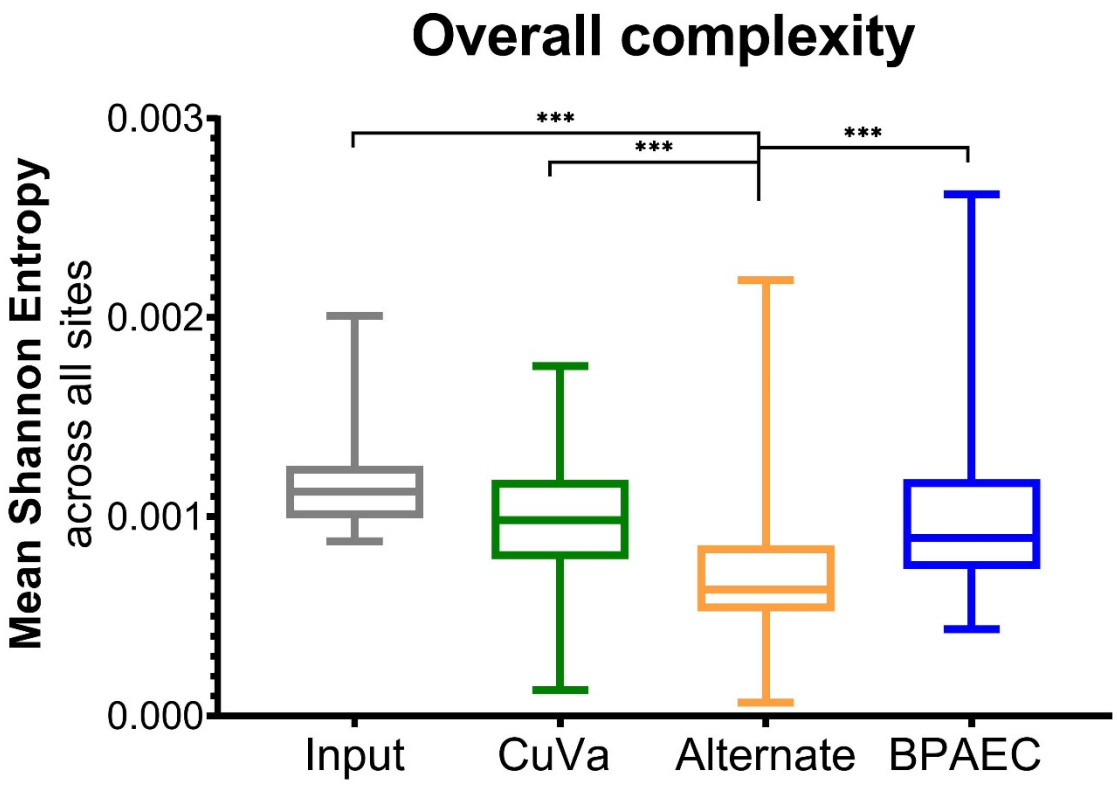

Figure 2.7 – Alternatingly Passaged Virus has Lower Overall Genetic Complexity. BTV17-ALT exhibits the lowest overall complexity when analyzed across segments and passages. Shannon entropy was calculated as a measure of population complexity across the coding sequences of BTV17-INPUT, BTV17-CUVA, BTV17-ALT, and BTV17-BPAEC. Shannon entropy was calculated for each segment, and cumulative data from all segments is shown by box-and-whisker plots (median, interquartile range, and min/max are depicted). Box-and-whisker plots for BTV17-CUVA, -ALT, and -BPAEC were constructed using the mean Shannon entropy of all segments across passages 3, 6, and 9.

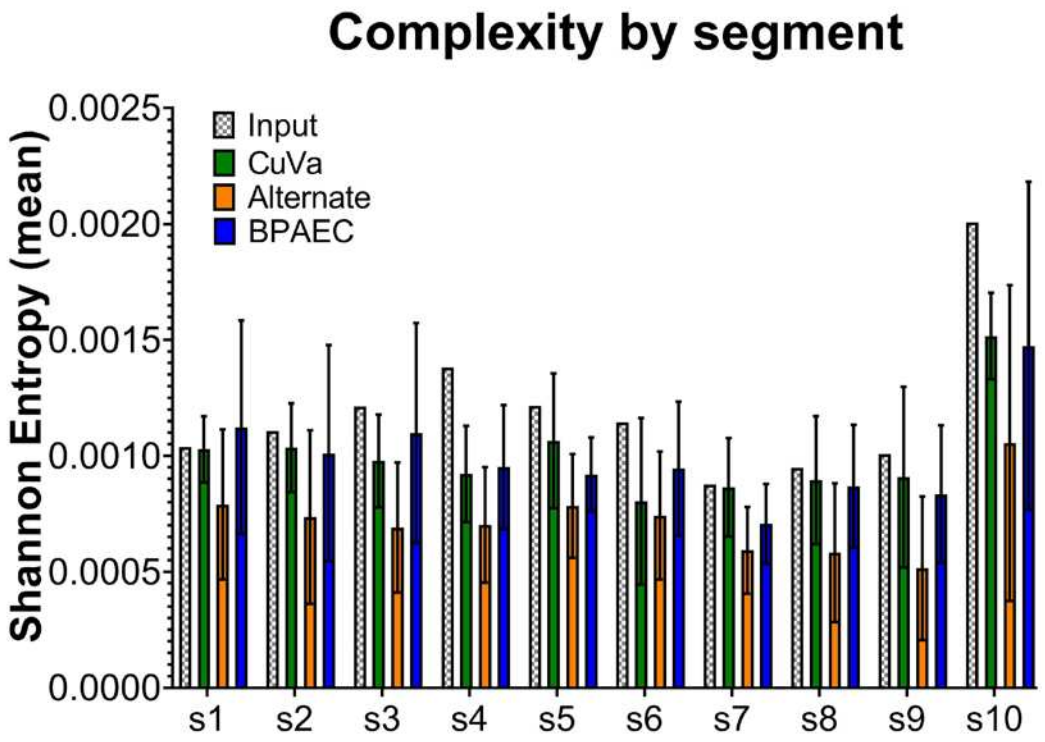

Figure 2.8 – Segment 10 Demonstrates Greater Complexity Compared to Other Segments. BTV17-INPUT, -CUVA, -ALT, and -BPAEC demonstrate similar population complexity across all segments, although segment 10 shows increased overall complexity compared to the other segments. For BTV17-CUVA, -ALT, and -BPAEC, mean Shannon entropy (and standard deviation) for each segment across passages 3, 6, and 9 is shown.

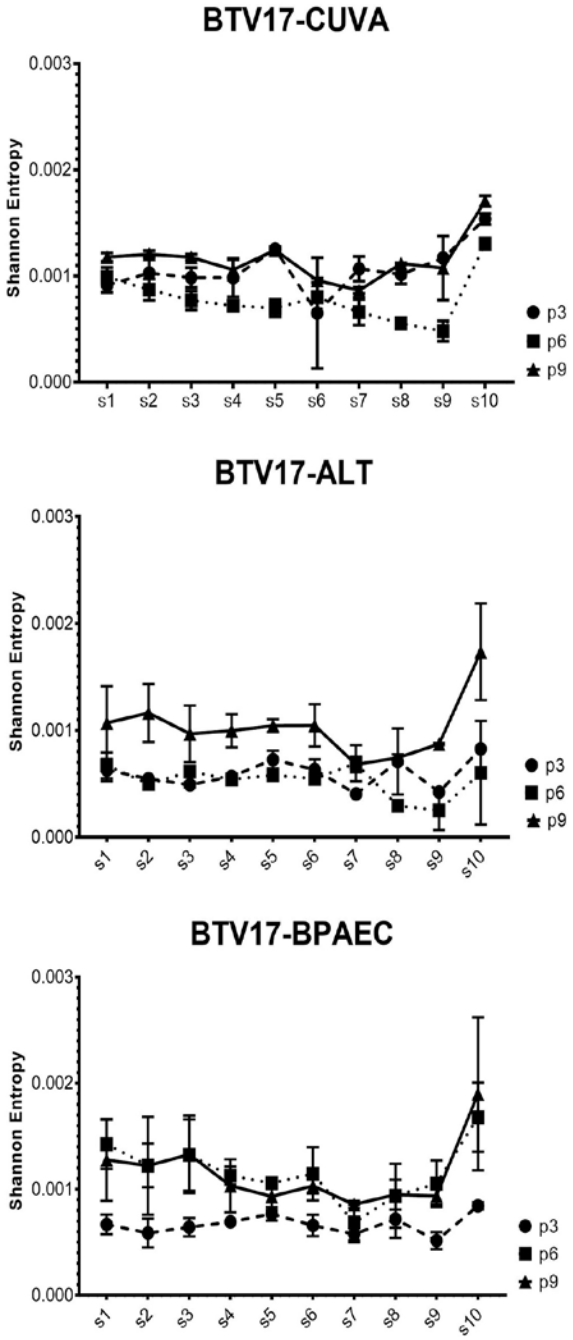

Figure 2.9 – Genetic Complexity Varies by Passage. BTV17-CUVA, -ALT, and -BPAEC demonstrate variable Shannon entropy within each segment across passages 3, 6, and 9, although segment 10 generally demonstrates a greater degree of complexity compared to other segments. Mean Shannon entropy (and range) for each segment and passage is shown. Virus harvested from passage 3 is connected by dashed line; virus from passage 6 is connected by dotted line; virus from passage 9 is connected by solid line.

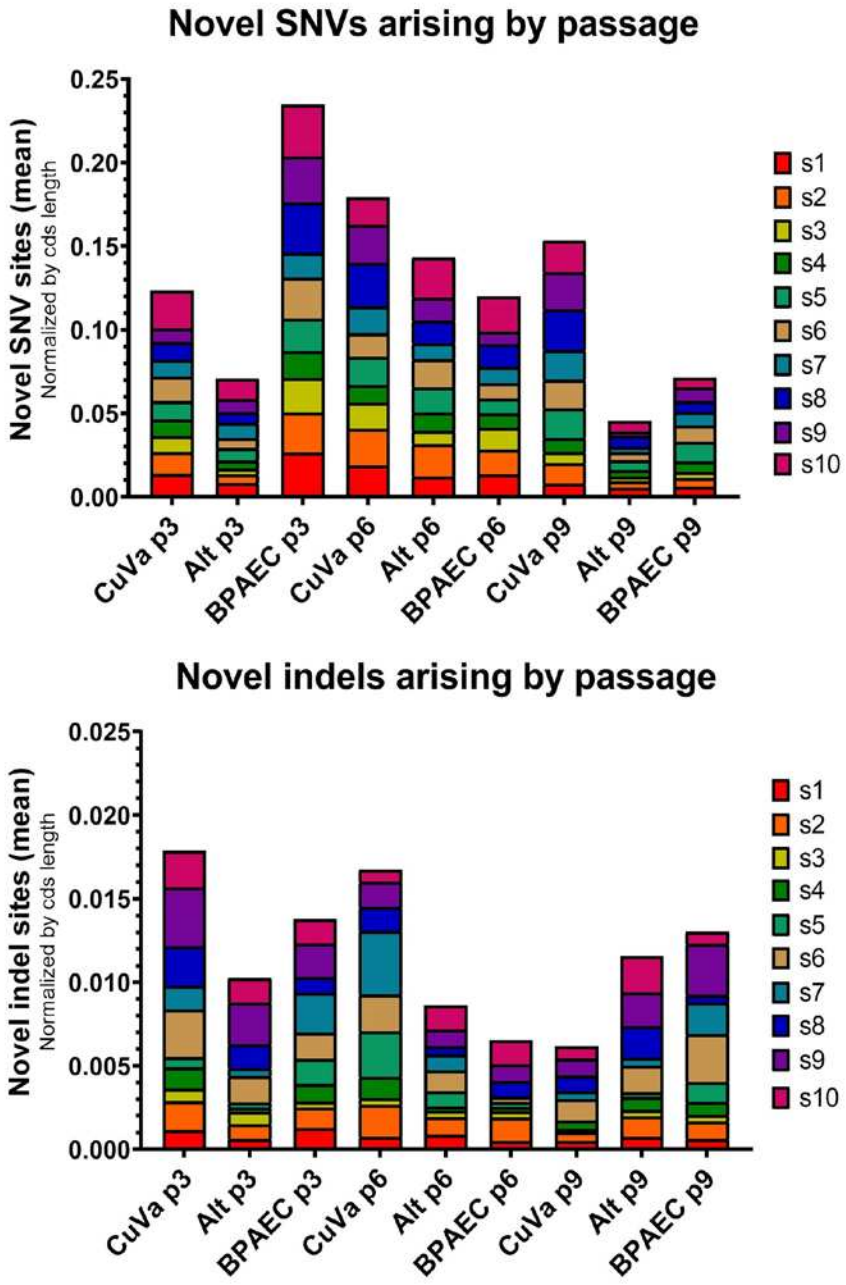

Figure 2.10 – SNVs and Indels Arise across Passages. Variable numbers of novel SNVs and indels (those that were not present in prior passage across each lineage) arise across passages. The total number of novel SNVs or indels was calculated for each sample and normalized by the nucleotide length of the coding sequence (cds) of each segment. The mean number of normalized novel sites per segment is plotted according to passage and cell culture condition. Novel indels occur nearly 10-fold less frequently than novel SNVs.

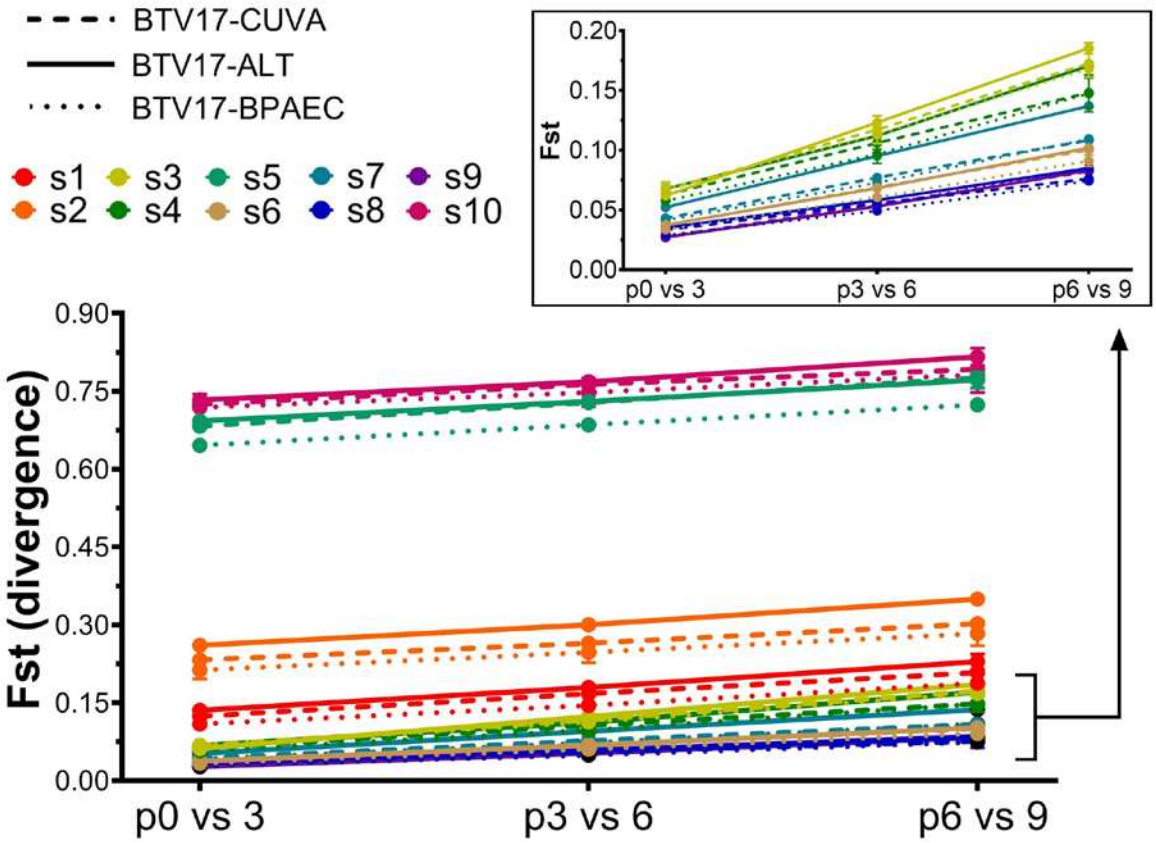

Figure 2.11 – BTV Exhibits Minimal Divergence between Passages. Fixation index (F_{ST}), or the genetic divergence from passage to passage, shows consistent trends regardless of cell culture condition. Marked divergence from BTV17-INPUT is evident in segments 5 and 10 by passage 3, but thereafter divergence remains steady across cell culture conditions and passages (cumulative F_{ST} is shown). Dashed lines represent BTV17-CUVA, solid lines represent BTV17-ALT, and dotted lines represent BTV17-BPAEC. Mean F_{ST} and range are depicted at each point, although error bars are often vanishingly small.

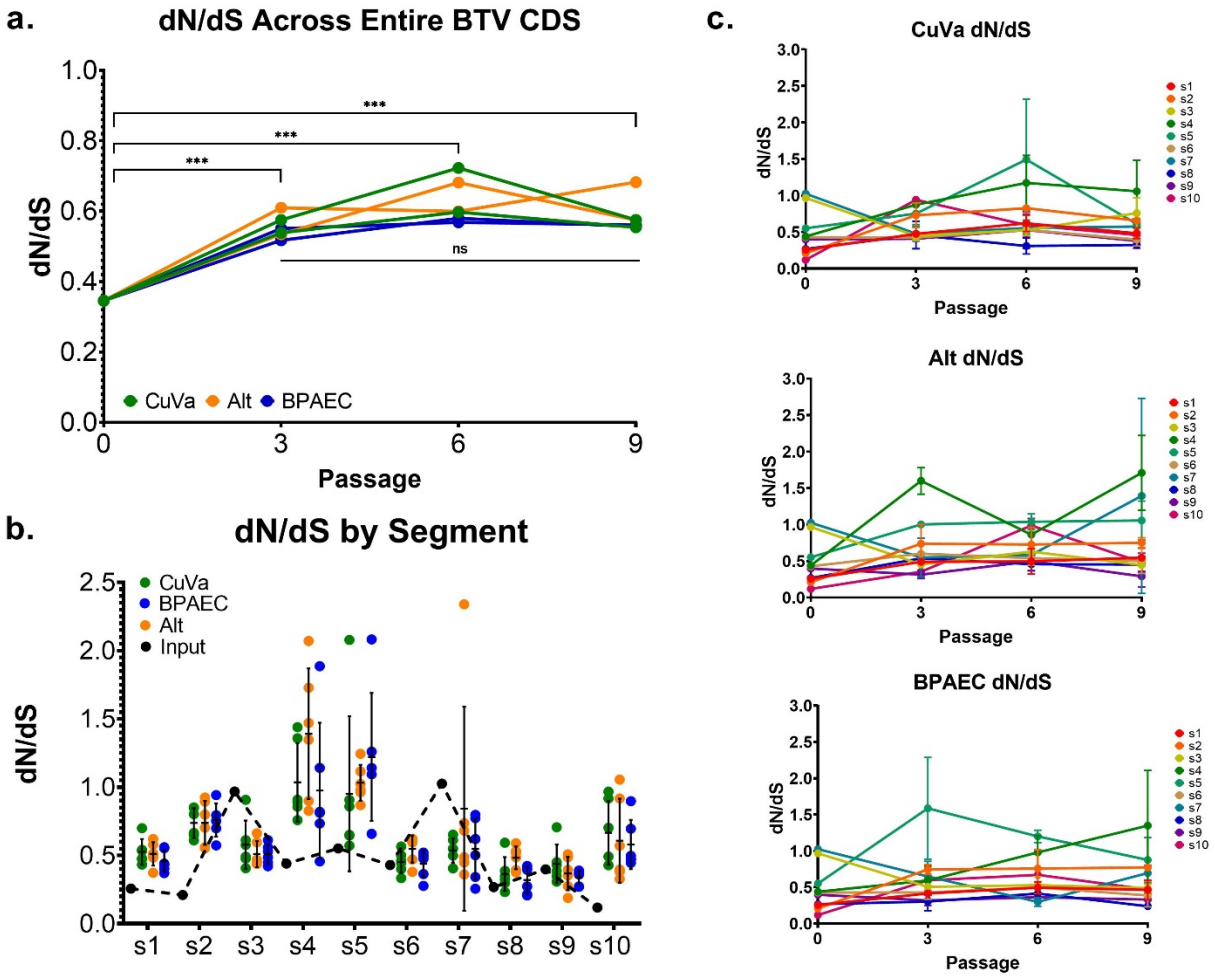

Figure 2.12 – BTV Demonstrates Strong Overall Purifying Selection. The proportion of nonsynonymous (dN) to synonymous (dS) changes was used as an estimate of selection, demonstrating that all samples (BTV17-INPUT, -CUVA, -ALT, and -BPAEC) are under overall negative selection. **a)** dN/dS for each sample was calculated across the entire BTV coding sequence (inclusive of all ten segments), and BTV17-INPUT had significantly lower dN/dS than passaged viruses ($p < 0.0005$). **b)** dN/dS from all passages and replicates are shown. Error bars depict mean and standard deviation of each segment according to cell culture condition. BTV17-INPUT is shown by black dots and dashed line. **c)** dN/dS of each segment is shown according to each passage in each cell culture condition. Mean and range for each segment is shown at each passage.

REFERENCES

1. Maclachlan NJ, Mayo CE, Daniels PW, Savini G, Zientara S, Gibbs EPJ. Bluetongue. *Rev Sci Tech*. 2015;34(2):329-340. doi:10.20506/rst.34.2.2360.

2. Schwartz-Cornil I, Mertens PPC, Contreras V, et al. Bluetongue virus: virology, pathogenesis and immunity. *Vet Res*. 2008;39(46). doi:10.1051/vetres:2008023.

3. Maan S, Maan NS, Belaganahalli MN, et al. Full-genome sequencing as a basis for molecular epidemiology etudies of bluetongue virus in India. *PLoS One*. 2015;10(6):e0131257. doi:10.1371/journal.pone.0131257.

4. Wright M. Serological and genetic characterisation of putative new serotypes of bluetongue virus and epizootic haemorrhagic disease virus isolated from an alpaca. Dissertation Thesis, North-West University Potchefstroom Campus. 2013.

5. Ostlund EN. Report of the committee on bluetongue and bovine retroviruses. *Proc Annu Meet US Anim Health Assoc*. 2007;111:209-213.

6. Mcvey DS, Drolet BS, Ruder MG, et al. Orbiviruses: a North American perspective. *Vector-Borne Zoonot*. 2015;15(6):335-338. doi:10.1089/vbz.2014.1699.

7. Maclachlan NJ, Wilson WC, Crossley BM, et al. Novel serotype of bluetongue virus, western North America. *Emerg Infect Dis*. 2013;19(4):665-666. doi:10.3201/eid1904.120347.

8. Schirtzinger EE, Jasperson DC, Ostlund EN, Johnson DJ, Wilson WC. Recent US bluetongue virus serotype 3 isolates found outside of Florida indicate evidence of reassortment with co-circulating endemic serotypes. *J Gen Virol*. 2018;99(2):157-168. doi:10.1099/jgv.0.000965.

9. Van der Sluijs M, de Smit AJ, Moormann R. Vector independent transmission of the vector-borne bluetongue virus. *Crit Rev Microbiol*. 2016;42(1):57-64. doi:10.3109/1040841X.2013.879850.

10. Bréard E, Schulz C, Sailleau C, et al. Bluetongue virus serotype 27: experimental infection of goats, sheep and cattle with three BTV-27 variants reveal atypical characteristics and likely direct contact transmission BTV-27 between goats. *Transbound Emerg Dis*. 2018;65(2). doi:10.1111/tbed.12780.

11. Tanya VN, Greiner EC, Gibbs E. Evaluation of *Culicoides insignis* (Diptera: Ceratopogonidae) as a vector of bluetongue virus. *Vet Microbiol*. 1992;32:1-14.

12. Tabachnick WJ. *Culicoides variipennis* and bluetongue virus epidemiology in the United States. *Annu Rev Entomol*. 1996;41:23-43.

13. Ruder MG, Lysyk TJ, Stallknecht DE, et al. Transmission and epidemiology of bluetongue and epizootic hemorrhagic disease in North America: current perspectives, research gaps, and future directions. *Vector-Borne Zoonot*. 2015;15(6):348-363. doi:10.1089/vbz.2014.1703.

14. Vigil SL, Ruder MG, Shaw D, et al. Apparent range expansion of *Culicoides* (Hoffmania) *insignis* (Diptera: Ceratopogonidae) in the southeastern United States. *J Med Entomol*. 2018;55(4):1043-1046. doi:10.1093/jme/tjy036.

15. Mellor PS. Replication of arboviruses in insect vectors. *J Comp Path*. 2000;123:231-247. doi:10.1053/jcpa.2000.0434.

16. Stewart M, Hardy A, Barry G, et al. Characterization of a second open reading frame in genome segment 10 of bluetongue virus. *J Gen Virol*. 2015;96:3280-3293. doi:10.1099/JGV.0.000267.

17. Mertens PP, Pedley S, Cowley J, et al. Analysis of the roles of bluetongue virus outer capsid proteins VP2 and VP5 in determination of virus serotype. *Virology*. 1989;170(2):561-565.

18. Zhang X, Boyce M, Bhattacharya B, et al. Bluetongue virus coat protein VP2 contains sialic acid-binding domains, and VP5 resembles enveloped virus fusion proteins. *Proc Nat Acad Sci*. 2010;107(14):6292-6297. doi:10.1073/pnas.0913403107.

19. Forzan M, Wirblich C, Roy P. A capsid protein of nonenveloped bluetongue virus exhibits membrane fusion activity. *Proc Nat Acad Sci*. 2004;101(7):2100-2105.

20. Forzan M, Marsh M, Roy P. Bluetongue virus entry into cells. *J Virol*. 2007;81(9):4819-4827. doi:10.1128/JVI.02284-06.

21. Kar AK, Iwatani N, Roy P. Assembly and intracellular localization of the bluetongue virus core protein VP3. *J Virol*. 2005;79(17):11487-11495. doi:10.1128/JVI.79.17.11487-11495.2005.

22. Boyce M, Wehrfritz J, Noad R, Roy P. Purified recombinant bluetongue virus VP1 exhibits RNA replicase activity. *J Virol*. 2004;78(8):3994-4002. doi:10.1128/JVI.78.8.3994-4002.2004.

23. Matsuo E, Roy P. Bluetongue virus VP1 polymerase activity in vitro: template dependency, dinucleotide priming and cap dependency. *PLoS One*. 2011;6(11). doi:10.1371/journal.pone.0027702.

24. Roy P. Bluetongue virus: dissection of the polymerase complex. *J Gen Virol*. 2008;89:1789-1804. doi:10.1099/vir.0.2008/002089-0.

25. Boyce M, Celma CCP, Roy P. Bluetongue virus non-structural protein 1 is a positive regulator of viral protein synthesis. *Virol J*. 2012;9(178). doi:10.1186/1743-422X-9-178.

26. Kar A, Bhattacharya B, Roy P. Bluetongue virus RNA binding protein NS2 is a modulator of viral replication and assembly. *BMC Mol Biol*. 2007;8(1):4. doi:10.1186/1471-2199-8-4.

27. Celma CCP, Roy P. A viral nonstructural protein regulates bluetongue virus trafficking and release. *J Virol*. 2009;83(13):6806-6816. doi:10.1128/JVI.00263-09.

28. Ratinier M, Shaw AE, Barry G, et al. Bluetongue virus NS4 protein is an interferon antagonist and a determinant of virus virulence. *J Virol*. 2016;90(11):5427-5439. doi:10.1128/JVI.00422-16.

29. Fajardo T, Sung PY, Roy P. Disruption of specific RNA-RNA interactions in a double-stranded RNA virus inhibits genome packaging and virus infectivity. *PLoS Pathog*. 2015;11(12):e1005321. doi:10.1371/journal.ppat.1005321.

30. Sung PY, Roy P. Sequential packaging of RNA genomic segments during the assembly of bluetongue virus. *Nucleic Acids Res*. 2014;42(22):13824-13838. doi:10.1093/nar/gku1171.

31. Sung PY, Vaughan R, Rahman SK, et al. The interaction of bluetongue virus VP6 and genomic RNA is essential for genome packaging. *J Virol*. 2019;93(5):e02023-18. doi:10.1128/JVI.02023-18.

32. Ma EJ, Hill NJ, Zabilansky J, Yuan K, Runstadler JA, Delong EF. Reticulate evolution is favored in influenza niche switching. *Proc Nat Acad Sci*. 2016;113(19):5335-5339. doi:10.1073/pnas.1522921113.

33. Lowen AC. It's in the mix: Reassortment of segmented viral genomes. *PLOS Pathog*. 2018;14(9). doi:10.1371/journal.ppat.1007200.

34. McDonald SM, Nelson MI, Turner PE, Patton JT. Reassortment in segmented RNA viruses: mechanisms and outcomes. *Nat Rev Microbiol*. 2016;14:448-460. doi:10.1038/nrmicro.2016.46.

35. Deardorff ER, Fitzpatrick KA, Jerzak GVS, Shi PY, Kramer LD, Ebel GD. West Nile virus experimental evolution in vivo and the trade-off hypothesis. *PLoS Pathog*. 2011;7(11). doi:10.1371/journal.ppat.1002335.

36. Lequime S, Fontaine A, Ar Gouilh M, Moltini-Conclois I, Lambrechts L. Genetic drift, purifying selection and vector genotype shape dengue virus intra-host genetic diversity in mosquitoes. *PLoS Genet*. 2016;12(6). doi:10.1371/journal.pgen.1006111.

37. Holmes EC. Patterns of intra- and interhost nonsynonymous variation reveal strong purifying selection in dengue virus. *J Virol*. 2003;77(20):11296-11298. doi:10.1128/JVI.77.20.11296-11298.2003.

38. Coffey LL, Vasilakis N, Brault AC, Powers AM, Tripet F, Weaver SC. Arbovirus evolution in vivo is constrained by host alternation. *Proc Nat Acad Sci*. 2008;105(19):6970-6975. doi: 10.1073pnas.0712130105.

39. Engel D, Jöst H, Wink M, et al. Reconstruction of the evolutionary history and dispersal of Usutu virus, a neglected emerging arbovirus in Europe and Africa. *MBio*. 2016;7(1). doi:10.1128/mBio.01938-15.

40. Forrester NL, Guerbois M, Seymour RL, Spratt H, Weaver SC. Vector-borne transmission imposes a severe bottleneck on an RNA virus population. *PLoS Pathog*. 2012;8(9). doi:10.1371/journal.ppat.1002897.

41. Grubaugh ND, Weger-Lucarelli J, Murrieta RA, et al. Genetic drift during systemic arbovirus infection of mosquito vectors leads to decreased relative fitness during host switching. *Cell Host Microbe*. 2016;19(4):481-492. doi:10.1016/j.chom.2016.03.002.

42. Ciota AT. The role of co-infection and swarm dynamics in arbovirus transmission. *Virus Res*. 2019;265:88-93. doi:10.1016/j.virusres.2019.03.010.

43. Ciota AT, Kramer LD. Insights into arbovirus evolution and adaptation from experimental studies. *Viruses*. 2010;2(12):2594-2617. doi:10.3390/V2122594.

44. Lauring AS, Andino R. Quasispecies theory and the behavior of RNA viruses. *PLoS Pathog*. 2010;6(7). doi:10.1371/journal.ppat.1001005.

45. Caporale M, Gialleonorado L Di, Janowicz A, et al. Virus and host factors affecting the clinical outcome of bluetongue virus infection. *J Virol*. 2014;88(18):10399-10411. doi:10.1128/JVI.01641-14.

46. Sanjuán R, Nebot MR, Chirico N, Mansky LM, Belshaw R. Viral mutation rates. *J Virol*. 2010;84(19):9733-9748. doi:10.1128/JVI.00694-10.

47. Peck KM, Lauring AS. Complexities of viral mutation rates. *J Virol.* 2018;92(14). doi:10.1128/JVI.01031-17.

48. Bonneau KR, Mullens BA, Maclachlan NJ. Occurrence of genetic drift and founder effect during quasispecies evolution of the VP2 and NS3/NS3A genes of bluetongue virus upon passage between sheep, cattle, and *Culicoides sonorensis*. *J Virol*. 2001;75(17):8298-8305. doi:10.1128/JVI.75.17.8298-8305.2001.

49. Gould AR, Eaton BT. The amino acid sequence of the outer coat protein VP2 of neutralizing monoclonal antibody-resistant, virulent and attenuated bluetongue viruses. *Virus Res*. 1990;17:161-172.

50. Heidner HW, Maclachlan NJ, Fuller FJ, et al. Bluetongue virus genome remains stable throughout prolonged infection of cattle. *J Gen Virol*. 1988;69:2629-2636.

51. MacLachlan N, Fuller F. Genetic stability in calves of a single strain of bluetongue virus. *Am J Vet Res*. 1986;47(4):762-764.

52. DeMaula CD, Jutila MA, Wilson DW, Maclachlan NJ, Wilson DW, Jutila MA. Infection kinetics, prostacyclin release and cytokine-mediated modulation of the mechanism of cell death during bluetongue virus infection of cultured ovine and bovine pulmonary artery and lung microvascular endothelial cells. *J Gen Virol*. 2001;82(4):787-794. doi:10.1099/0022-1317-82-4-787.

53. Reed LJ, Muench H. A simple method of estimating fifty percent endpoints. *Am J Epidemiol*. 1938;27(3):493-497. doi:10.1093/oxfordjournals.aje.a118408.

54. McHolland LE, Mecham JO. Characterization of cell lines developed from field populations of *Culicoides sonorensis* (Diptera: Ceratopogonidae). *J Med Entomol*. 2003;40(3):348-351. doi:10.1603/0022-2585-40.3.348.

55. Ortega J, Crossley B, Dechant JE, Drew CP, James MacLachlan N. Fatal bluetongue virus infection in an alpaca (*Vicugna pacos*) in California. *J Vet Diagn Invest*. 2010;22:134-136. doi:10.1177/104063871002200129.

56. Capella-Gutiérrez S, Silla-Martínez JM, Gabaldón T. trimAl: a tool for automated alignment trimming in large-scale phylogenetic analyses. *Bioinformatics*. 2009;25(15):1972-1973. doi:10.1093/bioinformatics/btp348.

57. Fu L, Niu B, Zhu Z, Wu S, Li W. CD-HIT: accelerated for clustering the next-generation sequencing data. *Bioinformatics*. 2012;28(23):3150-3152. doi:10.1093/bioinformatics/bts565.

58. Langmead B, Salzberg SL. Fast gapped-read alignment with Bowtie 2. *Nat Methods*. 2012;9(4):357-359. doi:10.1038/nmeth.1923.

59. Wilm A, Aw PPK, Bertrand D, et al. LoFreq: A sequence-quality aware, ultra-sensitive variant caller for uncovering cell-population heterogeneity from high-throughput sequencing datasets. *Nucleic Acids Res*. 2012;40(22):11189-11201. doi:10.1093/nar/gks918.

60. Grubaugh ND, Fauver JR, Rückert C, et al. Mosquitoes transmit unique West Nile virus populations during each feeding episode. *Cell Rep*. 2017;19(4):709-718. doi:10.1016/j.celrep.2017.03.076.

61. Reynolds J, Weir BS, Cockerham CC. Estimation of the coancestry coefficient: basis for a short-term genetic distance. *Genetics*. 1983;105:767-779.

62. Fumagalli M, Vieira FG, Korneliussen TS, et al. Quantifying population genetic differentiation from next-generation sequencing data. *Genetics.* 2013;195:979-992. doi:10.1534/genetics.113.154740.

63. Rozas J, Ferrer-Mata A, Sánchez-DelBarrio JC, et al. DnaSP 6: DNA sequence polymorphism analysis of large data sets. *Mol Biol Evol*. 2017;34(12):3299-3302. doi:10.1093/molbev/msx248.

64. Nei M, Gojobori T. Simple methods for estimating the numbers of synonymous and nonsynonymous nucleotide substitutions. *Molec Biol Evol*. 1986;3:418-426. doi:10.1093/oxfordjournals.molbev.a040410.

65. Jukes TH, Cantor CR. Evolution of protein molecules. In: *Mammalian Protein Metabolism*. Academic Press; 1969:21-132. doi:10.1016/B978-1-4832-3211-9.50009-7.

66. Kryazhimskiy S, Plotkin JB. The population genetics of dN/dS. *PLoS Genet*. 2008;4(12). doi:10.1371/journal.pgen.1000304.

67. Jerzak GVS, Brown I, Shi PY, Kramer LD, Ebel GD. Genetic diversity and purifying selection in West Nile virus populations are maintained during host switching. *Virology*. 2008;374:256-260. doi:10.1016/j.virol.2008.02.032.

68. Jerzak G, Bernard KA, Kramer LD, Ebel GD. Genetic variation in West Nile virus from naturally infected mosquitoes and birds suggests quasispecies structure and strong purifying selection. *J Gen Virol*. 2005;86(8):2175-2183. doi:10.1099/vir.0.81015-0.

69. Boyle DB, Amos-Ritchie R, Broz I, et al. Evolution of bluetongue sirus serotype 1 in northern Australia over 30 years. *J Virol*. 2014;88(24):13981-13989. doi:10.1128/JVI.02055-14.

70. Carpi G, Holmes EC, Kitchen A. The evolutionary dynamics of bluetongue virus. *J Mol Evol*. 2010;70:583-592. doi:10.1007/s00239-010-9354-y.

71. Jenkins GM, Rambaut A, Pybus OG, Holmes EC. Rates of molecular evolution in RNA viruses: a quantitative phylogenetic analysis. *J Mol Evol*. 2002;54:156-165. doi:10.1007/s00239-001-0064-3.

72. Brackney DE, Beane JE, Ebel GD. RNAi targeting of West Nile virus in mosquito midguts promotes virus diversification. *PLoS Pathog*. 2009;5(7):e1000502. doi:10.1371/journal.ppat.1000502.

73. Brackney DE, Schirtzinger EE, Harrison TD, Ebel GD, Hanley KA. Modulation of flavivirus population diversity by RNA interference. *J Virol*. 2015;89(7):4035-4039. doi:10.1128/JVI.02612-14.

74. Schnettler E, Ratinier M, Watson M, et al. RNA interference targets arbovirus replication in *Culicoides* cells. *J Virol*. 2013;87(5):2441-2454. doi:10.1128/JVI.02848-12.

75. Mills MK, Nayduch D, Michel K. Inducing RNA interference in the arbovirus vector, *Culicoides sonorensis*. *Insect Mol Biol*. 2015;24(1):105-114. doi:10.1111/imb.12139.

76. Muller HJ. The relation of recombination to mutational advance. *Mutat Res*. 1964;1:2-9. doi:10.1016/0027-5107(64)90047-8.

77. Cvijović I, Good BH, Desai MM. The effect of strong purifying selection on genetic diversity. *Genetics*. 2018;209(4):1235-1278. doi:10.1534/genetics.118.301058.

78. Otsuki K, Yamamoto H, Tsubokura M. Studies on avian infectious bronchitis virus. *Arch Virol*. 1979;60:25-32.

79. Van Niekerk M, Freeman M, Paweska JT, et al. Variation in the NS3 gene and protein in South African isolates of bluetongue and equine encephalosis viruses. *J Gen Virol*. 2003;84:581-590. doi:10.1099/vir.0.18749-0.

80. Ftaich N, Ciancia C, Viarouge C, et al. Turnover rate of NS3 proteins modulates bluetongue virus replication kinetics in a host-specific manner. *J Virol*. 2015;89(20):10467-10481. doi:10.1128/JVI.01541-15.

81. Boyce M, Mccrae MA, Boyce P, Kim JT. Inter-segment complementarity in orbiviruses: a driver for co-ordinated genome packaging in the *Reoviridae*? *J Gen Virol*. 2016;97:1145-1157. doi:10.1099/jgv.0.000400.

82. McCrone JT, Lauring AS. Measurements of intrahost viral diversity are extremely sensitive to systematic errors in variant calling. *J Virol*. 2016;90(15):6884-6895. doi:10.1128/JVI.00667-16.

CHAPTER 3 – IN VITRO REASSORTMENT BETWEEN ENDEMIC BLUETONGUE VIRUSES FEATURES GLOBAL SHIFTS IN SEGMENT FREQUENCIES AND PREFERRED SEGMENT COMBINATIONS

Introduction

Bluetongue virus (BTV, genus *Reoviridae*, family *Orbivirus*) is associated with significant economic and animal health impacts worldwide. Composed of ten segments of double-stranded RNA (dsRNA) and transmitted by hematophagous *Culicoides* midges, BTV can cause severe disease in susceptible ruminants and has been identified as an important, re-emerging arbovirus with significant animal health implications.[1,2] BTV circulates year-round in tropical climates, and seasonally in more temperate and cooler environments.[3] Its range is defined by the presence of one or more competent vector species (*Culicoides* spp.) capable of transmitting the virus between ruminant hosts.

Recent episodes of BTV incursion into previously BTV-free regions has highlighted the role of climate change and animal and vector movement as important mediators of the spread of this virus.[4–6] Moreover, virus-specific factors such as mutation and reassortment may also contribute to the ability of BTV to invade new regions or cause disease outbreaks in otherwise enzootic areas. The BTV genome is replicated via an RNA-dependent RNA polymerase, which – as with other RNA viruses – lacks proof-reading ability and thus is subject to error-prone transcription.[7–9] For many RNA viruses, this is considered an important mechanism contributing to genetic diversification and overall fitness; the mutation rate and replication rate strike a delicate balance allowing these viruses to rapidly adapt through the generation of massive viral populations.[8,10] RNA arboviruses have much lower rates of mutation despite the production of

large viral populations, which is believed to be secondary to the fitness tradeoffs that occur during the alternating host transmission cycle.[11,12] In vitro and in vivo studies of BTV from our lab and others indicate that this virus has a low overall rate of genetic diversity at the single-nucleotide level, and that virus transmitted between *Culicoides* and ruminant hosts generally remains relatively stable at the consensus level.[13,14]

Reassortment – or the generation of progeny viruses that contain genome segments from more than one parental strain – appears to contribute significantly to the overall genetic diversification and evolution of bluetongue virus. Extensive reassortment has been demonstrated both in vitro and in vivo with various strains of BTV, and several studies of field isolates have demonstrated that BTV reassortment is widespread in naturally transmitted viral infections.[15–22] Coinfection of the vector or ruminant host with more than one strain of BTV is prerequisite for reassortment to occur, but thereafter, it has been suggested that reassortment has very few limitations.

Some studies, particularly those analyzing field samples, have detected potential segment-specific trends in reassortment, but most experimental approaches have generally failed to establish definitive segment combinations that are more likely to occur than others.[20] The sheer number of potential segment combinations between BTV strains (1,024 different reassortants are possible with two strains) makes robust investigation of reassortment trends time- and labor-intensive, which has hampered investigations in this area.

Here, we apply whole genome sequencing and a novel amplicon-based sequencing approach to detect global shifts in segment frequencies and reassortment events between two enzootic North American BTV strains (BTV-2 and BTV-10) to better understand features of reassortment between these two viruses in an in vitro system. This coinfection system provides

an interesting lens through which to assess BTV reassortment in general, as BTV-2 remains very limited in its distribution in North America, although it is considered enzootic.[23,24] Thus, the potential for this virus to reassort with other BTVs may lend important information in terms of its overall ability to spread, and could provide insight for our understanding of how incursive BTV strains may intermingle with already enzootic strains to become widespread in a new region.

Materials and Methods

Viruses

Two endemic bluetongue virus strains were used to established single-virus infections or coinfections in vitro. BTV-2 and BTV-10 were obtained from ATCC and had been passaged three and seven times in BHK 21 cells prior to the initiation of the experiment, respectively. The BTV-2 strain was isolated from asymptomatic sentinel cattle in 1982 in Florida and subsequently submitted to ATCC (Bluetongue virus, type 2, ATCC® VR-983™).[25,26] The BTV-10 virus used in this study (Bluetongue virus, type 10, strain 8, ATCC® VR-187™) was originally isolated from a sheep in California in 1952.[27]

These strains were chosen due to their enzootic nature, traceability, and distinguishability using molecular assays. Shotgun metagenomics and bioinformatics approaches have reduced ability to differentiate highly genetically homogenous sequences, as probabilistic assembly algorithms cannot accurately discriminate between identical sequences. We therefore selected this pair of viruses due to their relatively low nucleotide identity that would allow us to rapidly distinguish them using metagenomic sequencing (Table 3.1).

Cell culture

Low-passage BHK 21 cells were maintained in Eagle's Minimum Essential Medium (EMEM) with 10% heat-inactivated fetal bovine serum (FBS), 10% tryptose phosphate broth, and 1% penicillin-streptomycin (10,000 U/ml). Cells were maintained at 37°C with 5% CO_2 and passaged at ~90% confluency every 3-4 days.

Growth curves

BTV-2 and BTV-10 were introduced in duplicate to confluent cultures of BHK 21 cells at a multiplicity of infection (MOI) of 0.2 TCID50/ml. A negative control flask inoculated with an equal volume (1 ml) of EMEM without virus was also included. Viral inoculum was allowed to incubate with cells for 1 hr at 37°C, and then an additional 4 ml of maintenance media was added to each flask. Five hundred µl of cell culture supernatant was collected at 1 hr, 6 hr, 12 hr, 24 hr, 48 hr, and 72 hr post-inoculation and stored at -80°C until further analysis. Tissue culture infectious dose (TCID50) was calculated from the supernatant collected at each time point to characterize the viral growth kinetics of each virus.

Viral passages

Following initial virus characterization, BTV-2 and BTV-10 were used to inoculate flasks of confluent BHK 21 cells in triplicate. To establish single-virus infections, virus was diluted in EMEM to reach an MOI of 0.2 TCID50/ml. One ml of diluted virus was then added to a confluent monolayer of BHK 21 cells in triplicate. To establish coinfections, each virus was diluted to a final MOI of 0.2 TCID50/ml in EMEM and 1 ml of inoculum containing 0.1 TCID50/ml of each virus was added to confluent flasks of BHK-21 cells in triplicate. Another flask of cells was inoculated with EMEM as a negative control. After 1 hr of incubation at 37°C, an additional 4 ml of maintenance media was added to each flask.

Virus was harvested from cell cultures at 72-96 hr post-inoculation, when cytopathic effect (CPE) was approximately 80-90%. Freshly harvested virus was used to initiate the next round of infections on BHK 21 cells immediately following collection. Viruses were passaged blindly so as to avoid freeze-thaw cycles. Three hundred µl of virus was also reserved to perform TCID50s at each passage. Remaining harvested virus was aliquoted into 1 ml vials and stored at -80°C for downstream analysis.

TCID50

TCID50s were performed for viral quantification to determine initial MOI, viral titers during growth curves, and levels of infectious virus at each passage throughout the course of the study. Ten-fold dilutions of virus stocks were prepared in triplicate from 10^{-1} to 10^{-8}. Fifty µl of each dilution of virus (or EMEM for negative controls) was added to a well in a 96-well microtitration plate. BHK 21 cells were seeded at a density of 1.55 x 10^4 cells per well, along with 50 µl of EMEM. Fifty µl of maintenance medium was added to each well at 24 and 72 hr post-inoculation, and plates were stained with crystal violet solution and read at 96 hr. The Reed-Muench equation was used to determine the TCID50/ml for each virus.[28]

qRT-PCR

Nucleic acid was extracted either manually or on the KingFisher Flex robot (Thermo Fisher, Waltham, MA) using Applied Biosystem's MagMAX Pathogen RNA/DNA kit (Foster City, CA) according to manufacturer's instructions.

A pan-BTV qRT-PCR assay targeting segment 10 was performed as described by Ortega et al.[29] Quantitative RT-PCR was performed using SuperScript III Platinum One-Step qRT-PCR reagents (Invitrogen, Carlsbad, CA) at half-reaction volumes, and thermocycling conditions were

carried out as previously described.[29] Samples from each passage were screened throughout the course of the study.

Whole genome sequencing

Samples from passages 1, 3, and 7 were prepared for shotgun metagenomic sequencing. Samples were DNased according to manufacturer's instructions using TURBO DNA-*free* kit (Invitrogen), except the amount of DNase was increased to 4U per sample to maximize DNase activity. Following DNase inactivation, 7.5 M LiCl solution was added to each sample to reach a final concentration of 2.0 M. Samples were incubated for 16-18 hours at 4°C, then centrifuged at 18,000 x *g* at 4°C for 20 min to selectively precipitate single-stranded RNA. Supernatant was subsequently used for downstream whole genome sequencing (WGS). Sample quality was determined with RNA High Sensitivity screentape on the TapeStation 2200 instrument (Agilent, Santa Clara, CA) to estimate RNA integrity and concentration prior to library preparation.

Sample libraries were prepared using KAPA RNA Hyper Prep kit (KAPA Biosystems, Basel, Switzerland) according to instructions, except reagents were used at half-reaction volumes with 5 µl of sample input. Libraries were assessed for DNA quality and concentration using Qubit broad-range or high sensitivity DNA reagents and the Qubit 2.0 fluorometer (Thermo Fisher), followed by High Sensitivity D1000 DNA screentape on the TapeStation 2200 machine. Samples were then pooled and size-selected for inserts from 300-800 basepairs (bp) in length using size fractionation on a 1% agarose gel. The desired region was excised from the gel and QIAquick Gel Extraction kit (Qiagen, Hilden, Germany) was used to purify the pooled DNA according to manufacturer's instructions.

Pooled, size-selected libraries were then re-analyzed using Qubit fluorometer and the TapeStation 2200 system as before. The pooled library was quantified further using KAPA

Library Quantification kit (KAPA Biosystems) according to kit instructions prior to loading on the flowcell. Libraries of approximately ~20 samples were sequenced using NextSeq 2x150 mid-output cartridges (Illumina Inc., San Diego, CA) on the Illumina NextSeq machine.

BTV analysis pipeline and bioinformatics

Consensus sequences of BTV-2 and BTV-10 input strains were determined via our lab's novel BTV bioinformatics pipeline as described in Chapter 5. Viral supernatant harvested from passages 1, 3, and 7 was similarly processed, with some minor changes. Briefly, libraries were demultiplexed and raw reads were trimmed to remove low quality bases and adapter sequences (TrimAL).[30] Cd-hit was then used to eliminate duplicate reads (where two or more reads had ≥ 96% pairwise identity in the first and last 30 base pairs).[31] Reads were aligned to the consensus sequences of the input viruses, BTV-2 and BTV-10, using Bowtie2 with default parameters, except `--end-to-end` and `--very sensitive` modifiers were used to reduce off-target mapping.[32] Finalized sequences were visually inspected in Geneious v. 10.2.2 to confirm alignment and mapping accuracy.

Plaque isolation

To identify the genotype of individual viruses and detect potential occurrences of reassortment, viral stocks harvested from passages 1, 3, and 7 co-infected cultures were serially diluted and used to establish infections on 6-well plates of BHK 21 cells. Six-well plates were set 48 hr prior to virus inoculation, with each well seeded with 1.0×10^5 cells in maintenance media.

Serial ten-fold dilutions of viral stocks from 10^{-1} to 10^{-8} were prepared in EMEM. Five hundred µl per well of 10^{-2} to 10^{-7} viral dilutions were used to inoculate confluent BHK 21 monolayers in duplicate. After 1 hr of incubation at 37°C, cells were washed once with PBS to remove unbound virus and then were overlaid with 2 ml of a 1:3 solution of 2% agarose in

Earle's balanced salt solution (EBSS):maintenance media. Plates were incubated at 37°C with 5% CO_2 for 48-72 hours, when cytopathic effect (CPE) were evident. Once CPE were detected, a second overlay containing 0.1% neutral red in media with agarose was added, after which cells were incubated until discrete plaques were visible.

Plaques were visualized using a transilluminator or by holding the plates up to a light. Individual plaques were picked and propagated once in BHK 21 cells in a 24- or 48-well plate format. Briefly, each agarose plug was added to 100 µl EMEM and 4.65 x 10^4 BHK 21 cells in 300 µl maintenance media in a well and propagated plaques were maintained at 37°C until CPE was complete. Viral supernatant was harvested, aliquoted, and then frozen at -80°C until downstream analyses were carried out.

Amplicon assay

Total nucleic acid from propagated plaques was extracted either manually or on the KingFisher Flex robot using Applied Biosystem's MagMAX Pathogen RNA/DNA kit as described above. Extracted RNA was subsequently used for amplicon-based sequencing to rapidly differentiate which parental strain contributed each of the ten segments comprising the progeny virus. Standards and negative controls were run in duplicate with each plate of samples. Standards were prepared from BTV-2 and BTV-10 stocks with equal Ct values (based on segment 10 qPCR; see above) as follows: standard 1, 100% BTV-2; standard 2, 90% BTV-2/10% BTV-10; standard 3, 50% BTV-2/50% BTV-10; standard 4, 10% BTV-2/90% BTV-10; standard 5, 100% BTV-10. These standards were used to ensure we could reliably detect all ten segments of each virus, as well as establish baseline levels of any off-target mapping that might occur for each virus and segment.

Custom primers incorporating Illumina TruSeq constructs were used to generate amplicons of each BTV segment following the two step PCR assay design described by Galan et al.[33] Illumina's TruSeq adapters were used to design a two-step PCR process to generate barcoded amplicons of each BTV segment. Full-length viral genome sequences of each parental strain were aligned and used to design consensus primers for each segment using the Primer3 plugin in Geneious v.10.2.[34] First round primers were designed to generate amplicons approximately 400-600 bp in length that were genetically distinct between BTV-2 and BTV-10 at multiple sites within the amplified region. These first round primers included two main features: a BTV segment-specific primer region and an adapter sequence complementary to the second round primer set (Appendix 2). Eight base pair dual-indexes were generated for forward and reverse round-two primers (96 unique indexes each) using BARCRAWL (Appendix 2).[35] Individual round-one primer pairs were confirmed to amplify their specific target in each parental genome and pooled equimolar into a 10-plex reaction. An initial test-run of the multiplex PCR with the standard samples (above) was sequenced in the Illumina MiSeq (Illumina, Inc.) and the concentration of each primer pair was adjusted empirically based on the relative efficiently of each primer pair (proportion of reads for each product).

The first round PCR included an initial template denaturation and primer annealing step with 2 µl of sample and 2 µl of 2 µM first-round primer pool heated at 95°C for 5 min and then immediately quenched on ice. The following master mix using components from SuperScript III One-step RT-PCR kit with Platinum Taq (Invitrogen) was then prepared and added to each reaction on ice for reverse transcription and round-one amplification: 5 µl of 2X Reaction Mix, 0.5 µl SuperScript III RT/Platinum Taq mix, 0.5 µl H2O. Thermocycling conditions were as follows: 56°C x 30 min → 94°C x 2 min → 14-16 cycles of [94°C x 15 s + 54°C x 45 s + 68°C x

30 s] → 68°C x 30 sec. Round-one product was treated with Exonuclease 1 from New England Biosciences (Ipswish, MA) according to kit instructions to remove excess primers.

The second round PCR included 1 µl each of forward and reverse barcoded primers (2 µM), in addition to a master mix containing the following components: 1 µl each of i5 and i7 primers (Appendix 2), 0.1 µl Platinum Taq High Fidelity DNA Polymerase (Invitrogen), 3.7 µl H_2O, 1 µl 10X Reaction Buffer, 0.7 µl MgCl2, and 0.5 µl 10 mM dNTP mix. PCR reaction conditions were as follows: 94°C x 2 min → 18-20 cycles of [94°C x 30 s + 52-54°C x 45 s + 72°C x 30 s] → 72°C x 30 s.

Second-round product was quantified using fluorometric quantification with Sybr Green (Thermo Fisher) on a plate reader (EnSpire Multimode Plate Reader, PerkinElmer, Waltham, MA). Up to 96 products were then pooled to approximately equimolar concentrations and purified with Agencourt AMPure XP beads (Brea, CA) (0.6x ratio). The pooled amplicon library was quantified on the Qubit 2.0 fluorometer and visualized using the Agilent TapeStation 2200 prior to KAPA qRT-PCR quantification. Library pools were sequenced on an Illumina MiSeq instrument using either 500 cycle Nano or 300 cycle Micro kits.

Amplicon assay bioinformatics

Illumina reads were demultiplexed with bcl2fastq v2.20.0.422 using default settings.[36] Primer and adapter sequences were trimmed using Cutadapt v1.13, and 3' bases were removed if they were below a minimum quality of Q30.[37] Reads less than 80 bp in length after trimming were removed from further analyses. Trimmed reads were mapped to the parental reference sequences in Bowtie2 v2.3.2 (Appendix 3).[32] Sorted bam files were made in samtools v1.5 and viewed in Geneious v.10.2.2 to confirm accurate mapping of reads to the correct parental strain(s).[38] The reads mapping to each parental strain were quantified and used to determine the

presence of reassortment in progeny viruses (presence of reads mapping to one or segment from both parental strains). Due to the presence of low-level mis-mapping of reads between BTV-2 and BTV-10 for certain segments in the amplicon assay, only plaques with >90% of all reads mapping to one parent segment or the other were included in our final analyses. Viruses with missing segments (i.e., those that did not get reads across all ten segments) were also excluded from downstream analyses.

Relative diversity

Simpson's diversity index was used to estimate the population complexity of viruses isolated from co-infected conditions. This measure is based upon the number of unique genotypes (richness) present in a population, as well as the relative abundance of each (evenness).[39] Simpson's diversity was calculated for each BTV-2+10 replicate from passages 1, 3, and 7 using the following equation: $D = \sum(p_i^2)$ where p_i is the relative abundance of each genotype. To normalize these data to a linear format and to allow for more intuitive comparisons, D for each sample was converted to Hill's N_2, which can be calculated by $N_2 = 1/D$.[40] Hill's N_2, or the effective diversity of the population, represents the number of equally abundant genotypes required to be present to generate the level of diversity detected by Simpson's index.[40,41]

Statistics

Chi-square analysis and Fisher's exact test were performed to determine whether significant trends existed in terms of segment-linkages and reassortment for amplicon-based genotypes, with $p < 0.05$ considered significant. Two-way repeated measures ANOVA with Tukey's post hoc was used to determine whether significant trends in segment frequencies from

metagenomic data occurred across passages, with $p < 0.05$ considered significant. Statistical analyses were carried out with GraphPad Prism v. 8.0.

Results

BTV-2 and BTV-10 share similar growth kinetics in BHK 21 cells

To ensure we did not unfairly bias our coinfection experiment with one virus growing more rapidly than the other, we performed growth curves for both BTV-2 and BTV-10 in BHK 21 cells prior to initiating coinfections. BTV-2 and BTV-10 were propagated in duplicate at an MOI of 0.2 TCID50/ml on BHK 21 cells. Virus supernatant collected at 1, 6, 12, 24, 48, and 72 hours post-infection was titered via TCID50, and constructed growth curves demonstrated that BTV-2 and BTV-10 had similar growth kinetics in the target cell type (BHK 21) (Figure 3.1).

Infectious titer and viral copy number of each replicate was tracked across each passage by TCID50 and qPCR, respectively, and remained relatively constant between replicates and infection conditions (single vs. coinfection) (Appendix 4).

BTV-2 and BTV-10 consensus sequences do not change across passages

Previous studies have reported that BTV remains largely genetically stable across passages in vitro and during experimental transmission in vivo.[13] To understand whether this phenomenon also occurs in BHK 21 cells, which are interferon deficient and hence may provide a permissive environment for genetic diversification, or whether coinfection might drive the occurrence of mutations, we assessed the consensus sequences of BTV-2, BTV-10, and BTV-2+10 at the beginning (passage 0, input viruses) and the end of our passage series (passage 7, output viruses) using whole genome sequencing (WGS).[42] Consensus sequences were constructed for each segment and coding sequences of passage 0 viruses were aligned to those of passage 7 viruses. For certain segments (Table 3.2), full coding sequences could not be

determined due to the very low frequency of these segments in co-infected cultures by passages 3 and 7. There were no consensus changes detected between passages 0 and 7, regardless of infection condition (single vs. coinfection).

Metagenomic sequencing reveals consistent global shifts in segment frequencies during BTV-2 and BTV-10 coinfection

As has been performed for influenza virus, whole genome metagenomic sequencing was used to detect global shifts in segment frequencies during BTV coinfection as an estimator of reassortment trends.[43] BTV-2 and BTV-10 were used to establish coinfections on BHK 21 cells in triplicate at an MOI of 0.2 TCID50/ml for each virus and passaged blindly for seven consecutive passages. Viral supernatant collected from each BTV-2+10 replicate was harvested after passages 1, 3, and 7 and prepared for WGS to assess the segment composition of the viral population present at each time point.

Reads from each sample were aligned to both BTV-2 and BTV-10 via our bioinformatics pipeline (Table 3.2). The number of reads per segment aligning to either parent strain was normalized as a percent by the total number of reads per segment.

Following a single passage in BHK 21 cells, viral populations from BTV-2+10 coinfections demonstrated early, consistent changes in overall segment composition of the viral milieu. While all ten segments from both BTV-2 and BTV-10 were present and well-represented after one passage, all replicates demonstrated a consistent shift towards BTV-2, with approximately ⅔ of reads for each segment aligning to BTV-2, and only ⅓ of reads aligning to BTV-10. This trend occurred across all ten segments in each replicate (mean: 67%, range 60-75%) (Figure 3.2).

By the third passage, marked trends in segment frequencies were more evident, with prominent shifts towards BTV-2 across most segments (Figure 3.2). This was most remarkable for segments 7 and 8, where >98% of reads aligned to BTV-2. Segments 5 and 10 were notable exceptions to this trend, however, maintaining relatively substantial contributions from both BTV-2 (~65% of viral reads) and BTV-10 (~35% of viral reads) within the viral population present at passage 3.

In general, the trends in segment contributions from each BTV parent strain noted at passage 3 persisted after seven passages, with shifts towards BTV-2 becoming more pronounced across most segments. No BTV-10 reads were detected for either segment 7 or 8 in two of three replicates. In one replicate, two segment 7 reads aligned to BTV-10. BTV-2 and BTV-10 contributed roughly equivalent proportions of segment 5 reads, while segment 10 shifted heavily towards BTV-2 (84% of viral reads). In contrast to passage 3, segment 9 demonstrated substantial representation of both parent strains in passage 7.

Two-way repeated measures ANOVA with Tukey's post-hoc to correct for multiple comparisons was used to determine whether shifts in segment frequencies along the course of passages were statistically significant. The overall contribution of BTV-10 segments 1, 2, 3, 4, 7, 8, and 10 significantly decreased from passage 1 to passages 3 and 7 (all $p < 0.05$). Reads aligning to BTV-10 segment 9 were significantly increased from passages 1 and 3 to passage 7 ($p < 0.05$). No significant differences were detected in the number of reads aligning to BTV-10 segment 6 across passages.

Amplicon-based sequencing of individual plaques demonstrates frequent reassortment between BTV-2 and BTV-10

We used a novel, amplicon-based sequencing assay to rapidly differentiate the genotypes of individual viral plaques isolated from passages 1, 3, and 7. Viruses were plaque isolated on BHK 21 cells and then individual plaques were picked and propagated once.

We successfully sequenced 32 plaques from passage 1, 44 plaques from passage 3, and 51 plaques from passage 7 that had a clear genotype across all ten segments (>90% of reads aligning to one parent strain or the other) without evidence of plaque bleed over (Figure 3.3). Similar to our WGS results, we found that no plaques had either segment 7 or 8 contributed by BTV-10 in passages 3 and 7, and that both parental strains of BTV were well-represented across plaques in segments 5 and 9.

Interestingly, although BTV-10 contributed only ~⅓ of segment 10 viral reads in passage 3 and ~⅕ of segment 10 viral reads in passage 7 via metagenomic sequencing, we detected a high frequency of plaques with BTV-10 segment 10 by our plaque assay method (Figure 3.4). We also found that certain segments that were well-represented in our metagenomic sequencing data were not detected by our plaque assay approach; in particular, BTV-10 contributed approximately 40% of segment 6 viral reads in passage 7 according to WGS, but not a single plaque with BTV-10 segment 6 was identified. A similar, although less striking, trend was noted for BTV-10's segment 2. It is important to note that these two "missing" BTV-10 segments were detectable in our amplicon assay positive control standards, as well as in propagated plaques that did not have clear genotypes or appeared to have plaque bleed-over, indicating that viruses with these BTV-10 segments may have had delayed or diminished cytopathic effect on BHK 21 cells.

Diversity indices increase during coinfection, but segment-specific trends are evident in both metagenomic and amplicon-based sequencing assays, demonstrating preferred reassortant segment combinations

To better understand the genetic diversity generated by BTV-2 and BTV-10 coinfection, we calculated Simpson's diversity index and Hill's N_2 for each replicate from passages 1, 3, and 7.[39–41] While all 20 potential segments from BTV-2 and BTV-10 were represented after the first passage, effective diversity was actually quite low due to the large number of plaques that had all ten segments contributed by BTV-2. Although certain BTV-10 segments all but disappeared from co-infected viral populations by passages 3 and 7, effective diversity nevertheless was increased from passage 1 (Figure 3.5).

There were 8 unique genotypes identified in passage 1, 17 in passage 3, and 17 in passage 7 (across all replicates). While the number of unique reassortant viruses was relatively high in passages 3 and 7, there were consistent trends in terms of which segments were involved in reassortment events (segments 5, 9, 10 frequently; segments 1, 3, and 4 infrequently), and these were noted in each replicate. In general, most isolated viruses appeared to have a BTV-2 backbone that occasionally accepted certain BTV-10 segments (Figure 3.3).

Chi-square analysis and Fisher's exact test was used to assess the overall independence of segments 1-10 for BTV-2 and BTV-10 for plaque genotypes identified at passage 7. Highly significant relationships ($p < 0.0009$) were noted between segment 5 and all other segments, except segment 10 (ns). Similarly, segments 9 and 10 exhibited highly significant relationships to all other segments ($p < 0.0001$), except as noted above (s5 and s10, ns) and between s9 and s10 (non-significant).

Discussion

Reassortment amongst bluetongue viruses is a complex phenomenon, and our understanding of the features that drive or restrict the occurrence of reassortment remains limited. Here, we applied whole genome sequencing and a novel, amplicon-based sequencing approach to characterize the occurrence of reassortment between two endemic bluetongue viruses in a relaxed, in vitro system.

We selected BHK 21 cells as our model system for this particular study for two main reasons. First, both BTV-2 and BTV-10 grow similarly in BHK 21 cells, allowing us to avoid unfairly biasing our experiment with one virus simply outcompeting the other. Second, BHK 21 cells are interferon-deficient and therefore provide a relaxed environment for BTV replication.[42] We sought to understand how readily reassortment occurs between these two viruses, so we used a highly permissive in vitro system to simply query the extent to which these viruses share compatible segments.

Our findings highlight the plasticity with which BTV may reassort, given the appropriate conditions. This corroborates the findings of Shaw et al., who investigated reassortment between BTV-1 and BTV-8 in an in vitro system and found that the viruses reassorted extensively.[44] Our work also correlates to the findings of a much earlier series of reassortment studies where BTV-10 (BT-8) and BTV-17 (strain 262) were investigated in Vero cells and in vivo using shifts in electropherotype as a hallmark of reassortment.[15–17,19] These studies found that reassortment occurred readily between BTV-10 and BTV-17 viruses, both in vitro and in vivo.

In their 2013 study, Shaw et al. noted potential trends in terms of which segments were most likely to be detected in reassortant viruses (segments 1, 2, and 7 donated by BTV-8, for instance) after four passages.[44] However, this group concluded overall that reassortment was

highly flexible and no specific trends were apparent during BTV-1 and BTV-8 coinfection. In contrast, we found consistent, repeatable trends in segment frequencies both in our metagenomic sequencing approach and when we assessed the specific composition of individual viruses. These trends were noted after only three passages in BHK 21 cells, and became even more pronounced, albeit with slight shifts, by passage 7. We even found that some segments went "extinct" in our reassortment experiment. All replicates demonstrated highly similar trends at each time point. This suggests that there may be specific, preferred segment combinations that arise during BTV-2 and BTV-10 reassortment, favoring a BTV-2 backbone that accepts certain segments from BTV-10.

In assessing the specific trends that we detected in both our metagenomic sequencing approach and our amplicon-based genotyping assay, one of the most striking findings was that BTV-10 segments 7 and 8 essentially disappeared from the viral milieu over the course of our BTV-2+10 passage series. Remarkably, this occurred despite 100% shared identity at the putative amino acid level between BTV-2 and BTV-10's segment 7. The concurrent disappearance of both of these segments, despite identical BTV-2 and BTV-10 VP7 proteins, suggests an interaction between segments 8 and 7 during viral replication, either at the RNA-RNA level or at the protein-RNA level. The disappearance of BTV-10 segments 7 and 8 may be attributable to some underlying functionality that allows BTV-2's segments 7 and 8 to be selectively incorporated during viral replication and packaging. While segment 8's NS2 protein is known to be an essential component of viral inclusion bodies (VIBs) and plays a key role in recruiting and binding viral ssRNAs for assembly, direct NS2-segment 7 interactions have not been described to date.[45,46]

These findings are also important because they allude to specific segment linkages that might limit the spectrum of fit reassortant viruses that can be generated during BTV coinfection. When Shaw et al. generated mono-reassortants with segments from BTV-1 or BTV-8 onto the reciprocal virus's backbone, they found deleterious effects when BTV-8 segment 7 was incorporated into the BTV-1 backbone.[44] They also found that segment 8 mono-reassortants demonstrated consistently decreased titers 8 hours post infection compared to wild-type viruses. Collectively, these findings suggest that segment 7 and 8 mismatches may negatively affect viral fitness.

BTV-2 and BTV-10 demonstrated distinct cytopathic effect (CPE) phenotypes during infection, with BTV-10 causing profound, rapid cell lysis, and BTV-2 resulting in less profound lysis and comparatively prominent cell rounding and cytomegaly. BTV-2+10 replicates increasingly adopted this BTV-2-like CPE phenotype during the passage series. The BTV-2-like CPE phenotype observed during coinfection may point to the complete incorporation of BTV-2 segment 8 and disappearance of BTV-10 segment 8 by passage 7, as NS2 (encoded by segment 8) has been found to play a key role in disrupting mitosis in BTV-infected cells.[18] Certain strains of BTV have been linked to aberrant mitosis in BHK 21 cells and other cell types (Vero, BPAEC), which was associated with NS2 accumulation near kinetochores.[18] Thus the shift in phenotype observed during BTV-2+10 coinfection may reflect specific properties of the BTV-2 segment 8 protein as it interacts with cell machinery during mitosis, which may represent an adaptive advantage of BTV-2's segment 8 (at least for in vitro propagation).

Metagenomic sequencing also revealed that certain segments from BTV-10 were more likely to reassort onto a BTV-2 backbone than others. Specifically, we saw high frequencies of both BTV-2 and BTV-10 contributing segments 5, 6, and 9 in passage 7 co-infected conditions.

Segment 5 encodes the NS1 protein, which is associated with microtubules and has been shown to enhance BTV translation; segment 6 encodes VP5, one of the two major outer capsid proteins; and segment 9 encodes VP6 and NS4.[47,48] VP6 is the RNA helicase, while NS4 is translated from another open reading frame and acts as an interferon antagonist.[49,50] Specific interactions between these three segments have not been described, nor do these segments share the highest nucleotide or amino acid identity of the ten segments between the BTV-2 and BTV-10 used in our study. At least for segments 5 and 9, it appears that a BTV-2 backbone virus can accept these segments from either parental strain successfully.

As BTV-10 segment 6 was not identified in any of our plaques, it is difficult to draw conclusions about possible linkages between this segment and others. This highlights another key finding from our study – namely, that plaque assays failed to fully capture the genetic diversity present in our viral populations. Individual plaque genotypes largely corresponded with metagenomic sequencing findings, but we found that certain segments that were present at high levels by whole genome sequencing (e.g., BTV-10 segment 6) were not detected among our plaque-isolated viruses. While it is possible that the trends detected via our whole genome sequencing approach were due to the detection of non-viable viruses, we believe it is more likely that the differences between our metagenomic sequencing and plaque-based assays are attributable to inherent variations in the replication kinetics and phenotypes of reassortant viruses. Indeed, the persistence of these segments (e.g.., segment 6 from BTV-10) over multiple passages indicates that viruses carrying these “undetected” segments are either directly viable or viable via complementation with other viruses.

Not only does this emphasize the importance of whole genome sequencing in capturing viral population composition, but it also demonstrates that complete reliance upon plaque assays to understand reassortment may fail to detect important trends in segment frequencies.

Corroborating this further, we found an overrepresentation of reassortant isolates with BTV-10 segment 10. While our WGS data indicated that BTV-10 segment 10 was actually the minor allele present in the population, selection of individual plaques seemed to disproportionately favor plaques with BTV-10 segment 10. In early experiments based on electropherotype using BTV-10 (BT-8) and BTV-17 (strain 262) in Vero cells, Ramig et al. found a higher than expected number of reassortant plaques with BTV-10 segment 10, even when BTV-10 was added at a lower MOI.[17] They also found that segment 8 was significantly more likely to be contributed by the opposite virus (BTV-17). Similar findings were noted in *Culicoides variipennis* (now *sonorensis*) coinfections.[16,17]

The NS3/3a protein, encoded by segment 10, is associated with the development of CPE in mammalian cells, due in part to its viroporin-like activity.[51] Some groups have shown that single-amino acid residue changes in NS3 affect the development of CPE in vitro, as well as the virulence of BTV in IFNAR$^{-/-}$ mice.[52] The frequent detection of plaques with BTV-10 segment 10 in our study and others, therefore, may be related to a more dramatic viroporin activity and CPE phenotype generated by viruses incorporating BTV-10 segment 10 compared to BTV-2's segment 10.

The MOI which we used for coinfection (0.1 TCID50 of each virus) may have impacted the occurrence of reassortment and the segment-specific trends that we detected. For other segmented viruses such as influenza, higher MOIs are linked with increased frequency of reassortment, so we may have detected different trends had we used a different MOI.[53] The

biological relevance of very high MOIs for either mammalian or insect BTV infection is questionable given the small volumes of blood ingested and expectorate released during *Culicoides* feeding. However, repeated experiments with higher MOIs are warranted to investigate this phenomenon further.

In terms of the broader ecological relevance of this work, certain details are of note, particularly in reference to our selection of BTV-2 as one of the two strains used here. BTV-2 was first detected in the U.S. in 1982 in Florida.[25] It has been infrequently identified on subsequent occasions, most commonly in Florida and the southeast.[23,54,55] In 2010, BTV-2 was isolated from a dairy heifer in California, leading to concerns about the expansion of this virus throughout more of North America.[24,56] BTV-2 is now considered enzootic in the U.S., but it has remained limited in its distribution. While underlying causes remain poorly understood, various factors including reduced vector competence of *C. sonorensis* – the predominant vector species of BTV in the U.S. – for BTV-2 likely contribute to this phenomenon.[23,24,57] Importantly, our finding of reassortment between BTV-2 and BTV-10 indicates that this virus has the ability to reassort with other enzootic strains of BTV, potentially allowing for expansion of a reassortant BTV-2 to areas where this virus has previously failed to circulate. Vector competence studies focusing on reassortant BTV-2 viruses are necessary to better estimate the risk that this poses.

The ATCC strain of BTV-2 has not been fully sequenced prior to this study, although it is putatively related to the OnaB strain of BTV-2, one of two BTV-2 electropherotypes isolated from sentinel cattle in Florida in 1982.[25,26] Various groups have sequenced portions of the OnaB BTV-2, although the putative OnaB strain was isolated multiple times from different animals in 1982 and 1983 (and again, later in Florida), and it is not clear whether all "1982 OnaB" strains are identical at the nucleotide level (despite their shared electropherotype).[23,26,54,58,59] Whole

genome sequencing of BTV-2 VR-983 revealed high identity with the 2010 BTV-2 isolate from California (GenBank: JQ822248-JQ822257) across all ten genome segments (99.8-100% nucleotide identity).[24] Consistent with the findings for BTV-2 California 2010, our sequences for BTV-2 VR-983 were nearly identical to the reported sequences for BTV-2 Florida 1982 OnaB across segments 4-10, while segments 1, 2, and 3 were not.[24] However, the identities of the specific, U.S.-origin BTV-2 viruses used to generate some of the sequences for segments 1-3 are not always clear.[59–61] This highlights the important role that WGS can play in establishing the genetic identity of all ten segments of BTV's dsRNA, and refines our ability to characterize the various BTV-2 strains that were originally isolated from 1982 Florida samples by a variety of techniques. The whole genome sequence determined for the ATCC strain of BTV-2 (VR-983) – which was last propagated in our lab in 2005 – is >99.8% identical to the 2010 California isolate of BTV-2, suggesting that this particular BTV-2 strain has been present in the U.S. prior to its initial detection on a California dairy in 2010.

Finally, metagenomic sequencing coupled with amplicon-based genotyping of plaques is a highly useful approach for investigating reassortment in a rapid, cost-efficient manner. Our findings highlight the utility of WGS in reassortment studies, especially when considering viruses with a relatively large number of segments, such as those in the family *Reoviridae*. BTV, with ten genome segments, can generate up to 1,024 possible reassortants in the case of two co-infecting viruses. Robust analysis of population make-up during BTV coinfection using standard plaque assay-based methods thus requires thousands of individual plaques to be genotyped, rapidly becoming both labor- and cost-prohibitive in most cases. Even then, this premise is based on the assumption that all viable viruses generate plaques on the selected cell type, which is not necessarily valid. As such, WGS becomes a useful tool for detecting population-wide shifts in

segment frequencies secondary to coinfection and provides a lens into potential reassortment events that arise, broadening our understanding of the global segment trends that accompany this important feature of segmented viruses.

Table 3.1 – Pairwise Identity of BTV-2 and BTV-10.

	S1	S2	S3	S4	S5	S6	S7	S8	S9	S10
% Nucleotide Identity	89.2%	52.4%	93.2%	89.7%	91.6%	69.4%	93.7%	89.3%	88.1%	81.9%
% Amino acid Identity	97.8%	40.9%	99.6%	96.4%	97.3%	77.9%	100%	90.4%	86.9%	93.9%

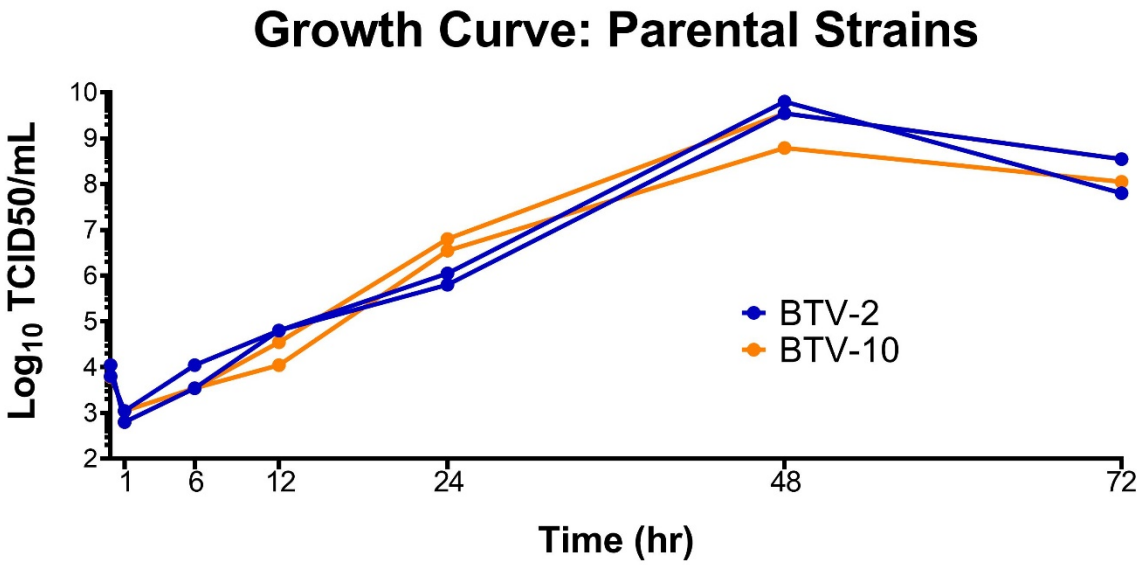

Figure 3.1 – Parental Strains have Similar Growth Kinetics. BTV-2 and BTV-10 demonstrate similar growth kinetics in BHK 21 cells. Growth curves were performed in duplicate, with a starting MOI of 0.2 TCID50/ml. Supernatant was collected at 1, 6, 12, 24, 48, and 72 hr post infection and TCID50s were performed at each time point to determine infectious titer.

Table 3.2 – Coding Sequence Coverage, All Samples. CDS = coding sequence.

		% CDS coverage, BTV-2			% CDS coverage, BTV-10			Total reads, BTV-2			Total reads, BTV-10			Mean CDS depth, BTV-2			Mean CDS depth, BTV-10		
Passage	Segment	2+10A	2+10B	2+10C	2+10A	2+10B	2+10C	2+10A	2+10B	2+10C	2+10A	2+10B	2+10C	2+10A	2+10B	2+10C	2+10A	2+10B	2+10C
1	1	100%	100%	100%	100%	100%	100%	3655	2466	3461	1851	1240	1966	119	81	116	60	41	65
	2	100%	100%	100%	100%	100%	100%	2822	2023	4236	1509	1025	2190	124	90	192	66	47	99
	3	100%	100%	100%	100%	100%	100%	2677	1962	2661	1455	1104	1795	126	93	128	68	53	86
	4	99.9%	99.9%	99.5%	99.8%	99.7%	99.9%	1866	1392	1800	915	610	762	121	92	119	59	41	51
	5	100%	100%	100%	100%	100%	100%	3966	3046	4805	2129	1848	2512	299	259	368	161	141	193
	6	100%	100%	100%	100%	100%	100%	2697	2015	3793	1482	1153	1274	214	163	310	119	94	105
	7	100%	100%	100%	100%	100%	100%	2724	2371	2744	930	865	1191	323	282	329	110	105	144
	8	100%	100%	100%	100%	100%	100%	4028	3481	4660	1772	1414	1841	466	408	555	207	171	223
	9	100%	100%	100%	100%	100%	100%	4492	3474	4862	2324	1667	2256	550	430	621	282	208	286
	10	100%	100%	100%	100%	100%	100%	1577	1243	2036	1014	836	1156	274	221	371	188	158	217
3	1	100%	99.9%	100%	99.8%	97.8%	99.9%	1640	1453	1253	345	325	262	53	47	41	11	10	9
	2	100%	100%	100%	99.97%	99.9%	100%	1083	1024	921	355	309	246	48	45	41	16	14	11
	3	99.8%	100%	100%	99.90%	100%	100%	1093	1000	835	266	247	165	51	46	39	12	11	8
	4	99.8%	99.7%	99.0%	99.4%	95.8%	99.5%	903	952	795	138	146	129	59	62	52	9	10	9
	5	100%	100%	100%	99.4%	99.7%	100%	1718	1818	1589	914	1040	779	130	136	120	67	76	59
	6	100%	100%	100%	100%	100%	97.7%	1349	1575	1377	285	250	215	106	124	110	23	20	18
	7	100%	100%	100%	97%	100%	79.6%	1433	1824	1352	32	30	25	168	217	159	4	4	3
	8	100%	100%	100%	83.1%	71.5%	93.2%	2600	3081	2517	32	23	32	303	355	298	4	3	4
	9	100%	100%	100%	100%	100%	100%	2610	3123	2372	655	934	634	318	380	297	78	113	78
	10	100%	100%	100%	100%	100%	100%	596	725	593	331	435	327	102	127	106	62	82	59
7	1	100%	100%	98.6%	98.9%	99.9%	84%	664	1389	307	153	298	69	22	45	10	5	10	2
	2	100%	100%	100%	98%	97.8%	79.4%	509	961	216	112	223	65	22	42	10	5	10	3
	3	100%	100%	100%	80.9%	95.6%	57.9%	590	1099	231	61	108	37	28	51	11	3	5	2
	4	100%	100%	99.7%	91.3%	91.6%	48.7%	450	886	181	50	65	17	30	58	11	3	4	1
	5	99.6%	100%	100%	100%	100%	100%	357	645	157	455	706	184	26	48	11	34	53	14
	6	100%	100%	100%	100%	100%	100%	300	565	121	153	426	107	24	44	9	13	34	9
	7	100%	100%	100%	ND	21.7%	ND	538	852	261	ND	2	ND	59	97	28	ND	0	ND
	8	100%	100%	100%	ND	ND	ND	1018	1792	448	ND	ND	ND	118	210	50	ND	ND	ND
	9	99.8%	100%	100%	99.8%	100%	99.8%	224	537	105	207	479	111	27	65	13	25	59	13
	10	100%	100%	100%	100%	100%	99.4%	278	532	153	42	94	35	49	90	24	8	17	7

ND = not detected.

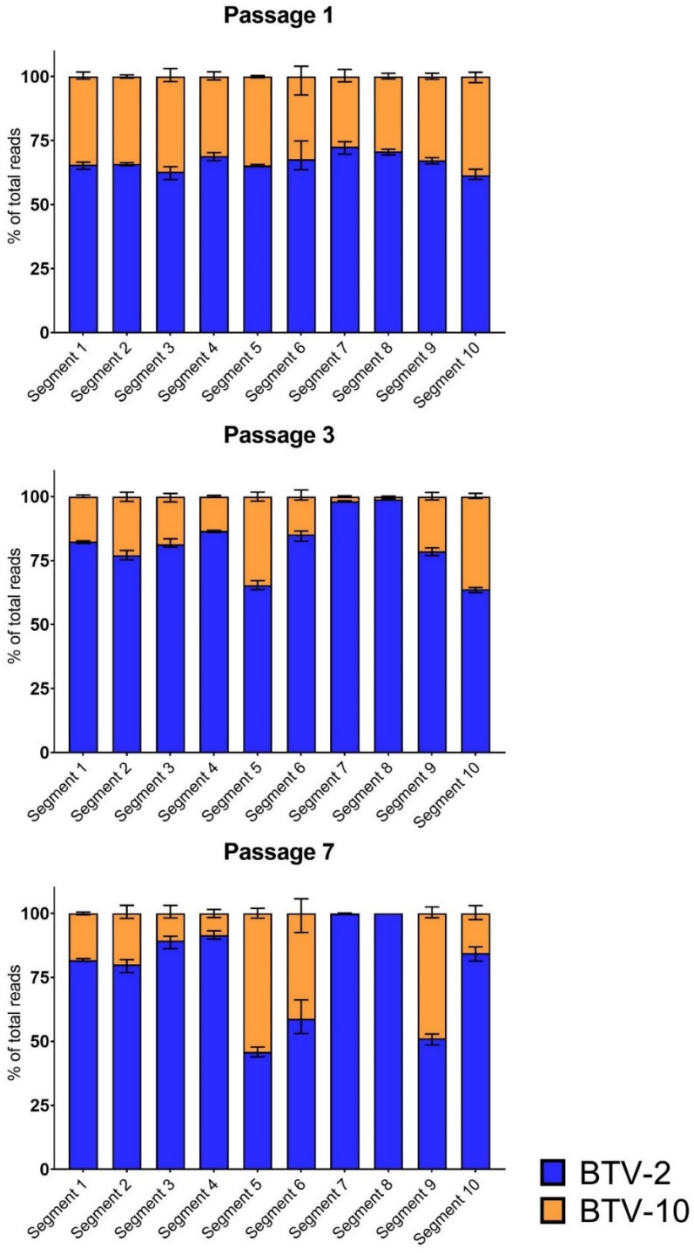

Figure 3.2 – Whole Genome Sequencing Reveals Global Shifts in Segment Frequencies. Metagenomic sequencing shows distinct trends across segments 1-10 during BTV-2+10 coinfection over seven passages. Percent of total viral reads per segment aligning to either input strain are shown. Error bars depict mean and range across replicates.

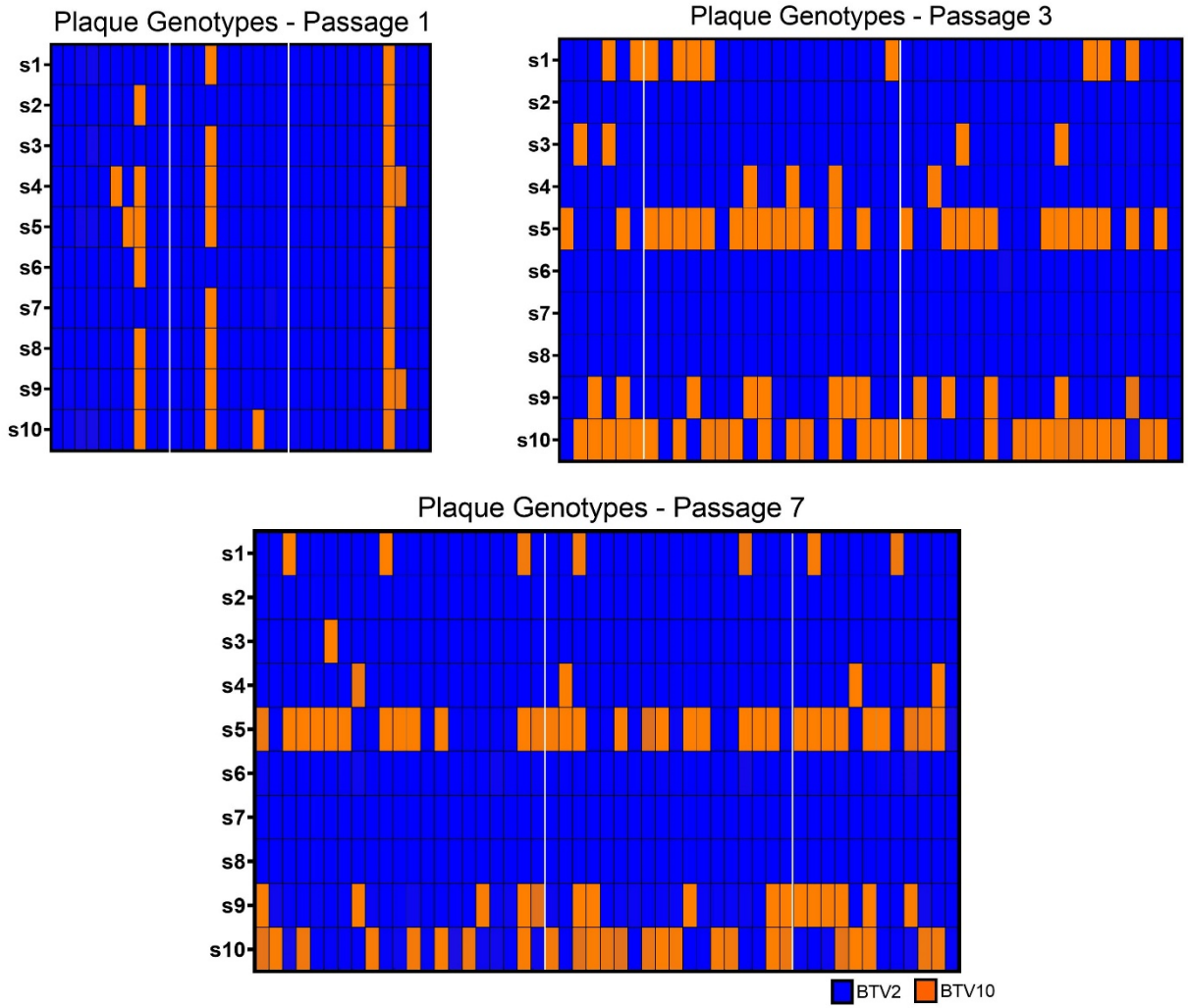

Figure 3.3 – Plaque Genotypes Demonstrate Selection for BTV-2 Segments. Plaque genotypes from passages 1, 3, and 7 demonstrate a dominant BTV-2 backbone that accepts certain segments from BTV-10. Each column represents the full ten segments of an individual plaque. Plaques isolated from each replicate are demarcated by white margins.

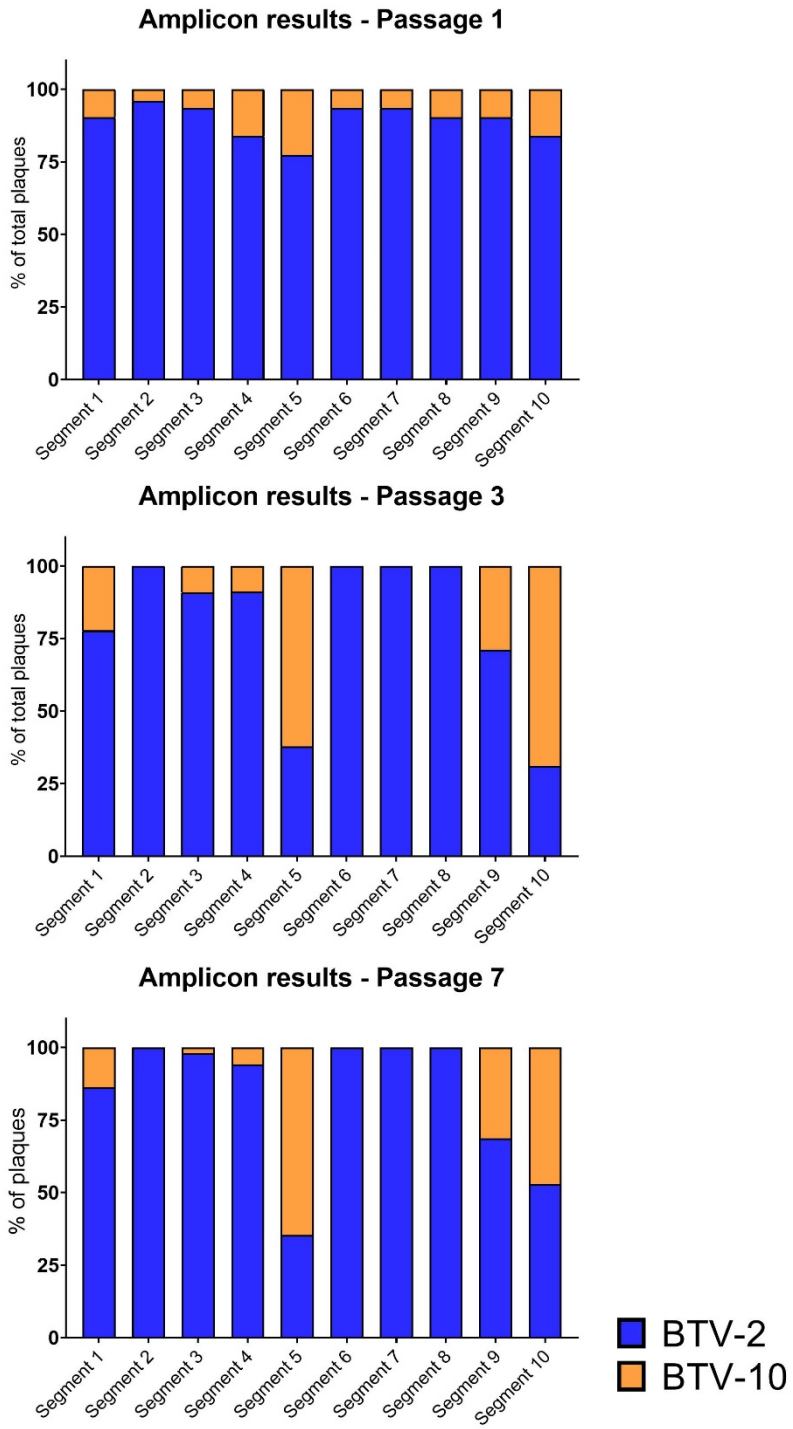

Figure 3.4 – Amplicon-based Genotyping Corroborates Metagenomic Sequencing Trends, but Reveals Potential Biases of Plaque Assays. Cumulative data across all coinfection replicates was used to create relative % of plaques with each segment represented by either input virus (BTV-2 vs. BTV-10).

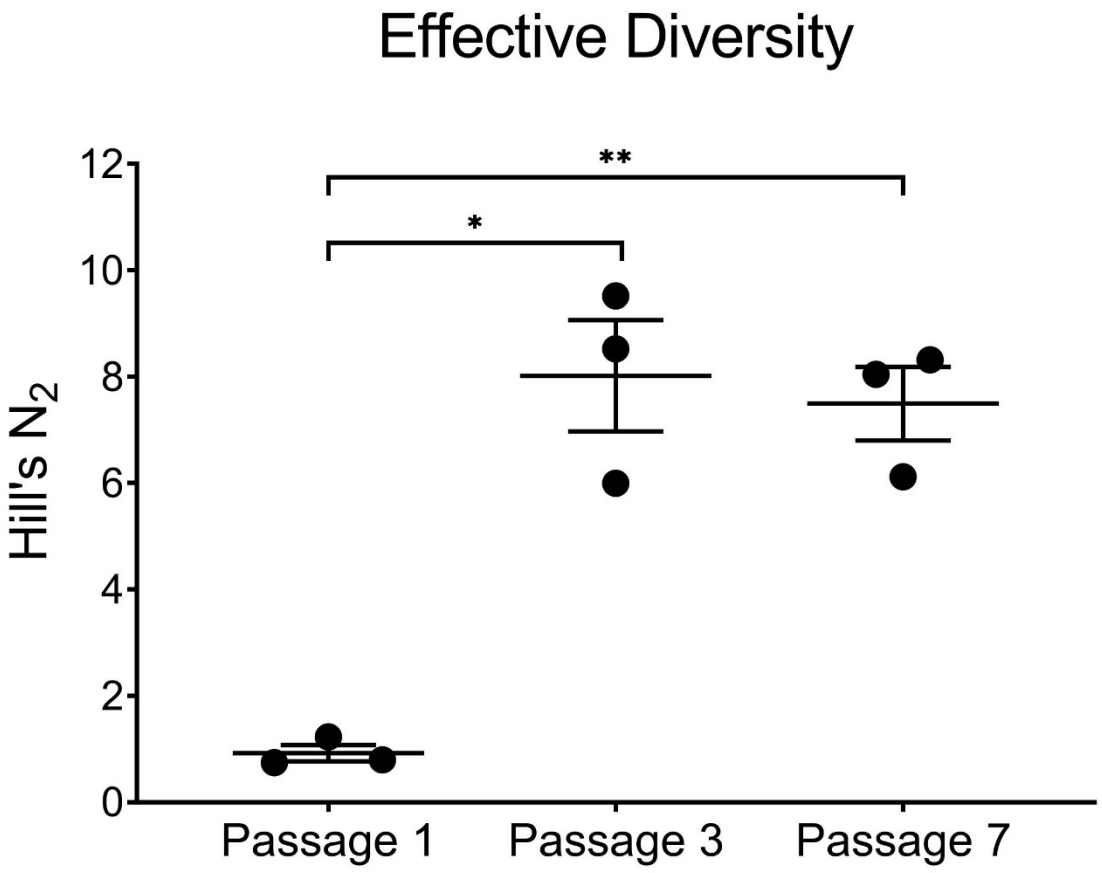

Figure 3.5 – Effective Diversity Increases by Passages 3 and 7. Hills N_2 and effective diversity is increased by passages 3 and 7 in co-infected cultures (* $p = 0.02$, ** $p = 0.009$; paired t-test). Each replicate is depicted, with mean and standard deviation shown for each passage.

REFERENCES

1. Maclachlan NJ, Mayo CE, Daniels PW, Savini G, Zientara S, Gibbs EPJ. Bluetongue. *Rev Sci Tech*. 2015;34(2):329-340. doi:doi.org/10.20506/rst.34.2.2360.

2. Maclachlan NJ, Zientara S, Wilson WC, Richt JA, Savini G. Bluetongue and epizootic hemorrhagic disease viruses: recent developments with these globally re-emerging arboviral infections of ruminants. *Curr Opin Virol*. 2019;34:56-62. doi:10.1016/j.coviro.2018.12.005.

3. Paul E, Gibbs J, Greiner EC. The epidemiology of bluetongue. *Comp Immun Microbiol Infect Dis*. 1994;17(4):207-220.

4. Baylis M, O'Connel L, S. MP. Rates of bluetongue virus transmission between *Culicoides sonorensis* and sheep. *Med Vet Entomol*. 2008;22(3):228-237. doi:10.1111/j.1365-2915.2008.00732.x.

5. Niedbalski W. The evolution of bluetongue virus: genetic and phenotypic diversity of field strains. *Pol J Vet Sci*. 2013;16(3):611-616. doi:10.2478/pjvs-2013-0086.

6. Wilson A, Mellor P. Bluetongue in Europe: vectors, epidemiology and climate change. *Parasitol Res*. 2009;103(Suppl 1):S69-S77. doi:10.1007/s00436-008-1314-8.

7. Matsuo E, Roy P. Bluetongue virus VP1 polymerase activity in vitro: template dependency, dinucleotide priming and cap dependency. *PLoS One*. 2011;6(11). doi:10.1371/journal.pone.0027702.

8. Lauring AS, Frydman J, Andino R. The role of mutational robustness in RNA virus evolution. *Nat Rev Microbiol*. 2013;11:327-336. doi:10.1038/nrmicro3003.

9. Smith EC. The not-so-infinite malleability of RNA viruses: viral and cellular determinants of RNA virus mutation rates. *PLos Pathog*. 2017;13(4). doi:10.1371/journal.ppat.1006254.

10. Lauring AS, Andino R. Quasispecies theory and the behavior of RNA viruses. *PLoS Pathog*. 2010;6(7). doi:10.1371/journal.ppat.1001005.

11. Ciota AT, Kramer LD. Insights into arbovirus evolution and adaptation from experimental studies. *Viruses*. 2010;2(12):2594. doi:10.3390/V2122594.

12. Jenkins GM, Rambaut A, Pybus OG, Holmes EC. Rates of molecular evolution in RNA viruses: a quantitative phylogenetic analysis. *J Mol Evol*. 2002;54:156-165. doi:10.1007/s00239-001-0064-3.

13. Bonneau KR, Mullens BA, Maclachlan NJ. Occurrence of genetic drift and founder effect during quasispecies evolution of the VP2 and NS3/NS3A genes of bluetongue virus upon passage between sheep, cattle, and *Culicoides sonorensis*. *J Virol*. 2001;75(17):8298-8305. doi:10.1128/JVI.75.17.8298-8305.2001.

14. Caporale M, Di Gialleonorado L, Janowicz A, et al. Virus and host factors affecting the clinical outcome of bluetongue virus infection. *J Virol*. 2014;88(18):10399-10411. doi:10.1128/JVI.01641-14.

15. Samal SK, Livingston CW, Mcconnell S, Ramig RF. Analysis of mixed infection of sheep with bluetongue virus serotypes 10 and 17: evidence for genetic reassortment in the vertebrate host. *J Virol*. 1987;61(4):1086-1091.

16. Samal BK, El Hussein A, Holbrook FR, Beaty BJ, Ramig RF. Mixed infection of *Culicoides variipennis* with bluetongue virus serotypes 10 and 17: evidence for high frequency reassortment in the vector. *J Gen Virol*. 1987;68:2319-2329.

17. Ramig RF, Garrison C, Chen D, Bell-Robinson D. Analysis of reassortment and superinfection during mixed infectino of Vero cells with bluetongue virus serotypes 10 and 17. *J Gen Virol*. 1989;70:2595-2603.

18. Shaw AE, Brüning-Richardson A, Morrison EE, et al. Bluetongue virus infection induces aberrant mitosis in mammalian cells. *Virol J*. 2013;10(319). doi:10.1186/1743-422X-10-319.

19. El Hussein A, Ramig RF, Holbrook FR, Beaty BJ. Asynchronous mixed infection of *Culicoides variipennis* with bluetongue virus serotypes 10 and 17. *J Gen Virol*. 1989;70:3355-3362.

20. Nomikou K, Hughes J, Wash R, et al. Widespread reassortment shapes the evolution and epidemiology of bluetongue virus following European invasion. *PLoS Pathog*. 2015;11(8). doi:10.1371/journal.ppat.1005056.

21. Schirtzinger EE, Jasperson DC, Ostlund EN, Johnson DJ, Wilson WC. Recent US bluetongue virus serotype 3 isolates found outside of Florida indicate evidence of reassortment with co-circulating endemic serotypes. *J Gen Virol*. 2018;99(2):157-168. doi:10.1099/jgv.0.000965.

22. Greenbaum BD, Li O, Poon L, Levine AJ, Rabadan R. Viral reassortment as an information exchange between viral segments. *Proc Nat Acad Sci*. 2012;109(9):3341-3346. doi:10.1073/pnas.1113300109.

23. Mecham JO, Johnson DJ. Persistence of bluetongue virus serotype 2 (BTV-2) in the southeast United States. *Virus Res*. 2005;113:116-122. doi:10.1016/J.VIRUSRES.2005.04.022.

24. Gaudreault NN, Mayo CE, Jasperson DC, et al. Whole genome sequencing and phylogenetic analysis of bluetongue virus serotype 2 strains isolated in the Americas including a novel strain from the western United States. *J Vet Diagn Invest*. 2014;26(4):553-557. doi:10.1177/1040638714536902.

25. Gibbs EP, Greiner EC, Taylor WP, Barber TL, House JA, Pearson JE. Isolation of bluetongue virus serotype 2 from cattle in Florida: serotype of bluetongue virus hitherto unrecognized in the Western Hemisphere. *Am J Vet Res*. 1983;44(12):2226-2228.

26. Barber T, Collisson E. Implications of a new bluetongue serotype for the U.S. livestock industry. *Proc Annu Meet US Anim Health Assoc*. 1983;87:90-104.

27. McKercher DG, McGowan B, Howarth JA, Saito JK. A preliminary report on the isolation and identification of the bluetongue virus from sheep in California. *J Am Vet Med Assoc*. 1953;122(913):300-301.

28. Reed LJ, Muench H. A simple method of estimating fifty percent endpoints. *Am J Epidemiol*. 1938;27(3):493-497. doi:10.1093/oxfordjournals.aje.a118408.

29. Ortega J, Crossley B, Dechant JE, Drew CP, MacLachlan NJ. Fatal bluetongue virus infection in an alpaca (*Vicugna pacos*) in California. *J Vet Diagn Invest*. 2010;22:134-136. doi:10.1177/104063871002200129.

30. Capella-Gutiérrez S, Silla-Martínez JM, Gabaldón T. trimAl: a tool for automated alignment trimming in large-scale phylogenetic analyses. *Bioinformatics*. 2009;25(15):1972-1973. doi:10.1093/bioinformatics/btp348.

31. Fu L, Niu B, Zhu Z, Wu S, Li W. CD-HIT: accelerated for clustering the next-generation sequencing data. *Bioinformatics*. 2012;28(23):3150-3152. doi:10.1093/bioinformatics/bts565.

32. Langmead B, Salzberg SL. Fast gapped-read alignment with Bowtie 2. *Nat Methods*. 2012;9(4):357-359. doi:10.1038/nmeth.1923.

33. Galan M, Pons J-B, Tournayre O, et al. Metabarcoding for the parallel identification of several hundred predators and their prey: Application to bat species diet analysis. *Mol Ecol Resour*. 2018;18(3):474-489. doi:10.1111/1755-0998.12749.

34. Untergasser A, Cutcutache I, Koressaar T, et al. Primer3-new capabilities and interfaces. *Nucleic Acids Res*. 2012;40(15). doi:10.1093/nar/gks596.

35. Frank DN. BARCRAWL and BARTAB: software tools for the design and implementation of barcoded primers for highly multiplexed DNA sequencing. *BMC Bioinformatics*. 2009;10(362). doi:10.1186/1471-2105-10-362.

36. bcl2fastq2 Conversion Software v2.20. 2019. www.illumina.com/company/legal.html.

37. Martin M. Cutadapt removes adapter sequences from high-throughput sequencing reads. *EMBnet J*. 2011;17(1):10-12. doi:doi.org/10.14806/ej.17.1.200.

38. Li H, Handsaker B, Wysoker A, et al. The sequence alignment/map format and SAMtools. *Bioinformatics*. 2009;25(16):2078-2079. doi:10.1093/bioinformatics/btp352.

39. Simpson E. Measurement of diversity. *Nature*. 1949;163:688.

40. Hill MO. Diversity and evenness: a unifying notation and its consequences. *Ecology*. 1973;54(2):427-432. doi:10.2307/1934352.

41. Richard M, Herfst S, Tao H, Jacobs NT, Lowen AC. Influenza A virus reassortment is limited by anatomical compartmentalization following coinfection via distinct routes. *J Virol*. 2018;92(5). doi:10.1128/JVI.02063-17.

42. Otsuki K, Yamamoto H, Tsubokura M. Studies on avian infectious bronchitis virus. *Arch Virol*. 1979;60:25-32.

43. Zeldovich KB, Liu P, Renzette N, et al. Positive selection drives preferred segment combinations during influenza virus reassortment. *Mol Biol Evol*. 2015;32(6):1519-1532. doi:10.1093/molbev/msv044.

44. Shaw AE, Ratinier M, Nunes SF, et al. Reassortment between two serologically unrelated bluetongue virus strains is flexible and can involve any genome segment. *J Virol*. 2013;87(1):543-557. doi:10.1128/JVI.02266-12.

45. Kar A, Bhattacharya B, Roy P. Bluetongue virus RNA binding protein NS2 is a modulator of viral replication and assembly. *BMC Mol Biol*. 2007;8(1):4. doi:10.1186/1471-2199-8-4.

46. Lymperopoulos K, Noad R, Tosi S, Nethisinghe S, Brierley I, Roy P. Specific binding of bluetongue virus NS2 to different viral plus-strand RNAs. *Virology*. 2006;353:17-26. doi:10.1016/j.virol.2006.04.022.

47. Boyce M, Celma CCP, Roy P. Bluetongue virus non-structural protein 1 is a positive regulator of viral protein synthesis. *Virol J*. 2012;9(178). doi:10.1186/1743-422X-9-178.

48. Mertens PP, Pedley S, Cowley J, et al. Analysis of the roles of bluetongue virus outer capsid proteins VP2 and VP5 in determination of virus serotype. *Virology*. 1989;170(2):561-565.

49. Sung PY, Vaughan R, Rahman SK, et al. The interaction of bluetongue virus VP6 and genomic RNA is essential for genome packaging. *J Virol*. 2019;93(5):e02023-18. doi:10.1128/JVI.02023-18.

50. Ratinier M, Shaw AE, Barry G, et al. Bluetongue virus NS4 protein is an interferon antagonist and a determinant of virus virulence. *J Virol*. 2016;90(11):5427-5439. doi:10.1128/JVI.00422-16.

51. Han Z, Harty RN. The NS3 protein of bluetongue virus exhibits viroporin-like properties. *J Biol Chem*. 2004;279(41):43092-43097. doi:10.1074/jbc.M403663200.

52. Ftaich N, Ciancia C, Viarouge C, et al. Turnover rate of NS3 proteins modulates bluetongue virus replication kinetics in a host-specific manner. *J Virol*. 2015;89(20):10467-10481. doi:10.1128/JVI.01541-15.

53. Marshall N, Priyamvada L, Ende Z, Steel J, Lowen AC. Influenza virus reassortment occurs with high frequency in the absence of segment mismatch. *PLoS Pathog*. 2013;9(6). doi:10.1371/journal.ppat.1003421.

54. Collisson EW, Barber TL, Paul E, Gibbs J, Greiner EC. Two electropherotypes of bluetongue virus serotype 2 from naturally infected calves. *J Gen Virol*. 1985;66:1279-1286.

55. Collisson EW, Barber TL. Isolation and identification of bluetongue virus: a serotype new to the U.S. *Prog Clin Biol Res*. 1985;178:319-327.

56. Maclachlan NJ, Wilson WC, Crossley BM, et al. Novel serotype of bluetongue virus, western North America. *Emerg Infect Dis*. 2013;19(4):665-666. doi:10.3201/eid1904.120347.

57. Tanya VN, Greiner EC, Shroyer DA, Gibbs EPJ. Vector competence parameters of *Culicoides variipennis* (Diptera: Ceratopogonidae) for bluetongue virus serotype 2. *J Med Entomol*. 1993;30(1):204-208.

58. Bonneau KR, Zhang N, Zhu J, et al. Sequence comparison of the L2 and S10 genes of bluetongue viruses from the United States and the People's Republic of China. *Virus Res*. 1999;61(2):153-160. doi:10.1016/S0168-1702(99)00034-9.

59. Guang-Yuh H, Ming X, Li JK. Analyses and conservation of sequences among the cognate L3 segments of the five United States bluetongue viruses. *Virus Res*. 1994;32(3):381-389. doi:10.1016/0168-1702(94)90086-8.

60. Kowalik TF, Yang YY, Li JK. Molecular cloning and comparative sequence analyses of bluetongue virus S1 segments by selective synthesis of specific full-length DNA copies of dsRNA genes. *Virology*. 1990;177(2):820-823. doi:10.1016/0042-6822(90)90557-8.

61. Hwang GY, Chiou JF, Yang YY, Li JK. High-sequence conservation among the United States bluetongue viruses cognate M2 genes which encode the nonstructural NS1 tubule protein. *Virology*. 1993;192(1):321-327. doi:10.1006/viro.1993.1036.

CHAPTER 4 –INFECTION OF *CULICOIDES SONORENSIS* WITH ENDEMIC STRAINS OF BLUETONGUE VIRUS DEMONSTRATES TEMPERATURE- AND VIRUS-SPECIFIC EFFECTS ON VIROGENESIS

Introduction

Arboviruses represent one of several important types of pathogens anticipated to increase in range and frequency with the progression of climate change.[1,2] These viruses are transmitted by arthropod vectors and represent an emergent disease threat to both human and animal populations in many parts of the world. Bluetongue virus (BTV), the type species of genus *Orbivirus* (family *Reoviridae*), is an arboviral disease of ruminants that is transmitted by biting midges of the *Culicoides* genus (Diptera: Ceratopogonidae). BTV can affect both wild and domestic ruminants and severe disease is characterized by symptoms reflective of the virus's ability to cause profound vasculitis.[3] Animals may develop high fevers, edema, coronitis, mucosal erosions, and respiratory distress, among other signs.[4] Production declines, animal losses, and trade restrictions contribute to BTV's significant economic impact.[5]

BTV has classically been distributed throughout much of the tropics and subtropics, with seasonal circulation in more temperate regions ranging from approximately 35° South to 40° North.[6,7] The virus's range is defined by the presence of any of a large number of competent vector species of the genus *Culicoides*. More than 1,300 species of *Culicoides* exist worldwide, but to date only approximately 30 species have been demonstrated to transmit BTV.[8–10] Of the numerous species of *Culicoides* present in North America (>150), only a handful are considered to be key BTV vectors.[11,12] These include *Culicoides sonorensis*, which is the predominant BTV vector in North America, and *C. insignis*.[13–16] While *C. sonorensis* is distributed throughout

much of the United States (U.S.), *C. insignis* localizes to the southeast U.S., predominantly Florida.[17]

BTV serotype is defined by the VP2 outer capsid protein, which is the major antigenic determinant of this virus. Of 29 currently described serotypes of BTV, *C. sonorensis* and *C. insignis* are implicated in the spread of five enzootic serotypes found in North America: BTV-2, BTV-10, BTV-11, BTV-13, and BTV-17.[18] BTV-3 is considered an exotic serotype, but recently seems to have established a presence throughout the southeastern and central regions of the U.S.[19]

The VP2 protein is encoded by one of ten genomic segments of double-stranded RNA (segment 2) that make up the BTV genetic structure. BTV's segmented genome provides this virus and related viruses an additional mechanism of genetic diversification beyond the accumulation of mutations or recombination. Reassortment is a phenomenon that can occur during coinfection, where progeny viruses inherit genome segments from more than one parent virus.[20] Reassortment plays an important role in the overall genetic diversification of bluetongue virus and its relatives, as has been demonstrated both in vitro and in vivo.[21–28] While reassortment is known to occur in both the insect vector and ruminant hosts, the features that contribute to and modulate the occurrence of this phenomenon are only somewhat understood.

Various groups have shown that climatic conditions such as temperature have an important effect on vectorial life traits and the rate of BTV virogenesis in the vector, with higher temperatures being associated with more rapid BTV replication.[29–32] This is important for a number of reasons in terms of ensuring accurate predictive strategies and mitigation efforts (i.e., predicting BTV circulation during peak temperature seasons), in addition to assessing the

potential impacts of progressive climate change. Warmer climates are likely to result in shifts in vector distributions and may enhance BTV transmission.

How temperature affects viral reassortment in the vector is unknown. More rapid virogenesis at higher temperatures would presumably be associated with increased rates of viral reassortment, but this has not been investigated. The potential for extensive BTV reassortment and its association with temperature could significantly impact surveillance and mitigation strategies, as well as our understanding of how BTV may spread to naive populations and the likelihood of reassortant BTV viruses affecting animals in otherwise enzootic areas.

Here, we investigate the effect of temperature on the reassortment of two enzootic BTV strains – BTV-2 and BTV-10 – in laboratory-reared *Culicoides sonorensis*. Among other things, we find that BTV-2 replicates poorly in *C. sonorensis*, highlighting potential reasons why this BTV serotype has failed to expand widely across North America despite its persistence in the Southeast. However, in some instances, BTV-2 did appear to replicate, particularly when *C. sonorensis* were infected at higher titers of virus. When taken together with other work from our lab that BTV-2 and BTV-10 can reassort readily in vitro, these findings indicate that reassortment between BTV-2 and BTV-10 may not only be feasible, but may provide an opportunity for segments from BTV-2 to become more widespread in North America.

Materials and Methods

Viruses

BTV-10 California 1952 (strain 8, ATCC VR-187) and BTV-2 Florida 1982 (ATCC VR-983) were obtained from ATCC and had been passed eight times and four times in BHK 21 cells, respectively.[33–35] Whole genome sequences of each virus were previously determined by our lab (Chapter 3).

Infectious titers were estimated via 50% tissue culture infectious dose (TCID50). Briefly, ten-fold dilutions of each virus were prepared and 50 µl of each dilution was introduced in triplicate to a 96-well microtitration plate. BHK 21 cells were added (1.55×10^4 cells per well) along with 50 µl EMEM, and virus and cells were incubated at 37°C with 5% CO_2 for 96 hours. At 96 hrs, cells were stained with crystal violet solution, and infectious titer of each virus was determined using the Reed-Muench equation.[36]

BTV-2 and BTV-10 infection in Culicoides cell line

Previous results from our lab show that BTV-2 and BTV-10 grow similarly and are able to reassort in BHK 21 cells. However, since this may be a cell-type specific phenomenon, we opted to examine the replication kinetics of these viruses in CuVaW3 cells as a way to better estimate the overall susceptibility of *Culicoides sonorensis* to BTV-2 and BTV-10.[37]

The CuVaW3 line is derived from *Culicoides sonorensis* embryos from the Ausman colony, which was isolated in Weld Co., Colorado.[37] One-step viral growth curves were performed for each virus at an MOI of ~0.2 TCID50. BTV-2 and BTV-10 were used to inoculate confluent monolayers of CuVaW3 cells in duplicate. One ml of inoculum was added to each flask (25 cm^2) and incubated for 1 hr at 27°C with frequent rocking. An additional 4 ml of maintenance media (modified from Wechsler et al., Appendix 1) was added to each flask after incubation, and infected cells were maintained at 27°C with no CO_2 supplementation.[38] Five hundred µl of viral supernatant was collected from each flask at 2, 6, 12, 24, 48, 72, and 96 hr post-inoculation and immediately stored at -80°C until TCID50s could be performed. Appropriate negative controls were included at each step.

Culicoides maintenance and infection

One-to-two day old *Culicoides sonorensis* from the AK colony (isolated in Idaho in 1973 and maintained at USDA ARS, Manhattan, KS) were obtained from USDA ARS and allowed to acclimate for at least 24 hr at 25°C on a 12:12 light cycle with 10% sugar water provided *ad libitum* prior to being infected with BTV via virus-spiked blood meal.[39,40] *C. sonorensis* were 3-4 days old at feeding.

Defibrinated sheep blood (Hemostat Laboratories, Dixon, CA, or Lampire Biological Laboratories, Everett, PA) was screened for BTV virus and antibodies via qRT-PCR and cELISA (VMRD, Pullman WA), respectively. Blood was then spiked with BTV and was made available to *Culicoides* in glass bell feeders through parafilm membranes. During feeding, blood was maintained at 37°C. *Culicoides* were allowed to feed for 1 hr 30 min to permit as many females as possible the opportunity to consume a blood meal. Following this, *Culicoides* were chilled at -20°C for 5 min and then sorted into groups using a modified chill table. Only blood-fed females were retained. These were divided into groups of several hundred *Culicoides* per container based on BTV infection status (Table 4.1). Five to ten blood-fed females were immediately harvested from each group (BTV-2 only, BTV-10 only, BTV-2+10, and negative) and screened for uptake of virus via BTV qRT-PCR.

Containers were made of non-treated paper tubes (Rigid Paper Tube Corporation, Wayne, NJ) with sheer pantyhose over the lid to permit air exchange and feeding. Sugar water (10% w/v) was available at all times via a cotton wick in each container. *Culicoides* were offered a BTV-negative blood meal for ~30 min every 3-4 days as above, and were maintained at one of three temperatures (20°C, 25°C, 30°C) with a 12:12 light cycle for the remainder of the experiment.

Initial experiments were performed in two parts due to limitations in the number of *Culicoides* that could be obtained and housed at one time. BTV-2+10 coinfection experiments were performed first (Experiment 1), followed by BTV-2 and BTV-10 single infections and survival experiments (Experiment 2) (Table 4.1). The same BTV stocks were used for each iteration of experiments, and negative control groups were included with each.

Culicoides collections

Following initial infection, subsets of blood-fed females were collected over the course of two to three weeks. Our goal was to track BTV virogenesis via qRT-PCR across temperatures and time, in addition to determining whether the temperature at which midges were held (20°C, 25°C, or 30°C) would affect the generation of reassortant BTV.

For both singly exposed (BTV-2 or BTV-10) and co-exposed (BTV-2+10) groups, five *Culicoides* were collected in triplicate from each temperature every other day until there were no midges remaining. Five midges from the negative group were also collected approximately weekly to ensure that they remained BTV-negative throughout the course of the study (data not shown). After collection, *Culicoides* were immediately stored at -80°C until further analysis (qRT-PCR).

Starting on day 3, and then continuing every four days until the end of the experiment, groups of n=10 midges from the BTV-2+10 co-exposed group were collected in triplicate from each temperature for plaque assays. Quantitative RT-PCR was also performed on midges from these time points.

In both cases, bugs were vigorously homogenized with a sterile pestle in Eagle's Minimum Essential Medium (EMEM) at a volume of 50 µl per midge (ie, 250 µl for groups of n=5 and 500 µl for groups of n=10). Homogenates were centrifuged briefly, and then 50 µl of

supernatant was collected for qRT-PCR and stored at -80°C until extractions were performed. For the co-exposed groups of n=10 bugs, 400 µl of homogenate was sterile-filtered (0.22 µM Millex-GV syringe filter, MilliporeSigma, Burlington, MA) and diluted further in EMEM at 1:2, 1:10, 1:100, 1:1,000, and 1:10,000 dilutions for plaque assays, which were performed immediately after collection.

Plaque assays

BHK 21 cells were seeded in 6-well plates 48 hr prior to setting up plaque assays (1.0 x 10^5 cells/well). Cells were maintained in EMEM with 10% heat-inactivated fetal bovine serum (FBS), 10% tryptose phosphate broth, and 1% penicillin streptomycin (10,000 U/ml). Cells were kept at 37°C with 5% CO_2 supplementation.

Confluent monolayers were washed once with PBS pH 7.4 prior to inoculation with dilutions of *Culicoides* homogenate. Five hundred µl of each dilution was added to a well and incubated for 1 hr at 37°C with frequent rocking to disperse the virus. After incubation, the inoculum was removed and cells were washed once with PBS pH 7.4, followed by overlay of with 2 ml of 3:1 BHK media:2% agarose in Earle's Buffered Salt Solution (EBSS). Plates were incubated at 37°C for 96 hr, or until plaques became evident. At this time, 1 ml of overlay (3:1 BHK media:2% agarose in EBSS with ~0.1% neutral red stain) was added. Plaques were picked 8-24 hr after the second overlay when plaques were visibly apparent. Agarose plugs were taken from well-isolated plaques and were propagated in individual wells of a 24- or 48-well plate with BHK 21 cells (4.65 x 10^4 per well). Propagated virus was harvested when cytopathic effect (CPE) was advanced; harvested viruses were promptly stored at -80°C until further analysis.

Extraction and DNase treatment

Nucleic acids were extracted from *Culicoides* homogenates and viral supernatants using Applied Biosystem's MagMAX RNA/DNA Pathogen kit (Invitrogen, Carlsbad, CA) according to manufacturer's instructions. Extractions were performed either manually or using the KingFisher Flex robot (Thermo Fisher, Waltham, MA).

Extracted insect homogenates were treated with DNase 1, RNase free (Thermo Fisher). Briefly, 12 µl of extracted nucleic acid from each sample was treated with 2 µl of DNase 1 and 2 µl of 10X buffer. Samples were incubated at 37°C x 30 min, and then 2 µl of EDTA was added to each sample and heated at 65°C x 10 min to inactivate the DNase.

qRT-PCR

Extracted, DNased samples were subsequently screened in duplicate for the presence of BTV using a universal BTV qRT-PCR that detects BTV segment 10 as previously described using SuperScript III One-step qRT-PCR reagents (Thermo Fisher) at half-reaction volumes.[41]

To normalize any variations in extraction efficiency, a qRT-PCR based on *Culicoides* mitochondrial cytochrome *c* oxidase subunit 1 (*cox*1) was also performed in duplicate on each sample. Primers were selected based on previously published work (BFculicFm and C1-N-2191) and a HEX-based probe (3'HEX- TGAATACTT/ZEN/CCTCCTTCTCTTTCTT - 3IABkFQ/5', Integrated DNA Technologies, Coralville, IA) was designed based on GenBank sequences of this gene using Geneious v.10.2.2.[42–44] SuperScript III One-step qRT-PCR reagents and volumes were the same as those used for BTV qRT-PCR, except samples did not undergo the initial 95°C denaturation step in the presence of primers, as was performed for BTV.[41] Appropriate positive and negative controls for both BTV and *Culicoides cox*1 were run with each plate. A no-reverse

transcriptase (no-RT) control was run to confirm that DNAse treatment was effective (ie, no amplification of *cox*1 in absence of reverse transcriptase).

To ensure that the BTV qPCR and *Culicoides cox*1 qPCR were comparable, we ran side-by-side qPCRs in triplicate on serial dilutions of extracted, DNased, BTV-infected midges to determine the relative efficiencies of each primer/probe set. Both targets had similar slopes and efficiencies ($R^2 = 0.99$ for both BTV and *cox*1) under the qPCR conditions used (Appendix 5). To correct for any variations in extraction efficiency, BTV Ct values were normalized by *Culicoides cox*1 using the ΔCt method based on mean Ct values for BTV and *cox*1 for each sample.

BTV segment-specific sequencing of plaques

The genotype of individual plaques propagated from co-exposed bugs was then determined using a novel, amplicon-based sequencing approach that can rapidly distinguish between BTV-2 and BTV-10 across all ten segments of genomic dsRNA. As described in Chapter 3, we used a two-step PCR approach to create amplicons of regions of each BTV-2 and BTV-10 segment that could be differentiated by several non-homologous nucleotides within each amplified sequence. Briefly, 2 µl of nucleic acid from propagated viruses (isolated from BTV-2+10 co-exposed *Culicoides*) was used as input. Primer combinations and concentrations were as those described in Chapter 2, except with slight variations in round one primer concentrations (Appendix 6). Bioinformatics analysis and processing were as described in Chapter 2.

In some cases, segment 2 did not receive sufficient sequencing reads. In these cases, segment 2-based, serotype-specific qRT-PCR was performed on extracted plaques as described in Chapter 5.[45]

Exposure of Culicoides to high titer BTV-2

BTV-2 did not grow well in *C. sonorensis* at the titer used in Experiments 1 and 2. To test whether we could successfully infect *C. sonorensis* by increasing the viral titer delivered in the blood meal. We infected smaller groups of *C. sonorensis* at titers 30- and 50-fold higher than our initial dose (BTV-2 LO: 3.06 x 10^6, and BTV-2 HI: 5.1 x 10^6 TCID50/ml, respectively). Infected midges (n = 127 for BTV-2 LO; n = 87 for BTV-2 HI) were then held at 25C on a 12:12 light cycle and provided a negative blood meal every 3-4 days as outlined for earlier infections. Duplicate groups of n = 50 midges infected at the low and high dose were also maintained to monitor survival at the different titers. Experiments were terminated at day 14, as our earlier experiments had shown that midges held at 25°C demonstrated productive virogenesis several days before this time point.

At days 7, 11, and 14 post blood meal, we harvested four groups of n = 5 *Culicoides* from each group (BTV-2 LO and BTV-2 HI) for screening via BTV qRT-PCR. At day 14, a group of n = 5 bugs from each group was homogenized in EMEM and filtered as described for plaque assay preparation. Insect homogenates were subsequently used to inoculate confluent 25cm^2 flasks of BHK 21 cells. *Culicoides* homogenate was diluted in EMEM to reach a total volume of 1 ml, which was used to inoculate monolayers. The monolayers were incubated along with virus for 1 hr at 37°C, and then an additional 4 ml of maintenance media was added to each flask. Flasks were incubated for 96 hr and monitored for the development of cytopathic effect (CPE) daily. If flasks developed CPE, virus and cells were harvested for extraction and BTV qRT-PCR as described above. BTV serotype was confirmed using the same qRT-PCR protocol described above, except with serotype-specific, segment 2-based primers and probe designed to detect BTV-2.[45]

Results

BTV-2 and BTV-10 exhibit similar replication kinetics in Culicoides-derived cell line

Previous work from our lab has demonstrated that BTV-2 and BTV-10 have similar growth kinetics in BHK 21 cells. However, as BHK 21 cells are a non-native cell type for BTV, we wanted to establish whether these viruses could replicate to the same level in *Culicoides*-derived cells to better approximate the virus-host interactions present in our in vivo infection experiments. When infected at an MOI of ~0.2 TCID50, CuVaW3 cells supported similar growth kinetics for both BTV-2 and BTV-10 (Figure 4.1).

BTV-2 replicates poorly compared to BTV-10 in C. sonorensis

We then used these same virus stocks to infect *C. sonorensis* midges through an infective blood meal at a total dose of ~1 x 10^5 TCID50/ml. Midges were infected with either BTV-2, BTV-10, or BTV-2+10 and held at one of three temperatures (20°C, 25°C, or 30°C) for the remainder of the experiment. Quantitative RT-PCR was used to track BTV virogenesis for each virus or virus combination in pools of bugs, and BTV Ct values were normalized by *Culicoides cox*1 Ct values (ΔCt) to account for any variations in extraction efficiency between samples.

Midges infected with BTV-10 or BTV-2+10 demonstrated signs of productive virogenesis (i.e., Ct values lower than day 0 infection levels) during the course of the experiment as early as day 4 post-infection in the higher temperature groups (Figure 4.2). In contrast, at no time point did the Ct values of midges infected with BTV-2 drop below baseline values, regardless of temperature (Figures 4.2-4.4).

We then attempted to infect smaller groups of *C. sonorensis* with higher titers of BTV-2 (~3 x 10^6 and 5 x 10^6) to see if midges were susceptible at higher doses of virus. Interestingly, we found that some pools of midges did demonstrate productive virogenesis when exposed to

titers 30- or 50-fold higher than our initial single-virus infection experiments. At day 7, one of four pools from our highest dose (BTV-2 HI) had BTV Ct values that approached baseline Ct values. An analogous finding was identified in a single pool from the BTV-2 LO group on day 14. Survival rates were similar between BTV-2 HI and BTV-2 LO groups (data not shown).

Temperature affects BTV replication in C. sonorensis, with higher temperatures generating more rapid virogenesis

Midges infected with BTV-2, BTV-10, and BTV-2+10 were screened in pools of n=5 in triplicate at regular intervals over the course of infection via BTV qRT-PCR to detect productive virogenesis. Our goal was to better understand how temperature affects BTV virogenesis (specifically of BTV-2 and BTV-10) and to determine whether different temperatures affected the occurrence of reassortment. Homogenates from midges prepared for plaque assays (n=10 per pool, days 3, 7, 11, 15, 19, and 23) were also extracted and screened for BTV via qRT-PCR. All samples were normalized by *Culicoides* mitochondrial *cox*1 qRT-PCR values to obtain a ΔCt value. Normalized BTV Ct values were calculated using the ΔCt method (Ct_{BTV} - Ct_{cox1} = $\Delta Ct_{normalized}$). To make figures more intuitive, values were expressed as -ΔCt.

Rate of blood meal digestion appeared to vary between incubation temperatures. While BTV rapidly reached near-undetectable limits in midges held at 30°C early in infection (by day 2), *Culicoides* held at 20°C reached comparable BTV Ct values only at 4 days post-blood meal (Figure 4.5). Insects held at 25°C also demonstrated slightly slower rates of BTV digestion than those at 30°C, although they were overall comparable between the two upper temperatures. Normalized BTV Ct values for 20°C midge pools were statistically lower (i.e., more virus still present) at day 2 post-infection than 25°C or 30°C midge pools ($p < 0.003$, two-way ANOVA

with Tukey's post-hoc), and significantly higher (i.e., less virus present) BTV Ct values at day 4 post-infection compared to 30°C midges ($p < 0.005$).

Productive BTV virogenesis was considered to exist when *cox*1-normalized BTV Ct values dropped below the baseline BTV Ct level (determined as the mean normalized BTV Ct value from day 0 post-blood meal: $\Delta Ct = 7.5$). At 30°C, productive virogenesis was first detected on day 4 for BTV-10 and BTV-2+10 (Figure 4.2). For midges at 25°C, productive BTV-10 virogenesis was first detected on day 10, and in the co-exposed group at day 8 (Figure 3). Midges held at 20°C only demonstrated decreased BTV Ct values starting at days 15 and 16 for BTV-2+10 and BTV-10, respectively (Figure 4.4).

Linear regressions were used to analyze the rate of virogenesis for each virus and temperature. Samples with undetectable BTV via qPCR were excluded from these calculations. Regressions were calculated based on $-\Delta Ct$ values starting at the day where BTV copy numbers were at their lowest point to account for variations in rate of blood meal digestion. Linear regressions demonstrate that BTV virogenesis is more rapid at 30°C than at lower temperatures. In addition, a greater proportion insect pools demonstrated productive virogenesis among 30°C groups compared to 20°C or 25°C groups (Figure 4.6).

In experiments with lower titer exposure, BTV-2 exposed insects failed to demonstrate productive virus replication, although BTV-2 was still detectable by qPCR in many of our pools, particularly at early time points. Interestingly, BTV-2 Ct values became largely undetectable around the same time points that BTV-10 and BTV-2+10 began to reach levels indicative of productive virogenesis at each respective temperature.

Temperature affects midge survival rates, regardless of BTV infection status

To establish whether BTV infection affected midge survival, we performed survival experiments in duplicate with each virus (BTV-2, BTV-10, BTV-2+10, negative) at each temperature. Groups of n=50 *Culicoides* per container were maintained at the same temperatures (20°C, 25°C, 30°C) as experimental groups, but were only used to count the number of midges that died each day.

Midges at 30°C died at faster rates than either of the lower temperatures, regardless of infection status (Figure 4.7). Those held at 25°C died at similar rates to those at 30°C, although delayed by a day or two, and infection status did not seem to affect survival rates. Insects at 20°C survived the longest across all infection types. While *Culicoides* with single-virus infections survived at similar rates across the experiment at 20°C, co-exposed midges died at a faster rate initially compared to uninfected and singly infected insects. Insects that took a BTV-negative blood meal and held at 20°C survived the longest of all groups, and had higher survival rates than infected *Culicoides* held at the same temperature.

BTV-2 and 10 reassortment is infrequent or absent in C. sonorensis

Pools of co-exposed midges from each temperature were prepared in triplicate for plaque assays every four days during the course of the experiment. Plaques were first isolated from *Culicoides* at 25°C and 30°C on day 7, and from *Culicoides* at 20°C on day 11 (Table 4.2). Thereafter, plaques were detected from one or more pools of insects from all temperatures at each time point (until no midges were remaining at a respective temperature). Occasionally, infrequent plaques (e.g., <5 at lowest dilutions) were detected from pools of midges with low viral copy numbers, although these were not considered to be “productive virogenesis.”

Plaques were propagated once on BHK 21 cells and then selected plaques were prepared for genotyping via amplicon-based sequencing. As midges at all temperatures generated plaques by day 11, we randomly selected 23 plaques from 20°C midges, 27 from 25°C midges, and 9 plaques from 30°C midges from day 11 for genotyping. Of these, 20/23, 25/27, and 9/9 plaques from the 20°C, 25°C, and 30°C groups, respectively, had at least 8/10 segments successfully genotyped. Initial results demonstrated that 92% of 540 possible segments were derived from BTV-10. No plaques demonstrated any segments derived from BTV-2, although the amplicon assay failed to detect 8% of all segments (Figure 4.8).

As a follow up and to determine whether reassortment might be more likely after a longer incubation period, we screened 12 randomly selected plaques from day 23 midges that had been maintained at 20°C. Of these, all plaques demonstrated at least 9/10 segments derived from BTV-10 (Figure 4.9). A high percentage (50%) of plaques failed to generate reads aligning to either parent strain for segment 2. One plaque had a minimal number of reads aligning to BTV-2 for segment 2, although no other plaques demonstrated any BTV-2-derived segments.

Discussion

Understanding how temperature affects virogenesis and reassortment among BTV strains is vital for our ability to accurately predict potential BTV incursions and epizootics, both in North America and worldwide. While temperature has a well-described effect on the extrinsic incubation period (EIP) of various vector-borne diseases including BTV, little is known in regard to how or whether environmental factors such as temperature can affect the frequency of reassortment among segmented arboviruses.[30,31,46–48] This study, therefore, represents one of the first attempts to better characterize the impact of temperature on rates of reassortment in arthropod vectors.

Two previous studies have assessed whether *C. sonorensis* midges are competent vectors for BTV-2, yet found differing results.[49] An initial study carried out shortly after BTV-2 was first detected in Florida in 1982 was performed using two strains of BTV-2, one of which was the BTV-2 OnaB 1982 strain.[50] This is putatively the same strain as that which was deposited at ATCC and subsequently used in our study. Consistent with our findings, very low rates of infection were found in *C. sonorensis* (~2%, from the AA, or Sonora, colony in this early study).[50,51] However, the viral titers used to infect midges in this experiment were not specified.

Subsequently, Tanya et al. used *C. sonorensis* from an unspecified colony to investigate their competence for BTV-2 OnaB 1983.[49] This isolate of BTV-2 was also detected in Ona, FL, but from a different year than the isolate used in the prior study. While the electropherotype of BTV-2 OnaB 1982 and BTV-2 OnaB 1983 were reportedly the same, no sequencing data currently exists to confirm this.[52] Tanya et al. found that BTV-2 OnaB 1983 was readily transmitted to sheep from infected midges, and that the oral infection rate of *C. sonorensis* was ~46% when blood meal BTV titers were 4.5 $\log_{10}$.[49] This titer of BTV-2 is less than what was provided to midges in our experiments, and significantly less than the high titer doses we eventually used. Collectively, these conflicting findings highlight the numerous factors that can impact the likelihood of productive BTV infection following oral exposure to this virus.

While our overarching findings failed to directly address the question of the effect of temperature on reassortment, we nonetheless obtained valuable information regarding BTV virogenesis in *C. sonorensis*. Similar to early findings with BTV-2, our study highlights the role that host species may play in the overall transmission and dispersion of various strains of BTV. It implicates poor infectability of BTV-2 in *C. sonorensis* – the predominant BTV vector in North America – as a primary factor for the failure of this particular serotype to become widely

established in the U.S.[53] Given that BTV-2 continues to circulate in the southeast U.S., particularly in Florida, where the BTV-2-competent vector *C. insignis* exists, it is likely that this vector species plays a key role in the circulation and range of BTV strains.[54] The expansion of *C. insignis* and reports of BTV-2 reassortment in vitro (Chapter 3) and in the field allude to potential increases in the range of this serotype within North America.[17,53] A better understanding of the likelihood of BTV reassortment in *C. insignis* is fundamental as we approach questions involving BTV evolution and ecology in North America.

The *C. sonorensis* midges infected in our study demonstrated much higher rates of infection with BTV-10 compared to BTV-2. We suspect that the productive virogenesis detected in our midges infected with BTV-2+10 predominantly reflects the replication of BTV-10, as implied by the findings of our plaque genotyping assay.

Viruses must overcome a variety of barriers to successfully infect an arthropod host and eventually become transmissible. These include the mesenteron infection barrier, the mesenteron escape barrier, the salivary gland infection barrier, and the salivary gland escape barrier.[55–57] *Culicoides* are also believed to have a dissemination barrier that restricts BTV replication beyond the gut cells.[55] Our findings indicate that BTV-2 OnaB 1982 may only rarely be able to overcome the mesenteron escape barrier in *C. sonorensis* from the AK colony, given that BTV Ct values never indicated productive BTV-2 virogenesis at biologically relevant oral infection titers. Interestingly, the VP7 protein (encoded by segment 7) – which is responsible for viral core particle binding to *Culicoides* cells – has an identical amino acid sequence between the BTV-10 and BTV-2 strains used in our study.[58,59] This implies that additional factors beyond successful VP7-mediated cell binding likely modulate BTV-2's ability to effectively infect *Culicoides*

sonorensis. Additional studies with intrathoracic inoculation of midges are warranted to better understand these barriers to infection.

We observed differing rates of *Culicoides* death at different temperatures, which was largely independent of infection status. This is consistent with findings from other vector studies, predominantly in mosquitoes, where higher incubation temperatures drive more rapid vector mortality.[47,60] At our lowest temperature (20°C), however, we detected distinctions in mortality rate between non-infected, singly-infected, and co-exposed midges. Similar findings have been noted subsequent to arboviral infections in mosquito vectors, although these trends were only noted at our lowest incubation temperature.[61–63] Increased mortality at 20°C may be associated with reduced ability to control viral infection at lower temperatures. Notably, this trend was present among midges infected with BTV-2 as well as BTV-10, particularly from day 10 forward. The most dramatic mortality rate was detected in midges co-exposed to BTV-2+10. Collectively, these findings suggest that there may be an important interaction between infection status, temperature, and vector survival. Despite the rare incidence of successful BTV-2 infection in midges in our initial experiments, it appears that exposure to BTV-2 at sub-infective doses may nonetheless affect midge survival at cooler temperatures, alluding to other potential underlying causes for absence of robust BTV-2 virogenesis at biologically relevant infection titers. This finding has implications for understanding the complex interactions of vector competence, environmental temperature, and overall survival rates, and will contribute to our ability to better model and predict BTV outbreaks and incursions in the face of climate change.

Finally, we noted that a greater proportion of midges held at 30°C demonstrated high BTV copy numbers, indicating increased virus production in these insects. Although we did not directly measure how high rates of BTV replication affected vector competence or infectious

titer, it stands to reason that greater virogenesis may be associated with increased BTV transmission and reassortment. Collectively, these findings highlight the complexities of virus-vector interactions that underlie bluetongue ecology in North America.

Table 4.1 – Groups of *C. sonorensis* Infected with BTV in Experiments 1 and 2.

	BTV-2			BTV-10			BTV-2+10			Negative		
Temperature	20°C	25°C	30°C	20°C	25°C	30°C	20°C	25°C	30°C	20°C	25°C	30°C
Experiment ID	2	2	2	2	2	2	1	1	1	-	1 / 2	-
Number of midges per container	n = 150 / n = 150	n = 165 / n = 153	n = 136 / n = 144	n = 150 / n = 150	n = 150 / n = 150	n = 150 / n = 185	n = 454 / n = 534	n = 614 / n = 741	n = 724 / n = 556	-	n = 312 / n = 252	-
Mean Bloodmeal BTV Titer (TCID50/ml)	1.02×10^5	1.02×10^5	1.02×10^5	1.06×10^5	1.06×10^5	1.06×10^5	BTV-2: 5.1×10^4 BTV-10: 5.3×10^4	BTV-2: 5.1×10^4 BTV-10: 5.3×10^4	BTV-2: 5.1×10^4 BTV-10: 5.3×10^4	-	-	-
Survival groups (Exp. 2 only)	n = 50 in duplicate	n = 50 in duplicate	n = 50 in duplicate	n = 50 in duplicate	n = 50 in duplicate	n = 50 in duplicate	n = 50 in duplicate	n = 50 in duplicate	n = 50 in duplicate	n = 50 in duplicate	n = 50 in duplicate	n = 50 in duplicate

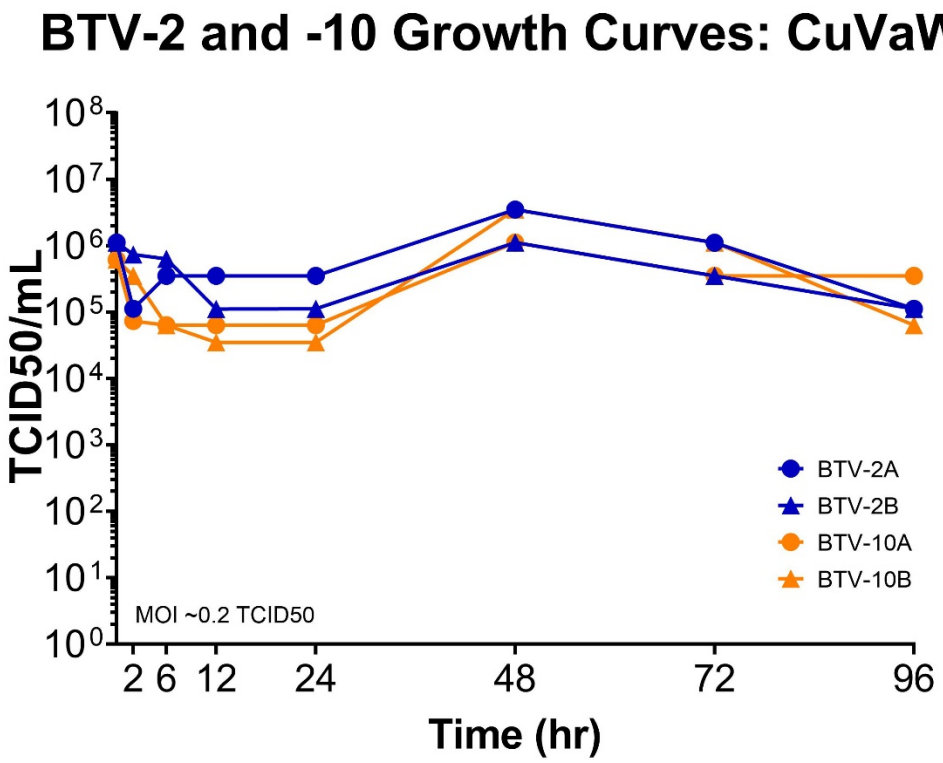

Figure 4.1 – BTV-2 and -10 Demonstrate Similar Growth Kinetics on CuVaW3 Cells. BTV-2 and BTV-10 one-step growth curves on CuVaW3 cells reflect similar growth kinetics between the two viruses in *Culicoides sonorensis*-derived cell line.

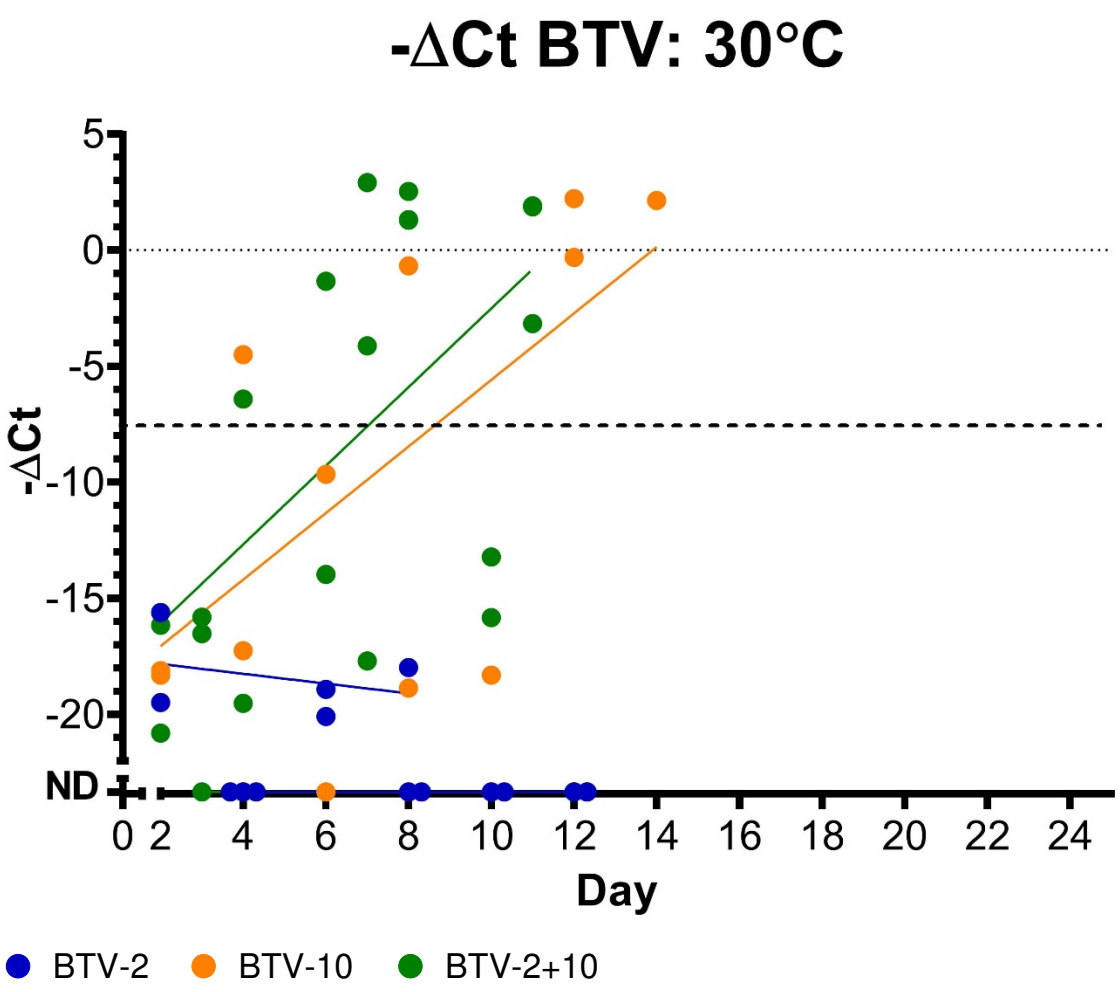

Figure 4.2 – BTV Virogenesis Occurs Rapidly in Midges Held at 30°C. BTV virogenesis is evident in pools of *Culicoides sonorensis* infected with BTV-10 and BTV-2+10 at 4 days after blood meal when held at 30°C. BTV-2 remains near undetectable limits across all days. Each point indicates a single pool of *Culicoides*, and ΔCt values are presented. ΔCt is calculated as the difference between mean BTV Ct values and *cox*1 Ct values for each sample. To make graphs more intuitive, -ΔCt values are presented. Dashed line indicates mean post-blood meal day 0 ΔCt across all infection groups (BTV-2, BTV-10, and BTV-2+10). Points depicted at "ND" (not detected), indicate undetectable BTV Ct values and were not included in linear regressions. BTV-2: $y = -0.21x - 17.41$ and $R^2 = 0.10$; BTV-10: $y = 1.43x - 19.93$ and $R^2 = 0.43$; BTV-2+10: $y = 1.69x - 19.45$ and $R^2 = 0.35$.

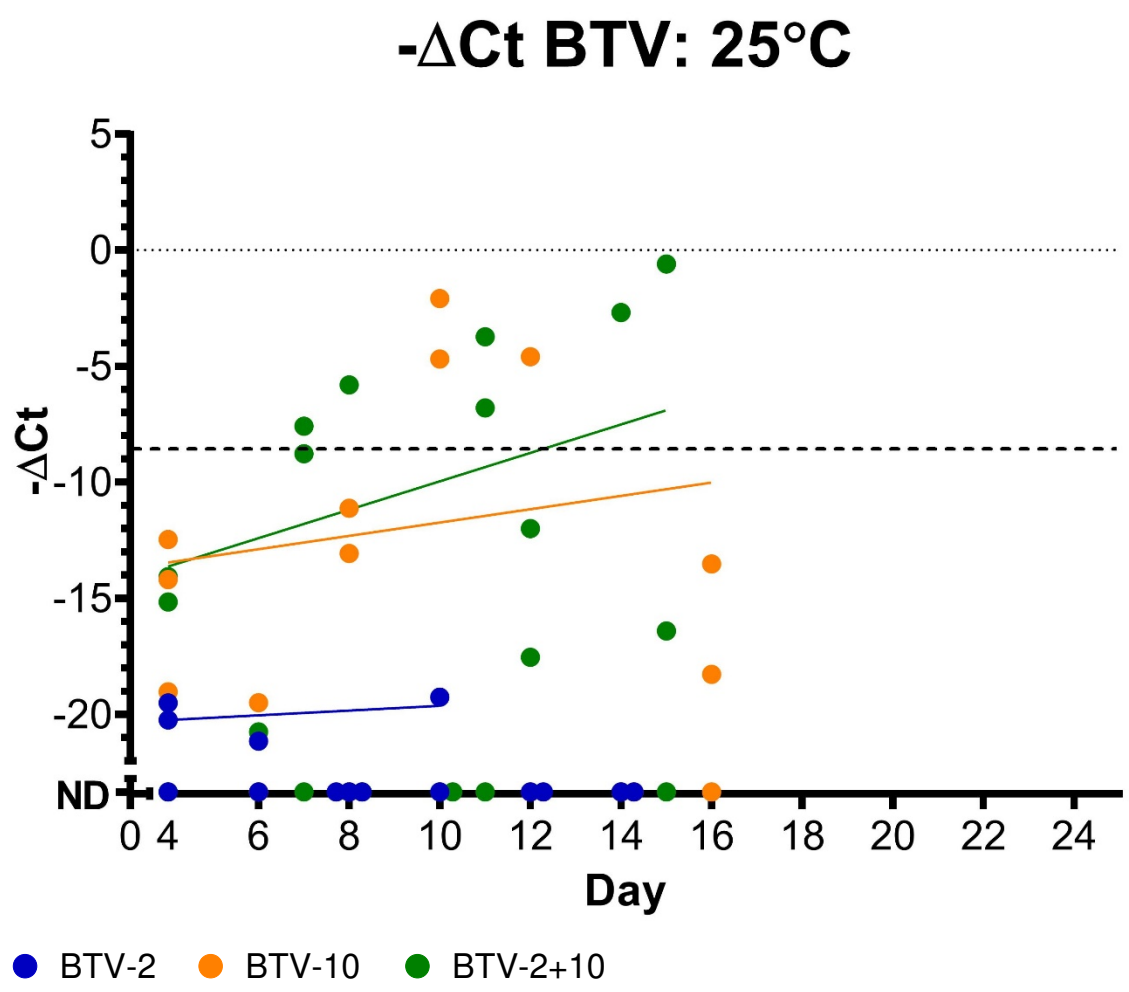

Figure 4.3 – Productive BTV Virogenesis is Noted by Day 7 in Midges Held at 25°C. BTV virogenesis is evident in pools of *Culicoides sonorensis* infected with BTV-10 and BTV-2+10 at 7-8 days after blood meal when held at 25°C. BTV-2 remains near undetectable limits across all days. Each point indicates a single pool of *Culicoides*, and ΔCt values are presented. ΔCt is calculated as the difference between mean BTV Ct values and *cox*1 Ct values for each sample. To make graphs more intuitive, -ΔCt values are presented. Dashed line indicates mean post-blood meal day 0 ΔCt across all infection groups (BTV-2, BTV-10, and BTV-2+10). Points depicted at "ND" (not detected), indicate undetectable BTV Ct values and were not included in linear regressions. BTV-2: $y = -0.18x - 18.51$ and $R^2 = 0.17$; BTV-10: $y = 0.28x - 14.52$ and $R^2 = 0.06$; BTV-2+10: $y = 0.76x - 17.72$ and $R^2 = 0.32$.

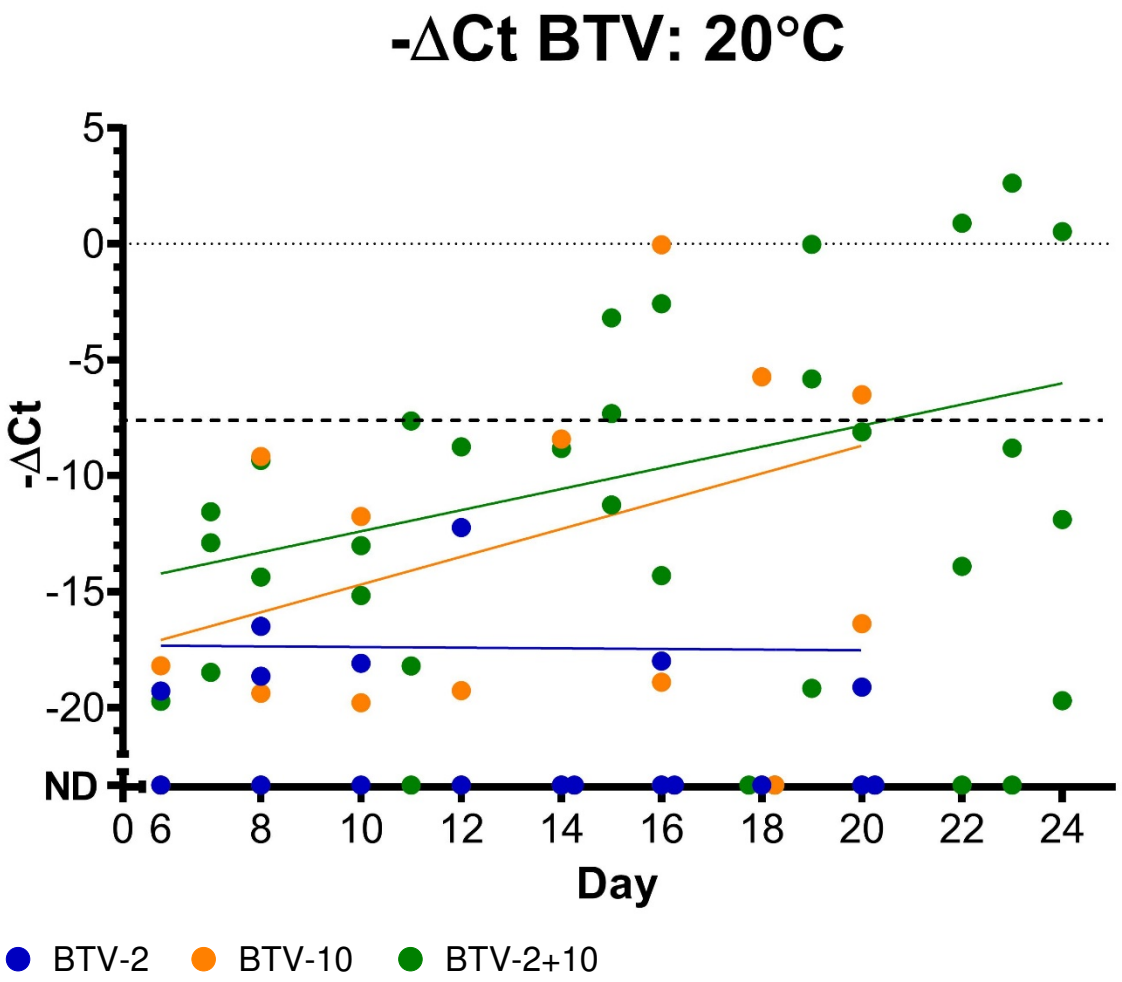

Figure 4.4 – BTV Virogenesis is Delayed in Midges Held at 20°C Compared to Warmer Temperatures. BTV virogenesis is evident in pools of *Culicoides sonorensis* infected with BTV-10 and BTV-2+10 at ~15 days after blood meal when held at 20°C. BTV-2 remains near undetectable limits across all days. Each point indicates a single pool of *Culicoides*, and ΔCt values are presented. ΔCt is calculated as the difference between mean BTV Ct values and *cox*1 Ct values for each sample. To make graphs more intuitive, -ΔCt values are presented. Dashed line indicates mean post-blood meal day 0 ΔCt across all infection groups (BTV-2, BTV-10, and BTV-2+10). Points depicted at "ND" (not detected), indicate undetectable BTV Ct values and were not included in linear regressions. BTV-2: $y = -0.01x - 17.25$ and $R^2 = 0.00$; BTV-10: $y = 0.60x - 20.68$ and $R^2 = 0.19$; BTV-2+10: $y = 0.46x - 16.96$ and $R^2 = 0.18$.

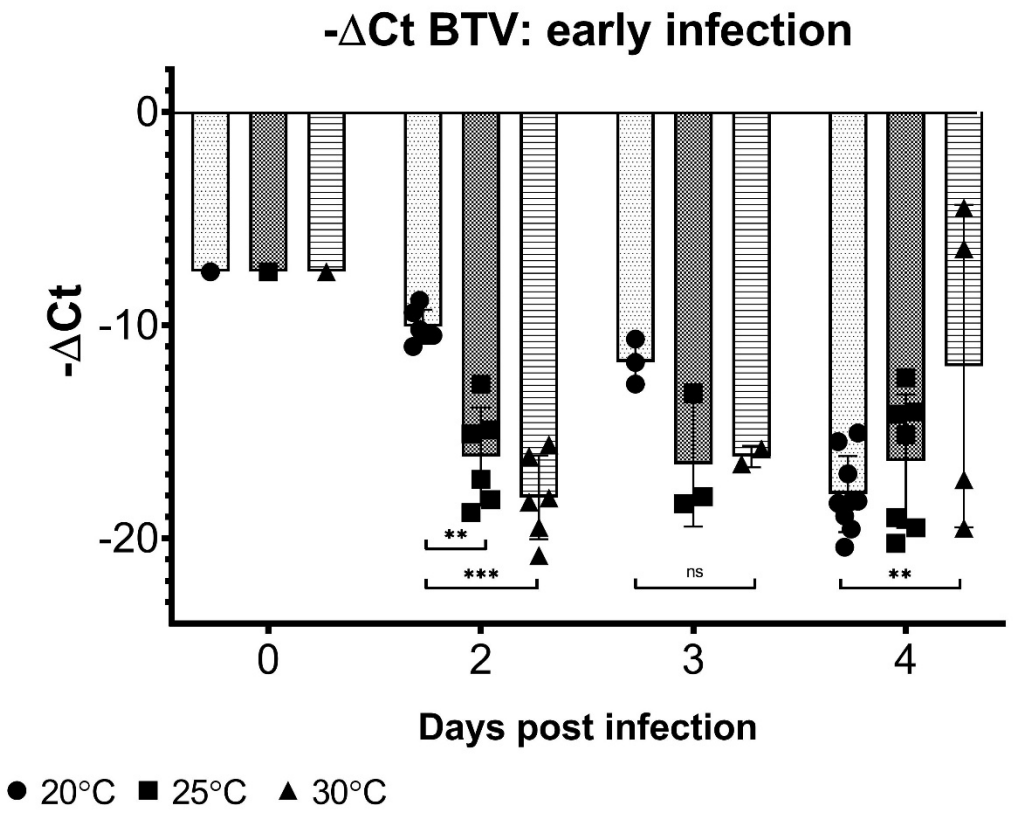

Figure 4.5 – Blood Meal Digestion Occurs More Rapidly in Midges Held at Warmer Temperatures. Early in infection (days 2-4 post blood meal), *Culicoides* held at different temperatures demonstrate different rates of blood meal digestion, with cooler temperatures (20°C) associated with slower decreases in BTV copy number over early infection compared to high temperatures. Day 0 –ΔCt values represent mean from pools collected immediately post blood meal. Midges collected from all viruses (BTV-2, BTV-10, and BTV-2+10) are represented at each time point. Two-way ANOVA with Tukey's post hoc was used to analyze differences between temperatures, with $p < 0.05$ considered significant.

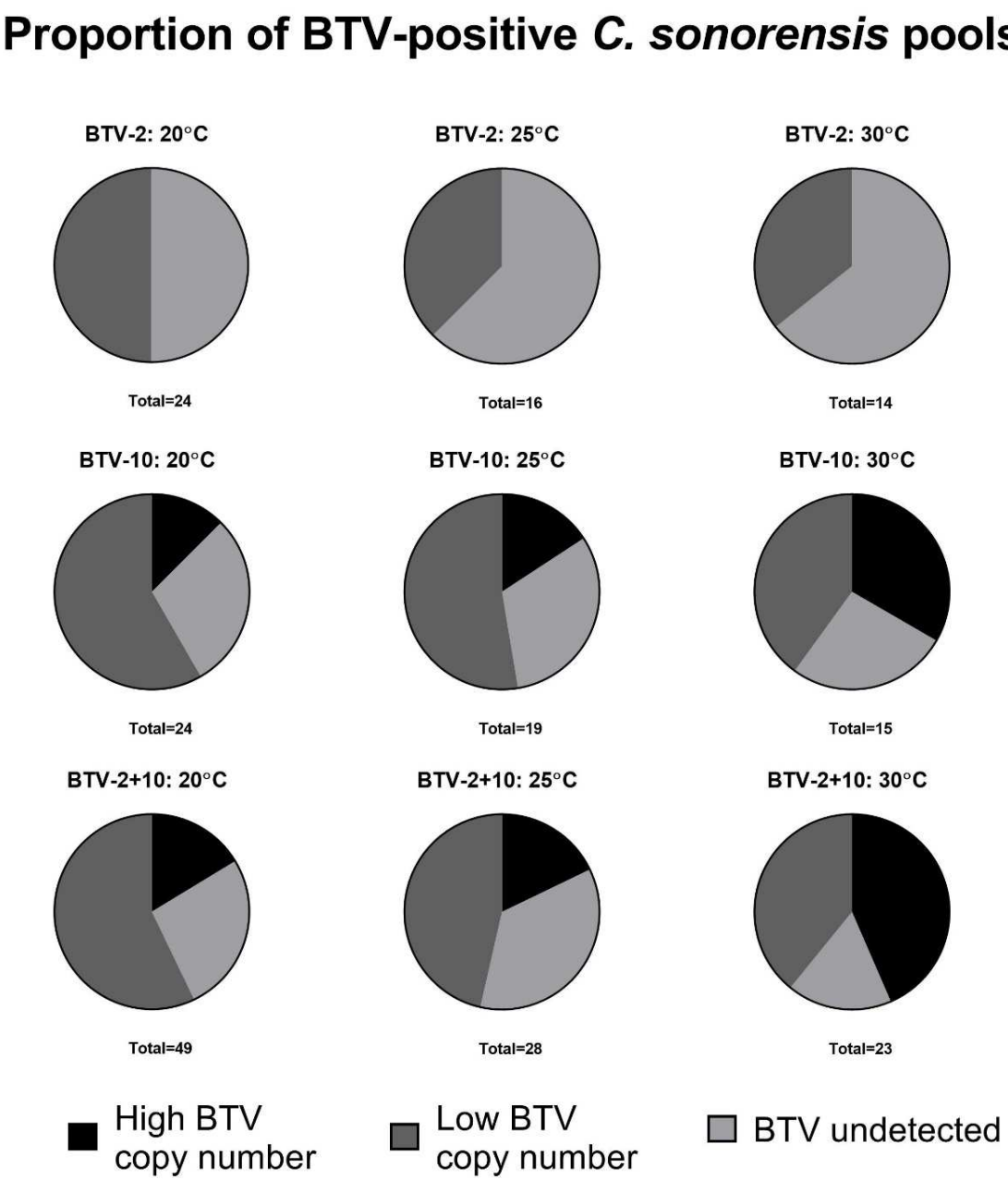

Figure 4.6 – A Higher Proportion of *C. sonorensis* Pools are BTV-positive at 30°C. A greater proportion of midge pools demonstrate productive BTV virogenesis (-ΔCt values greater than day 0 –ΔCt value, -7.5) at 30°C compared to lower temperatures. Insects infected with BTV-2 alone failed to demonstrate productive virogenesis regardless of incubation temperature.

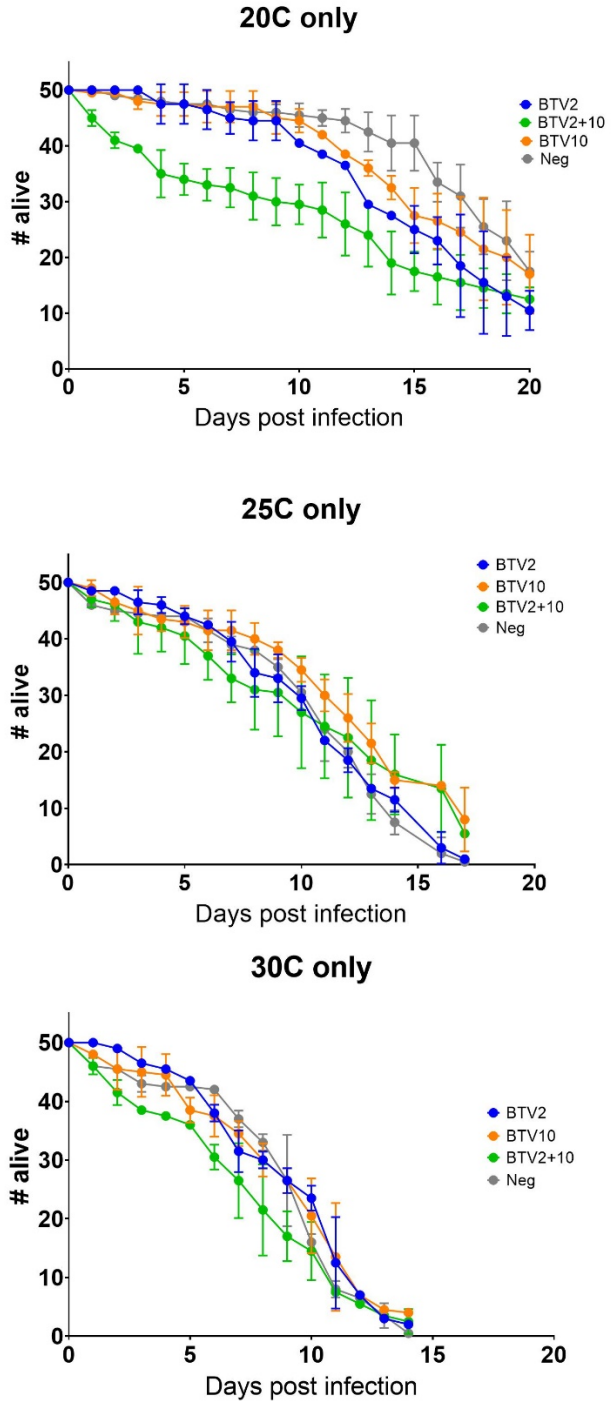

Figure 4.7 – *C. sonorensis* Maintained at Cooler Temperatures Outlive Those Held at Warm Temperatures. Temperature affects *Culicoides* mortality. Survival groups (n=50 per group) were infected in duplicate with virus via blood meal (BTV-2, BTV-10, BTV-2+10, or negative) at same titers as experimental groups. Survival groups were held respective temperatures (20°C, 25°C, or 30°C) for the duration of the experiment and survivors were counted daily.

Table 4.2 – Viable BTV can be Isolated from *Culicoides* Held at All Temperatures. Pools of midges (n=10 per pool) were homogenized in triplicate (A, B, C) and used to inoculate BHK 21 cells for plaque isolation at days 3, 7, 11, 15, 19, and 23 post-blood meal. Dashes (-) indicate replicates where no plaques were identified. Pools that produced ≥ 5 plaques are denoted by (+), and those that produced plaques rarely (< 5 plaques at lowest dilution) are indicated by (+/-). Days where no bugs were available to perform plaque assays are (n/a).

	20°C			25°C			30°C		
Days post-infection	**A**	**B**	**C**	**A**	**B**	**C**	**A**	**B**	**C**
3	-	-	-	-	-	-	-	-	-
7	-	-	-	+/-	-	+	-	-	+
11	+	+/-	+/-	+	+/-	+/-	+	+	+/-
15	+	+	+/-	+	+/-	+/-	n/a	n/a	n/a
19	-	-	+	n/a	n/a	n/a	n/a	n/a	n/a
23	+	-	-	n/a	n/a	n/a	n/a	n/a	n/a

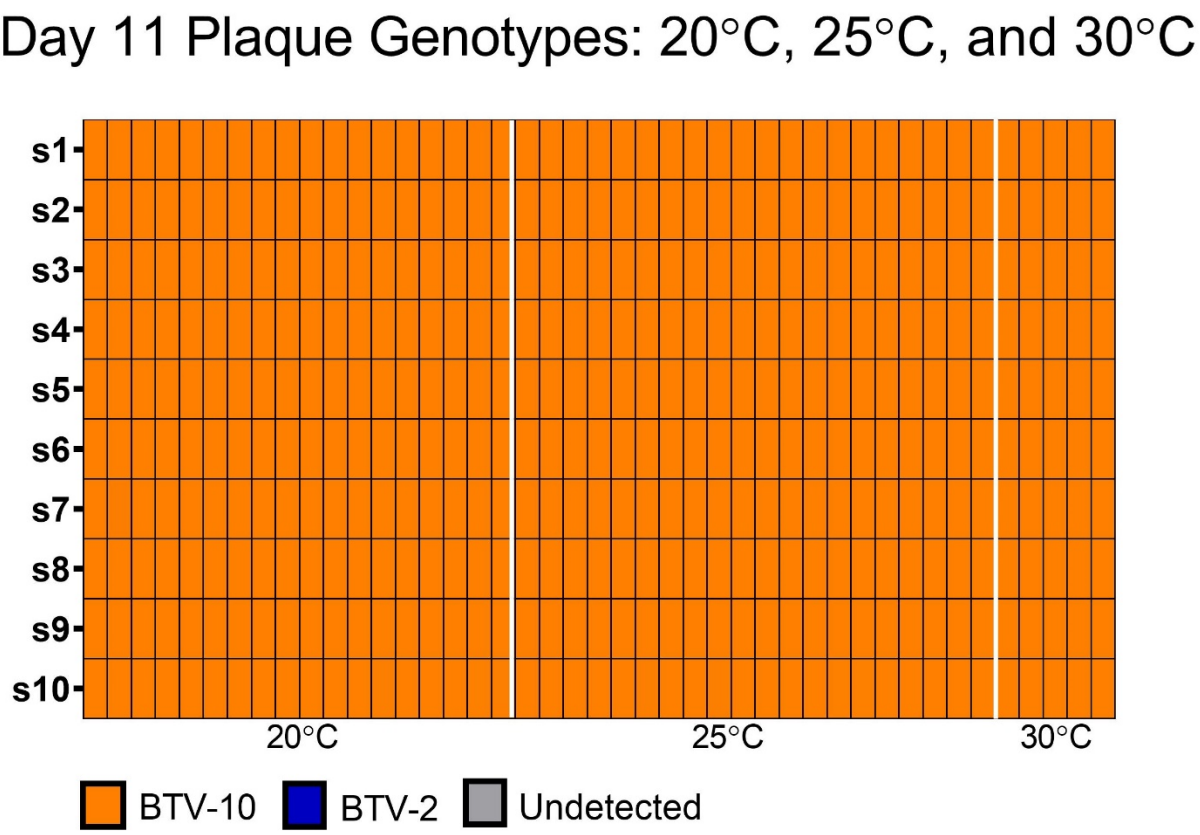

Figure 4.8 – Only BTV-10 is Detected in Plaques Isolated from *Culicoides* at Day 11 Post-infection. Plaque genotypes from plaque isolated viruses from pools of BTV-2+10 exposed midges collected on day 11 post infection. Each column represents the full ten segments of an individual plaque. Plaques isolated from each replicate are demarcated by white margins.

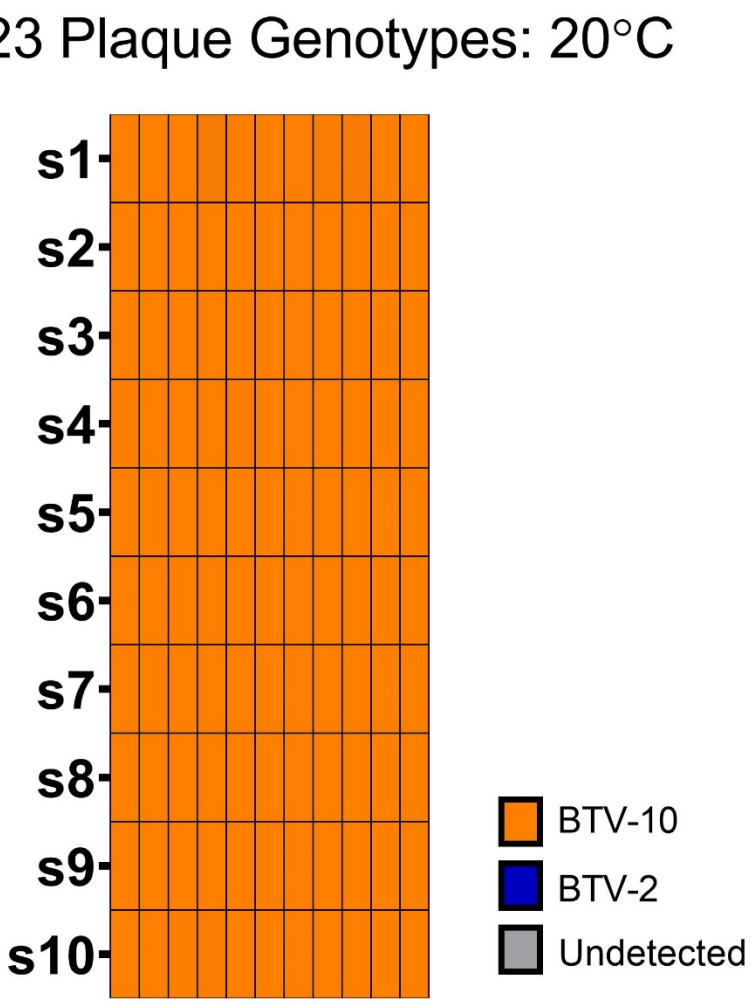

Figure 4.9 – Only BTV-10 is Detected in Plaques Isolated from *Culicoides* at Day 23 Post-infection. Plaque genotypes from plaque isolated viruses from pools of BTV-2+10 exposed midges collected on day 23 post infection. Each column represents the full ten segments of an individual plaque.

REFERENCES

1. Whitehorn J, Yacoub S. Global warming and arboviral infections. *Clin Med*. 2019;19(2):149-152. doi:10.7861/clinmedicine.19-2-149.

2. Baylis M. Potential impact of climate change on emerging vector-borne and other infections in the UK. *Environ Heal*. 2017;16(S1):112. doi:10.1186/s12940-017-0326-1.

3. Maclachlan NJ. Bluetongue: History, global epidemiology, and pathogenesis. *Prev Vet Med*. 2011;102(2):107-111. doi:10.1016/j.prevetmed.2011.04.005.

4. Maclachlan NJ, Drew CP, Darpel KE, Worwa G. The pathology and pathogenesis of bluetongue. *J Comp Pathol*. 2009;141(1):1-16. doi:10.1016/j.jcpa.2009.04.003.

5. Rushton J, Lyons N. Economic impact of bluetongue: a review of the effects on production. *Vet Ital*. 2015;51(4):401-406. doi:10.12834/VetIt.646.3183.1.

6. Samy AM, Peterson AT. Climate change influences on the global potential distribution of bluetongue virus. *PLoS One*. 2016. doi:10.1371/journal.pone.0150489.

7. Purse B V., Mellor PS, Rogers DJ, Samuel AR, Mertens PPC, Baylis M. Climate change and the recent emergence of bluetongue in Europe. *Nat Rev Microbiol*. 2005;3(2):171-181. doi:10.1038/nrmicro1090.

8. Foxi C, Delrio G, Falchi G, Marche MG, Satta G, Ruiu L. Role of different *Culicoides* vectors (Diptera: Ceratopogonidae) in bluetongue virus transmission and overwintering in Sardinia (Italy). *Parasit Vectors*. 2016;9(1):440. doi:10.1186/s13071-016-1733-9.

9. Borkent A. World Species of Biting Midges (Diptera: Ceratopogonidae); 2016. https://www.inhs.illinois.edu/files/4514/6410/0252/CeratopogonidaeCatalog.pdf.

10. Meiswinkel R, Gomulski LM, Delécolle J-C, Goffredo M, Gasperi G. The taxonomy of *Culicoides* vector complexes-unfinished business. *Vet Ital*. 2004;40(3):151-159.

11. Vigil SL, Wlodkowski JC, Parris J, et al. New records of biting midges of the genus *Culicoides Latreille* from the southeastern United States (Diptera: Ceratopogonidae). *Insecta mundi*. 2014;394:1-14.

12. Borkent A, Grogan WL. Article catalog of the New World biting midges north of Mexico (Diptera: Ceratopogonidae). *Zootaxa*. 2009;2273:1-48.

13. Tabachnick WJ. *Culicoides variipennis* and bluetongue virus epidemiology in the United States. *Annu Rev Entomol*. 1996;41:23-43.

14. Tabachnick WJ, Maclachlan NJ, Thompson LH, Hunt GJ, Patton JF. Susceptibility of *Culicoides variipennis sonorensis* to infection by polymerase chain reaction-detectable bluetongue in cattle blood. *Am J Trop Med Hyg*. 1996;54(5):481-485.

15. Holbrook FR, Tabachnick WJ, Schmidtmann ET, McKinnon CN, Bobian RJ, Grogan WL. Sympatry in the *Culicoides variipenni*s complex (Diptera: Ceratopogonidae): a taxonomic reassessment. *J Med Entomol*. 2000;37(1):65-76. doi:10.1603/0022-2585-37.1.65.

16. Tanya VN, Greiner EC, Gibbs EPJ. Evaluation of *Culicoides insignis* (Diptera: Ceratopogonidae) as a vector of bluetongue virus. *Vet Microbiol*. 1992;32:1-14.

17. Vigil SL, Ruder MG, Shaw D, et al. Apparent range expansion of *Culicoides* (Hoffmania) *insignis* (Diptera: Ceratopogonidae) in the southeastern United States. *J Med Entomol*. 2018;55(4):1043-1046. doi:10.1093/jme/tjy036.

18. Maan S, Maan NS, Belaganahalli MN, et al. Full-genome sequencing as a basis for molecular epidemiology studies of bluetongue virus in India. *PLoS One*. 2015;10(6):e0131257. doi:10.1371/journal.pone.0131257.

19. Schirtzinger EE, Jasperson DC, Ostlund EN, Johnson DJ, Wilson WC. Recent US bluetongue virus serotype 3 isolates found outside of Florida indicate evidence of reassortment with co-circulating endemic serotypes. *J Gen Virol*. 2018;99(2):157-168. doi:10.1099/jgv.0.000965.

20. McDonald SM, Nelson MI, Turner PE, Patton JT. Reassortment in segmented RNA viruses: mechanisms and outcomes. *Nat Rev Microbiol*. 2016;14:448-460. doi:10.1038/nrmicro.2016.46.

21. Ramig RF, Garrison C, Chen D, Bell-Robinson D. Analysis of reassortment and superinfection during mixed infectino of Vero cells with bluetongue virus serotypes 10 and 17. *J Gen Virol*. 1989;70:2595-2603.

22. Shaw AE, Ratinier M, Nunes SF, et al. Reassortment between two serologically unrelated bluetongue virus strains is flexible and can involve any genome segment. *J Virol*. 2013;87(1):543-557. doi:10.1128/JVI.02266-12.

23. Maan S, Maan NS, Belaganahalli MN, et al. Genome sequence of bluetongue virus type 2 from India: evidence for reassortment between outer capsid protein genes. *Genome Announc*. 2015;3(2). doi:10.1128/genomeA.00045-15.

24. Dal Pozzo F, Martinelle L, Thys C, et al. Experimental co-infections of calves with bluetongue virus serotypes 1 and 8. *Vet Microbiol*. 2013. doi:10.1016/j.vetmic.2013.01.016.

25. Samal BK, El Hussein A, Holbrook FR, Beaty BJ, Ramig RF. Mixed infection of *Culicoides variipennis* with bluetongue virus serotypes 10 and 17: evidence for high frequency reassortment in the vector. *J Gen Virol*. 1987;68:2319-2329.

26. Van Den Bergh C, Coetzee P. Reassortment of bluetongue virus vaccine serotypes in cattle. *J S Afr Vet Assoc.* 2018;80:1019-1028.

27. Batten CA, Maan S, Shaw AE, Maan NS, Mertens PPC. A European field strain of bluetongue virus derived from two parental vaccine strains by genome segment reassortment. *Virus Res*. 2008;137(1):56-63. doi:10.1016/j.virusres.2008.05.016.

28. Nomikou K, Hughes J, Wash R, et al. Widespread reassortment shapes the evolution and epidemiology of bluetongue virus following European invasion. *PLoS Pathog*. 2015;11(8). doi:10.1371/journal.ppat.1005056.

29. Lysyk TJ, Danyk T. Effect of temperature on life history parameters of adult *Culicoides sonorensis* (Diptera: Ceratopogonidae) in relation to geographic origin and vectorial capacity for bluetongue virus. *J Med Entomol*. 2007;44(5):741-751. doi:10.1093/jmedent/44.5.741.

30. Carpenter S, Wilson A, Barber J, et al. Temperature dependence of extrinsic incubation period of orbiviruses in *Culicoides* biting midges. *PLoS One*. 2011;6(11). doi:10.1371/journal.pone.0027987.

31. Wittmann EJ, Mellor PS, Baylis M. Effect of temperature on the transmission of orbiviruses by the biting midge, *Culicoides sonorensis*. *Med Vet Entomol*. 2002;16(2):147-156. doi:10.1046/j.1365-2915.2002.00357.x.

32. Mullens BA, Tabachnick WJ, Holbrook FR, Thompson LH. Effects of temperature on virogenesis of bluetongue virus serotype 11 in *Culicoides variipennis sonorensis*. *Med Vet Entomol*. 1995;9(1):71-76. http://www.ncbi.nlm.nih.gov/pubmed/7696691.

33. McKercher DG, McGowan B, Howarth JA, Saito J. A preliminary report on the isolation and identification of the bluetongue virus from sheep in California. *J Am Vet Med Assoc*. 1953;122(913):300-301.

34. Gibbs EP, Greiner EC, Taylor WP, Barber TL, House JA, Pearson JE. Isolation of bluetongue virus serotype 2 from cattle in Florida: serotype of bluetongue virus hitherto unrecognized in the Western Hemisphere. *Am J Vet Res*. 1983;44(12):2226-2228.

35. Barber T, Collisson E. Implications of a new bluetongue serotype for the U.S. livestock industry. *Proc Annu Meet US Anim Health Assoc*. 1983;87:90-104.

36. Reed LJ, Muench H. A simple method of estimating fifty percent endpoints. *Am J Epidemiol*. 1938;27(3):493-497. doi:10.1093/oxfordjournals.aje.a118408.

37. McHolland LE, Mecham JO. Characterization of cell lines developed from field populations of *Culicoides sonorensis* (Diptera: Ceratopogonidae). *J Med Entomol*. 2003;40(3):348-351. doi:10.1603/0022-2585-40.3.348.

38. Wechsler SJ, McHolland LE, Tabachnick WJ. Cell lines from *Culicoides variipennis* (Diptera: Ceratopogonidae) support replication of bluetongue virus. *J Invertebr Pathol*. 1989;54:385-393.

39. Jones RH, Foster AM. Relevance of laboratory colonies of the vector in arbovirus research - *Culicoides variipennis* and bluetongue. *Am J Trop Med Hyg*. 1978;27(1):168-177.

40. Nayduch D, Cohnstaedt LW, Saski C, et al. Studying *Culicoides* vectors of BTV in the post-genomic era: resources, bottlenecks to progress and future directions. *Virus Res*. 2014;182:43-49. doi:10.1016/j.virusres.2013.12.009.

41. Ortega J, Crossley B, Dechant JE, Drew CP, MacLachlan NJ. Fatal bluetongue virus infection in an alpaca (*Vicugna pacos*) in California. *J Vet Diagn Invest*. 2010;22:134-136. doi:10.1177/104063871002200129.

42. Bellis G, Dyce A, Gopurenko D, Mitchell A. Revision of the Immaculatus group of *Culicoides* Latreille (Diptera: Ceratopogonidae) from the Australasian region with description of two new species. *Zootaxa*. 2013;3680(1):15-37.

43. Hopken MW, Ryan BM, Huyvaert KP, Piaggio AJ. Picky eaters are rare: DNA-based blood meal analysis of *Culicoides* (Diptera: Ceratopogonidae) species from the United States. doi:10.1186/s13071-017-2099-3.

44. Dallas JF, Cruickshank RH, Linton Y-M, et al. Phylogenetic status and matrilineal structure of the biting midge, *Culicoides imicola*, in Portugal, Rhodes and Israel. *Med Vet Entomol*. 2003;17(4):379-387. doi:10.1111/j.1365-2915.2003.00454.x.

45. Maan S, Maan NS, Belaganahalli MN, et al. Development and evaluation of real time RT-PCR assays for detection and typing of bluetongue virus. *PLoS One*. 2016;11(9). doi:10.1371/journal.pone.0163014.

46. Samuel GH, Adelman ZN, Myles KM. Temperature-dependent effects on the replication and transmission of arthropod-borne viruses in their insect hosts. *Curr Opin Insect Sci*. 2016;16:108-113. doi:10.1016/j.cois.2016.06.005.

47. Shapiro LLM, Whitehead SA, Thomas MB. Quantifying the effects of temperature on mosquito and parasite traits that determine the transmission potential of human malaria. *PLoS Biol*. 2017;15(10):e2003489. doi:10.1371/journal.pbio.2003489.

48. Reisen WK, Meyer RP, Presser SB, Hardy JL. Effect of temperature on the transmission of Western equine encephalomyelitis and St. Louis encephalitis viruses by *Culex tarsalis* (Diptera: Culicidae). *J Med Entomol*. 1993;30(1):151-160. doi:10.1093/jmedent/30.1.151.

49. Tanya VN, Greiner EC, Shroyer DA, Gibbs EPJ. Vector competence parameters of *Culicoides variipennis* (Diptera: Ceratopogonidae) for bluetongue virus serotype 2. *J Med Entomol*. 1993;30(1):204-208.

50. Barber T, Jones R. Bluetongue virus, serotype 2: vector transmission and pathogenicity for sheep. *Proc Annu Meet US Anim Heathl Assoc*. 1984;88:545-555.

51. Jones R. The laboratory colonization of *Culicoides variipennis* (Coq.). *J Econ Entomol*. 1957;50(1):107-108.

52. Collisson EW, Barber TL, Paul E, Gibbs J, Greiner EC. Two electropherotypes of bluetongue virus serotype 2 from naturally infected calves. *J Gen Virol*. 1985;66:1279-1286.

53. Mecham JO, Johnson DJ. Persistence of bluetongue virus serotype 2 (BTV-2) in the southeast United States. *Virus Res*. 2005;113:116-122. doi:10.1016/j.virusres.2005.04.022.

54. Tanya VN, Greiner EC, Gibbs EPJ. Evaluation of *Culicoides insignis* (Diptera: Ceratopogonidae) as a vector of bluetongue virus. *Vet Microbiol*. 1992;32(1):1-14. doi:10.1016/0378-1135(92)90002-B.

55. Fu H, Leake CJ, Mertens PPC, Mellor PS. The barriers to bluetongue virus infection, dissemination and transmission in the vector, *Culicoides variipennis* (Diptera: Ceratopogonidae). *Arch Virol*. 1999;144:747-761.

56. Agarwal A, Parida M, Dash PK. Impact of transmission cycles and vector competence on global expansion and emergence of arboviruses. *Rev Med Virol*. 2017;27(5):e1941. doi:10.1002/rmv.1941.

57. Jennings DM, Mellor PS. Variation in the responses of *Culicoides variipennis* (Diptera, Ceratopogonidae) to oral infection with bluetongue virus. *Arch Virol*. 1987;95(3-4):177-182.

58. Tan BH, Nason E, Staeuber N, Jiang W, Monastryrskaya K, Roy P. RGD tripeptide of bluetongue virus VP7 protein is responsible for core attachment to *Culicoides* cells. *J Virol*. 2001;75(8):3937-3947. doi:10.1128/JVI.75.8.3937-3947.2001.

59. Xu G, Wilson W, Mecham J, Murphy K, Zhou EM, Tabachnick W. VP7: an attachment protein of bluetongue virus for cellular receptors in *Culicoides variipennis*. *J Gen Virol*. 1997;78:1617-1623.

60. Christofferson RC, Mores CN. Portential for extrinsic incubation temperature to alter interplay between transmission potential and mortality of dengue-infected *Aedes aegypti*. *Environ Health Insights*. 2016;10:119-123. doi:10.4137/EHI.S38345.

61. Scott TW, Lorenz LH. Reduction of *Culiseta melanura* fitness by eastern equine encephalomyelitis virus. *Am J Trop Med Hyg*. 1998;59(2):341-346.

62. Faran ME, Turell MJ, Romoser W, et al. Reduced survival of adult *Culex pipiens* infected with Rift Valley fever virus. *Am J Trop Med H yg*. 1987;37(2):403-409.

63. Martin E, Moutailler S, Madec Y, Failloux AB. Differential responses of the mosquito *Aedes albopictus* from the Indian Ocean region to two chikungunya isolates. *BMC Ecol*. 2010;10(8). doi:10.1186/1472-6785-10-8.

CHAPTER 5 – CHARACTERIZING THE GENETIC DIVERSITY OF BLUETONGUE VIRUSES CIRCULATING AMONG COLORADO RUMINANTS, 2015 AND 2018

Introduction

Bluetongue is a globally distributed, arthropod-borne disease of ruminants that is transmitted by *Culicoides* biting midges (Diptera: Ceratopogonidae). Bluetongue virus (BTV, family *Reoviridae*, genus *Orbivirus*), the etiologic agent of bluetongue disease, is composed of ten segments of double-stranded RNA (dsRNA) that encode seven structural proteins (VP1 - VP7) and four non-structural proteins (NS1, NS2, NS3/3a, and NS4).[1–4] BTV is frequently classified according to serotype, which is determined by the outer capsid protein VP2 (encoded by segment 2). Wild and domestic ruminants – particularly sheep – infected with BTV can develop severe disease characterized by systemic vasculitis accompanied by mucosal ulcerations, facial edema, pulmonary congestion, and coronitis, among other signs.[5–7] Within enzootic regions, ruminants may also develop clinically inapparent BTV infections.[8]

There are 29 serotypes of BTV recognized worldwide, with certain serotypes circulating regionally based on the presence of competent vector species.[8,9] Surveillance for ongoing spread of BTV and incursion of novel serotypes remains important, as bluetongue is an economically significant disease with financial losses attributable to animal sickness and death, production declines, and non-tariff trade restrictions.[10,11] The incursion of BTV serotype 8 (BTV-8) into northern Europe during 2006 highlighted concerns regarding vector expansion related to climate change and the ongoing spread of this arbovirus.[12] Total economic losses reached more than 150 million € in the initial years of the BTV-8 outbreak with a multitude of farms and animals affected.[10,11]

Historically, BTV serotypes 10, 11, 13, and 17 have been considered enzootic in North America, with occasional reports of other, non-enzootic serotypes (1, 3, 5, 6, 9, 12, 14, 18, 19, 22, and 24) detected in the southern United States (most commonly Florida).[2,12,13] BTV-2 is also considered enzootic in the United States, although its range is largely restricted to Florida, where additional potential vectors exist (*Culicoides insignis*) in addition to *C. sonorensis*, which is the dominant BTV vector in North America.[2,12,14–16] In 2010, BTV serotype 2 (BTV-2) was identified in clinically affected cattle in California but subsequent reports of serotype 2 in western states have been limited.[17,18]

Bluetongue virus circulates seasonally across much of the United States (U.S.), including in states such as Colorado and Wyoming in the Rocky Mountain West.[16,19–21] BTV also continues to expand northward into the upper half of the U.S. and into Canada, causing outbreaks in wild and domestic ruminants.[22–24] While much work has been performed regarding seasonal BTV infection and vector dynamics in some parts of the country (particularly on California dairies) and outside of North America, our understanding of BTV seasonal transmission dynamics and genetic diversity across various North American ecosystems remains limited.[24–34] Colorado provides a unique ecosystem to study BTV because of its distinct winter season, varied elevations, aridness, and high concentration of livestock and wild ruminants across the state.

A significant number of ruminants is infected with BTV during the summer and fall months but with inapparent clinical presentation, and as a result these animals are rarely identified due to lack of sentinel animal surveillance.[25,26] Thus, while numerous studies have indicated that there is extensive co-circulation of BTV strains, the absence of routine sentinel animal surveillance across enzootic regions severely blunts our ability to track and understand BTV evolutionary dynamics.[25,35–39] Moreover, the incursion of exotic BTV strains may go

undetected for extended periods of time if host animals are asymptomatic for infection, as often occurs in cattle.[40]

Reassortment, or the exchange of genome segments between different strains of BTV, can occur during coinfection in the ruminant or insect host and is a major contributor to BTV genetic diversification and evolution.[35,38,41–47] Reassortant viruses are frequently identified and can be important agents of disease outbreaks, even in BTV-enzootic regions.[48–56] However, diagnosis and surveillance for BTV is often based upon serology and sometimes serotype-specific PCR assays targeting segment 2, both of which fail to provide complete information about the remaining nine segments of genomic RNA. Thus, extensive reassortment likely goes undetected with traditional diagnostic methods.

Previous groups have investigated BTV genetic diversity in Colorado using a Sanger sequencing-based approach to analyze a limited subset of BTV segments (2, 7, and 10) in ruminants and *Culicoides* insects collected in Colorado during the 1980s and 1990s.[20,21] While White et al. found evidence of reassortment in their isolates, they determined that analysis of only three of the ten BTV genome segments was insufficient to characterize BTV epidemiology.[20] More recently, several groups have used whole genome sequencing (WGS) to study BTV, both in lab and in field studies.[2,8,35,52] The application of WGS permits simultaneous identification of all ten segments of genomic RNA, thereby facilitating detection of reassortment and mutations and providing a finer-resolution perspective on BTV genetic diversity. Field studies of BTV have demonstrated reassortment among BTV strains, but are often limited by opportunistic sampling strategies that, by their nature, most commonly sample BTV from overtly ill animals. Thus there is substantial BTV circulation that contributes to the overall genetic repertoire of the virus, but likely goes undetected with traditional sampling techniques. Our

understanding of naturally occurring BTV reassortment in North America, therefore, remains limited.

Here, we apply a cross-sectional and sentinel animal survey coupled with WGS to understand BTV transmission dynamics and genetic variability in the state of Colorado across one field season. We also describe the detection of non-enzootic BTV serotype 3 (BTV-3) in a nonclinical sentinel animal, corroborating reports that BTV-3 may be widely circulating in North America.[2] We compare the findings of our sentinel animal surveillance with opportunistic sampling of clinically ill, BTV-infected sheep from Colorado three years after our initial field study and demonstrate that this type of sampling method may fail to capture the majority of BTV genetic diversity present in the region. Additionally, we describe the presence of at least one exotic BTV segment among 2018 isolates. These findings contribute to our overall understanding of the genetic diversity of BTV in the Rocky Mountain states and highlight the role that sentinel animal surveillance plays in characterizing the ongoing evolution of BTV in North America.

Materials and Methods

Sentinel animal surveillance, 2015

A total of 150 calves from five dairy herds were enlisted from December 2014 to March 2015 and tested until December 2015. These dairies represented a longitudinal transect of five geographically distinct regions of the state (Figure 5.1). Monthly collections of serum and whole blood from each calf were analyzed respectively by BTV-specific cELISA (VMRD, Pullman, WA), BTV qRT-PCR assays, and serotype-specific qRT-PCR assays. Positive BTV qRT-PCR samples were isolated for BTV on bovine pulmonary artery endothelial cells (BPAEC) and samples were processed for whole genome sequencing (WGS). Dams of calves that were virus-

positive by qRT-PCR at initial sampling were also evaluated by cELISA for serological evidence of BTV infection (seroconversion). All sentinel surveillance work was approved by the Colorado State University Institutional Animal Care and Use Committee (15-5975A) and performed in accordance with institutional regulations. Producer consent was obtained for each site prior to the initiation of animal work.

Surveillance of clinically diseased animals, 2018

During the fall of 2018, numerous sheep along the Front Range of Colorado developed signs of bluetongue disease, and whole blood samples were submitted to the CSU Veterinary Diagnostic Laboratory (CSU-VDL) for diagnosis. Clinical signs ranged from relatively mild (facial and aural edema) to severe (death). BTV and serotype-specific qRT-PCR were performed to confirm BTV infection. Positive whole blood samples with Ct values of <30 were used for virus isolation on *Culicoides* cells (CuVaW3 cell line, USDA-ARS, Manhattan KS) and successfully isolated samples were sequenced using WGS.[57]

Nucleic acid extraction and qPCR

Nucleic acid was extracted from whole blood samples using MagMAX Pathogen RNA/DNA kit (Applied Biosystems, Foster City, CA) according to manufacturer's instructions. Extracted material was then used to screen each sample for BTV using a universal quantitative RT-PCR assay that detects BTV segment 10 (NS3).[58] Reverse transcription and qRT-PCR were carried out with SuperScript™ III One-Step qRT-PCR kit (Invitrogen, Carlsbad, CA) at half-reaction volumes and were thermocycled as previously described.[58]

Serotype-specific qRT-PCR was performed on samples found to be BTV-positive. Reaction conditions and reagents were the same as those described above, except serotype-specific primers and probes targeting segment 2 were used.[59]

Cell culture and virus isolation

Whole blood samples that were BTV-positive by qRT-PCR were then prepared for virus isolation on bovine pulmonary artery endothelial cells (BPAEC) or CuVaW3 cells. Whole blood was diluted in sterile water to lyse cells and then centrifuged at 1,500 rpm for 10 min at 4°C to pellet debris. Supernatant was collected and diluted further in Eagle's Minimum Essential Medium (EMEM) and then 1 ml of diluted blood was used to inoculate a confluent monolayer of BPAEC or CuVaW3 cells. Virus and cells were incubated for 1 hr at 37°C (BPAEC) or 27°C (CuVaW3) and then inoculum was removed and cells were washed once with phosphate buffered saline solution (PBS, pH 7.4). BPAEC maintenance media (10% heat-inactivated fetal bovine serum (FBS), 50,000 U penicillin, 50,000 µg streptomycin, 1% non-essential amino acids in Advanced MEM) or CuVaW3 maintenance media (modified from Wechsler et al., Appendix 1) was then added and cells were incubated at 37°C with 5% CO_2 (for BPAEC) or 27°C without CO_2 supplementation (for CuVaW3).[60]

For viruses isolated on BPAECs, cells were harvested when cytopathic effect (CPE) was evident. If CPE did not develop within 7 days, cells and media were harvested and used to inoculate a fresh flask of confluent BPAEC cells. This was repeated for 3-4 passages, after which virus isolation attempts were discontinued if CPE did not develop.

Conversely, for viruses isolated on CuVaW3 cells – which do not develop CPE when infected with BTV – qRT-PCR was used to track BTV Ct values during the course of infection and virus was harvested when Ct values had dropped into the mid-20s, indicating productive virogenesis. CuVaW3 virus isolation was performed in triplicate. For successful isolates, virus was harvested and aliquoted in 1 ml vials and stored at -80°C until downstream analysis.

Whole genome sequencing

Samples that were successfully cell culture isolated were subsequently prepared for whole genome sequencing (WGS). Nucleic acid was extracted from isolates using MagMAX Pathogen RNA/DNA Kit according to manufacturer's instructions for low cell content samples. Following extraction, samples were treated with 2-4 U of DNase in 0.1 volume buffer (TURBO DNA-*free*^{TM} Kit, Thermo Fisher, Waltham, MA), followed by a 0.5 - 1 hr incubation at 37°C. DNase was inactivated with 0.2 volumes of inactivation reagent and centrifuged (10,000 x g for 1.5 min) at room temperature. Supernatant was then collected and treated with LiCl to reach a 2.0 M final concentration so as to selectively precipitate single-stranded RNA (ssRNA). Samples were incubated for 16-18 hours at 4°C and then centrifuged (18,000 x g at 4°C for 20 min) to pellet ssRNA before collecting supernatant. Remaining salt was removed using a 1.25x MagMAX Pathogen RNA/DNA Kit clean-up.

Sample libraries were prepared for WGS using ScriptSeq v2 RNA-seq library preparation kit (Epicentre, Madison, WI; for 2015 samples) or KAPA RNA HyperPrep kit (KAPA Biosystems, Basel, Switzerland; for 2018 samples). Library preparations were carried out per manufacturer's instructions, with the following exceptions: 1) for libraries prepared with the ScriptSeq v2 kit, the initial fragmentation time was reduced to 1 min 30 sec at 80C, and 2) for libraries prepared with the KAPA RNA HyperPrep Kit, all reagents and samples were used at half-reaction volumes. Unique indices (ScriptSeq Index PCR Primers from Epicentre, or KAPA Dual-indexed Adapters from KAPA Biosystems) were annealed to each sample library. Following amplification, the concentration of each sample was measured using Agilent's D1000 ScreenTape Assay on the 2200 TapeStation System (Agilent, Santa Clara, CA). Samples were pooled according to molarity of inserts in the 300-800 base pair (bp) range and product was

fractionated on a 1% agarose gel. Library inserts of the desired size (300-800 bp in length) were excised from the gel and purified using the QIAquick Gel Extraction kit (Qiagen, Hilden, Germany). Pooled, size-selected libraries were then screened for concentration and quality using the D1000 ScreenTape assay and KAPA Library Quantification Kit (KAPA Biosystems) as specified by the manufacturer. Pools of 15-20 samples were sequenced on the Illumina NextSeq instrument using mid-output 300 cycle NextSeq v2 reagents (Illumina Inc., San Diego, CA).

Sequencing and bioinformatics pipeline

Samples were demultiplexed and raw reads were entered into a pre-processing bioinformatics pipeline that used TrimAL(for ScriptSeq libraries) or trimmomatic (for KAPA RNA HyperPrep libraries) to remove bases and sequences with low quality scores, as well as adapter sequences.[61,62] Cd-hit was used to eliminate duplicate reads where two or more reads had ≥ 96% pairwise identity in the first and last 30 base pairs.[63] Following initial processing steps, reads were iteratively aligned using Bowtie2 with default parameters to a database of unique GenBank BTV sequences to generate the consensus sequences of all ten segments for each sample.[64] Consensus sequences were visually inspected in Geneious v.10.2.2 to confirm alignment accuracy.

For samples isolated in triplicate (2018 clinical sheep samples), consensus sequences from each replicate were generated in the same way as above. As isolates did not show sequence variation across replicates, sequences from triplicate samples were collapsed into a single, representative consensus sequence for each segment, which was then used for downstream analyses.

In cases where samples had <100% coverage of the coding region of all ten BTV segments, de novo assembly of contigs was performed using SPAdes.[65] Contigs were then

analyzed using BLAST (https://blast.ncbi.nlm.nih.gov/Blast.cgi) and mapped to the consensus sequences generated by the previous step using Geneious v.10.2.2 to fill gaps in sequence data.

Phylogenetic analysis

Successfully sequenced isolates with sufficient coding region coverage across all ten segments were subsequently analyzed to determine the genetic relatedness of Colorado isolates to each other and to other enzootic and non-enzootic North American BTV isolates (Table 5.1). Consensus sequences were trimmed to remove 5' and 3' untranslated regions (UTRs) and then were aligned using the MUSCLE plugin in Geneious v.10.2.2. Trees were prepared for each segment alignment using HYK genetic distances with 1,000 bootstrapping replicates and EHDV-1 (GenBank: MF600026-35) as the outgroup.[66] Nodes with >70% support were considered statistically supported.

Results

Sentinel animal surveillance demonstrates widespread seasonal circulation of bluetongue virus in Colorado ruminants

Of the 150 calves screened for BTV infection during the 2015 field season, 28 became BTV PCR positive and seroconverted over the course of the season. Despite this significant prevalence, none of the cattle that were screened during this time demonstrated signs of disease.

Serial screening of calves demonstrated peak BTV Ct values from September to November, with maximal seroconversion by November. After initial detection of BTV infection via qRT-PCR, calves remained PCR-positive for up to three months, which was the end of the study (December, 2015).

BTV serotype was determined by segment 2-specific qRT-PCR. The predominant serotype circulating in subclinical cattle and sheep that were sampled in 2015 was BTV-17. Four

of the five enzootic BTV serotypes (10, 11, 13, and 17) were detected by qRT-PCR, and for viruses that were successfully isolated, serotype was confirmed via WGS. No overt co-infections were detected via serotype-specific qRT-PCR.

Considerable genetic diversity is present among bluetongue viruses circulating in Colorado sentinel ruminants

To better understand the genetic diversity of BTV circulating in sub-clinically infected Colorado ruminants, we used WGS to obtain sequence data across all ten BTV genome segments for viruses that were successfully isolated in cell culture.

Virus from 10 BTV-positive whole blood samples had sufficient sequencing output for further analysis. A novel bioinformatics pipeline was used to compile contigs and determine the genetic identity of each isolate across all ten segments. Isolates generally clustered into clades with other enzootic BTV isolates in constructed phylogenies, with some isolates (CO4 and 8; CO13 and 15) remaining nearly identical across all 10 genome segments. While CO4 and CO8 were isolated from two different calves at the same site, CO13 and CO15 were isolated from animals from geographically distinct sites. Moreover, certain Colorado isolates shared high (CO4 and CO8, >99.8% and CO18, >99.6%) nucleotide identity across all ten segments with historical BTV isolates from California (identified as BTV-17 CA 1988 and BTV-10 CA 1952 ATCC VR-187 in our phylogenies, respectively).

Despite the occasional appearance of these apparently stable BTV genotypes, Colorado isolates showed relatively marked diversity across segments, with variable degrees of shared nucleotide identity among isolates (Table 5.2), likely indicating the occurrence of reassortment as well as differing rates of genetic drift across segments. Consistent with their function as outer capsid proteins and antigenic determinants, segments encoding VP2 and VP5 (segments 2 and 6,

respectively) showed the greatest overall variation in nucleotide identity between Colorado isolates, while segments 5 and 9 (encoding NS1 and VP6/NS4, respectively) shared the highest identity within this subset of samples (Table 5.2).

While serotype-specific qPCR did not identify coinfections of any sentinel animals, WGS data indicated at least one animal (CO12) with probable BTV coinfection. Segments 2, 6, and 10 had complete or near-complete sequence data for more than one distinct segment genotype (Figures 5.3, 5.7, and 5.11).

2018 BTV isolates from clinically affected sheep show relatively less diversity than 2015 isolates

Twelve clinical sheep from different sites along the Front Range of Colorado were screened and found to be BTV-positive by qRT-PCR during the fall of 2018. None of the herds from which samples were submitted reported a history of BTV vaccination. Serotype-specific qRT-PCR successfully identified BTV serotype for 10 of 12 samples; two samples with high BTV NS3 qRT-PCR Ct values could not be detected by the serotype assay. Of these samples, nine were identified as BTV-17 and one sample was serotyped as BTV-11. Eight whole blood samples had Ct values <30 and were considered candidates for virus isolation, of which five were successfully isolated.

We then performed WGS to better understand the genetic diversity of BTV circulating during the 2018 field season. All five sequenced samples were identified as BTV serotype 17, confirming the results of serotype-specific qRT-PCRs for each of these samples. Overall, 2018 samples were related to 2015 Colorado isolates, although many 2018 viruses shared higher nucleotide identity with BTV isolates from Texas rather than 2015 Colorado isolates (Figures 5.2 – 5.11). Four of the five BTV isolates from clinical sheep were nearly identical (≥ 99.8%) across all segments, despite geographical distance between farms where isolations were made.

Segments 5 and 9 shared high identity among all isolates from both 2015 and 2018 and were highly similar across time points.

Reassortment is readily apparent among field isolates, although spatio-temporal relationships do not reveal clear lineages of reassortants

Reassortment events seem to play a clear role in the genetic variability detected among Colorado isolates from 2015, and to a lesser extent, 2018. Isolates frequently demonstrated high identity between certain segments, while other segments were much more distantly related. CO2, for instance, shared >96% identity with CO13 and CO15 across nine segments, but only 68.2% similarity in segment 2. Similarly, CO3 appears to be composed of common, Colorado-enzootic segments 3, 5, 9, and 10; however, segments 2, 4, 6, and 8 were more closely related to BTV isolates from Florida. Importantly, WGS results from this sample identified CO3 as BTV-3, an exotic serotype.

In the same way, reassortment was evident among isolates from 2018, albeit to a lesser extent. Most strikingly in this group of viruses, CO421 shared high identity with other 2018 isolates across segments 1 and 2, but was much more distantly related in other segments, especially segments 7 and 10. CO421 segment 7 was most closely related to an exotic segment from Guatemala (BTV-18, GenBank acc. KY092034) previously detected in Texas in 2008 (BTV-12, GenBank acc. KX164085), indicating probable reassortment. Interestingly, isolates SEW, ICE, 127, and 212 shared high segment 10 identity with 2015 Colorado isolates, while CO421 remained clustered with Texas isolates, most likely due to additional reassortment events.

While reassortment and single-nucleotide mutations are evident among Colorado isolates, 2015 and 2018 Colorado isolates were monophyletic across segments 1, 3, 5, and 9.

Discussion

Supporting the findings of other recent reports, we detected a reassortant, exotic BTV serotype 3 circulating in at least one of our sentinel animals.[2] While our BTV-3 isolate demonstrated evidence of reassortment with regionally circulating bluetongue viruses, it clustered with Florida BTV-3 isolates in segments 2, 6, and 8. This contrasts with the probable lineage of other recently identified BTV-3 isolates detected outside of Florida, which are considered to have originated from Central American/Caribbean strains.[2]

The sentinel calf from which BTV-3 was isolated did not have clinical signs. BTV-3 has not been subsequently detected in Colorado, indicating that this serotype may be circulating silently or that it is only present at very low levels in the region. Clarke et al. found that BTV-3 caused relatively mild disease in experimentally infected white-tailed deer, and it is possible that BTV-3 may be less frequently detected in the U.S. due to its more mild disease phenotype.[67]

Additionally, population dynamics dictate that it is difficult for novel genotypes to become established in endemic regions due to the abundance of well-established virus strains, making it unlikely for an exotic virus to supplant circulating strains unless it confers a marked fitness advantage.[20,68] Thus, BTV-3 may currently be outcompeted by enzootic BTV viruses in North America. However, given that host antibody responses are predominantly targeted towards BTV's VP2 outer capsid protein (encoded by segment 2), it would seem likely that novel serotypes would have a competitive advantage in enzootic locations due to the lack of neutralizing antibodies present at the population level. However, we have yet to detect evidence of increased BTV-3 circulation in Colorado after the initial detection of this exotic serotype, indicating that there may be some combination of surveillance, environmental, host, and viral factors that temper BTV-3's detection or expansion in the U.S.

We found that the majority of sheep with clinical bluetongue disease submitted to the CSU-VDL in the fall of 2018 had evidence of infection with BTV-17. Despite its enzootic nature, BTV-17 is commonly associated with disease outbreaks in North America.[19] Similar to the findings of White et al., we detected relatively high nucleotide identity within segment 2 (98.5-100% NI between 2015 and 2018 BTV-17 isolates), but more substantial genetic differences between these 2015 and 2018 viruses in segments 7 (92.5-95% NI) and 10 (82.9-97% NI), likely indicating reassortment of these segments.[20] In their work on the evolution of BTV in Europe, Nomikou et al. found that segments 2, 6, 7, and 10 were often dissociated between isolates across time, and our results corroborate these findings.[35]

Opportunistic sampling of clinically affected sheep may underestimate regional BTV genetic diversity compared to that observed during sentinel animal surveillance. In contrast to our 2015 sentinel animal findings, four of five 2018 BTV isolates had nearly identical sequences across all ten segments. While isolates from 2018 appeared to be composed of largely enzootic-derived segments, there were clear genetic signatures distinguishing 2018 BTV isolates from those collected in 2015. This may represent the introduction of divergent BTV strains from other parts of the U.S., or may indicate the accumulation of nucleotide variants across the span of several years. It is possible that the difference in method of isolation between 2015 and 2018 caused an artefactual appearance of genetic drift in our more recent isolates. However, this is unlikely, as partial sequence data from WGS performed directly from whole blood of at least one sample showed consistent sequences from input virus and isolated virus (data not shown) and studies have indicated that insect-cell versus mammalian-cell culture isolation of BTV results in minimal changes to the consensus sequences.[69]

We found evidence of reassortment and significant genetic diversity among BTV isolates recovered in 2015, indicating that we likely underestimate the degree of reassortment and influx of new segments in this region with common opportunistic sampling strategies. Given Colorado's robust livestock population and high concentration of feedlots, the potential for introduction of BTV viruses from other areas remains high, and this may be reflected by the relatively diverse viral genotypes detected in our sentinel animals.[70] However, in both 2015 and 2018, Colorado isolates were monophyletic across segments 1, 3, 5, and 9. This correlates with findings from Nomikou et al., who identified segments 1, 3, 4, 5, 8, and 9 as having similar times-to-most-recent-common-ancestor in their extensive analysis of European BTV evolution.[35] It is uncertain and not well established if these specific segments are linked in evolutionary space by RNA interactions, protein interactions, host- or vector-derived factors, or some combination thereof.

These findings demonstrate the importance of robust BTV sentinel surveillance strategies across North America, as significant genetic diversity appears to go undetected with routine, opportunistic surveillance. In addition, the results of our study reinforce the utility of WGS in BTV surveillance programs to detect the occurrence of low-frequency, exotic segments that may contribute to reassortment and the overall genetic diversification of BTV in otherwise enzootic areas. Additional factors may influence BTV diversity in North America warranting further investigation include the role of the vector, environmental and meteorological determinants, and vertebrate immunity and community composition.

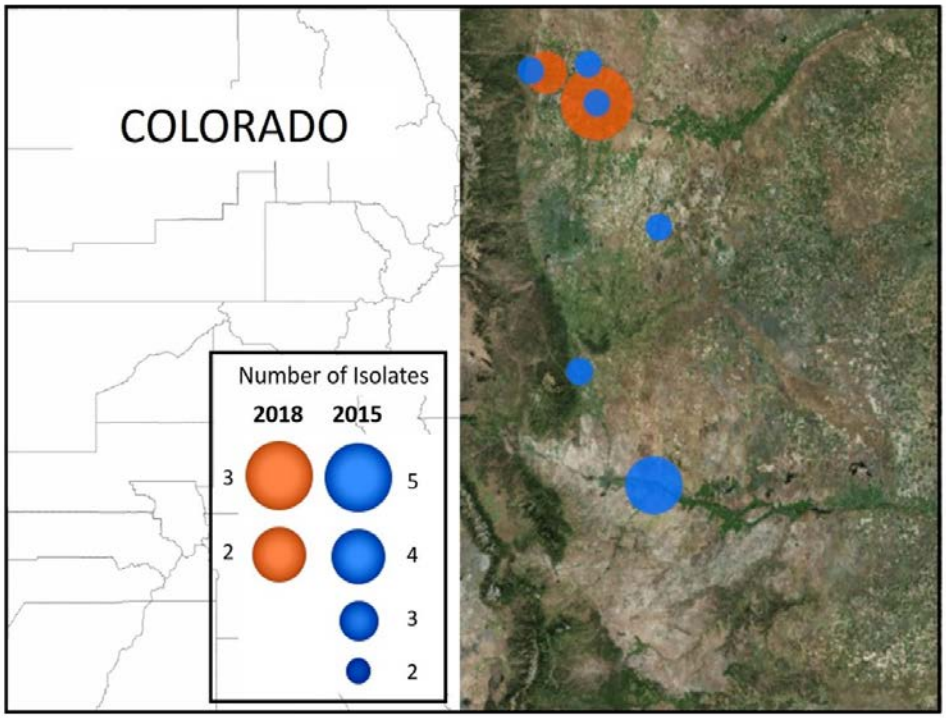

Figure 5.1 – Map of Colorado Isolates by Site. BTV isolates from 2015 sentinel work are indicated by blue circles, while clinical isolates are indicated in orange. The size of the circle indicates the number of isolates per location.

Table 5.1 – Sample IDs. Ten samples were isolated from sentinel cattle in 2015, and five samples were isolated from clinically affected sheep in 2018. CO12 had near-complete sequences for more than one serotype-defining segment; this sample was ultimately assigned as BTV-10 as this segment had the greatest % coverage compared to the other two serotypes detected.

Isolate ID	Year of Isolation	Species	Serotype
BTV3 Colorado 2015 CO3 (CO3)	2015	Bovine	BTV-3
BTV17 Colorado 2015 CO4 (CO4)	2015	Bovine	BTV-17
BTV11 Colorado 2015 CO5 (CO5)	2015	Bovine	BTV-11
BTV10 Colorado 2015 CO7 (CO7)	2015	Bovine	BTV-10
BTV17 Colorado 2015 CO8 (CO8)	2015	Bovine	BTV-17
BTV10 Colorado 2015 CO12* (CO12)	2015	Bovine	BTV-10 BTV-11 BTV-17
BTV17 Colorado 2015 CO13 (CO13)	2015	Bovine	BTV-17
BTV13 Colorado 2015 CO14 (CO14)	2015	Bovine	BTV-13
BTV17 Colorado 2015 CO15 (CO15)	2015	Bovine	BTV-17
BTV10 Colorado 2015 CO18 (CO18)	2015	Bovine	BTV-10
BTV17 Colorado 2018 CO127 (CO127)	2018	Ovine	BTV-17
BTV17 Colorado 2018 CO212 (CO212)	2018	Ovine	BTV-17
BTV17 Colorado 2018 CO421 (CO421)	2018	Ovine	BTV-17
BTV17 Colorado 2018 COICE (COICE)	2018	Ovine	BTV-17
BTV17 Colorado 2018 COSEW (COSEW)	2018	Ovine	BTV-17

Table 5. 2 – Colorado Isolates Share Higher Identities in 2018 than 2015 across All Segments. The mean pairwise identity and range for each segment are shown for different groups assessed in this study. The first row shows mean nucleotide identities among isolates from 2018 (n = 5); the second row shows the same data for 2015 isolates (n = 10).

	S1	S2	S3	S4	S5	S6	S7	S8	S9	S10
% Identity:	99.4%	99.5	99.2	97.9	98.6	98.8	96.8	98.5	97.8	93.4
CO 2018	98.5-100%	98.7-100%	98.1-100%	94.9-100%	96.4-100%	97.0-100%	92.1-100%	96.3-100%	94.6-100%	83.5-100%
% Identity:	97	68.7	96.4	96.6	98.2	85.4	90.8	96.5	97.5	89.9
CO 2015	92.3-100%	48.8-100%	93.4-100%	88.2-100%	96.6-100%	70.9-100%	78.6-100%	88.7-100%	95.2-100%	82-100%

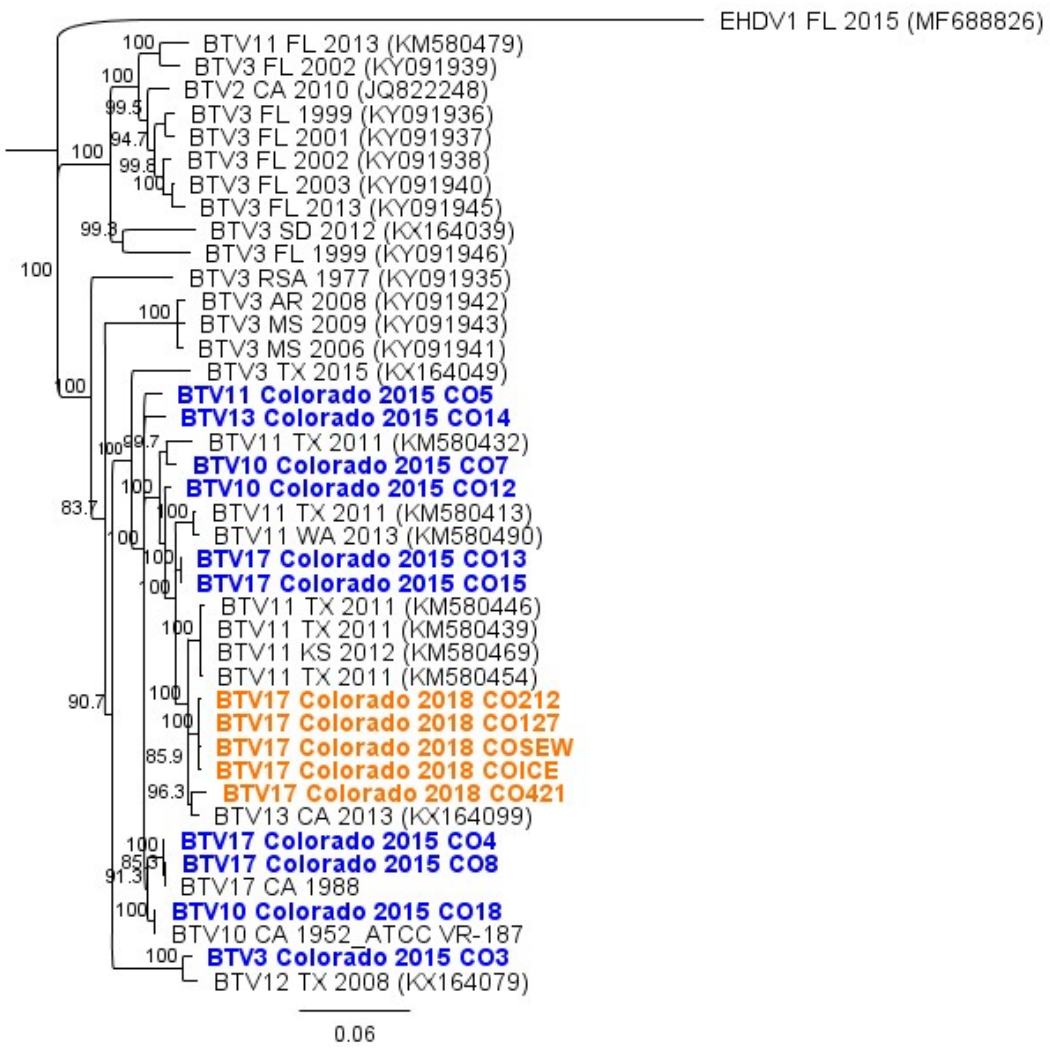

Figure 5.2 – Segment 1 Phylogenetic Tree. 2015 isolates are shown in blue; 2018 isolates are depicted in orange. Neighbor-joining trees were prepared from coding sequence alignments (3909 bp) using HKY genetic distances with 1,000 bootstrapping replicates. EHDV-1 was used as the outgroup. Nodes with >70% support are considered statistically supported. GenBank accession numbers of non-Colorado isolates are included in parentheses.

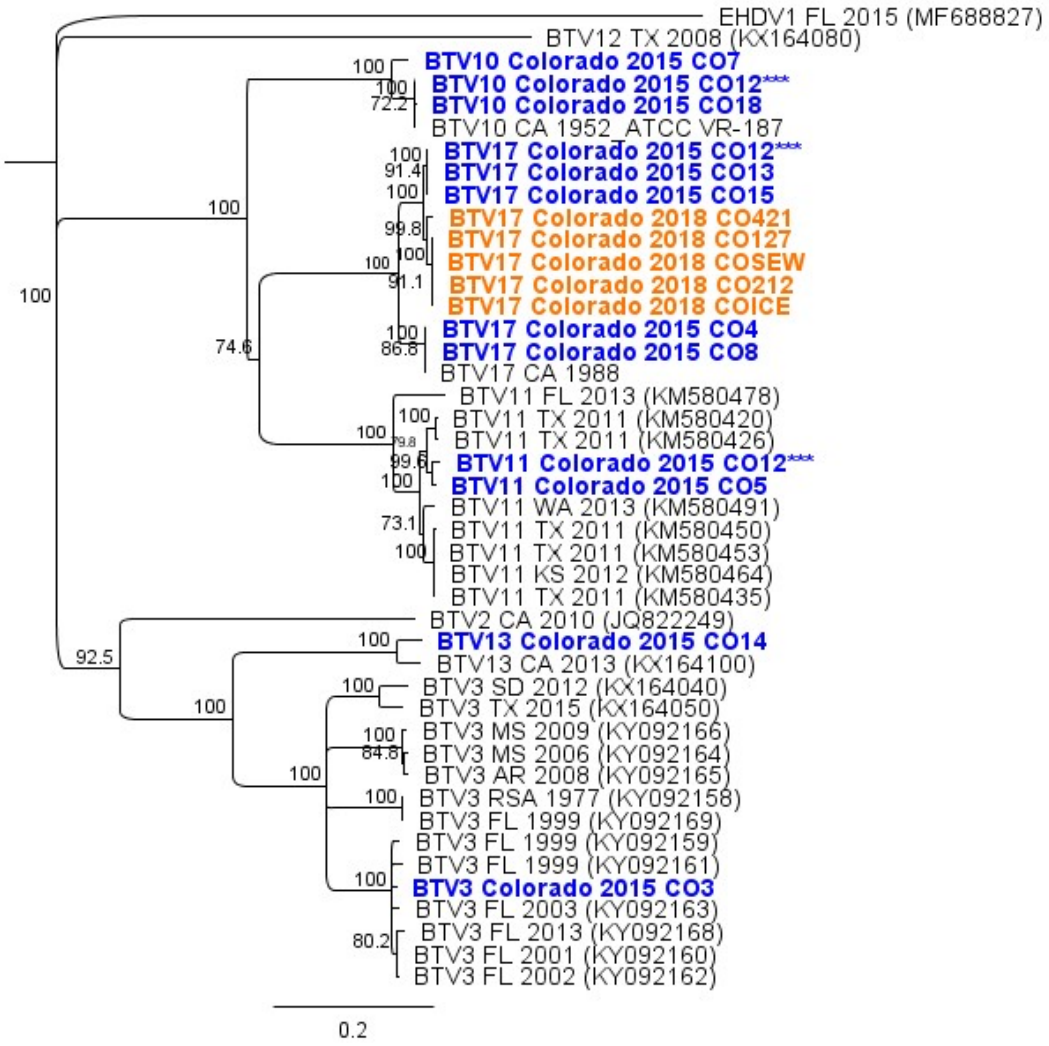

Figure 5.3 – Segment 2 Phylogenetic Tree. 2015 isolates are shown in blue; 2018 isolates are depicted in orange. Neighbor-joining trees were prepared from coding sequence (cds) alignments (2880 bp) using HKY genetic distances with 1,000 bootstrapping replicates. EHDV-1 was used as the outgroup. Nodes with >70% support are considered statistically supported. BTV10 Colorado 2015 CO12 demonstrated coinfection (sequences aligning to distinct segment 2 sequences from this isolate are depicted with asterisks). Segment 2 reads from CO12 had 100% of BTV-10 segment 2; 97% coverage of BTV-17 segment 2 (gap from nucleotide 938-1120); and 93% coverage of BTV-11 segment 2 (gap from nucleotide 1616-1685). GenBank accession numbers of non-Colorado isolates are included in parentheses.

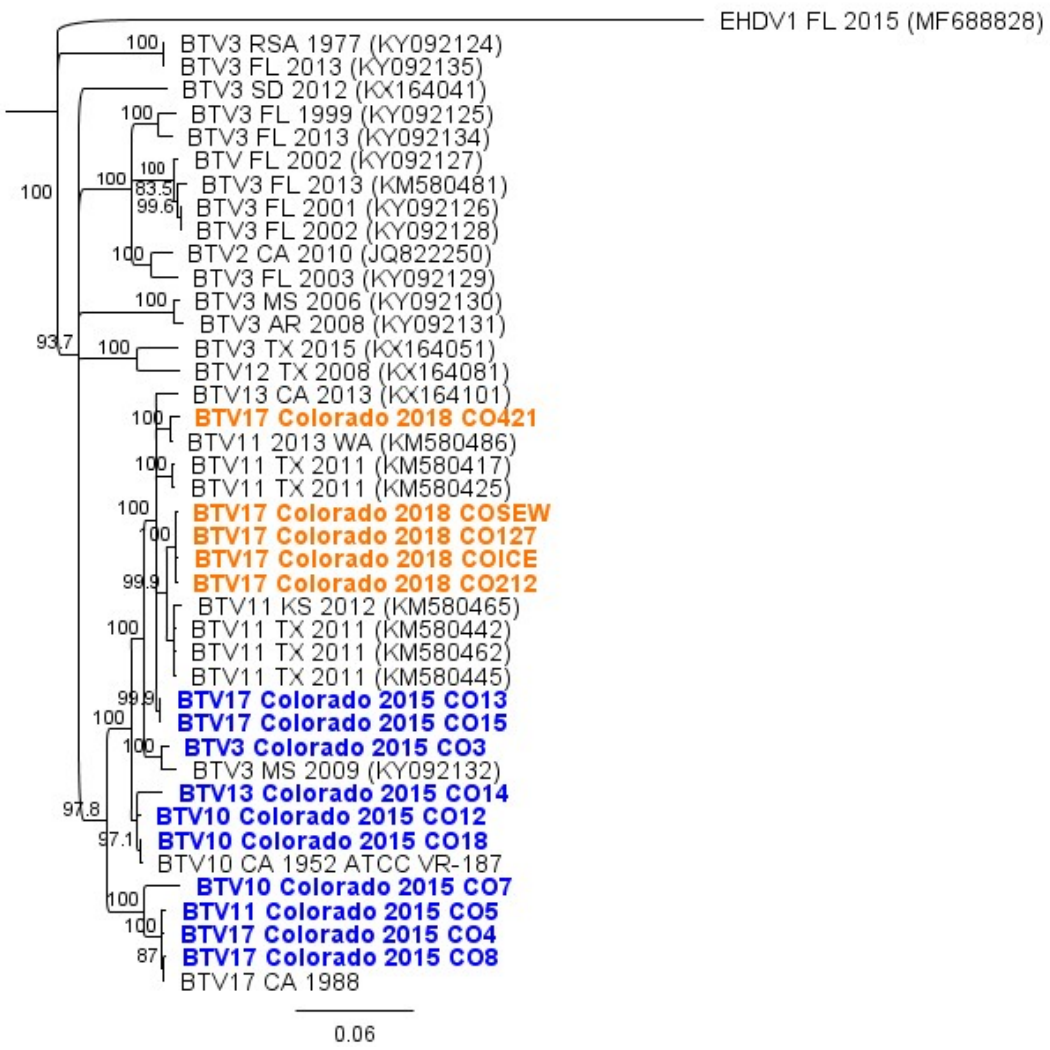

Figure 5.4 – Segment 3 Phylogenetic Tree. 2015 isolates are shown in blue; 2018 isolates are depicted in orange. Neighbor-joining trees were prepared from coding sequence alignments (2706 bp) using HKY genetic distances with 1,000 bootstrapping replicates. EHDV-1 was used as the outgroup. Nodes with >70% support are considered statistically supported.

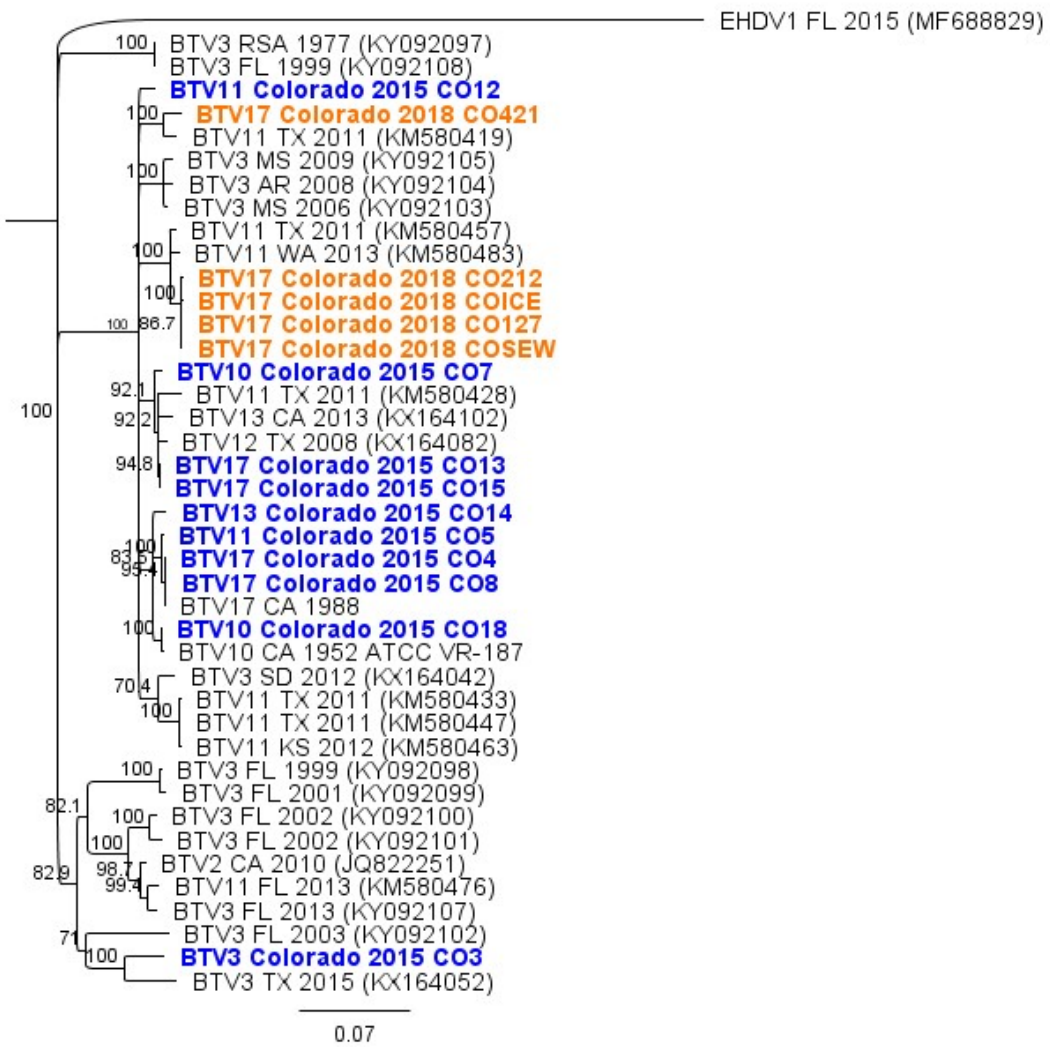

Figure 5.5 – Segment 4 Phylogenetic Tree. 2015 isolates are shown in blue; 2018 isolates are depicted in orange. Neighbor-joining trees were prepared from coding sequence alignments (1935 bp) using HKY genetic distances with 1,000 bootstrapping replicates. EHDV-1 was used as the outgroup. Nodes with >70% support are considered statistically supported. GenBank accession numbers of non-Colorado isolates are included in parentheses.

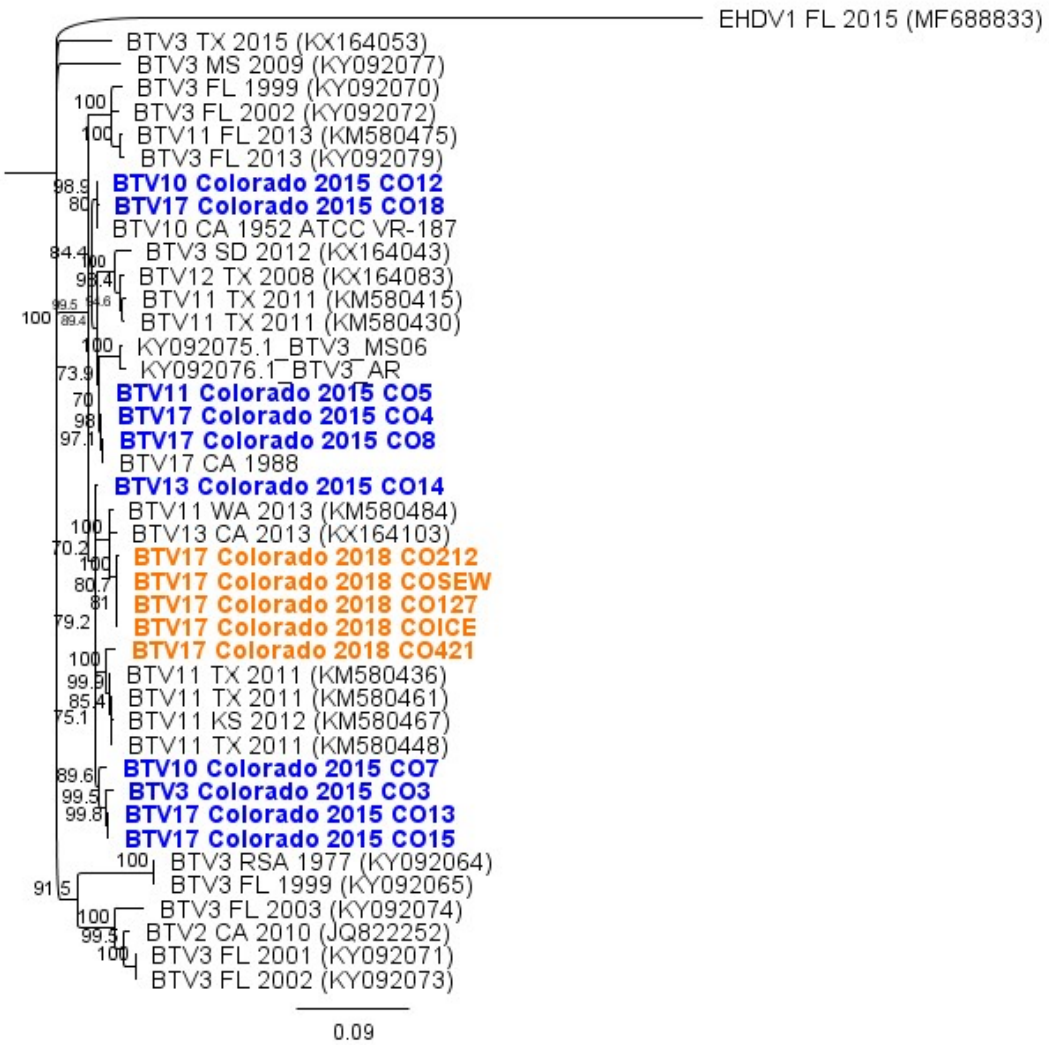

Figure 5.6 – Segment 5 Phylogenetic Tree. 2015 isolates are shown in blue; 2018 isolates are depicted in orange. Neighbor-joining trees were prepared from coding sequence alignments (1659 bp) using HKY genetic distances with 1,000 bootstrapping replicates. EHDV-1 was used as the outgroup. Nodes with >70% support are considered statistically supported. GenBank accession numbers of non-Colorado isolates are included in parentheses.

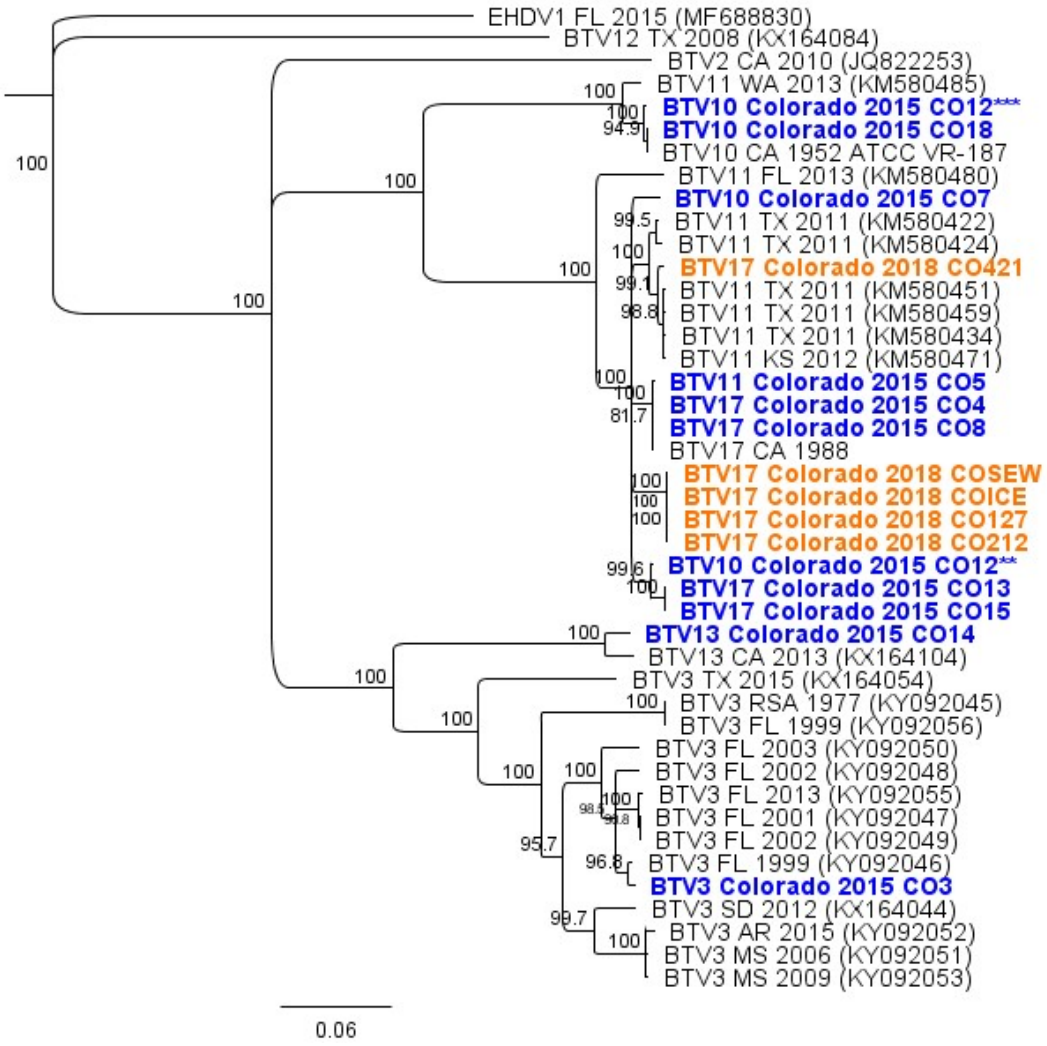

Figure 5.7 – Segment 6 Phylogenetic Tree. 2015 isolates are shown in blue; 2018 isolates are depicted in orange. Neighbor-joining trees were prepared from coding sequence alignments (1581 bp) using HKY genetic distances with 1,000 bootstrapping replicates. EHDV-1 was used as the outgroup. Nodes with >70% support are considered statistically supported. BTV10 Colorado 2015 CO12 demonstrated coinfection (sequences aligning to distinct segment 6 sequences from this isolate are depicted with asterisks). Both segment 6s that CO12 reads aligned to had 100% cds coverage. GenBank accession numbers of non-Colorado isolates are included in parentheses.

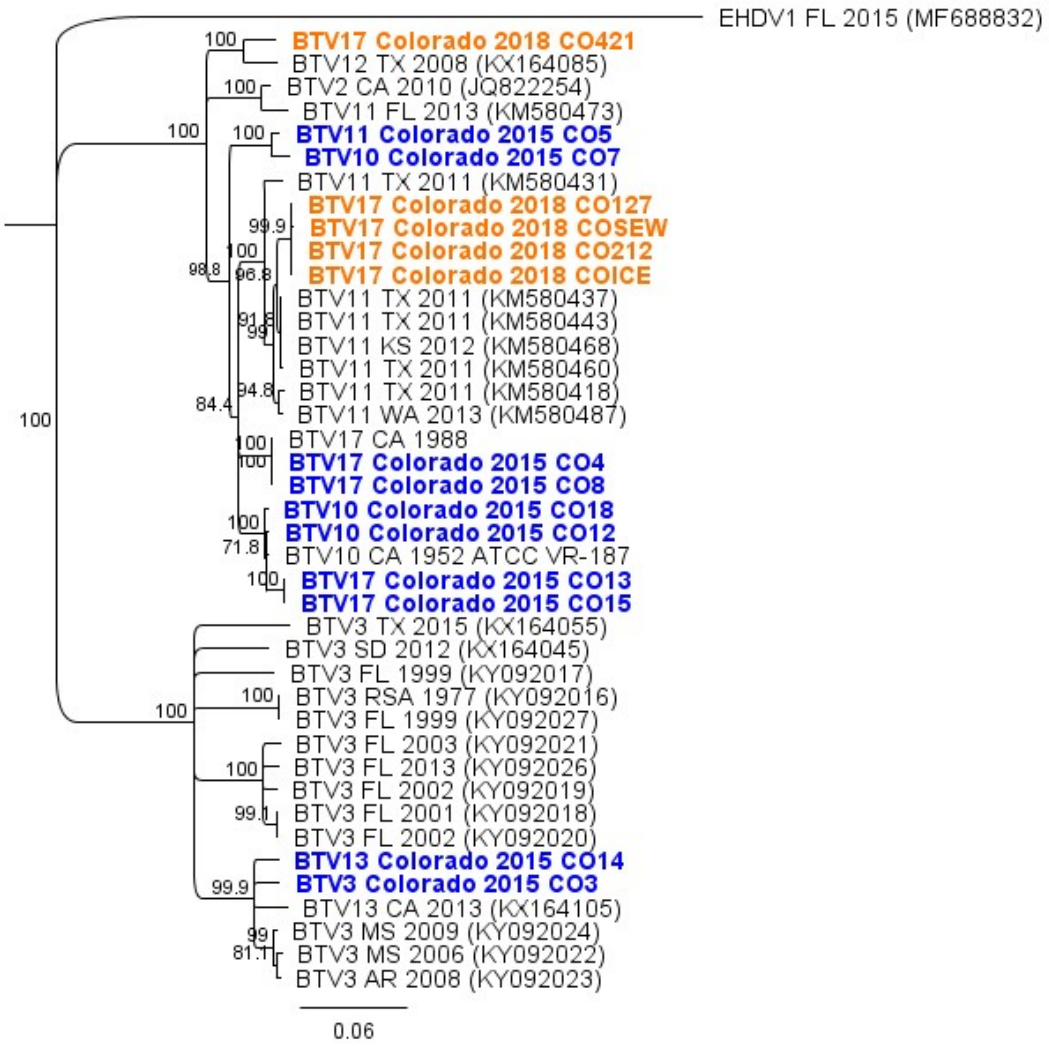

Figure 5.8 – Segment 7 Phylogenetic Tree. 2015 isolates are shown in blue; 2018 isolates are depicted in orange. Neighbor-joining trees were prepared from coding sequence alignments (1050 bp) using HKY genetic distances with 1,000 bootstrapping replicates. EHDV-1 was used as the outgroup. Nodes with >70% support are considered statistically supported. GenBank accession numbers of non-Colorado isolates are included in parentheses.

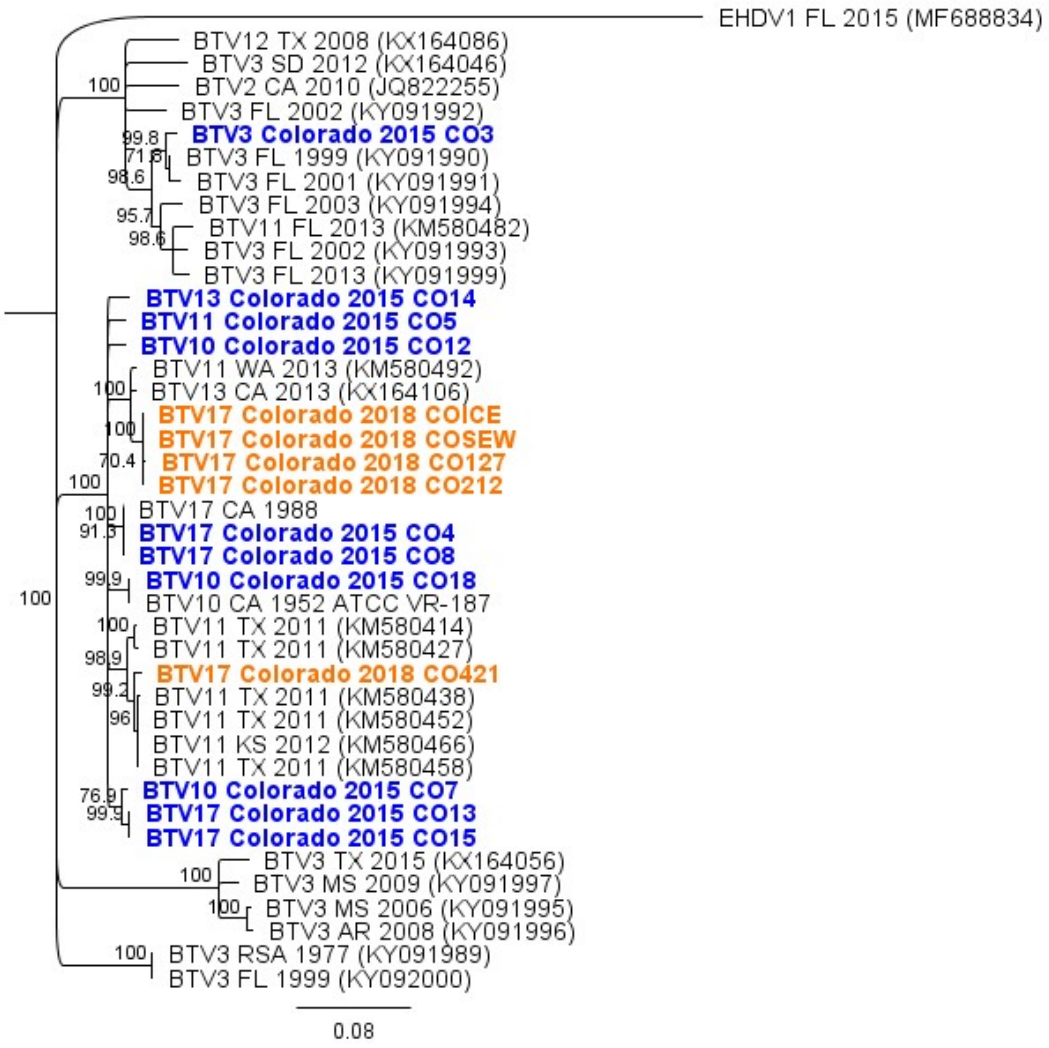

Figure 5.9 – Segment 8 Phylogenetic Tree. 2015 isolates are shown in blue; 2018 isolates are depicted in orange. Neighbor-joining trees were prepared from coding sequence alignments (1065 bp) using HKY genetic distances with 1,000 bootstrapping replicates. EHDV-1 was used as the outgroup. Nodes with >70% support are considered statistically supported. GenBank accession numbers of non-Colorado isolates are included in parentheses.

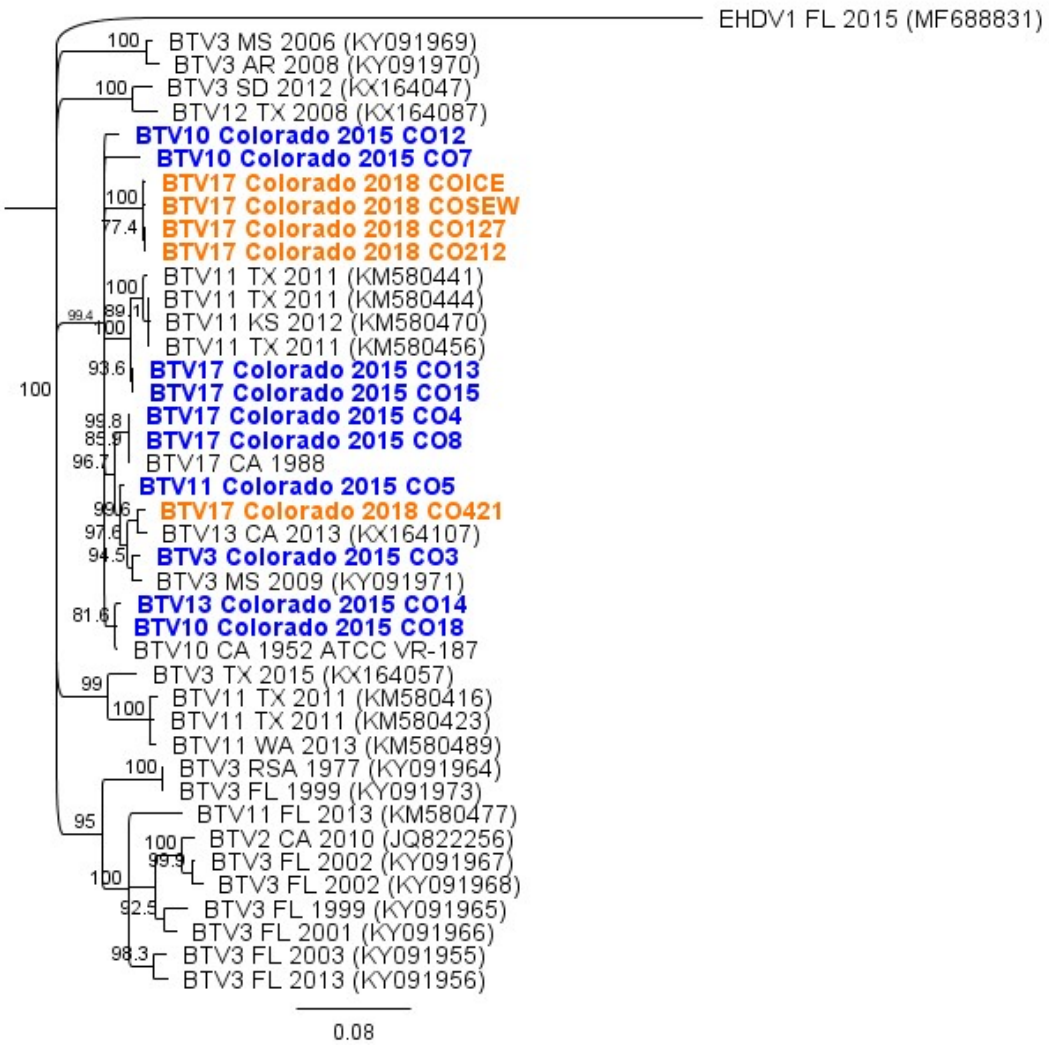

Figure 5.10 – Segment 9 Phylogenetic Tree. 2015 isolates are shown in blue; 2018 isolates are depicted in orange. Neighbor-joining trees were prepared from coding sequence alignments (990 bp) using HKY genetic distances with 1,000 bootstrapping replicates. EHDV-1 was used as the outgroup. Nodes with >70% support are considered statistically supported. GenBank accession numbers of non-Colorado isolates are included in parentheses.

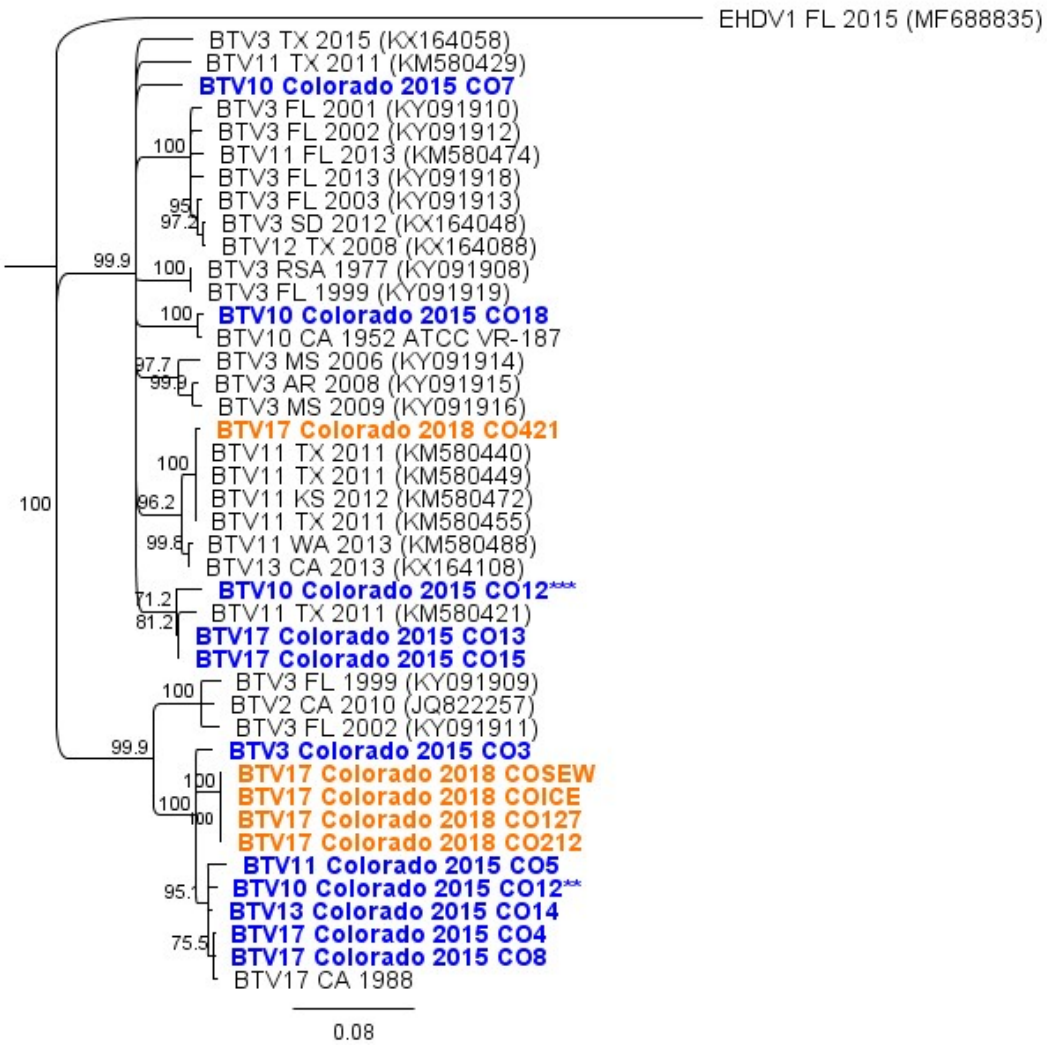

Figure 5.11 – Segment 10 Phylogenetic Tree. 2015 isolates are shown in blue; 2018 isolates are depicted in orange. Neighbor-joining trees were prepared from coding sequence alignments (690 bp) using HKY genetic distances with 1,000 bootstrapping replicates. EHDV-1 was used as the outgroup. Nodes with >70% support are considered statistically supported. BTV10 Colorado 2015 CO12 demonstrated coinfection (sequences aligning to distinct segment 10 sequences from this isolate are depicted with asterisks). Both segment 10s that CO12 reads aligned to had 100% cds coverage. GenBank accession numbers of non-Colorado isolates are included in parentheses.

REFERENCES

1. Ratinier M, Shaw AE, Barry G, et al. Bluetongue virus NS4 protein is an interferon antagonist and a determinant of virus virulence. *J Virol*. 2016;90(11):5427-5439. doi:10.1128/JVI.00422-16.

2. Schirtzinger EE, Jasperson DC, Ostlund EN, Johnson DJ, Wilson WC. Recent US bluetongue virus serotype 3 isolates found outside of Florida indicate evidence of reassortment with co-circulating endemic serotypes. *J Gen Virol*. 2018;99(2):157-168. doi:10.1099/jgv.0.000965.

3. Ratinier M, Caporale M, Golder M, et al. Identification and characterization of a novel non-structural protein of bluetongue virus. *PLoS Pathog*. 2011;7(12). doi:10.1371/journal.ppat.1002477.

4. Belhouchet M, Mohd Jaafar F, Firth AE, Grimes JM, Mertens PPC, Attoui H. Detection of a fourth orbivirus non-structural protein. *PLoS One*. 2011;6(10):e25697. doi:10.1371/journal.pone.0025697.

5. Maclachlan NJ, Nunamaker RA, Katz JB, et al. Detection of bluetongue virus in the blood of inoculated calves: comparison of virus isolation, PCR assay, and in vitro feeding of *Culicoides variipennis*. *Arch Virol*. 1994;136:1-8.

6. Schwartz-Cornil I, Mertens PPC, Contreras V, et al. Bluetongue virus: virology, pathogenesis and immunity. *Vet Res*. 2008;39(46). doi:10.1051/vetres:2008023.

7. Maclachlan NJ, Mayo CE, Daniels PW, Savini G, Zientara S, Gibbs EPJ. Bluetongue. *Rev Sci Tech*. 2015;34(2):329-340. doi:doi.org/10.20506/rst.34.2.2360.

8. Maan S, Maan NS, Belaganahalli MN, et al. Full-genome sequencing as a basis for molecular epidemiology etudies of bluetongue virus in India. *PLoS One*. 2015;10(6). doi:10.1371/journal.pone.0131257.

9. Wright M. Serological and genetic characterisation of putative new serotypes of bluetongue virus and epizootic haemorrhagic disease virus isolated from an alpaca. Dissertation Thesis, North-West Univ Potchefstroom Campus. 2013.

10. Wilson A, Mellor P. Bluetongue in Europe: vectors, epidemiology and climate change. *Parasitol Res*. 2009;103(Suppl 1):S69-S77. doi:10.1007/s00436-008-1314-8.

11. Hoogendam K. International study on the economic consequences of outbreaks of bluetongue serotype 8 in north-western Europe Leeuwarden: *Van Hall Institute*; 2007.

12. Maclachlan NJ. Globlal implications of the recent emergence of bluetongue virus in Europe. *Vet Clin Food Anim*. 2010;26:163-171. doi:10.1016/J.CVFA.2009.10.012.

13. Ostlund EN. Report of the committee on bluetongue and bovine retroviruses. *Proc Annu Meet US Anim Health Assoc*. 2007;111:209-213.

14. Tanya VN, Greiner EC, Gibbs EPJ. Evaluation of *Culicoides insignis* (Diptera: Ceratopogonidae) as a vector of bluetongue virus. *Vet Microbiol*. 1992;32:1-14.

15. Maclachlan NJ, Wilson WC, Crossley BM, et al. Novel serotype of bluetongue virus, western North America. *Emerg Infect Dis*. 2013;19(4):665-666. doi:10.3201/eid1904.120347.

16. Tabachnick WJ. *Culicoides variipennis* and bluetongue virus epidemiology in the United States. *Annu Rev Entomol*. 1996;41:23-43.

17. Mcvey DS, Drolet BS, Ruder MG, et al. Orbiviruses: a North American perspective. *Vector-Borne Zoonot*. 2015;15(6):335-338. doi:10.1089/vbz.2014.1699.

18. Gaudreault NN, Jasperson DC, Dubovi EJ, Johnson DJ, Ostlund EN, Wilson WC. Whole genome sequence analysis of circulating bluetongue virus serotype 11 strains from the United States including two domestic canine isolates. *J Vet Diagn Invest*. 2015;27(4):442-448. doi:10.1177/1040638715585156.

19. Miller MM, Brown J, Cornish T, et al. Investigation of a bluetongue disease epizootic caused by bluetongue virus serotype 17 in sheep in Wyoming. *J Am Vet Med Assoc*. 2010;237(8):955-959. doi:10.2460/javma.237.8.955.

20. White DM, Blair CD, Beaty BJ. Molecular epidemiology of bluetongue virus in northern Colorado. *Virus Res*. 2006;118:39-45. doi:10.1016/j.virusres.2005.11.008.

21. White DM, Wilson WC, Blair CD BB. Studies on overwintering of bluetongue viruses in insects. *J Gen Virol*. 2005;86:453-462.

22. Clavijo A, Munroe F, Zhou EM, Booth TF, Roblesky K. Incursion of bluetongue virus into the Okanagan Valley, British Columbia. *Can Vet J*. 2000;41:312-314.

23. Samy AM, Peterson AT. Climate change influences on the global potential distribution of bluetongue virus. *PLoS One*. 2016;11(3):e0150489. doi:10.1371/journal.pone.0150489.

24. Ruder MG, Lysyk TJ, Stallknecht DE, et al. Transmission and epidemiology of bluetongue and epizootic hemorrhagic disease in North America: current perspectives, research gaps, and future directions. *Vector-Borne Zoonot*. 2015;15(6):348-363. doi:10.1089/vbz.2014.1703.

25. Mayo CE, Mullens BA, Reisen WK, et al. Seasonal and interseasonal dynamics of bluetongue virus infection of dairy cattle and *Culicoides sonorensis* midges in northern California – implications for virus overwintering in temperate zones. *PLoS One*. 2014;9(9). doi:10.1371/journal.pone.0106975.

26. Gerry AC, Mullens BA, Maclachlan NJ, Mecham JO. Seasonal transmission of bluetongue virus by *Culicoides sonorensis* (Diptera: Ceratopogonidae) at a southern California dairy and evaluation of vectorial capacity as a predictor of bluetongue virus transmission. *J Med Entomol*. 2001;38(2):197-209.

27. Mayo CE, Gardner IA, Mullens BA, et al. Anthropogenic and meteorological factors influence vector abundance and prevalence of bluetongue virus infection of dairy cattle in California. *Vet Microbiol*. 2012;155:158-164. doi:10.1016/j.vetmic.2011.08.029.

28. Mayo C, Shelley C, MacLachlan NJ, Gardner I, Hartley D, Barker C. A deterministic model to quantify risk and guide mitigation strategies to reduce bluetongue virus transmission in California dairy cattle. *PLoS One*. 2016;11(11). doi:10.1371/journal.pone.0165806.

29. Mayo CE, Osborne CJ, Mullens BA, et al. Seasonal variation and impact of waste-water lagoons as larval habitat on the population dynamics of *Culicoides sonorensis* (Diptera:Ceratpogonidae) at two dairy farms in northern California. *PLoS One*. 2014;9(2). doi:10.1371/journal.pone.0089633.

30. Lhor Y. Spatial and seasonal distribution of *Culicoides* species in Morocco in relation to the transmission of bluetongue viruses. *Br J Virol*. 2015;2(6):88-95. doi:10.17582/journal.bjv/2015.2.6.88.95.

31. Foxi C, Delrio G, Falchi G, Marche MG, Satta G, Ruiu L. Role of different *Culicoides* vectors (Diptera: Ceratopogonidae) in bluetongue virus transmission and overwintering in Sardinia (Italy). *Parasit Vectors*. 2016;9(1):440. doi:10.1186/s13071-016-1733-9.

32. Diarra M, Fall M, Fall AG, et al. Seasonal dynamics of *Culicoides* (Diptera: Ceratopogonidae) biting midges, potential vectors of African horse sickness and bluetongue viruses in the Niayes area of Senegal. *Parasit Vectors*. 2014;7(1):147. doi:10.1186/1756-3305-7-147.

33. Turner J, Bowers RG, Baylis M. Modelling bluetongue virus transmission between farms using animal and vector movements. *Sci Rep*. 2012;2:319. doi:10.1038/srep00319.

34. Carvalho LPC, Silva FS. Seasonal abundance of livestock-associated *Culicoides* species in northeastern Brazil. *Med Vet Entomol*. 2014;28:228-231. doi:10.1111/mve.12043.

35. Nomikou K, Hughes J, Wash R, et al. Widespread reassortment shapes the evolution and epidemiology of bluetongue virus following European invasion. *PLoS Pathog*. 2015;11(8). doi:10.1371/journal.ppat.1005056.

36. Sugiyama K, Bishop DHL, Roy P. Analyses of the genomes of bluetongue viruses recovered in the United States. *Virology*. 1982;114:210-217.

37. Lima L, Guimarães B, César J, et al. Identification of bluetongue virus serotypes 1, 4, and 17 co- infections in sheep flocks during outbreaks in Brazil. *Res Vet Sci*. 2017. doi:10.1016/j.rvsc.2017.09.001.

38. Oberst RD, Squire KRE, Stott JL, Chuang RY, Osburn BI. The coexistence of multiple bluetongue virus electropherotypes in individual cattle during natural infection. *J Gen Virol*. 1985;66:1901-1909.

39. Squire KRE, Osburn BI, Chuang RY, Doi RH. A survey of electropherotype relationships of bluetongue virus isolates from the western United States. *J Gen Virol*. 1983;64:2103-2115.

40. Maclachlan NJ, Jagels G, Rossitto P V, Moore PF, Heidner HW. The pathogenesis of experimental bluetongue virus infection of calves. *Vet Pathol*. 1990;27:223-229.

41. Shaw AE, Ratinier M, Nunes SF, et al. Reassortment between two serologically unrelated bluetongue virus strains is flexible and can involve any genome segment. *J Virol*. 2013;87(1):543-557. doi:10.1128/JVI.02266-12.

42. Stott JL, Oberst RD, Blanchard-Channell M, Osburn BI. Genome segment reassortment between two serotypes of bluetongue virus in a natural host. *J Virol*. 1987;61(9):2670-2674.

43. Oberst RD, Stott JL, Blanchard-Channell M, Osburn BI. Genetic reassortment of bluetongue virus serotype 11 strains in the bovine. *Vet Microbiol*. 1987;15:11-18.

44. Ramig RF, Garrison C, Chen D, Bell-Robinson D. Analysis of reassortment and superinfection during mixed infectino of Vero cells with bluetongue virus serotypes 10 and 17. *J Gen Virol*. 1989;70:2595-2603.

45. Samal BK, El Hussein A, Holbrook FR, Beaty BJ, Ramig RF. Mixed infection of *Culicoides variipennis* with bluetongue virus serotypes 10 and 17: evidence for high frequency reassortment in the vector. *J Gen Virol*. 1987;68:2319-2329.

46. El Hussein A, Ramig RF, Holbrook FR, Beaty BJ. Asynchronous mixed infection of *Culicoides variipennis* with bluetongue virus serotypes 10 and 17. *J Gen Virol*. 1989;70:3355-3362.

47. Dal Pozzo F, Martinelle L, Thys C, et al. Experimental co-infections of calves with bluetongue virus serotypes 1 and 8. *Vet Microbiol*. 2013. doi:10.1016/j.vetmic.2013.01.016.

48. Qin S, Yang H, Zhang Y, et al. Full genome sequence of the first bluetongue virus serotype 21 (BTV-21) isolated from China: evidence for genetic reassortment between BTV-21 and bluetongue virus serotype 16 (BTV-16). *Arch Virol*. 2018;163(5):1379-1382. doi:10.1007/s00705-018-3718-9.

49. Shafiq M, Minakshi P, Bhateja A, Ranjan K, Prasad G. Evidence of genetic reassortment between Indian isolate of bluetongue virus serotype 21 (BTV-21) and bluetongue virus serotype 16 (BTV-16). *Virus Res*. 2013;173(2):336-343. doi:10.1016/j.virusres.2013.01.009.

50. Batten CA, Maan S, Shaw AE, Maan NS, Mertens PPC. A European field strain of bluetongue virus derived from two parental vaccine strains by genome segment reassortment. *Virus Res*. 2008;137(1):56-63. doi:10.1016/j.virusres.2008.05.016.

51. Maan S, Maan NS, Pullinger G, et al. The genome sequence of bluetongue virus type 10 from India: evidence for circulation of a western topotype vaccine strain. *J Virol*. 2012;86(10):5971-5972. doi:10.1128/JVI.00596-12.

52. Maan NS, Maan S, Guimera M, et al. The genome sequence of a reassortant bluetongue virus serotype 3 from India. *J Virol*. 2012;86(11):6375-6376. doi:10.1128/JVI.00671-12.

53. Maan S, Maan NS, Guimera M, et al. Genome sequence of a reassortant strain of bluetongue virus serotype 23 from western India. *J Virol*. 2012;86(12):7011-7012. doi:10.1128/JVI.00731-12.

54. Hornyák Á, Malik P, Marton S, Dóró R, Cadar D, Bányai K. Emergence of multireassortant bluetongue virus serotype 4 in Hungary. *Infect Genet Evol*. 2015;33:6-10. doi:10.1016/j.meegid.2015.03.036.

55. Kumar L, Batra K, Chaudhary D, et al. Full-genome sequence analysis of a reassortant strain of bluetongue virus serotype 16 from southern India. *Genome Announc*. 2016;4(4). doi:10.1128/genomeA.00783-16.

56. Lorusso A, Costessi A, Pirovano W, Marcacci M, Cammà C, Savini G. Complete genome sequence analysis of a reassortant strain of bluetongue virus serotype 16 from Italy. *Genome Announc*. 2013;1(4). doi:10.1128/genomea.00622-13.

57. McHolland LE, Mecham JO. Characterization of cell lines developed from field populations of *Culicoides sonorensis* (Diptera: Ceratopogonidae). *J Med Entomol*. 2003;40(3):348-351. doi:10.1603/0022-2585-40.3.348.

58. Ortega J, Crossley B, Dechant JE, Drew CP, James MacLachlan N. Fatal bluetongue virus infection in an alpaca (*Vicugna pacos*) in California. *J Vet Diagn Invest*. 2010;22:134-136. doi:10.1177/104063871002200129.

59. Maan S, Maan NS, Belaganahalli MN, et al. Development and evaluation of real time RT-PCR assays for detection and typing of bluetongue virus. *PLoS One*. 2016;11(9). doi:10.1371/journal.pone.0163014.

60. Wechsler SJ, McHolland LE, Tabachnick WJ. Cell lines from *Culicoides variipennis* (Diptera: Ceratopogonidae) support replication of bluetongue virus. *J Invertebr Pathol*. 1989;54:385-393.

61. Capella-Gutiérrez S, Silla-Martínez JM, Gabaldón T. trimAl: a tool for automated alignment trimming in large-scale phylogenetic analyses. *Bioinformatics*. 2009;25(15):1972-1973. doi:10.1093/bioinformatics/btp348.

62. Bolger AM, Lohse M, Usadel B. Trimmomatic: a flexible trimmer for Illumina sequence data. *Bioinformatics*. 2014;30(15):2114-2120. doi:10.1093/bioinformatics/btu170.

63. Fu L, Niu B, Zhu Z, Wu S, Li W. CD-HIT: accelerated for clustering the next-generation sequencing data. *Bioinformatics*. 2012;28(23):3150-3152. doi:10.1093/bioinformatics/bts565.

64. Langmead B, Salzberg SL. Fast gapped-read alignment with Bowtie 2. *Nat Methods*. 2012;9(4):357-359. doi:10.1038/nmeth.1923.

65. Bankevich A, Nurk S, Antipov D, et al. SPAdes: a new genome assembly algorithm and its applications to single-cell sequencing. *J Comput Biol*. 2012;19(5):455-477. doi:10.1089/cmb.2012.0021.

66. Edgar RC. MUSCLE: multiple sequence alignment with high accuracy and high throughput. *Nucleic Acids Res*. 2004;32(5):1792-1797. doi:10.1093/nar/gkh340.

67. Clarke LL, Ruder MG, Kienzle-Dean C, Carter D, Stallknecht D, Howerth EW. Experimental infection of white-tailed deer (*Odocoileus virginianus*) with bluetongue virus serotype 3. *J Wildl Dis*. 2019;55(3). doi:10.7589/2018-06-159.

68. De la Torre J, Holland J. RNA virus quasispecies populations can suppress vastly superior mutant progeny. *J Virol*. 1990;64(12):6278-6281.

69. Caporale M, Di Gialleonorado L, Janowicz A, et al. Virus and host factors affecting the clinical outcome of bluetongue virus infection. *J Virol*. 2014;881. Capor(18):10399-10411. doi:10.1128/JVI.01641-14.

70. 2018 State Agriculture Overview: Colorado. https://www.nass.usda.gov/Quick_Stats/Ag_Overview/stateOverview.php?state=COLORADO.

CHAPTER 6 – CONCLUSION

Bluetongue virus remains an economically important, re-emerging disease threat throughout North America and worldwide. Persistent knowledge gaps regarding its evolution and ecology have hindered our ability to effectively predict and prevent outbreaks. Moreover, climate change is expected to continue to reshape the distribution of bluetongue virus (BTV), likely accelerating the rate of BTV incursions and the introduction of non-enzootic serotypes into new regions.

The research presented here builds upon previous work to offer a unique perspective that takes into account both the evolutionary traits of this virus as well as ecological factors that influence its evolution. We applied a number of sequencing technologies and experimental approaches to answer specific questions about BTV's overall genetic stability and viral population structure both in vitro and in vivo.

First, we leveraged a well-characterized in vitro system to determine how BTV's alternating-host transmission cycle impacts the occurrence of genetic variation within a single virus strain across passages. Using whole genome sequencing to detect the occurrence and frequency of single-nucleotide variants (SNVs), we applied several specific measures to understand the viral population dynamics at play in our system. Our findings demonstrate that the BTV genome remains highly genetically stable, even when passaged exclusively in invertebrate cells.

Given our findings of the remarkable genome stability of a single virus strain, we next queried how reassortment might affect BTV's evolution. Again, we applied an in vitro system and novel sequencing approaches to understand reassortment between BTV-2 and BTV-10. Our

results indicate that reassortment occurs readily between these two strains. However, global shifts in segment frequencies arise across passages, possibly indicating a preferred virus backbone. Despite the segment-specific trends that arose, it is interesting to note that measures of effective diversity (which were based on individual plaque genotypes and thus likely underestimated the true diversity detected via metagenomic sequencing) significantly increased during the course of coinfection. This is in contrast to the findings of our first chapter, where measures of population complexity were essentially unchanged across passages. Although these estimates of diversity are not directly comparable, these findings nevertheless allude to the prominent role that reassortment likely plays in BTV's evolution.

We then used these same viruses to investigate how incubation temperature might affect virogenesis and reassortment in *Culicoides sononensis*, the predominant BTV vector in North America. Unexpectedly, we found that BTV-2 generally failed to infect midges unless introduced at very high titers, highlighting the complexities of virus-vector interactions and their role in modulating arbovirus expansion. We also detected temperature- and virus-specific effects on midge survival, which is significant for our understanding of BTV ecology and will help refine forthcoming predictive modeling efforts.

Finally, we explored the genetic diversity of BTV isolates circulating among ruminants along the Front Range of Colorado using whole genome sequencing. Due to the large livestock and wildlife populations in Colorado, this region provides an ideal geospatial location for BTV surveillance. In addition to detecting evidence of reassortment, we identified exotic serotype 3 in at least one cow with inapparent BTV infection in 2015, as well as the presence of other exotic BTV segments in isolates collected in 2018. These findings underscore the necessity of sentinel animal surveillance and the vital importance of whole genome sequencing to capture the true

complexity and considerable genetic diversity of bluetongue viruses circulating in North America.

In addition to investigating the impact of temperature on BTV reassortment between strains that are equally infectious to *C. sonorensis*, future work should explore the myriad other factors that affect virus-vector-host interactions. The mechanistic unknowns of BTV reassortment following coinfection and the RNA- or protein-based interactions that permit or limit the generation of successful reassortant progeny also warrant further investigation. On a broader level, the roles that host immunity, RNAi, host community structure, coinfection with other viral species, and microbiome composition play in shaping BTV's evolution should also be investigated.

APPENDIX 1 – CUVAW3 MAINTENANCE MEDIA

Maintenance media for CuVaW3 cells was prepared from a modified recipe based off that described by Weschsler et al., courtesy of recommendations from collaborators at USDA-ARS in Manhattan, KS.[1,2]

Add the following to 1 liter of HyClone cell culture grade water:

24.5 g powdered Schneider's Drosophila Media

0.4 g sodium bicarbonate

0.06 g L-glutamine

0.006 g reduced glutathione

0.03 g L-asparagine

0.45 U bovine insulin*

2.1 g sodium hydroxide pellets

0.6 g calcium chloride

Adjust pH to ~6.7 with 12.1 N HCl

Sterile-filter solution with 0.22 µm vacuum filter

Add 15% heat-inactivated, insect-cell tested fetal bovine serum

*Bovine insulin was not used for CuVaW3 cell culture described in Chapter 2.

1. Wechsler SJ, McHolland LE, Tabachnick WJ. Cell lines from *Culicoides variipennis* (Diptera: Ceratopogonidae) support replication of bluetongue virus. *J Invertebr Pathol*. 1989;54:385-393.
2. McHolland LE, Mecham JO. Characterization of cell lines developed from field populations of *Culicoides sonorensis* (Diptera: Ceratopogonidae). *J Med Entomol*. 2003;40(3):348-351. doi:10.1603/0022-2585-40.3.348.

Appendix 2 – Amplicon Assay Primers. Round 1 amplicon assay, BTV-specific primer sequences and concentrations. Final primer cocktail concentration (in µM) is shown for each primer.

	Sequence	µM
S1_560F	TCC AGG GGA ATA GAG ATT TAT C	0.12
S1_1033R	TCG TGC GAG CCY AAW TTT TG	0.12
S2_1210F	TGG CGA TGT KTA CTT YAC MTT GCG	0.11
S2_1601R	GCA TCY TTY TCG AAA TCG ATT GTA AG	0.11
S3_2282F	TMC AGT TYC GAG CGG CTT TAA G	0.10
S3_2684R	GAG CGA TTG GGT GAT GTC CA	0.10
S4_1484F	TCG TGG GCG ATG AAT TTT GCT	0.08
S4_1961R	TCA CCT AGC AGT CAC GCA TTA TAA G	0.08
S5_177F	TCG ATG ATY GCA GCA ACT GAT G	0.08
S5_587R	TGT GCT GTC CAC GAA TGC CAA	0.08
S6_715F	TAG GCG GCR TCW GAA GAA GTG	0.10
S6_1099R	YGG GAT CTT AAA YYT CAT CAT YAC	0.10
S7_246F	TTT TGG ACC GAT ATC GCC AGA	0.05
S7_701R	TGT CCA TCC CAC GCT ATA ATG C	0.05
S8_594F	TTG GAT GAW GAG GCC AAA GAG AT	0.09
S8_1048R	CTT AGA GAC AAA AGC AAC ACG CT	0.09
S9_455F	TAC GGT ACG AAG ATT GAT GTT TAC AG	0.09
S9_902R	TTC CAA TGC GGA TCT CCA GTT G	0.09
S10_184F	TAA ATY CTG GAC AAA GCG ATG TC	0.07
S10_549R	ACT YTT TGC GCA AAC CAT CAT CA	0.07

TruSeq adapter tags sit upstream of forward and reverse primers:

Forward: CTA CAC GAC GCT CTT CCG ATC [BTV-specific primer sequence, from table]
Reverse: CAG ACG TGT GCT CTT CCG ATC [BTV-specific primer sequence, from table]
Second round dual-index PCR primers.

i7 primer: CAA GCA GAA GAC GGC ATA CGA GAT [8-mer barcode] C AGA CGT GTG CTC TTC CGA TC
i5 primer: AAT GAT ACG GCG ACC ACC GAG ATC TAC ACG TTC TCT TAC A [8-mer barcode] CTA CAC GAC GCT CTT CCG ATC T

APPENDIX 3 – BOWTIE2 PARAMETERS USED FOR AMPLICON ANALYSIS

```
cmd="bowtie2
 -x $bt_index
 -q
 -1 $f1
 -2 $f2
 -D 120
 -R 60
 -X 600
 --rg-id 1
 --rg SM:1
 --local
 --qc-filter
 --score-min C,160,1
 --no-unal
 --no-mixed
 --maxins 700
 --time
 --al-conc ${output_prefix}.conc_hits.fastq
 --threads 24
```

1. Langmead B, Salzberg SL. Fast gapped-read alignment with Bowtie 2. *Nat Methods*. 2012;9(4):357-359. doi:10.1038/nmeth.1923.

APPENDIX 4 – TITERS AND CT VALUES, PASSAGES 1-7

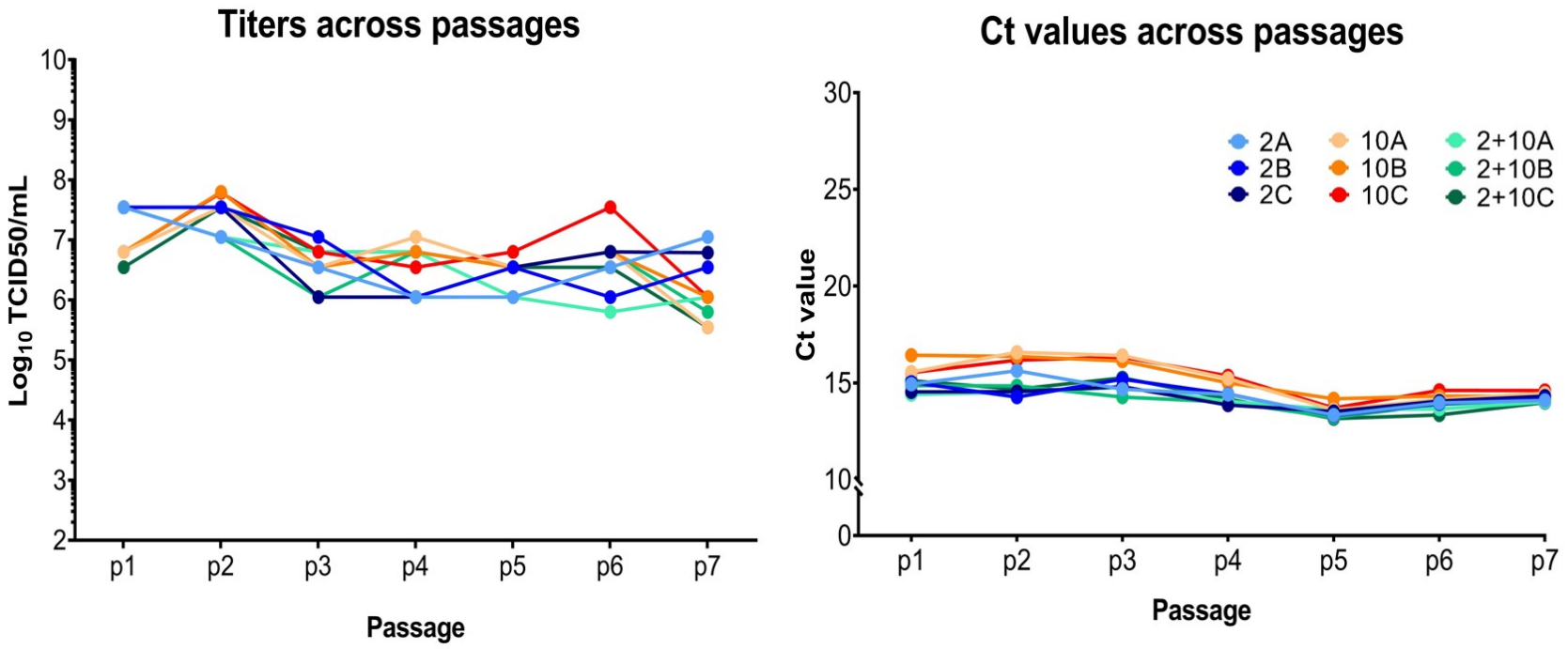

Appendix 4 – Titers and Ct Values, Passages 1-7. 50% tissue culture infectious dose (TCID50) across passages and replicates is shown on the left hand panel, and BTV segment 10 Ct values across passages and replicates is shown on the right. Figures related to material presented in Chapter 3.

APPENDIX 5 – COMPARATIVE EFFICIENCIES OF BTV VS COX1, RT-PCR

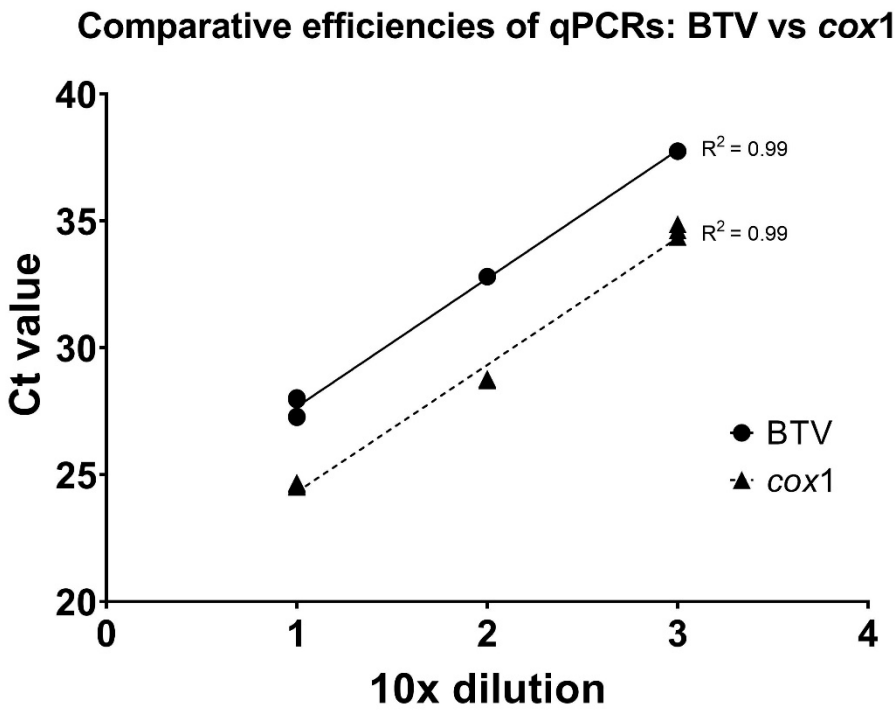

Appendix 5 – Comparative Efficiencies of BTV vs Cox1, RT-PCR. Comparative efficiencies of BTV and *Culicoides* mitochondrial cytochrome oxidase 1 gene (*cox*1) qRT-PCR after DNase treatment. Ten-fold dilutions were prepared of a pool of BTV-infected midges, and each dilution was screened in triplicate for each target. Linear regressions and R^2 values were prepared using Graph Pad Prism 8.0. Figure relates to material presented in Chapter 4.

APPENDIX 6 – MODIFIED AMPLICON ASSAY PRIMERS

Appendix 6 – Modified Amplicon Assay Primers. Round-one PCR of amplicon assay, BTV-specific primer sequences and concentrations. Final primer cocktail concentration (in µM) is shown for each primer. **P**rimer concentrations for day 11 propagated plaques (D11) and day 23 propagated plaques (D23) are shown. Relates to material presented in Chapter 4.

	Sequence	D11, µM	D23, µM
S1_560F	TCC AGG GGA ATA GAG ATT TAT C	0.13	0.12
S1_1033R	TCG TGC GAG CCY AAW TTT TG	0.13	0.12
S2_1210F	TGG CGA TGT KTA CTT YAC MTT GCG	0.10	0.11
S2_1601R	GCA TCY TTY TCG AAA TCG ATT GTA AG	0.10	0.11
S3_2282F	TMC AGT TYC GAG CGG CTT TAA G	0.08	0.10
S3_2684R	GAG CGA TTG GGT GAT GTC CA	0.08	0.10
S4_1484F	TCG TGG GCG ATG AAT TTT GCT	0.08	0.08
S4_1961R	TCA CCT AGC AGT CAC GCA TTA TAA G	0.08	0.08
S5_177F	TCG ATG ATY GCA GCA ACT GAT G	0.13	0.08
S5_587R	TGT GCT GTC CAC GAA TGC CAA	0.13	0.08
S6_715F	TAG GCG GCR TCW GAA GAA GTG	0.13	0.10
S6_1099R	YGG GAT CTT AAA YYT CAT CAT YAC	0.13	0.10
S7_246F	TTT TGG ACC GAT ATC GCC AGA	0.08	0.05
S7_701R	TGT CCA TCC CAC GCT ATA ATG C	0.08	0.05
S8_594F	TTG GAT GAW GAG GCC AAA GAG AT	0.08	0.09
S8_1048R	CTT AGA GAC AAA AGC AAC ACG CT	0.08	0.09
S9_455F	TAC GGT ACG AAG ATT GAT GTT TAC AG	0.10	0.09
S9_902R	TTC CAA TGC GGA TCT CCA GTT G	0.10	0.09
S10_184F	TAA ATY CTG GAC AAA GCG ATG TC	0.08	0.07
S10_549R	ACT YTT TGC GCA AAC CAT CAT CA	0.08	0.07